

A STUDY OF THE CORRESPONDENCE RULE IN A  
VISCOELASTIC STRESS ANALYSIS

Geoffrey Frank Howard

A Thesis Submitted in Fulfilment of the  
Requirement for the degree of  
Master of Philosophy  
Faculty of Engineering  
The University of Aston in Birmingham

May 1973

THESIS  
539.31  
How

27 June 73 - 163207



## SYNOPSIS

This thesis is mainly concerned with two fields of investigation; the viscoelastic behaviour of plastics, and the numerical solution of engineering problems by means of finite element methods.

The basic equations describing linear elastic behaviour are modified to give corresponding equations for linear viscoelastic materials, and various theoretical models are used to describe viscoelastic behaviour.

The stiffness matrix for a tapered element of a beam is derived for cases where the shear stress is neglected and where its effect is allowed for, and numerical solutions are obtained for various bending problems. Bending is also considered as a plane stress problem, using triangular elements.

By combining the results obtained from linear viscoelastic theory and finite element methods theoretical solutions are obtained for a number of more difficult viscoelastic problems, and the results are compared with those obtained by experiment. Theoretical and experimental results are also given for certain non-linear viscoelastic problems.

Finally methods of designing in plastics are discussed in relation to the results previously obtained.

Throughout, extensive use is made of computer solutions, and the development of the programs is detailed in the Appendix.



## CONTENTS

	Page
CHAPTER 1: INTRODUCTION	1
CHAPTER 2: NOTATION	4
CHAPTER 3: CONTINUUM MECHANICS	7
3.1 Stress and Strain	8
3.2 Linear elasticity	11
3.3 Stress functions	11a
3.4 Linear viscoelasticity	15
CHAPTER 4: SOLUTION OF PROBLEMS IN LINEAR VISCOELASTICITY	26
4.1 Creep tests on Perspex	27
4.2 The effect of loading rate in a creep test	28
4.3 Viscoelastic beam on a flexible base	32
4.4 Thin viscoelastic cylinder with internal pressure	38
CHAPTER 5: NUMERICAL SOLUTION OF ENGINEERING PROBLEMS	44
5.1 Methods of solution	45
CHAPTER 6: SOLUTION OF ELASTIC PROBLEMS USING FINITE ELEMENT METHODS	54
6.1 Finite element of a uniform beam	54
6.2 Elastic structures	56
6.3 Elastic beams	60
6.4 Finite element method applied to a tapered beam	67
6.5 Improved stiffness matrix for a tapered element	74
6.6 Further investigation of the errors in the end deflection of a finite element of varying taper	78



	Page
CHAPTER 6 continued..	
6.7 End deflection of a uniform wedge	82
6.8 Effect of shear stress on the stiffness matrix of an element of a beam	84
6.9 General solution for a tapered beam	92
6.10 Use of the general program for a tapered beam	96
6.11 Finite element method applied to a plane stress problem	98
CHAPTER 7: SOLUTION OF LINEAR VISCOELASTIC PROBLEMS USING FINITE ELEMENT METHODS	109
7.1 Perspex frame	110
7.2 Cylinder of varying wall thickness subjected to an internal pressure	112
7.3 Application of the finite element method to a plane stress viscoelastic problem	122
CHAPTER 8: BENDING OF NON-LINEAR ELASTIC BEAMS	132
8.1 Strains in a non-linear beam	132
8.2 Finite element solution using a non- linear stress-strain law	135
8.3 Finite element solution using numerical values of stress and strain	143
8.4 General computer solution for non-linear materials	151
CHAPTER 9: NON-LINEAR VISCOELASTICITY	153
9.1 Non-linear behaviour of plastics	153
9.2 Intermittent loading of a tensile test piece	155



	Page
CHAPTER 9 continued..	
9.3 The deflection of a tapered non-linear viscoelastic beam	161
9.4 Design in plastics	164
CHAPTER 10: GENERAL DISCUSSION	171
CHAPTER 11: CONCLUSIONS	175
APPENDIX	178
REFERENCES	192



## CHAPTER 1

### INTRODUCTION

With the increasing use of plastics as stressed members, as for example in the case of pressure vessels, some relatively simple but reasonably accurate design methods are highly desirable. It was intended that the work recorded here would eventually show possible ways in which the problems of designing in plastics could be approached.

Before dealing with the relatively difficult problems to be solved for plastics it was first necessary to consider the fundamental behaviour of a material and to be able to describe the states of stress and strain. By introducing the simple stress-strain relations for a linear elastic material, elasticity theory then provided a method of finding an exact solution for elastic problems.

It was then necessary to be able to describe the time-dependent behaviour of plastics, and by assuming that this behaviour is linearly viscoelastic various mathematical models may be introduced to describe this type of behaviour. By choosing suitable models the behaviour of a real material (Perspex) was described in mathematical form and it was seen that, by using the correspondence rule, a solution to a particular problem for a viscoelastic material could be obtained from the solution of the corresponding problem with an elastic material.



At a fairly early stage it became obvious that, because of the complexity of the exact solutions for any except the most simple examples, some form of numerical solution would be worth considering. Of the methods investigated the finite element method appeared to be best suited to the work in hand, and this method was used almost exclusively thereafter.

The finite element method using beam-type elements was applied to examples on elastic beams and frames, and the stiffness matrix was derived for a tapered element. To increase the accuracy of this method in cases where shear stresses are not negligible, the stiffness matrices for both uniform and tapered elements were modified to allow for shear effects.

An alternative finite element method was applied to bending problems by using triangular constant-strain triangles, treating the beam as a two-dimensional continuum, and the effect of varying the number of elements was investigated.

Finite element methods were then applied to various problems for a linear viscoelastic material. These were (i) a frame (ii) a pressurised cylinder with a rigid end and (iii) a square plate subjected to compressive stresses. The material was Perspex in each case, and theoretical and experimental results were compared.

Since the behaviour of any real plastic is non-linearly visco-elastic except at low stresses, a method of calculating deflections of beams of non-linear elastic and non-linear viscoelastic materials was



developed. The theoretical results were again compared with experimental values for the deflection of a tapered Perspex beam.

A solution was also obtained for a second non-linear problem. This was the case of a member subjected to intermittent loads, and theoretical and experimental values of strain were compared.

As a result of the theoretical investigations and experimental work, it was possible to make certain suggestions concerning the problems of designing in plastics, and these are given in Chapter 9.

In the numerical methods extensively used, large numbers of linear equations had to be solved. The coefficients were most conveniently evaluated by using a digital computer, and various programs were written to evaluate and store these coefficients and to solve the equations. Details of the development of these programs together with the programs themselves are given in the Appendix.



CHAPTER 2

NOTATION

a A	Coefficients
[A]	Matrix of coefficients
b	Element width
$b_1$	= $y_2 - y_3$ etc.
[B]	Matrix of coordinates
$c_1$	= $x_3 - x_2$ etc.
c	Coefficient
C	Viscoelastic parameter = $\frac{1}{3G} \left( \frac{\bar{\gamma}}{\zeta} - 1 \right)$
$d, d_1, d_2$	Depth of element
D	= $Eh^3/[12(1 - \nu^2)]$
[D]	Matrix of elastic constants
$e_{ij}$	Component of deviatoric strain
E	Young's modulus
$E(t)$	Time-dependent value of E
$\bar{E}$	= $1/C(1 - e^{-\zeta t})$
F	Force
$F_i$	Generalized force
G	Modulus of rigidity
h	Thickness
I	Second moment of area
k	Stiffness
[K]	Stiffness matrix
K	Bulk modulus



$\ell$	Length of element
$L$	Length of beam
$[L]$	Matrix of coefficients
$m$	$\left\{ \begin{array}{l} \text{Viscoelastic parameter} = \beta(1 + \gamma)^{\frac{1}{2}} \\ \text{Taper of element} = (d_1 - d_2)/\ell \end{array} \right.$
$m_i$	$= \frac{1}{\epsilon_i^2} \int_0^i \sigma \epsilon d\epsilon$
$M$	Moment
$n$	Index in non-linear stress-strain law
$p$	Rate of loading, pressure
$P_0$	Force
$p, q$	Coefficients
$P, Q$	Differential operators
$r$	$\left\{ \begin{array}{l} \text{Radius} \\ \text{Rate of application of stress} \\ \text{Ratio } d_2/d_1 \end{array} \right.$
$\left. \begin{array}{l} r_1, r_2, \\ r_3, r_4, \end{array} \right\}$	Elements of flexibility matrix
$R$	Radius of curvature
$s$	Laplace transform parameter
$s_{ij}$	Component of deviatoric stress
$t, T$	Time
$u$	Component of displacement
$u_i$	Generalized displacement
$U$	Strain energy
$U^*$	Complementary strain energy
$v$	Component of displacement



$V$	Total potential energy
$V^*$	Total complementary energy
$w$	Deflection
$x$	Distance from end of element
$y$	Distance from neutral axis
$\alpha$	Angle
$\alpha_i$	Coefficient
$\beta$	Elastic parameter = $(k/4EI)^{1/4}$
$\gamma$	= $G/\eta$
$\gamma_{ij}$	Engineering shear strain
$\delta_{ij}$	Kronecker delta
$\epsilon_{ij}$	Component of strain tensor
$\epsilon_m$	Spherical strain
$\zeta$	Viscoelastic parameter
$\eta$	Viscosity
$\theta$	Angle
$\theta_1\theta_2$	Viscoelastic parameters = $E/3\eta$
$\nu$	Poisson's ratio
$\nu(t)$	Time-dependent value of $\nu$
$N$	"Poisson's" ratio for distortion = 0.5
$\sigma$	Normal stress
$\tau_{ij}$	Component of stress tensor
$\tau_m$	Spherical stress
$\phi$	Stress function
$\Omega$	Potential energy of generalized forces.



CHAPTER 3

CONTINUUM MECHANICS

Since the ultimate aim of the work recorded here was the solution of problems concerned with design in plastics, it was first necessary to study the fundamental behaviour of a material subjected to a number of stresses. The states of stress and strain at any point in a continuum are most conveniently described by using the stress and strain tensors, both of which may be used for any type of material. To determine the strains due to prescribed stresses (or vice versa) in a real material it is then necessary to introduce a stress-strain relationship. The simplest form of this relationship is  $\text{Stress/Strain} = \text{Constant}$  which applies to a linear elastic material, and so many of the earlier results recorded below (in particular in Chapter 6) were obtained for this type of material.

For a linear viscoelastic material, the stress-strain ratio is a function of time, but by using a Laplace transformation, equations connecting stress and strain are obtained similar to those for a linear elastic material. Subsequent analysis may then proceed making use of a correspondence rule as explained in 3.4. By using this method, the more complicated equations encountered in linear viscoelastic problems may usually be solved.

In the case of non-linear viscoelastic materials, the stress-strain ratio is a function of stress (or strain) and time, and no



general method of stress analysis for this type of material seems to be in use at present. This is unfortunate as all plastics exhibit a considerable amount of non-linearity except at very low stresses. In this thesis, some basic investigations are described.

### 3.1 Stress and strain

The state of stress at any point in a 3-dimensional continuum will in general be described by the 9 stress components. These will be the 3 normal components and 6 shear components corresponding to any 3 mutually perpendicular axes. These stresses are conveniently represented as  $\tau_{ij}$  ( $i, j = 1, 2, 3$ ) where  $i = j$  denotes a normal stress and  $i \neq j$  denotes a shear stress. By considering a rotation of the reference axes it may be shown that  $\tau_{ij}$  satisfies the law of transformation for the components of a second order tensor, and that therefore  $\tau_{ij}$  is a second-order tensor. In matrix form the components are shown as:-

$$\begin{bmatrix} \tau_{11} & \tau_{12} & \tau_{13} \\ \tau_{21} & \tau_{22} & \tau_{23} \\ \tau_{31} & \tau_{32} & \tau_{33} \end{bmatrix}$$

If  $\tau$  is a principal stress then

$$\begin{vmatrix} \tau_{11} - \tau & \tau_{12} & \tau_{13} \\ \tau_{21} & \tau_{22} - \tau & \tau_{23} \\ \tau_{31} & \tau_{32} & \tau_{33} - \tau \end{vmatrix} = 0$$

Expanding this determinant gives a cubic equation

$$\tau^3 - I_1\tau^2 + I_2\tau - I_3 = 0$$

where  $I_1, I_2$  and  $I_3$  are the invariants of the matrix.



There will be 3 roots of this cubic equation giving the 3 principal stresses, and it may be shown that their directions are orthogonal.

A given stress tensor may be decomposed into deviatoric and spherical components showing shearing and hydrostatic stressing separately. Thus:-

$$\begin{bmatrix} \tau_{11} & \tau_{12} & \tau_{13} \\ \tau_{21} & \tau_{22} & \tau_{23} \\ \tau_{31} & \tau_{32} & \tau_{33} \end{bmatrix} = \begin{bmatrix} \tau_{11} - \tau_m & \tau_{12} & \tau_{13} \\ \tau_{21} & \tau_{22} - \tau_m & \tau_{23} \\ \tau_{31} & \tau_{32} & \tau_{33} - \tau_m \end{bmatrix} + \begin{bmatrix} \tau_m & 0 & 0 \\ 0 & \tau_m & 0 \\ 0 & 0 & \tau_m \end{bmatrix}$$

$$\text{or } \tau_{ij} = s_{ij} + \delta_{ij}\tau_m$$

$$\text{where } \tau_m = \frac{1}{3} \tau_{kk}$$

(3.1.1)

This decomposition is of great use when modelling material behaviour. It is often found that inelastic behaviour is related to the deviator as in the viscoelastic behaviour of plastics.

There will also be, in general, nine components of strain at a point. It should be noted that whilst  $\epsilon_{ij}$  ( $i=j$ ) is a ratio of a change of length to the original length,  $\epsilon_{ij}$  ( $i \neq j$ ) is the change of a right angle, and the usual engineering shear strain  $\gamma_{ij} = 2\epsilon_{ij}$  being the sum of two equal angles  $\epsilon_{ij}$  and  $\epsilon_{ji}$ .

The strain tensor will also have principal values in 3 perpendicular directions.



Of particular importance later, is the fact that the strain tensor may be decomposed into deviatoric and spherical components.

$$\epsilon_{ij} = e_{ij} + \delta_{ij}\epsilon_m \quad (3.1.2)$$

where  $\epsilon_m = \frac{1}{3}\epsilon_{kk}$

In a continuum, stresses and strains will usually vary from point to point, but their variations are not arbitrary as various conditions have to be satisfied.

These are:-

(a) Equilibrium of stresses

There are two conditions here

(i)  $\bar{T}_i = \tau_{ji}n_j$  on the surface where  $\bar{T}_i$  is the component of the surface traction. (3.1.3)

(ii)  $\tau_{ji,j} + F_i = 0$  within the continuum where  $F_i$  is a body force.

It may also be shown that  $\tau_{ij} = \tau_{ji}$  (i.e. the stress tensor is symmetric), so that there will be in general 6 unknown stress components at any point and only 3 equations from (i) or (ii) above, so that the problem is statically indeterminate.

(b) Compatibility of strains

If  $u_i$  ( $i = 1,2,3$ ) are the components of a small displacement then the strains are:-

$$\epsilon_{ij} = \frac{1}{2}(u_{i,j} + u_{j,i}) \quad (3.1.4)$$

Also the strain may be found from:-

$\delta A_i = \epsilon_{ij}A_j + \omega_{ij}A_j$  where the  $A_j$  are the components of a radius vector, and the  $\delta A_i$  are the components of the change of the vector.



Here the second term denotes rigid body motion, so the remaining term gives  $\epsilon_{ij} = \frac{\delta A_i}{A_j}$  which is a pure strain effect. It follows that  $\epsilon_{ij} = \epsilon_{ji}$ , so that there will be six strain components to be determined from only three displacements. The strains may not therefore be chosen arbitrarily, but must satisfy the conditions of compatibility. These conditions ensure that adjacent parts of the continuum continue to fit together after straining, and result in six equations connecting the different strains which always apply providing the strains are small

$$\text{e.g. } \frac{\partial^2 \epsilon_x}{\partial y^2} + \frac{\partial^2 \epsilon_y}{\partial x^2} = \frac{\partial^2 \gamma_{xy}}{\partial x \partial y} \quad \text{is one of the six equations [1]}$$

### (c) Stress-strain relationship

Although the six strains may be expressed in terms of only three displacements, these cannot be determined without equations connecting stress and strain.

### 3.2 Linear elasticity

The well-known relationships between normal and shear stresses and strains may be used here. The general form of Hooke's law is

$$\epsilon_{ij} = \frac{1+\nu}{E} \tau_{ij} - \frac{\nu}{E} \tau_{kk} \delta_{ij} \quad (3.2.1)$$

but by using the deviatoric and spherical components of stress and strain an alternate form is:-

$$\begin{aligned} s_{ij} &= \frac{e_{ij}}{2G} \\ \epsilon_m &= \frac{\tau_m}{3K} \end{aligned} \quad (3.2.2)$$



By using either 3.2.1 or 3.2.2 together with 3.1.3 and 3.1.4 the stresses and displacements may be found.

### 3.3 Stress functions

In the general case of a 3-dimensional problem the 9 stress and 9 strain components will vary from point to point within the material, and these stresses and strains must satisfy equilibrium conditions (3 equations) compatibility conditions (6 equations) and the specified stress-strain relationship (9 equations) at each point. In addition, specified stress and/or displacement conditions must be satisfied on the boundary. The general solution will therefore involve the solution of a very large number of simultaneous partial differential equations, and an exact solution is virtually impossible.

Even in a two-dimensional system with only 3 stress and strain components at each point there are still too many equations for ease of solution. If, however, the stresses are embodied in a single stress function in such a way that equilibrium and compatibility conditions are automatically satisfied, then by carrying out prescribed operations on the stress function the 3 stresses of a 2-dimensional system are easily found, and by introducing the stress-strain relationship the corresponding strains may be found from only 3 equations.

It may be shown [1] that for a 2-dimensional system, the stress function  $\phi$  must satisfy the condition  $\nabla^2 \phi = \sigma_x + \sigma_y$  and since also  $\nabla^2(\sigma_x + \sigma_y) = 0$  for compatibility it follows that  $\nabla^4 \phi = 0$ . A stress



function for a particular set of conditions must satisfy this condition and also give the correct stresses at the boundaries.

For plane stress problems using Cartesian coordinates the 3 stresses are found from the stress function  $\phi$

$$\begin{aligned}\sigma_x &= \frac{\partial^2 \phi}{\partial y^2} \\ \sigma_y &= \frac{\partial^2 \phi}{\partial x^2} \\ \tau_{xy} &= -\frac{\partial^2 \phi}{\partial x \partial y}\end{aligned}\tag{3.3.1}$$

Similarly, using polar coordinates

$$\begin{aligned}\sigma_r &= \frac{1}{r} \frac{\partial \phi}{\partial r} + \frac{1}{r^2} \frac{\partial^2 \phi}{\partial \theta^2} \\ \sigma_\theta &= \frac{\partial^2 \phi}{\partial r^2} \\ \tau_{r\theta} &= -\frac{\partial}{\partial r} \left( \frac{1}{r} \frac{\partial \phi}{\partial \theta} \right)\end{aligned}\tag{3.3.2}$$

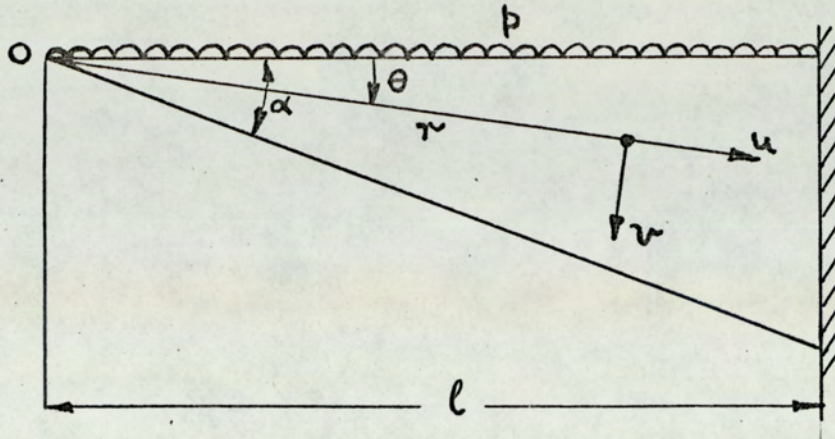
Also in polar coordinates the strains are found from the radial and tangential displacements  $u$  and  $v$  respectively by:-

$$\begin{aligned}\epsilon_\theta &= \frac{1}{r} \frac{\partial v}{\partial \theta} + \frac{u}{r} \\ \epsilon_r &= \frac{\partial u}{\partial r} \\ \gamma_{r\theta} &= \frac{1}{r} \frac{\partial u}{\partial \theta} + \frac{\partial v}{\partial r} - \frac{v}{r}\end{aligned}\tag{3.3.3}$$

An example illustrating the use of a stress function is shown on the next page. This particular example was chosen as it was later to be used for checking the finite element solution in 6.8.



Example



It was required to find the end deflection of a uniform wedge of unit width clamped at one end and carrying a uniformly distributed load along its top edge. For small angles of taper conventional beam theory can be expected to give reasonable results, but for larger angles the effect of shear stress will become more important and must be allowed for. The use of a stress function will of course automatically include the effect of shear stress.

Using polar coordinates, Timoshenko and Goodier<sup>[1]</sup> suggest the stress function.

$$\phi = C[r^2(\alpha - \theta) + r^2 \sin \theta \cos \theta - r^2 \cos^2 \theta \tan \alpha] \quad (3.3.4)$$

where  $C = p/[2(\tan \alpha - \alpha)]$

The three stresses are then found by using equations (3.3.2) and are given by

$$\begin{aligned} \sigma_r &= C[2(\alpha - \theta) - \sin 2\theta + \cos 2\theta \tan \alpha - \tan \alpha] \\ \sigma_\theta &= C[2(\alpha - \theta) + \sin 2\theta - 2\cos^2 \theta \tan \alpha] \\ \tau_{r\theta} &= -C[-1 + \cos 2\theta + \sin 2\theta \tan \alpha] \end{aligned} \quad (3.3.5)$$







The expressions found were:-

$$L = - \frac{C}{E} [(1+\nu) + 4\ln(\ell \sec\alpha) + 2(1-\nu) \frac{\alpha}{\tan\alpha}]$$

$$M = \frac{2C\ell}{E} [(1+\nu) + (1-\nu) \frac{\alpha}{\tan\alpha} + 2\ln(\sec\alpha)]$$

$$N = \frac{-2C\ell}{E} [(1+\nu)\alpha - \nu \tan\alpha]$$

The end deflection of the wedge was then found by substituting the values  $\theta = 0$  and  $r = 0$  in the above expression for  $v$  i.e.

$$(v)_{\theta=r=0} = \frac{p\ell}{E(\tan\alpha - \alpha)} [(1+\nu) + (1-\nu) \frac{\alpha}{\tan\alpha} + 2\ln(\sec\alpha)] \quad (3.3.6)$$

---

It was also found that by imposing the vertical constraint at the bottom face instead of the top face of the wedge only the last term of equation 3.3.6 was affected and this now became  $\tan^2\alpha$ . For angles up to about  $30^\circ$  there is little difference between the values of  $2\ln(\sec\alpha)$  and  $\tan^2\alpha$ , but for larger angles the difference is measurable, but the effect on the deflection is small.

### 3.4 Linear Viscoelasticity

Unlike linear elastic materials for which the stress-strain, load-deflection etc. relations are not time-dependent, a viscoelastic material can only have its behaviour fully described by including time as an independent variable [2] [3] [4].

Considering first the uniaxial stress-strain relation, a convenient form suggested by a spring-damper model is

$$p = Q_s$$



$$P\sigma = Q\epsilon$$

where  $P$  and  $Q$  are differential operators

$$P = \sum_0^m p_k \frac{d^k}{dt^k}, \quad Q = \sum_0^n q_k \frac{d^k}{dt^k} \quad (3.4.1)$$

By choosing suitable values for  $m$ ,  $n$ ,  $p_k$  and  $q_k$ , various mechanical models consisting of springs and dampers may be represented by this equation.

For example, a system comprising a spring and damper in ~~parallel~~ <sup>series</sup> gives a Maxwell body having the equation

$$\sigma + p_1 \dot{\sigma} = q_1 \dot{\epsilon} \quad (3.4.2)$$

The addition of a series spring to the ~~Maxwell~~ <sup>Kelvin</sup> combination produces the 3-parameter solid (Standard Linear Solid)

$$\sigma + p_1 \dot{\sigma} = q_0 \epsilon + q_1 \dot{\epsilon} \quad (3.4.3)$$

The coefficients  $p_k$  and  $q_k$  will be functions of the elastic and viscous properties for the material under consideration.

The viscoelastic stress-strain equation for a particular material is thus found as follows:-

- (a) A suitable model is chosen to describe the type of behaviour for a certain stress or strain pattern (e.g. In a simple creep test the stress is constant while strain varies with time).
- (b) Values of  $p_k$  and  $q_k$  are then found to give the best agreement with experimental results.



These values of  $p_k$  and  $q_k$  may then be used when the same material is stressed in a different way (e.g. in a beam where the stress varies with depth). The differential equation for the particular problem must be formulated in terms of  $p_k$  and  $q_k$ , and its solution will give the information required - perhaps the relation between deflection and time.

### Correspondence rule

It can be seen that when the differential equation for any viscoelastic problem is subjected to a Laplace transformation with respect to time, the coefficients are a combination of elastic and viscous constants and the transform parameter  $s$ . It may also be shown that the equation giving the solution of the viscoelastic problem is of exactly the same form as that for the corresponding elastic problem, but with elastic constants replaced by equivalent combinations of viscoelastic constants and  $s$ .

For example, consider the case of a body subjected to a shear stress  $\tau$ .

$$\text{Then for an elastic material } \epsilon = \frac{1}{2G} \tau$$

$$\text{and the Laplace transform is } \bar{\epsilon} = \frac{1}{2G} \bar{\tau}$$

Now for a Maxwell body equation 3.4.2 may be written as

$$\left(\frac{1}{2\eta} + \frac{1}{2G} \frac{\partial}{\partial t}\right)\tau = \frac{\partial \epsilon}{\partial t} \quad [4]$$

where  $\eta$  is the viscosity of the material.



The Laplace transform of this is  $(\frac{1}{2\eta} + \frac{s}{2G})\bar{\tau} = s\bar{\epsilon}$

and  $\bar{\epsilon} = \frac{s + G/\eta}{2Gs} \bar{\tau}$  or  $\mathcal{P}\bar{\tau} = \mathcal{Q}\bar{\epsilon}$  where in this case

$$\mathcal{P} = \frac{s + G/\eta}{2Gs} \quad \text{and} \quad \mathcal{Q} = 1$$

This is of exactly the same form as the expression for an elastic material with G replaced by  $\frac{Gs}{s + \frac{G}{\eta}}$ .

The stress-strain relation may therefore be expressed as

$$\frac{\bar{\tau}}{\bar{\epsilon}} = \frac{\mathcal{Q}}{\mathcal{P}} = 2G(s) \quad \text{where in this case} \quad G(s) = \frac{Gs}{s + \frac{G}{\eta}}$$

If the solution of an elastic problem is known the solution of the corresponding viscoelastic problem is then found by using the correspondence rule as follows:-

- (i) Take the Laplace transform of the elastic solution
- (ii) Replace the elastic constants by the appropriate equivalents as noted above (These equivalents will depend on the particular model of material behaviour chosen, but will always be the same for that model).
- (iii) Invert the modified transformed equation.

A good example of the use of the correspondence rule is given in obtaining equation 3.4.7 below for a creep test.

In order to relate  $p_k$  and  $q_k$  to the elastic and viscous constants, fundamental assumptions must be made about the behaviour



of the material. Since viscous effects seem to be mainly associated with a shearing action, it is convenient to decompose the original stress system into spherical and deviatoric components as noted in 3.1.1. The corresponding spherical strain (dilatation) and deviatoric strain (distortion) are given by 3.1.2.

Two sets of equations are therefore obtained and these are most easily expressed as Laplace transforms.

$$\begin{aligned} \text{Distortion } \mathcal{P}' \bar{s}_{ij} &= \mathcal{Q}' \bar{e}_{ij} \\ \text{Dilatation } \mathcal{P}'' \bar{\sigma}_{ii} &= \mathcal{Q}'' \bar{e}_{ii} \end{aligned} \tag{3.4.4}$$

A relatively simple, but usually quite adequate form of the second set of these equations is obtained by assuming elastic dilatation. In this case  $\mathcal{P}'' = 1$  and  $\mathcal{Q}'' = 3K$ . [3]

This assumption was therefore made for all subsequent work, with the exception of 4.3(a).

Since both uniaxial and two-dimensional systems were to be studied, the following results were required:-

Assuming Maxwell distortion the usual form of the equation

$$\dot{e}_{ij} = \frac{1}{2G} \dot{s}_{ij} + \frac{1}{2\eta} s_{ij}$$

where  $\eta$  is the viscosity of the material may be re-written as

$$\left(1 + \frac{1}{\gamma} \frac{\partial}{\partial t}\right) s_{ij} = 2\eta \frac{\partial}{\partial t} e_{ij}$$

so that  $\mathcal{P}' = 1 + \frac{S}{\gamma}$  and  $\mathcal{Q}' = 2\eta S$  where  $\gamma = \frac{G}{\eta}$ .



It may also be shown [3] that

$$E \rightarrow \frac{3\alpha'\alpha''}{2\beta'\alpha'' + 2\beta''} = \frac{9KGs}{(3K+G)s + 3K\gamma} \quad (3.4.5)$$

and  $\frac{\nu}{E} \rightarrow \frac{\beta'\alpha'' - 2\beta''}{3\alpha'\alpha''} = \frac{3K-2G}{18KG} \frac{s + \frac{3K}{3K-2G}\gamma}{s}$

Assuming 3-parameter distortion

$$\dot{e}_{ij} + \zeta e_{ij} = \frac{1}{2G} \dot{s}_{ij} + \frac{1}{2\eta} s_{ij}$$

or  $s_{ij} + \frac{1}{\gamma} \dot{s}_{ij} = 2\eta\zeta e_{ij} + 2\eta \dot{e}_{ij}$

and by comparison  $\mathcal{P}' = 1 + \frac{s}{\gamma}$ ,  $\mathcal{Q}' = 2\eta(\zeta + s)$

$$E \rightarrow \frac{9KG(\zeta + s)}{(3K+G)s + 3K\gamma + G\zeta} \quad (3.4.6)$$

and  $\frac{\nu}{E} \rightarrow \frac{3K-2G}{18KG} \left[ 1 + \frac{3K\gamma - 3K\zeta}{3K-2G} \frac{1}{\zeta + s} \right]$

Uni-axial constant stress (Creep condition)

The solution of the elastic problem is

$$\epsilon = \frac{\sigma}{E}$$

Maxwell distortion

Taking the Laplace transform of the above and replacing E by the appropriate combination gives



$$\begin{aligned}\bar{\epsilon} &= \frac{(3K+G)s+3K\gamma}{9KGs} \bar{\sigma} \\ &= \frac{3K+G}{9KG} \frac{s + \frac{3K\gamma}{3K+G}}{s} \bar{\sigma}\end{aligned}$$

and since  $\sigma$  is constant

$$\epsilon = \frac{3K+G}{9KG} \left(1 + \frac{3K\gamma}{3K+G} t\right) \sigma$$

which simplifies to 
$$\epsilon = \left(\frac{1}{E} + \frac{t}{3\eta}\right) \sigma \quad (3.4.7)$$

### 3-parameter distortion

The result is obtained by replacing E by the combination appropriate to a 3-parameter solid

$$\bar{\epsilon} = \frac{(3K+G)s+3K\gamma+G\zeta}{9KG(\zeta+s)} \bar{\sigma}$$

and hence 
$$\epsilon = \left\{ \frac{1}{E} + \frac{1}{3G} \left(\frac{\gamma}{\zeta} - 1\right) (1 - e^{-\zeta t}) \right\} \sigma$$
 when  $\sigma$  is a constant

or 
$$\epsilon = \left\{ \frac{1}{E} + C(1 - e^{-\zeta t}) \right\} \sigma \quad (3.4.8)$$

where 
$$C = \frac{1}{3G} \left(\frac{\gamma}{\zeta} - 1\right)$$

### Two-dimensional stress system (stresses constant)

The results are obtained in the same way as for a single stress except that both E and  $\frac{\nu}{E}$  must be replaced by their appropriate equivalents, and the net strain in a given direction is now the sum



of the strains in this direction due to the two stresses providing strains are small. This linear superposition may be used since linear viscoelasticity is being considered.

Consider now a system of two perpendicular stresses  $\sigma_x$  and  $\sigma_y$  for two types of material.

Maxwell distortion

$$\text{Due to } \sigma_x, \quad \underline{\epsilon_x = \left(\frac{1}{E} + \frac{t}{3\eta}\right)\sigma_x} \quad \text{if } \sigma_x \text{ is constant}$$

$$\text{Due to } \sigma_y \text{ for an elastic material } \quad \epsilon_x = \frac{\nu}{E} \sigma_y$$

The Laplace transform of the viscoelastic solution is then obtained using the correspondence rule

$$\bar{\epsilon}_x = \frac{s + \frac{3K}{3K-2G} \gamma}{s} \bar{\sigma}_y$$

and since  $\sigma_y$  is constant

$$\underline{\epsilon_x = -\left\{\left(\frac{1}{2G} - \frac{1}{E}\right) + \frac{t}{6\eta}\right\} \sigma_y}$$

Hence the net strain in this direction is

$$\underline{\epsilon_x = \left(\frac{1}{E} + \frac{t}{3\eta}\right)\sigma_x - \left\{\left(\frac{1}{2G} - \frac{1}{E}\right) + \frac{t}{6\eta}\right\}\sigma_y} \quad (3.4.9)$$

The corresponding expression for  $\epsilon_y$  is obtained by interchanging  $\sigma_x$  and  $\sigma_y$ .



3-parameter distortion

Again  $E$  and  $\frac{\nu}{E}$  are replaced by their appropriate equivalents and the strains due to the two stresses are added.

$$\dot{\epsilon}_x = \frac{(3K+G)s+3K\gamma+G\zeta}{9KG(\zeta+s)} \bar{\sigma}_x + \frac{3K-2G}{18KG} \left\{ 1 + \frac{3K\gamma-3K\zeta}{3K-2G} \frac{1}{\zeta+s} \right\} \bar{\sigma}_y$$

and since  $\sigma_x$  and  $\sigma_y$  are constants

(3.4.10)

$$\epsilon_x = \left\{ \frac{1}{E} + \frac{1}{3G} \left( \frac{\gamma}{\zeta} - 1 \right) (1 - e^{-\zeta t}) \right\} \sigma_x - \left\{ \left( \frac{1}{2G} - \frac{1}{E} \right) + \frac{1}{6G} \left( \frac{\gamma}{\zeta} - 1 \right) (1 - e^{-\zeta t}) \right\} \sigma_y$$


---

Again  $\epsilon_y$  may be found by interchanging  $\sigma_x$  and  $\sigma_y$

It will be seen that providing the stresses remain constant exact values of the strains may be found by using time-dependent values of  $E$  and  $\frac{\nu}{E}$  which are respectively the reciprocals of the coefficient of  $\sigma_x$  and the coefficient of  $\sigma_y$  above. It should be noted that  $E$  and  $G$  are initial or elastic values and since  $K$  has been assumed constant, the usual relations between the elastic constants may be used. Denoting a time-dependent "constant" by  $-(t)$  and using the expressions for  $E(t)$  and  $\frac{\nu}{E}(t) = \frac{\nu(t)}{E(t)}$  it may also be confirmed that these time-dependent values are subject to the same connections.

Then for the 3-parameter solid

$$\underline{E(t) = 1/\left\{ \frac{1}{E} + C(1-e^{-\zeta t}) \right\}} \quad (3.4.11)$$



If the initial value of Poisson's ratio is known the value of K may be calculated and so the value of  $\nu(t)$  may be found from the time dependent form of  $E = 3K(1-2\nu)$  giving

$$\underline{\nu(t) = \frac{1}{2} \left(1 - \frac{E(t)}{3K}\right)} \quad (3.4.12)$$

The expression for  $E(t)$  in 3.4.11 is in fact the reciprocal of the creep compliance defined as  $\frac{\text{Strain(varying)}}{\text{Stress(constant)}}$ .

It should be noted that  $E(t)$  is not the relaxation modulus which is  $\frac{\text{Stress(varying)}}{\text{Strain(constant)}}$  which will differ from the reciprocal of the creep compliance owing to the differing behaviour of the material when stress and strain are varied separately.

Using the parameters of 4.1 for Perspex these two quantities were compared in Table 3.1. It was found that:-

$$\frac{1}{\text{Creep compliance}} = \frac{E}{1 + EC(1 - e^{-\zeta t})} \quad (3.4.13)$$

$$\text{Relaxation modulus} = E[1 - EC(1 - e^{-(EC+1)\zeta t})]$$



Values for Perspex

Time hours	$\frac{1}{E \times \text{Creep compliance}} = A$	$\frac{\text{Relaxation modulus}}{E} = B$	$\frac{B-A}{A} \times 100$
0	1	1	0
1	0.9266	0.9108	-1.7
2	0.8900	0.8658	-2.7
3	0.8708	0.8431	-3.2
4	0.8604	0.8317	-3.4
5	0.8546	0.8259	-3.4
6	0.8515	0.8230	-3.4
8	0.8487	0.8208	-3.3

TABLE 3.1

It will be seen that the relaxation modulus has a maximum difference of 3.4% from  $E(t)$  at about 5 hours. This error then diminishes to -2.7% as  $t \rightarrow \infty$ .

Similarly using the result of 4.2.1 for a stress which increases uniformly from zero (ramp) it may be shown that in this case

$$\frac{\sigma}{\epsilon} = \frac{E}{(1+EC) - \frac{EC}{\zeta t}(1-e^{-\zeta t})} \quad (3.4.14)$$

This gave a maximum difference of +4.8% from the value of  $E(t)$  for a constant stress. This occurs at about 3 hours, and for longer times the difference diminishes and approaches zero for large values of  $t$ .



## CHAPTER 4

### SOLUTION OF PROBLEMS IN LINEAR VISCOELASTICITY

In Section 3.4 various theoretical viscoelastic models were studied, but no reference was made to any particular material. Before proceeding with any further theoretical investigations it was decided to obtain some experimental results for a particular material and then to choose a suitable theoretical model to fit these results. The material chosen was Perspex, as for moderate stresses its behaviour is approximately linear [6]; it is also readily available and is easily machined. Its mechanical properties are also little affected by small temperature changes and by contact with water or oil.

Since theoretical solutions had already been obtained for a constant uni-axial stress creep test for both Maxwell and 3-parameter distortion models (and elastic dilatation) in 3.4.7 and 3.4.8 and because this was a relatively straightforward test to carry out, a number of creep tests were carried out on Perspex test pieces for a number of different stresses. It was then possible, from the type of results obtained, to choose a suitable theoretical model and to find the values of the parameters necessary to fit the experimental results to the behaviour of this model. Because of the practical impossibility of applying the stress instantaneously the effect of applying the stress as a ramp was investigated theoretically. It was found that no correction was needed to allow for the manner in which the stress was applied in the tests.



Theoretical solutions were then obtained for two more difficult problems, initially using simple viscoelastic models because of the increased difficulty of the problems, but finally solutions were found using the theoretical model which was found to fit the results for Perspex. These results could then have been applied to Perspex. The second of these problems, the viscoelastic cylinder of 4.4, was capable of experimental investigation, and a more general theoretical solution obtained by using a finite element method was compared with experimental results in 7.2.

#### 4.1 Creep tests on Perspex

A number of creep tests were carried out on specimens cut from a Perspex sheet of 1/4 in nominal thickness, the actual cross-sectional dimensions of the specimens being 12.6 mm x 6.0 mm. A Denison creep testing machine was used to apply a constant axial pull, and the extension was measured with a Philips Type PR 9312 extensometer using a gauge length of 50 mm.

Fig. 4.1 shows how the strain varies with time for different values of the constant stress, and it is obvious that the strain-time relation is far from linear for the period considered, and accordingly the assumption of Maxwell distortion will fit the experimental data very imperfectly. The shape of the curves does, however, suggest that 3-parameter distortion may give a much better fit. Since a linear stress-strain relation was to be assumed the values of the 3 parameters must be independent of stress, and it was found that a reasonable representation of the experimental results



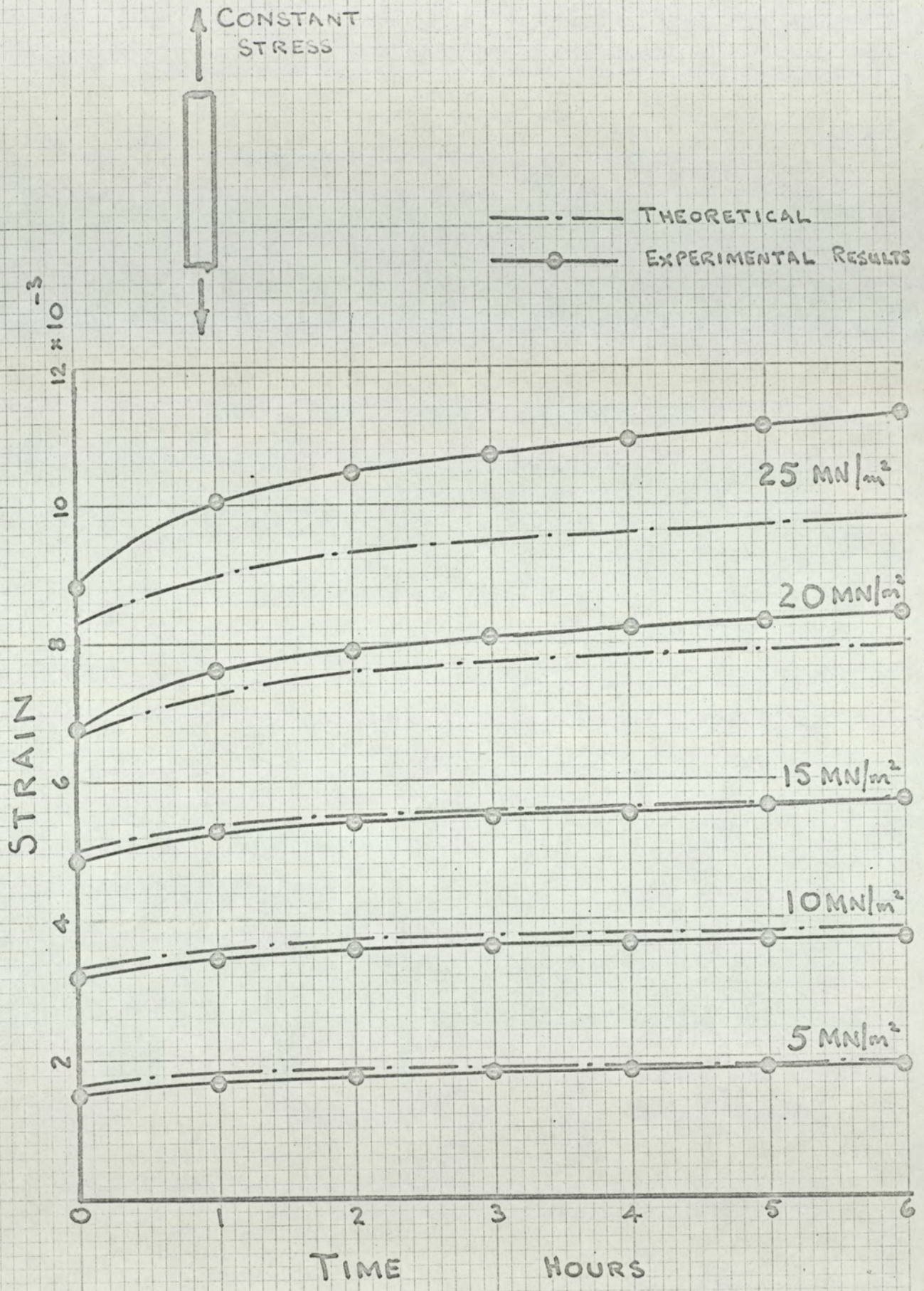


FIG.4.1



could be obtained with :-

$$E = 3000 \text{ MN/m}^2$$

$$C = \frac{1}{3G} \left( \frac{\gamma}{\zeta} - 1 \right) = 0.06 \times 10^{-3} \text{ m}^2/\text{MN}$$

$$\zeta = 0.58 \text{ h}^{-1}$$

$$\text{or } \underline{\epsilon = \left\{ \frac{1}{3000} + 0.06 \times 10^{-3} (1 - e^{-0.58t}) \right\} \sigma} \quad (4.1.1)$$

where  $t$  is the time in hours and  $\sigma$  is the stress in  $\text{MN/m}^2$ .

It will be seen that the assumption of linearity gives quite good results for stresses up to about  $20 \text{ MN/m}^2$ , but at higher stresses (the results for  $25 \text{ MN/m}^2$  only are shown) this assumption is hardly justifiable.

These results were used below in 7.1 and 7.2.

#### 4.2 The effect of loading rate in a creep test

In the creep tests of 4.1 it was not possible to apply the stress as a true step function as several seconds were required to increase the stress from zero to its final value. In order to determine if this finite loading time had any effect on the strains, a theoretical solution was obtained for a uniformly increasing stress giving the ramp function shown in Fig. 4A.



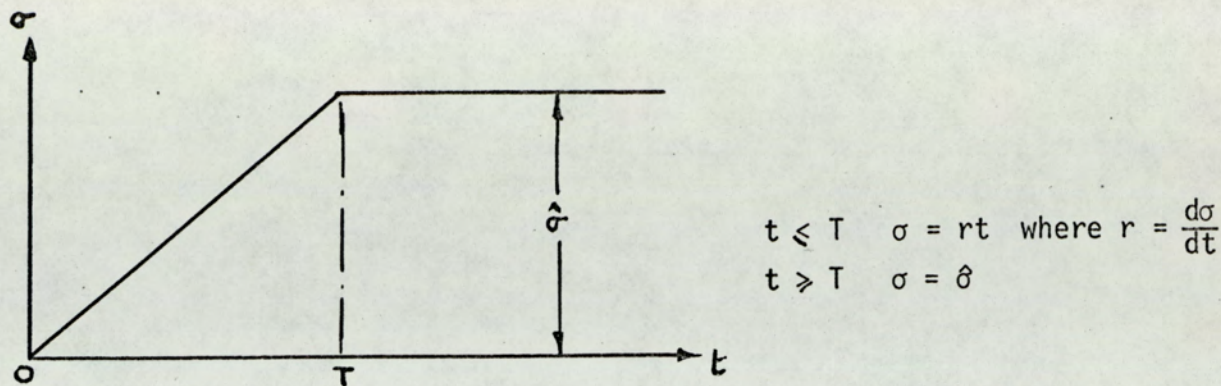


Fig. 4A

$t \leq T$

The solution of the elastic problem is  $\epsilon = \frac{\sigma}{E} = \frac{rt}{E}$

$\therefore \bar{\epsilon} = \frac{r}{E} \frac{1}{s^2}$  since  $r$  and  $E$  are constants.

For the viscoelastic problem considering 3-parameter distortion

$$\bar{\epsilon} = \frac{(3K+G)s+3K\gamma+G\zeta}{9KG(\zeta+s)} \frac{r}{s^2}$$

Hence  $\epsilon = \left(\frac{1}{E} + C\right)rt - C \frac{r}{\zeta}(1 - e^{-\zeta t})$  (4.2.1)

$t \geq T$

Now, a ramp may be obtained by superimposing on the original stress  $rt$  a negative stress of  $-r(t-T)$  when  $t \geq T$ .

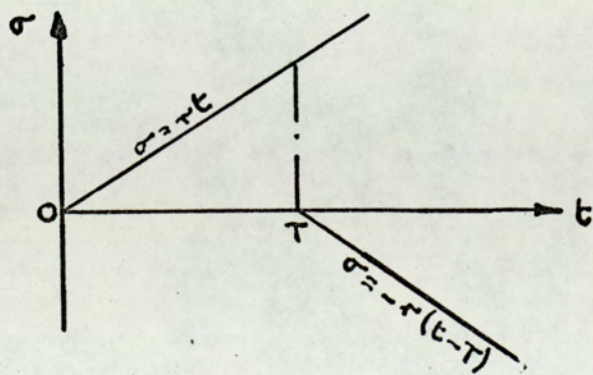


Fig. 4B.



Then for values of  $t \geq T$  the strain due to a stress applied as a ramp is the sum of the strains due to stresses  $rt$  and  $-r(t-T)$

$$\text{i.e. } \epsilon = \left(\frac{1}{E} + C\right)rt - C \frac{r}{\zeta}(1 - e^{-\zeta t}) + \left(\frac{1}{E} + C\right)\{-r(t-T)\} - C \frac{(-r)}{\zeta}(1 - e^{-\zeta(t-T)})$$

and since  $\delta = rT$

$$\epsilon = \left[\frac{1}{E} + C \left\{1 - \frac{1}{\zeta T} e^{-\zeta t} (e^{\zeta T} - 1)\right\}\right] \delta \quad (4.2.2)$$

For a step function as shown in 3.4.8.  $\epsilon = \left[\frac{1}{E} + C(1 - e^{-\zeta t})\right] \delta$

The strains will therefore vary in the manner shown in Fig. 4C.

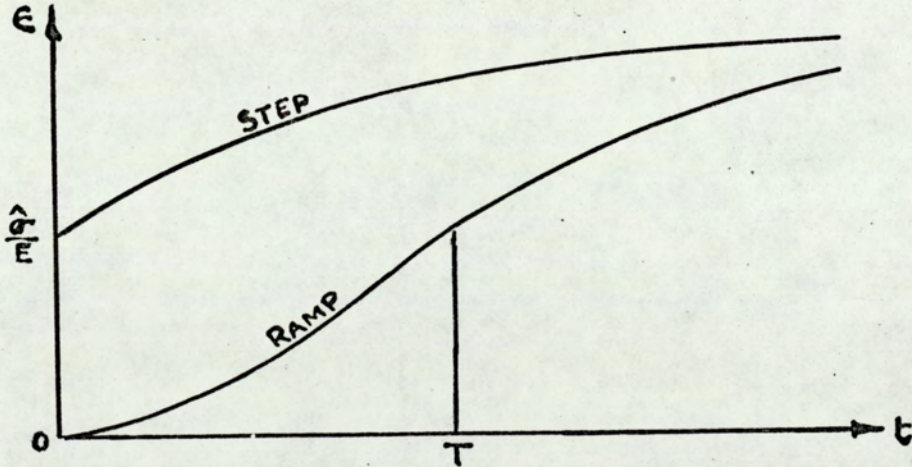


Fig. 4C

If the step stress is applied at  $t = 0$ , and the ramp stress begins to be applied at  $t = 0$ , there will obviously be considerable differences between the resulting strains for  $t < T$ . However when  $t \geq T$  the results may not differ so much.

$$\text{Thus } \Delta\epsilon = \epsilon_{\text{step}} - \epsilon_{\text{ramp}} = Ce^{-\zeta t} \left[ \frac{1}{\zeta T} (e^{\zeta T} - 1) - 1 \right] \delta \quad (4.2.3)$$



It is fairly obvious that  $\Delta\epsilon = 0$  when  $T = 0$  (i.e. the ramp then becomes a step) and when  $T = \infty$ . Inspection of the expression for  $\Delta\epsilon$  will also show that its value decreases as  $t$  increases, for a given value of  $T$ . The maximum value of  $\Delta\epsilon$  will therefore occur at the least value of  $t$  i.e. when  $t = T$ .

$$\text{Then } \underline{\Delta\epsilon_{\max} = C \left[ \frac{1}{\zeta T} - \left( \frac{1}{\zeta T} + 1 \right) e^{-\zeta t} \right] \delta} \quad (4.2.4)$$

It is found that the maximum value of  $\Delta\epsilon_{\max}$  is approximately  $0.3C\delta$  at  $\zeta T \approx 2$ .

This result was confirmed by calculating values of  $\Delta\epsilon_{\max}$  for various values of  $T$  using the parameters previously found for Perspex. These results are shown in Table 4.2.

$$\text{Perspex } E = 3 \times 10^3 \text{ MN/m}^2 \quad C = 0.06 \times 10^{-3} \text{ m}^2/\text{MN} \quad \zeta = 0.58 \text{ h}^{-1}$$

$$\epsilon_0 = \frac{\delta}{E}$$

$\zeta T$	$T_{\text{approx}}$	$\Delta\epsilon/\epsilon_0$
0.01	1 min	0.1%
0.05	5 min	0.4%
0.1	10 min	0.85%
0.5	1 h.	3.2%
1	2 h.	4.7%
1.5	2.5 h.	5.3%
2	3.5 h.	5.34%
5	8.5 h.	3.5%

Table 4.2



It will be seen that in this case, loading times of up to 10 min will give a maximum error of less than 1% in the strain, and the few seconds actually required to apply the maximum stress will have a negligible effect on the strain. It should be noted that this maximum error will in any case occur only at the end of the loading period, and will thereafter diminish.

#### 4.3 Viscoelastic beam on a flexible base

Since it was intended that later the effect of local bending stresses in a viscoelastic cylinder were to be studied, the simplest possible form of this problem was required. It is shown below that the cylinder problem may be solved by analogy with a beam on a flexible base. Timoshenko gives a solution of this problem for an elastic beam on an elastic base. [5].

Various types of beam and base were considered in the present report.

##### (a) Elastic base: Maxwell distortion and no dilatation for beam

Since there is no dilatation (i.e.  $K = \infty$ ) only deviatoric stresses and strains need be considered.

For a single stress  $\sigma$  and a single strain  $\epsilon$  equations 3.1.1 and 3.1.2 reduce to

$$s_{11} = \frac{2}{3} \sigma$$

$$e_{11} = \frac{2}{3}(1+\nu)\epsilon$$

(4.3.1)



In this first case the correspondence rule was not used, to demonstrate that although it is helpful in obtaining a solution, its use is not essential. Accordingly the stress-strain relationship for a Maxwell body is used i.e.

$$\left( \frac{1}{2G} \frac{\partial}{\partial t} + \frac{1}{2\eta} \right) s_{11} = \frac{\partial}{\partial t} \epsilon_{11} \quad [4]$$

When the expressions 4.3.1 are used, and noting that for bending  $\sigma = \frac{My}{I}$  and  $\epsilon = y \frac{\partial^2 w}{\partial x^2}$  we find that

$$\left( \frac{\partial}{\partial t} + \gamma \right) \frac{My}{I} = E \frac{\partial}{\partial t} \left( y \frac{\partial^2 w}{\partial x^2} \right)$$

Differentiating twice with respect to  $x$  and noting that  $\frac{\partial^2 M}{\partial x^2} = p$  and that for an elastic base  $p = -kw$

$$\frac{\partial}{\partial t} \left( \frac{EI}{k} \frac{\partial^4 w}{\partial x^4} + w \right) = -\gamma w$$

This partial differential equation is conveniently solved by using Laplace transforms, and using the condition of initial equilibrium

$$\frac{d^4 \bar{w}}{dx^4} = - \frac{k}{EI} \frac{s+\gamma}{s} \bar{w} \quad (4.3.2)$$

This is of exactly the same form as the equation for an elastic beam, except that  $E$  is replaced by  $\frac{Es}{s+\gamma}$ .

By using the correspondence rule, the solution could therefore have been started at this point.



The solution of this differential equation is

$$\bar{w} = e^{-mx} (\bar{A}\cos mx + \bar{B}\sin mx) + e^{mx} (\bar{C}\cos mx + \bar{D}\sin mx) \quad (4.3.3)$$

$$\text{where } m = \beta(1+\gamma)^{\frac{1}{4}} \quad \text{and } \beta = \left(\frac{k}{4EI}\right)^{\frac{1}{4}}$$

The values of the constants will depend on the end conditions for the beam.

Considering the case of an infinitely long beam with a single point load  $P$  at the origin, these conditions are:-

$$x = 0 \quad \frac{d\bar{w}}{dx} = 0, \quad Q = -\frac{P}{2}$$

$$x = \infty \quad \bar{w} = 0.$$

$$\text{Hence } \bar{w} = \frac{A'}{S} \left(1 + \frac{\gamma}{S}\right)^{\frac{1}{4}} e^{-mx} (\cos mx + \sin mx)$$

$$\text{where } A' = \frac{P}{8EI\beta^3}$$

By expanding  $\left(1 + \frac{\gamma}{S}\right)^{\frac{1}{4}}$ ,  $e^{-mx}$  and  $\cos mx + \sin mx$  as infinite series

$$\begin{aligned} \bar{w} = \frac{A'}{S} & \left[ 1 + \frac{1}{4} \frac{\gamma}{S} - \frac{3}{32} \left(\frac{\gamma}{S}\right)^2 + \dots \right] \left[ 1 - \left\{ 1 + \frac{1}{2} \frac{\gamma}{S} - \frac{1}{8} \left(\frac{\gamma}{S}\right)^2 + \dots \right\} (\beta x)^2 \right. \\ & \left. + \frac{2}{3} \left\{ 1 + \frac{3}{4} \frac{\gamma}{S} - \frac{3}{32} \left(\frac{\gamma}{S}\right)^2 + \dots \right\} (\beta x)^3 \right. \\ & \left. + \dots \dots \dots \right] \end{aligned}$$

By multiplying these series together and inverting the result term by term an expression for  $w$  is finally obtained



$$\begin{aligned}
 w = \frac{P}{8EI\beta^3} & \left[ \left\{ 1 + \frac{1}{4}\gamma t - \frac{3}{16}(\gamma t)^2 + \dots \right\} \right. \\
 & - \left\{ 1 + \frac{3}{4}\gamma t - \frac{3}{64}(\gamma t)^2 + \dots \right\} (\beta x)^2 \\
 & + \left\{ \frac{2}{3} - \frac{1}{12}\gamma t - \frac{1}{8}(\gamma t)^2 + \dots \right\} (\beta x)^3 \\
 & \left. + \dots \dots \dots \right]
 \end{aligned}
 \tag{4.3.4}$$

In practice, the value of  $\gamma t$  will usually be small and so only a few terms are needed in each  $t$  series, but for large values of  $x$  many  $x$  terms must be used to give an accurate answer. Fortunately the area of most interest is near the load where deflection and stress change most rapidly, and values of  $x$  are small here.

(b) Elastic base; Maxwell distortion, elastic dilatation for beam

This model is more likely to fit the actual behaviour of a plastic than the model of (a). Since it was seen that in (a) equation 4.3.2 could have been obtained directly by using the correspondence rule, this method was used here.

It was seen in 3.4 above that for this model the viscoelastic equivalent of  $E$  is  $\frac{9KGs}{(3K+G)s+3KY} = 1/\left(\frac{1}{E} + \frac{1}{3\eta s}\right)$ .

When  $E$  is replaced by this equivalent in the Laplace transform of the differential equation for an elastic beam, the corresponding equation becomes

$$\frac{d^4 \bar{w}}{dx^4} = -\frac{k}{EI} \left( 1 + \frac{E}{3\eta s} \right) \bar{w}
 \tag{4.3.5}$$

This could have been obtained from 4.3.2 by replacing  $\gamma$  by  $\frac{E}{3\eta}$ , and so the solution for this model may be found from 4.3.4 by the same substitution.



(c) Viscoelastic beam and base, Maxwell distortion, elastic dilatation for both

This model differs from that of (b) only in the behaviour of the base. It was seen in (b) that the  $1/E$  of an elastic solution is replaced by  $\frac{1}{E_1} (1 + \frac{E_1}{3\eta_1 s}) = \frac{s}{E_1} (s + \theta_1)$  where the suffix  $_1$  denotes a property of the beam, and  $\theta_1 = \frac{E_1}{3\eta_1}$ .

Similarly, for the base, since  $k \propto E_2$ .

$k$  will be replaced by  $\frac{k}{s(s+\theta_2)}$  where  $\theta_2 = \frac{E_2}{3\eta_2}$  and the suffix  $_2$  applies to the base.

Equation 4.3.5 now becomes

$$\frac{d^4 \bar{w}}{dx^4} = - \frac{k}{E_1 I} \left( \frac{s+\theta_1}{s+\theta_2} \right) \bar{w}$$

or 
$$\frac{d^4 \bar{w}}{dx^4} = - \frac{k}{E_1 I} \left( 1 + \frac{\theta_1 - \theta_2}{s+\theta_2} \right) \bar{w} \quad (4.3.6)$$

This is the same as equation 4.3.5 except that  $\frac{E}{3\eta s}$  is replaced by  $\frac{\theta_1 - \theta_2}{s + \theta_2}$ .

The solution may still be obtained from equation 4.3.3 providing  $m = \beta \left( 1 + \frac{\theta_1 - \theta_2}{s + \theta_2} \right)^{\frac{1}{4}}$ . By expanding this as a series and inverting each term separately, a solution may be obtained as in (a). Only the first few terms were derived giving:-



$$\begin{aligned}
 w = \frac{P}{8EI\beta^3} & \left[ \left\{ \left[ 1 + \left( \frac{1}{4}\theta_1 + \frac{3}{4}\theta_2 \right) t - \left( \frac{3}{64}\theta_1^2 - \frac{3}{32}\theta_1\theta_2 + \frac{3}{64}\theta_2^2 \right) t^2 + \dots \right] \right. \right. \\
 & \left. \left. + \left\{ \left[ 1 + \left( \frac{1}{4}\theta_1 + \frac{3}{4}\theta_2 \right) t + \dots \right] (\beta x)^2 \right. \right. \right. \\
 & \left. \left. + \left\{ \dots \right\} (\beta x)^3 \right. \right. \\
 & \left. \left. + \left\{ \dots \right\} \right. \right. \\
 & \left. \left. \left. \left. \left. \dots \right\} \right\} \right] \quad (4.3.7)
 \end{aligned}$$

There will also be terms of the type  $\frac{t}{\theta_2}(1 - e^{-\theta_2 t})$  which will normally be small.

It will therefore be seen that the general solution requires the evaluation of a large number of terms, which would be a tedious process.

There is however a special case of this solution. When the beam and base are of the same material, as they are for the viscoelastic cylinder of 4.4 where in effect the cylinder is both beam and base,  $\theta_1 = \theta_2$ . Equation 4.3.7 then gives an exact solution

$$w = \frac{P}{8EI\beta^3} e^{-\beta x} (\cos\beta x + \sin\beta x) \left( 1 + \frac{E}{3\eta} t \right)$$

or  $w = \left( 1 + \frac{E}{3\eta} t \right) w_{\text{elastic}} \quad (4.3.8)$

(d) Viscoelastic beam on viscoelastic base of the same material, 3-parameter distortion, elastic dilatation

It has been shown in 4.1 that this model describes the actual behaviour of Perspex quite well. The solution in this case therefore may be used when the results for a viscoelastic cylinder derived in 4.4 below are applied to Perspex.



Since  $\beta \propto \frac{k}{E}$  and here, as in (c)  $k$  and  $E$  vary in exactly the same way, the value of  $\beta$  is constant. The variation in  $w$  therefore depends solely on the variation of  $E$  and may be found from

$$w = \frac{P}{8E(t)I\beta^3} e^{-\beta x} (\cos\beta x + \sin\beta x) \quad (4.3.9)$$

where  $\frac{1}{E(t)} = \frac{1}{E} + C(1 - e^{-\zeta t})$  from 3.4.11.

#### 4.4 Thin viscoelastic cylinder with internal pressure

This problem may be conveniently solved by considering two separate effects. At points remote from any ring loads or couples, the cylinder will be subjected to the usual hoop and longitudinal membrane stresses which will be uniform in the case of a thin cylinder. Any local effects (e.g. a ring load and couple at a rigid end) will cause a longitudinal slice of the cylinder to bend, and so produces bending stresses which vary across the thickness of the shell and must be added to the membrane stresses. This local bending effect is analogous to a beam on an elastic base since the radial movement at any point on a longitudinal slice is opposed by the adjacent parts of the cylinder. Since the same material is involved whether its behaviour as a beam or as a base is under consideration, the local deflections may be derived from 4.3.9 which applies only if the properties of the beam and base are the same.

Consider, first, the membrane stresses

$$\text{Hoop stress } \sigma_y = \frac{pr}{h}$$

$$\text{Longitudinal stress } \sigma_x = \frac{pr}{2h}$$



Then assuming 3-parameter distortion and elastic dilatation equation 3.4.10 gives

$$\text{Hoop strain } \epsilon_y = \frac{pr}{h} \left[ \frac{1}{E} \left( 1 - \frac{\nu}{2} \right) - \frac{3}{4} C (1 - e^{-\zeta t}) \right]$$

and Increase of radius =  $r \epsilon_y$

$$\therefore \Delta r = \frac{pr^2}{h} \left[ \frac{1}{E} \left( 1 - \frac{\nu}{2} \right) - \frac{3}{4} C (1 - e^{-\zeta t}) \right] \quad (4.4.1)$$

It is interesting to note that the longitudinal strain found by interchanging  $\sigma_x$  and  $\sigma_y$  gives

$$\epsilon_x = \frac{pr}{h} \left( \frac{3}{2E} - \frac{1}{2G} \right) \text{ which is constant.}$$

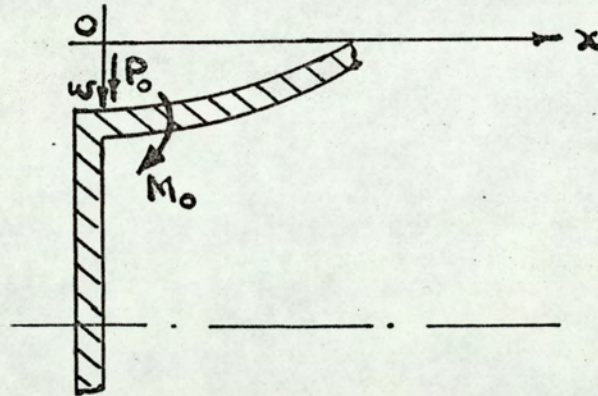


Fig. 4.D.

Assume now that the end of the cylinder is perfectly rigid. The slope and displacement at this end will then be zero.

These end conditions may be imposed by first assuming that the end of the cylinder is allowed to expand freely in a radial direction due to the internal pressure, and that a ring load  $P_0$  and moment  $M_0$  are then applied to return the end of the cylinder to its original position and to make the slope zero. The cylinder



is then equivalent to a beam on a flexible base where the unloaded position of the beam corresponds to the "free" expanded position of the cylinder (i.e. at a considerable distance from the end).

Because any bending of the wall of a cylinder produces two perpendicular stresses the usual flexural rigidity  $EI$  of a beam must be replaced by

$$D = E(t)h^3/[12(1-\{v(t)\}^2)] \text{ per unit width;}$$

$$\text{and } k = E(t)h/r^2 \quad [5]$$

$$\text{Then } \beta = \left[ \frac{3(1 - \{v(t)\}^2)}{r^2 h^2} \right]^{\frac{1}{2}} \quad (4.4.2)$$

It may be shown that the reduction of radius due to  $P_0$  and  $M_0$  is given by

$$w = \frac{1}{2\beta^3 D} e^{-\beta x} [ P_0 \cos\beta x - \beta M_0 (\cos\beta x - \sin\beta x) ] \quad [5]$$

If  $\Delta r$  is the "free" expansion (outwards) as found from 4.4.1, then applying the end conditions  $x = 0$ ,  $w = \Delta r$  (inwards) and  $\frac{\partial w}{\partial x} = 0$  gives  $P_0 = 4\beta^3 D \Delta r$  and  $M_0 = 2\beta^2 D \Delta r$

$$\text{and hence } w = \Delta r e^{-\beta x} (\cos\beta x + \sin\beta x). \quad (4.4.3)$$

Now the variation of  $\Delta r$  with time as given by (4.4.1) presents no problem, but unlike the beam on a flexible base of 4.3(d) where  $\beta$  is constant,  $\beta$  is now a function of  $v(t)$  which will also vary with time. To determine whether this effect is important the parameters found for Perspex in 4.1 were used to calculate the changes in  $E(t)$  and  $v(t)$ . It was found that in a period of 6 hours the value of



$E(t)$  decreases by 20%, and taking an initial value for  $\nu$  of 0.35, the value of  $\nu(t)$  increases by 8% during the same interval. The value of  $\beta$ , which is proportional to  $(1-\{\nu(t)\}^2)^{\frac{1}{4}}$  changes by only -0.5%, and it was thought that with a change of this magnitude a constant value could be assumed for  $\beta$  as this gave a much simpler solution. (It may be noted that the finite element solution of 7.2 below was obtained without making this assumption, and gave almost identical results.)

A further possible difficulty arose because 4.4.1 strictly only applies if stresses are constant, although in 3.4 it is shown that small variations of stress will have little effect on the value of  $E(t)$ . However, to determine whether there is an appreciable stress variation with time in the cylindrical shell, the position and magnitude of the maximum bending moment were investigated. The maximum bending stress is proportional to this moment and is thus easily found.

Now  $M \propto D \frac{\partial^2 w}{\partial x^2}$ , so from 4.4.3

$$M \propto D\beta^2 e^{-\beta x} (\cos\beta x - \sin\beta x)$$

This expression has a maximum value at  $x = \pi/2\beta$ , and since  $\beta \propto (1-\{\nu(t)\}^2)^{\frac{1}{4}}$  the variation in  $x$  for a given change of  $\beta$ , is easily found. As noted above, when the value of  $\nu(t)$  increases by 8%,  $\beta$  changes by -0.5% and therefore  $x$  changes by +0.5%.



Also  $\hat{M}$  may be shown to be proportional to  $D\beta^2$

$$\therefore \hat{M} \propto (1 - \{v(t)\}^2)^{-\frac{1}{2}}$$

and for the +8% change in  $v$  previously calculated the change in  $\hat{M}$ , and therefore in the maximum bending stress is only +1.2%. Since this bending stress is added to a constant longitudinal membrane stress the %change in the net stress must be less than 1.2%, and may be much less if the bending stress is appreciably smaller than the membrane stress.

There will be a further maximum bending moment of opposite sign to that found above at  $x = 0$ . There will this time be no variation in  $x$ , but as before  $\hat{M} \propto D\beta^2$  resulting in the same 1.2% change in stress as before.

A constant value of  $\beta$  is therefore assumed and the increase in radius is the difference between the "free" expansion and the inward deflection given by 4.4.3.

$$\text{i.e. } u = \Delta r [1 - e^{-\beta x}(\cos\beta x + \sin\beta x)] \quad (4.4.4)$$

where the value of  $\Delta r$  is found from 4.4.1 at any time  $t$ .

The local hoop stress due to bending effects may be found separately and added to the membrane stress, but the net hoop stress is easily found from the hoop strain.

Since  $\epsilon_y = \frac{1}{E(t)} (\sigma_y - v(t)\sigma_x)$  and also  $\epsilon_y = \frac{u}{r}$  where  $u$  is given by 4.4.4, the hoop stress is given by  $\sigma_y = E(t)\epsilon_y + v(t)\sigma_x$  where  $\sigma_x$  is the net longitudinal stress.



The expression 4.4.4 is easily evaluated for various values of  $x$  and  $t$ , and so, using values  $p = 1.5 \text{ MN/m}^2$ ,  $r = 75 \text{ mm}$ ,  $h = 6.25 \text{ mm}$  together with the previous values of  $E$ ,  $C$  and  $\zeta$  for Perspex and taking  $\nu$  as 0.35, Prog.1\* was written to find the changes of radius in a Perspex cylinder.

The theoretical results are shown in Fig. 4.4.1 where each column shows the change of radius in mm at a distance of  $X$  mm from the fixed end of the cylinder at  $T$  hours after the application of the pressure. It will be seen that at any time the cylinder takes up the shape of a damped sine wave which dies out at about 150 mm or one diameter from the end. There is also a steady increase in the deflections with increasing time, and it will be found that in a given time interval there is the same fractional increase in deflection for all values of  $X$ . This latter results from the assumption that  $\beta$  is constant, and will be referred to later in 7.2 where a finite element solution is obtained.

---

\* Details of all computer programs are given in the Appendix.



	T = 0	1	2	3	4	5	6
X = 0	0.0000	0.0000	0.0000	0.0000	0.0000	0.0000	0.0000
X = 10	0.0854	0.0906	0.0939	0.0959	0.0972	0.0980	0.0985
X = 20	0.2216	0.2352	0.2437	0.2490	0.2523	0.2544	0.2557
X = 30	0.3212	0.3409	0.3532	0.3609	0.3657	0.3687	0.3706
X = 40	0.3711	0.3939	0.4081	0.4170	0.4226	0.4260	0.4282
X = 50	0.3866	0.4103	0.4251	0.4344	0.4402	0.4438	0.4460
X = 60	0.3854	0.4091	0.4239	0.4331	0.4389	0.4425	0.4448
X = 70	0.3796	0.4029	0.4175	0.4266	0.4323	0.4358	0.4381
X = 80	0.3746	0.3976	0.4120	0.4210	0.4266	0.4301	0.4323
X = 90	0.3718	0.3946	0.4089	0.4178	0.4233	0.4268	0.4290
X = 100	0.3707	0.3934	0.4077	0.4166	0.4221	0.4256	0.4277
X = 110	0.3706	0.3933	0.4075	0.4164	0.4220	0.4254	0.4276
X = 120	0.3708	0.3936	0.4078	0.4167	0.4222	0.4257	0.4279
X = 130	0.3710	0.3938	0.4080	0.4169	0.4225	0.4260	0.4281
X = 140	0.3712	0.3940	0.4082	0.4171	0.4227	0.4261	0.4283
X = 150	0.3713	0.3940	0.4083	0.4172	0.4227	0.4262	0.4284
X = 160	0.3713	0.3941	0.4083	0.4172	0.4228	0.4262	0.4284
X = 170	0.3713	0.3941	0.4083	0.4172	0.4228	0.4262	0.4284
X = 180	0.3713	0.3940	0.4083	0.4172	0.4227	0.4262	0.4284

FIG. 4.4.1



CHAPTER 5

NUMERICAL SOLUTION OF ENGINEERING PROBLEMS

In Section 4, theoretical solutions were obtained for several viscoelastic problems. In the last of these (the viscoelastic cylinder), a solution was obtained by assuming that the parameter  $\beta$  was constant. While it was shown that this assumption was reasonable in the case mentioned, simplifications of this sort may not always be justifiable. For example, if the wall thickness of the cylinder is not constant, then the value of  $\beta$  may vary very considerably. In cases of this type it is not easy to invert the Laplace transform which is introduced by the use of the correspondence rule.

It was therefore decided that for more difficult examples of the type encountered in 4.4, the use of some form of numerical solution would enable a solution to be obtained more directly than by using an exact method. It is shown in Chapters 6 and 7 that numerical solutions of both elastic and viscoelastic problems are readily obtained.

Some of the possible numerical methods are considered below together with typical applications for elastic materials. The further application of a numerical method to linear viscoelastic materials is described in Chapter 7.



### 5.1 Methods of Solution

An exact solution to a problem will normally consist of two main steps:-

- (i) the derivation of the governing partial differential equation (except in very simple cases),
- (ii) the solution of this equation.

The use of a stress function may be helpful in some cases. An example of this approach is shown in 3.3 where the deflection at the end of a loaded wedge is obtained, but even when a suitable stress function is known, the determination of all the constants of integration is usually a lengthy process.

In some of the more standard problems (e.g. the torsion of non-circular bars) the differential equation is the same for any section and the difficulty lies in its solution. In this case some form of numerical solution may be used, and if a digital computer is used to solve the linear equations usually obtained a large number of these equations may be used so that an accurate answer is readily obtained. Two of the possible methods are:-

#### (a) Point matching

Using this method, a series solution of the partial differential equation is obtained. The solution would be exact with an infinite number of terms, but in practice only a finite number of terms can be considered. To find the coefficients in these terms, an equal number of points on the boundary are chosen, and the truncated



series is made to satisfy the boundary conditions exactly at the chosen points. In general the boundary conditions will not be satisfied exactly elsewhere.

An algebraic equation will thus be obtained for each point considered, and the solution of these simultaneous equations will give the required coefficients.

Example. Torsion of a square bar

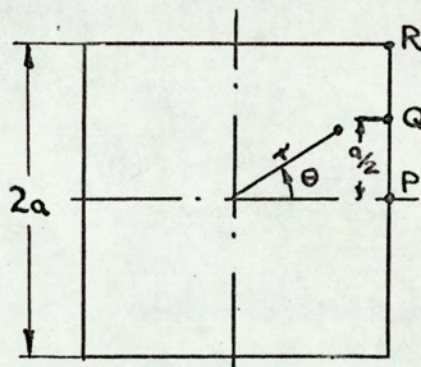


Fig. 5A.

Here  $\nabla^2\phi + 2G\alpha = 0$   
 within the region  
 and  $\phi = 0$  on the boundary  
 [1]

A possible solution of the differential equation is

$$\phi = -\frac{G\alpha r^2}{2} + A + Br^4 \cos 4\theta + Cr^8 \cos 8\theta + \dots$$

By choosing three points such as P, Q and R on the boundary and making  $\phi = 0$  in each case, three simultaneous equations in A, B and C will be obtained, and the solution of these will give the required approximate result.

In this case  $A = 0.58983 G\alpha a^2$

$$B = -0.09237 \frac{G\alpha}{a^2}$$

$$C = 0.00254 \frac{G\alpha}{a^6}$$

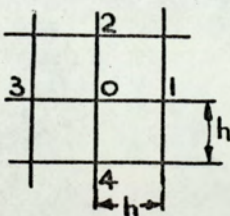


It will be seen that the values of the coefficients are diminishing rapidly, and that a quite accurate result is likely with only a few terms in the series.

Once the values of A, B and C have been found the torsional stiffness is found from  $M_t = 2 \iint \phi r \, dr \, d\theta$  and the shear stresses  $\tau_{zr} = \frac{1}{r} \frac{\partial \phi}{\partial r}$  and  $\tau_{z\theta} = - \frac{\partial \phi}{\partial r}$ .

(b) Finite difference method

If a mesh (usually square) is superimposed on the region under consideration, the governing partial differential equation will apply exactly at each node (i.e. point of intersection of two perpendicular lines). If, however, every partial derivative is replaced by its finite difference approximation, a separate algebraic equation, which satisfies the differential equation only approximately, will be obtained for each node. These approximate linear equations are then solved exactly.



For example at point 0 in the mesh shown  $\nabla^2 \phi \approx (\phi_1 + \phi_2 + \phi_3 + \phi_4 - 4\phi_0) / h^2$  the error being of the order of  $h^2$

Example. Torsion of non-circular bars

As before  $\nabla^2 \phi + 2G\alpha = 0$  within the region  
 $\phi = 0$  on the boundary



The approximate equation for each node will now be of the form

$$\phi_1 + \phi_2 - 4\phi_0 + \phi_3 + \phi_4 = -2G\alpha h^2$$

and the unknowns will be the values of  $\phi$ .

Because there may be several hundred equations to solve, the use of a digital computer is almost essential. Fortunately, if the equations are written in matrix form, the matrix of coefficients of  $\phi$  is banded and symmetric, thus greatly reducing the computer storage space required.

As with the point matching method, accuracy is increased by using more nodes, but alternatively a better finite difference approximation could be used by introducing more of the surrounding nodes. By using this method, errors in each equation may be reduced from the order of  $h^2$  to say  $h^4$ , but each equation will now be more complicated and there may be difficulties near the edge.

Difficulties will also occur with irregular boundaries. Approximations for the partial derivatives may be obtained in terms of the appropriate fractions of  $h$  between the central node and the boundary, but the matrix of coefficients is no longer symmetric, and so requires more computer storage space.

A third approach is:-

(c) Energy methods

In (b) it is shown that an approximate solution is obtained for an exact differential equation. In an energy method, a deflected shape or stress pattern in terms of unknown parameters is



initially assumed. For example, the deflected shape of a beam may be assumed to be given by  $w = \sum_{i=0}^{\infty} c_i \phi_i(x)$  where the  $\phi$ 's are known functions of  $x$ .

It is then possible to determine the strain energy of the solid and potential energy of the applied loads in terms of the unknown coefficients  $c_i$ , and by using the principle of stationary total potential energy (or complementary energy in the case of an assumed stress variation) the values of these coefficients may be found.

Problems on plate deflection are very satisfactorily handled by energy methods, and one example is shown below.

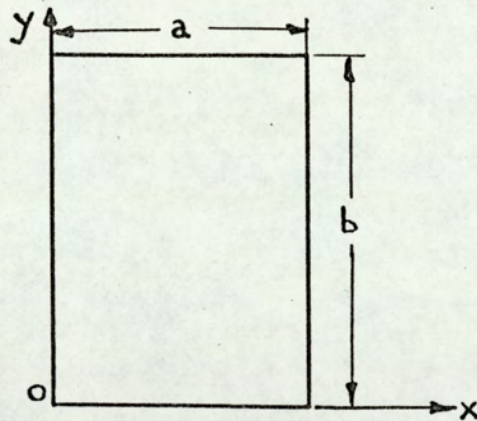


Fig. 5B

Consider a rectangular plate of uniform thickness which is simply supported at all edges and subjected to a uniform pressure  $p$ . In this case an infinite series is to be used and the chosen shape must satisfy the geometric boundary conditions, i.e.  $w = 0$  at  $x = 0$  and  $a$ , and at  $y = 0$  and  $b$ .

A possible shape is then:-

$$w = \sum_{m=1}^{\infty} \sum_{n=1}^{\infty} c_{mn} \sin \frac{m\pi x}{a} \sin \frac{n\pi y}{b}$$



For plates of polygonal form which are supported along their edges

the strain energy  $U = \frac{D}{2} \iint \left[ \frac{\partial^2 w}{\partial x^2} + \frac{\partial^2 w}{\partial y^2} \right]^2 dx dy$

$$\text{where } D = \frac{Eh^3}{12(1-\nu^2)}$$

$$\text{Hence } U = \frac{\pi^4 Dab}{8} \sum \sum c_{mn}^2 \left[ \frac{m^2}{a^2} + \frac{n^2}{b^2} \right]^2$$

Also the potential energy of the loads  $\Omega = - \iint pw dx dy$

gives  $\Omega = -p \sum \sum \frac{ab}{\pi^2} \frac{c_{mn}}{mn} (\cos m\pi - 1)(\cos n\pi - 1)$  which is zero for even values of  $m$  and  $n$ .

The total potential energy  $V = U + \Omega$

and for  $\delta V$  to be zero  $\frac{\partial V}{\partial c_{mn}} = 0$

$$\text{which gives } c_{mn} = \frac{16pa^4}{\pi D} \frac{1}{mn \left[ m^2 + \left( \frac{\pi}{r} \right)^2 \right]^2} \text{ where } r = \frac{b}{a}$$

The deflection at the centre of the plate is then

$$\begin{aligned} w_c &= \sum_{m=1,3}^{\infty} \sum_{n=1,3}^{\infty} c_{mn} \sin \frac{m\pi}{2} \sin \frac{n\pi}{2} \\ &= \sum \sum (-1)^{\frac{m+n}{2} + 1} c_{mn} \end{aligned}$$

A simple computer program was written to determine the values of  $c_{mn}$  and the central deflection from their summation. It was found that the coefficients decay rapidly and only 25 were taken (i.e.  $m, n = 1, 3 \dots 9$ ). The results obtained for plates of various shapes are given below.



b/a	Central deflection
1.0	0.00406 $\frac{pa^4}{D}$
1.2	0.00565
1.4	0.00709
1.6	0.00831
1.8	0.00932
2.0	0.01013
3.0	0.01224
4.0	0.01300
5.0	0.01322

TABLE 5.1

These results are almost identical with those given by Timoshenko [5].

The results given in Table 5.1 were obtained from an exact solution containing an infinite number of terms, although, of course, only a finite number can be evaluated.

Alternatively the Rayleigh-Ritz method may be used to give a series solution which contains a finite number of terms each of which must satisfy the geometrical boundary conditions. The number of terms required is first decided, and it is then only necessary to find the coefficient of each term. For example, in the plate bending problem already considered, a deflected shape described by



$w = c_1 \sin \frac{\pi x}{a} \sin \frac{\pi y}{b} + c_2 \sin \frac{3\pi x}{a} \sin \frac{3\pi y}{b}$  could be chosen. By using the principle stationary total potential energy  $\frac{\partial U}{\partial c_1} = 0$  and  $\frac{\partial U}{\partial c_2} = 0$ , and hence  $c_1$  and  $c_2$  may be found.

It is not even necessary for the series to be of the same type as the exact solution, so that in the plate bending problem, instead of a trigonometrical series the very simply described shape

$w = c \left(\frac{a}{2} - x\right)^2 \left(\frac{b}{2} - y\right)^2$  could be assumed. Then, as before,  $c$  is found from  $\frac{\partial U}{\partial c} = 0$ .

Similarly the deflected shape of a beam could be assumed to be given by the 4-term polynomial series  $w = c_i x^i$  ( $i=0,1,2,3$ ) and again the values of  $c_i$  are found from  $\frac{\partial U}{\partial c_i} = 0$ .

With a good choice of shape function, the Rayleigh-Ritz method can give extremely accurate results, and this is the basis of the finite element methods described below and used extensively in Chapter 6.

#### (d) The finite element method

Instead of choosing a particular deflection shape for the whole solid, the region may be considered to consist of a number (usually large) of separate finite elements, for each of which the shape function is of the same type. For example, in a plane stress situation an assumed deflection pattern  $u = a_1 + a_2 x + a_3 y$ , and  $v = a_4 + a_5 x + a_6 y$  could be assumed. This will apply to each element



but the values of  $a_1$ ,  $a_2$  and  $a_3$  will, in general, be different for each element, and their values are found by using the principle of stationary total potential energy.

In addition to considering the deflection within each element it is also necessary to ensure compatibility between that element and surrounding elements. Also, by using the principle of stationary total potential energy, equilibrium is satisfied on the average so that it is violated across a typical boundary.



## CHAPTER 6

### SOLUTION OF ELASTIC PROBLEMS USING FINITE ELEMENT METHODS

A solution of the cylinder problem of 4.4 was obtained in terms of the parameter  $\beta$ . While  $\beta$  is constant for a uniform elastic cylinder, its value varies slightly for a viscoelastic material, and an "exact" solution was only obtained by neglecting this change in  $\beta$ . For both elastic and viscoelastic materials any change in the wall thickness will affect the value of  $\beta$ , and the use of a constant value can no longer be justified. An exact solution will then be much more difficult, but as the membrane stresses are easily found even when the wall thickness varies, a solution is possible if the problem of a non-uniform beam on a non-uniform flexible base can be solved. Because of the nature of this problem, it was thought that a finite element method using beam-type elements offered the best method of approach.

To obtain experience in finite element methods, uniform beams were first considered, and later the same methods were applied to a tapered beam.

#### 6.1 Finite element of a uniform beam

Consider an element of length  $\ell$  of a beam of uniform flexural rigidity  $EI$ .



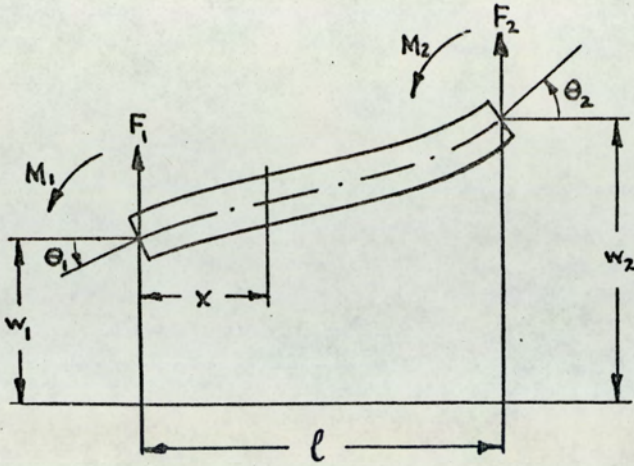


Fig. 6A.

As  $M = -M_1 + F_1 x$

The complementary strain energy of the element  $U^* = \int_0^l \frac{(-M_1 + F_1 x)^2}{2EI} dx$

The total complementary energy  $V^* = U^* + \Omega^*$

or  $V^* = \frac{1}{2EI} (M_1^2 l - M_1 F_1 l^2 + \frac{1}{3} F_1^2 l^3) - F_1 w_1 - F_2 w_2 - M_1 \theta_1 - M_2 \theta_2$

For equilibrium  $F_2 = -F_1$  and  $M_2 = -M_1 + F_1 l$

Hence  $V^*$  may be expressed in terms of  $F_1$  and  $M_1$ .

For stationary total complementary energy  $\frac{\partial V^*}{\partial F_1} = 0$  and  $\frac{\partial V^*}{\partial M_1} = 0$

Hence equations are obtained giving  $F_1$  and  $M_1$  in terms of the nodal displacements.

Similar expressions are obtained for  $F_2$  and  $M_2$ .

These equations are best expressed in matrix form

$$\begin{Bmatrix} F_1 \\ M_1 \\ F_2 \\ M_2 \end{Bmatrix} = EI \begin{bmatrix} \frac{12}{l^3} & \frac{6}{l^2} & -\frac{12}{l^3} & \frac{6}{l^2} \\ \frac{6}{l^2} & \frac{4}{l} & -\frac{6}{l^2} & \frac{2}{l} \\ -\frac{12}{l^3} & -\frac{6}{l^2} & \frac{12}{l^3} & -\frac{6}{l^2} \\ \frac{6}{l^2} & \frac{2}{l} & -\frac{6}{l^2} & \frac{4}{l} \end{bmatrix} \begin{Bmatrix} w_1 \\ \theta_1 \\ w_2 \\ \theta_2 \end{Bmatrix} \tag{6.1.1}$$

or  $\{F\} = [K] \{u\}$



The same stiffness matrix is obtained by the principle of stationary total potential energy as a special case of the stiffness matrix of a tapered element of 6.4 below.

If the beam is adequately supported it will be possible to invert the stiffness matrix  $[K]$  to give the inverse matrix  $[K]^{-1}$

$$\text{Then } \{u\} = [K]^{-1} \{F\}$$

and if the nodal forces are known the nodal displacements may be calculated. [9]

It will be seen that the stiffness matrix of 6.1.1 is symmetric. If a beam is divided into several elements joined at the nodes, then at each node common to two elements the conditions of equilibrium and compatibility must apply. This means that the nodal forces for the two elements must be added, and the nodal displacements must be the same for the two elements (otherwise there will be a discontinuity in the beam). The separate stiffness matrices for the two elements may therefore be combined by adding appropriate rows and columns, thus forming the combined stiffness matrix which is still symmetric. The formation of this combined matrix is more fully described below in 6.3 and in the Appendix.

## 6.2 Elastic structures

A structure may be regarded as an assemblage of separate members, each of which will in general have flexural and extensional deformations due to applied forces. Each of these members may be treated as a separate finite element joined to other elements at



the nodes. Equilibrium and compatibility conditions will apply at each node, so that a combined stiffness matrix for the whole structure may be formed as noted in 6.1. [10]

With certain types of structure, changes of length of the elements are small in comparison with the displacements due to bending, and under these conditions only bending effects need be considered.

Example

A typical example of this type of structure is the Portal frame shown in Fig. 6B, where each member has a length  $l$  and a flexural rigidity  $EI$ . It is required to find the slopes and deflections at B and C due to a horizontal force applied at C.

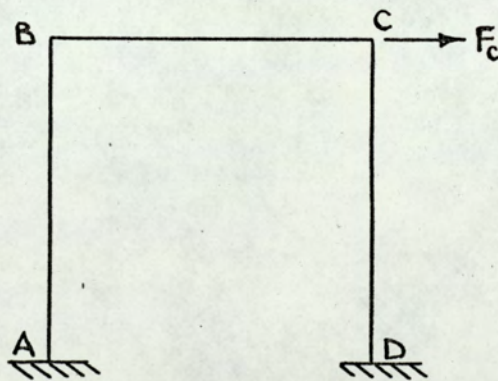


Fig. 6B.

The structure may be regarded as an assemblage of 3 separate elements joined at B and C as shown in Fig. 6C, and changes of length of these elements will be neglected.



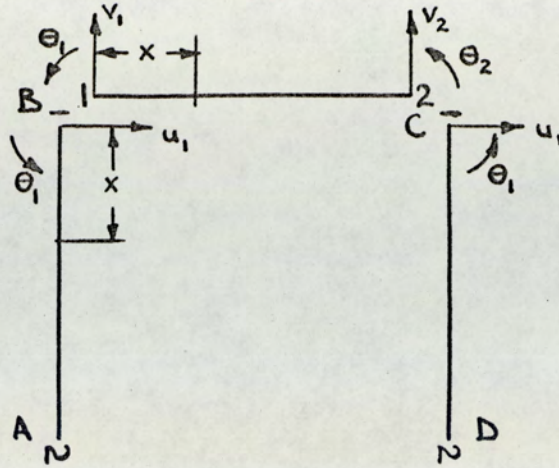


Fig. 6C.

For element AB  $u_2 = \theta_2 = 0, \quad u_1 = u_b, \quad \theta_1 = \theta_b$

Then from 6.1.1  $F_1 = \frac{12EI}{l^3} u_b + \frac{6EI}{l^2} \theta_b$

and  $M_1 = \frac{6EI}{l^2} u_b + \frac{4EI}{l} \theta_b$

Hence at a distance  $x$  from B, the bending moment

$$M = M_1 - F_1 x = \frac{6EI}{l^2} u_b + \frac{4EI}{l} \theta_b - \left( \frac{12EI}{l^3} u_b + \frac{6EI}{l^2} \theta_b \right) x$$

Then the strain energy of AB,  $U_{AB} = \int_0^l \frac{M^2}{2EI} dx$  may be expressed in terms of  $u_b$  and  $\theta_b$ .

For element CD  $u_2 = \theta_2 = 0, \quad u_1 = u_c, \quad \theta_1 = \theta_c$

Since the change of length of BC is assumed to be negligible  $u_c = u_b$  and hence the strain energy of CD is found from an identical expression to that for  $U_{AB}$ , except that  $\theta_b$  is replaced by  $\theta_c$ .



For element BC  $v_1 = v_2 = 0$  (since changes of length of AB and CD are neglected)  $\theta_1 = \theta_b$ ,  $\theta_2 = \theta_c$  (compatibility conditions for rigid joints at B and C).

$$\text{Then } F_1 = \frac{6EI}{l^2}\theta_b + \frac{6EI}{l^2}\theta_c$$

$$\text{and } M_1 = \frac{4EI}{l}\theta_b + \frac{2EI}{l}\theta_c$$

$M = M_1 - F_1x$  may then be used to find the strain energy of BC,  $U_{BC}$ .

Then the total potential energy of the system is given by

$$V = \Omega + U \\ = -F_c u_c - M_b \theta_b - M_c \theta_c + U_{AB} + U_{BC} + U_{CD}$$

where  $F_c$  is the horizontal force applied at C, and  $M_b$  and  $M_c$  are the couples applied at B and C.

Then by using the principle of stationary total potential energy

$$\frac{\partial V}{\partial F_c} = 0 \text{ gives } F_c = \frac{24EI}{l^3} u_c + \frac{6EI}{l^2} \theta_b + \frac{6EI}{l^2} \theta_c$$

and similar expressions may be obtained for  $M_b$  and  $M_c$  from

$$\frac{\partial V}{\partial \theta_b} = 0 \text{ and } \frac{\partial V}{\partial \theta_c} = 0$$

Expressed in matrix form the three equations give

$$\begin{Bmatrix} M_b \\ F_c \\ M_c \end{Bmatrix} = EI \begin{bmatrix} \frac{8}{l} & \frac{6}{l^2} & \frac{2}{l} \\ \frac{6}{l^2} & \frac{24}{l^3} & \frac{6}{l^2} \\ \frac{2}{l} & \frac{6}{l^2} & \frac{8}{l} \end{bmatrix} \begin{Bmatrix} \theta_b \\ u_c \\ \theta_c \end{Bmatrix}$$



Since, in the case considered,  $M_b = M_c = 0$  these equations are easily solved giving

$$\begin{aligned} u_c &= \frac{5}{84} \frac{F_c \ell^3}{EI} \\ \theta_b = \theta_c &= -\frac{F_c \ell^2}{28EI} \end{aligned} \quad (6.2.1)$$

Once the values of  $u_c$ ,  $\theta_b$  and  $\theta_c$  have been found 6.1.1 may be used to calculate the values of  $M_a$  and  $M_b$  (which by symmetry are respectively equal to  $M_d$  and  $M_c$ ).

$$\begin{aligned} M_a &= \frac{6EI}{\ell^2} u_b + \frac{2EI}{\ell} \theta_b = \frac{2}{7} F_c \ell \\ M_b &= \frac{4EI}{\ell} \theta_b + \frac{2EI}{\ell} \theta_c = -\frac{3}{14} F_c \ell \end{aligned}$$

These results were checked by using conventional beam deflection methods, by treating AB and CD as cantilevers subjected to end forces and couples and joined by a third beam BC. The conditions of equilibrium and compatibility must again be used for B and C. The results obtained were identical with those found by the finite element method.

### 6.3 Elastic beams

So far, each beam considered has been treated as a single finite element. In order to obtain more experience in the use of the finite element method, types of beam which are divided into several elements were next considered and the examples in this section show how the stiffness matrices for the whole beam are assembled, and check the accuracy of this method

As noted in 6.1, the stiffness matrix for an element of a uniform beam derived there may also be obtained by using the principle of stationary total potential energy. This method is used below in 6.4, and begins with an assumed deflection shape described by  $w = a_1 + a_2x + a_3x^2 + a_4x^3$ . Now if a uniform beam is subjected to end forces and couples only, conventional beam theory shows that



the deflected shape is represented exactly by this equation, and, given the values of the forces and couples and the end conditions, the values of the coefficients  $a_i$  may be determined. Since the stiffness matrix for one element is derived from an assumed (correct) shape which applies to the whole beam, the beam may be considered as a single finite element. This method was in fact used for the frame of 6.2.

If, however, point loads or couples are applied at points other than the ends to use previous results the beam must be divided into separate elements so that these forces may act at nodes which are common to adjacent elements. The stiffness matrix for the whole beam is then obtained by adding the stiffness matrices of the separate elements correctly and since the matrix for each element contains only 4 rows and columns, the resultant matrix will be banded with a band width of 7 elements. Again there will be no difference between the results obtained by this method and beam theory.

Distributed loads can, however, be only approximately represented by a system of point loads at the nodes. In the case of a uniformly distributed load the force on each element will be proportional to the length of the element, and could be equally divided between its ends.

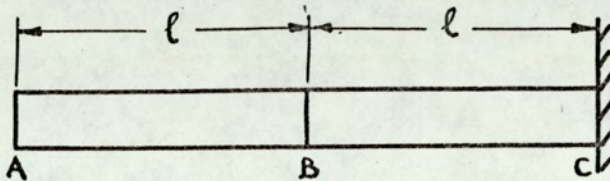
This is simple "static" lumping of the distributed load. More accurate results should be obtained by sharing out the load



from work consideration, i.e. the work done by the approximate lumped system must be equal to the work done by the distributed load.

If, however, a sufficient number of elements are used the simpler "static" lumping should give sufficiently accurate results.

Example 1



Consider a uniform cantilever of length  $L (=2\ell)$ . If this beam is divided into two elements of length  $\ell$ , AB and BC, their stiffness matrices will be identical. For equilibrium at node B,  $\Sigma F_b = 0$  and  $\Sigma M_b = 0$  and for compatibility of adjacent elements  $(w_b)_{AB}$  and  $(\theta_b)_{AB}$  must be equal to  $(w_b)_{BC}$  and  $(\theta_b)_{BC}$  respectively. Both these sets of conditions are satisfied if the third and fourth rows and columns of  $[K]_{AB}$  are added to the first and second rows and columns respectively of  $[K]_{BC}$ .

Using the stiffness matrix of 6.1.1 for each element, the combined stiffness matrix is:-



$$EI \begin{bmatrix} \frac{12}{l^3} & \frac{6}{l^2} & -\frac{12}{l^3} & \frac{6}{l^2} & 0 & 0 \\ \frac{6}{l^2} & \frac{4}{l} & -\frac{6}{l^2} & \frac{2}{l} & 0 & 0 \\ -\frac{12}{l^3} & -\frac{6}{l^2} & \frac{24}{l^3} & 0 & -\frac{12}{l^3} & \frac{6}{l^2} \\ \frac{6}{l^2} & \frac{2}{l} & 0 & \frac{8}{l} & -\frac{6}{l^2} & \frac{2}{l} \\ 0 & 0 & -\frac{12}{l^3} & -\frac{6}{l^2} & \frac{12}{l^3} & -\frac{6}{l^2} \\ 0 & 0 & \frac{6}{l^2} & \frac{2}{l} & -\frac{6}{l^2} & \frac{4}{l} \end{bmatrix}$$

which is still symmetric, as noted in 6.1.

Since in this case C is a fixed end,  $w_c = \theta_c = 0$ , so that the last two rows and columns of the stiffness matrix may be deleted giving the equations:-

$$\begin{Bmatrix} F_a \\ M_a \\ F_b \\ M_b \end{Bmatrix} = EI \begin{bmatrix} \frac{12}{l^3} & \frac{6}{l^2} & -\frac{12}{l^3} & \frac{6}{l^2} \\ \frac{6}{l^2} & \frac{4}{l} & -\frac{6}{l^2} & \frac{2}{l} \\ -\frac{12}{l^3} & -\frac{6}{l^2} & \frac{24}{l^3} & 0 \\ \frac{6}{l^2} & \frac{2}{l} & 0 & \frac{8}{l} \end{bmatrix} \begin{Bmatrix} w_a \\ \theta_a \\ w_b \\ \theta_b \end{Bmatrix} \quad (6.3.1)$$

If an end load  $-F$  is applied at A, then the nodal forces are  $F_a = -F, M_a = F_b = M_b = 0$ . Solution of the four equations above then

$$\text{gives } w_a = -\frac{FL^3}{3EI}, \quad \theta_a = \frac{FL^2}{2EI}, \quad w_b = -\frac{5}{84} \frac{FL^3}{EI}, \quad \theta_b = \frac{3}{8} \frac{FL^2}{EI}$$



which agree exactly with conventional beam theory. For this particular example, as only end forces are applied, one finite element would have given exactly the same end deflection and slope, so there is no increase in accuracy due to increasing the number of elements.

### Example 2

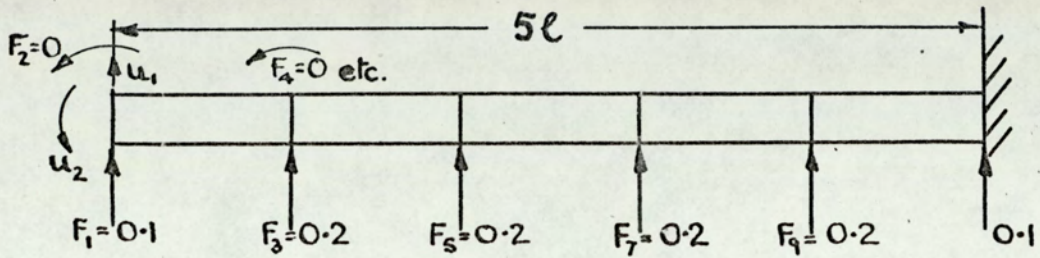
If the beam of Example 1 carries a uniformly distributed load of  $p$  per unit length along its whole length, by using "static" lumping a single finite element would approximate the distributed load by a force of  $-\frac{pL}{2}$  at each end. This gives an end deflection of  $-\frac{pL^4}{6EI}$  which is 33% high compared with the result from beam theory, and an end slope of  $-\frac{pL^3}{4EI}$  which is 50% high.

However, using two equal elements in Example 1, the nodal forces and moments at A and B are now  $\{-\frac{pL}{4}, 0, -\frac{pL}{4}, 0\}$  and the end deflection and slope by solving equations 6.3.1 are  $-\frac{13}{96}\frac{pL^4}{EI}$  (8 % high) and  $\frac{3}{16}\frac{pL^3}{EI}$  (12.5% high). By doubling the number of elements, the errors have therefore been reduced to about a quarter of their previous values. This is because the finite element method cannot exactly represent the deflected shape of a beam carrying a distributed load, but by increasing the number of elements the difference in any one element between the actual shape of the beam and the shape given by the finite element method is drastically reduced.

To obtain an even higher degree of accuracy the cantilever was divided into 5 equal elements, and since there are 2 constraints only



10 displacements and forces need be considered giving a 10 x 10 stiffness matrix. For simplicity EI is taken as unity, the length of each element  $l$  and the total load on the beam are also taken as unity. A uniformly distributed load is replaced by the nodal forces shown



Note  $F_1 F_3 \dots F_9$  are forces  
 $F_2 F_4 \dots F_{10}$  are moments (all zero here)  
 $u_1 u_3 \dots u_9$  are deflections  
 $u_2 u_4 \dots u_{10}$  are slopes

$$\begin{Bmatrix} 0.1 \\ 0 \\ 0.2 \\ 0 \\ 0.2 \\ 0 \\ 0.2 \\ 0 \\ 0.2 \\ 0 \end{Bmatrix} = \begin{bmatrix} 12 & 6 & -12 & 6 & & & & & & \\ & 6 & 4 & -6 & 2 & 0 & & & & \\ & -12 & -6 & 24 & 0 & -12 & 6 & & & \\ & & 6 & 2 & 0 & 8 & -6 & 2 & 0 & \\ & & & 0 & -12 & -6 & 24 & 0 & -12 & 6 \\ & & & & 6 & 2 & 0 & 8 & -6 & 2 \\ & & & & & 0 & -12 & -6 & 24 & 0 \\ & & & & & & 6 & 2 & 0 & 8 \end{bmatrix} \begin{Bmatrix} u_1 \\ u_2 \\ u_3 \\ u_4 \\ u_5 \\ u_6 \\ u_7 \\ u_8 \\ u_9 \\ u_{10} \end{Bmatrix}$$



A computer program [Prog. 2] was written to read in the forces and the non-zero elements of the stiffness matrix given above (all other elements were zero) and to solve the equations by the Gaussian elimination method, finding  $u_{10}$  first and then substituting back to find the other displacements in turn [7]. The factors  $E$ ,  $I$ ,  $\ell$  and  $F$  may then be re-introduced.

The results obtained from the computer program were:-

Node	1	2	3	4	5
Deflection	15.83	11.60	7.50	3.83	$1.10 \times \frac{F\ell^3}{EI}$
Slope	-4.25	-4.20	-3.95	-3.30	$-2.05 \times \frac{F\ell^2}{EI}$

where  $F$  is the total load on the beam and  $\ell$  is the length of each element.

The end deflection and slope are easily found from beam theory being  $\frac{F(5\ell)^3}{8EI} = 15.625 \frac{F\ell^3}{EI}$  and  $-\frac{F(5\ell)^2}{6EI} = -4.167 \frac{F\ell^2}{EI}$  respectively.

The end deflection is therefore 1.3% high and the end slope 1.6% high. These figures are acceptable for most purposes, but even more accurate values could be obtained by using more elements.

The computer program used to solve this problem is limited to cases where the beam has a uniform cross-section and all elements are of the same length. In 6.4 a finite element method is developed to allow for variation in both the depth and length of the element.



### 6.4 Finite element method applied to a tapered beam

Consider a beam of rectangular cross-section of uniform width  $b$ , but varying depth  $d$ . Let  $w_1$   $\theta_1$  and  $w_2$   $\theta_2$  be the deflections and slopes at the two ends of an element of length  $\ell$  and let  $x = 0$  at the left hand end of this element.

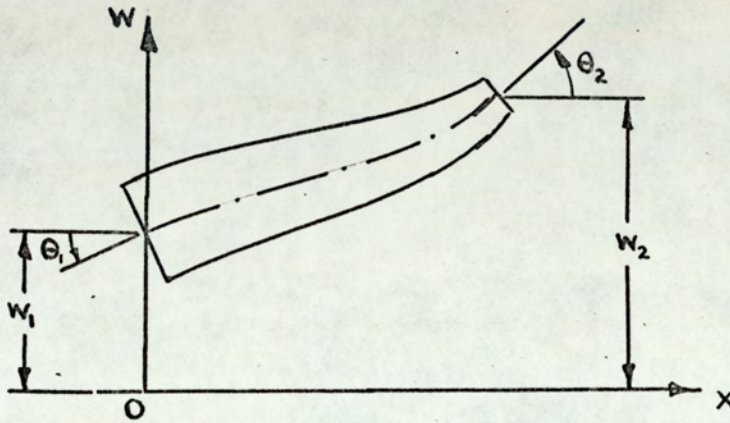


Fig. 6D.

Assume that at a distance  $x$  from this end the deflection  $w$  is given by:-

$$w = a_1 + a_2x + a_3x^2 + a_4x^3 \quad (6.4.1)$$

$$\text{Then } \theta = \frac{dw}{dx} = a_2 + 2a_3x + 3a_4x^2$$

Then by substituting  $x = 0$  and  $x = \ell$  in these two equations, expressions for  $w_1$   $\theta_1$   $w_2$  and  $\theta_2$  are obtained.

These may be written as

$$\{u\} = [L] \{a\}$$

where  $[L]$  is a  $4 \times 4$  matrix, the elements of which are functions of the length of the element  $\ell$ .

$$\text{Hence } \{a\} = [A] \{u\} \text{ where } [A] = [L]^{-1}$$

The deflection at any point in the element is



$$\begin{aligned} w &= [1 \quad x \quad x^2 \quad x^3] \{a\} \\ &= [1 \quad x \quad x^2 \quad x^3] [A] \{u\} \end{aligned}$$

Also the curvature of the neutral surface  $\frac{1}{R} = \frac{d^2 w}{dx^2}$  and the strain at a distance  $y$  from the neutral surface  $\epsilon = \frac{-y}{R}$  it follows that

$$\epsilon = -y \left[ \left( -\frac{6}{\ell^2} + \frac{12x}{\ell^3} \right) w_1 + \left( -\frac{4}{\ell} + \frac{6x}{\ell^2} \right) \theta_1 + \left( \frac{6}{\ell^2} - \frac{12x}{\ell^3} \right) w_2 + \left( -\frac{2}{\ell} + \frac{6x}{\ell^2} \right) \theta_2 \right]$$

For a linear elastic material  $\sigma = E\epsilon$  and the strain energy of the element  $U = \frac{1}{2} \int \{\sigma\}^t \{\epsilon\} d(\text{vol})$ .

$$\begin{aligned} \text{Hence } U &= \frac{Eb}{2} \iint y^2 \left[ \left( -\frac{6}{\ell^2} + \frac{12x}{\ell^3} \right) w_1 + \left( -\frac{4}{\ell} + \frac{6x}{\ell^2} \right) \theta_1 + \left( \frac{6}{\ell^2} - \frac{12x}{\ell^3} \right) w_2 \right. \\ &\quad \left. + \left( -\frac{2}{\ell} + \frac{6x}{\ell^2} \right) \theta_2 \right]^2 dx dy \end{aligned}$$

$$\text{or } U = \frac{Eb}{2} \iint y^2 [G(x,u)]^2 dx dy \tag{6.4.2}$$

Now consider the element of Fig. 6E tapering uniformly in depth from  $d_1$  to  $d_2$ . Then  $d = d_1 - mx$  where  $m = (d_1 - d_2)/\ell$

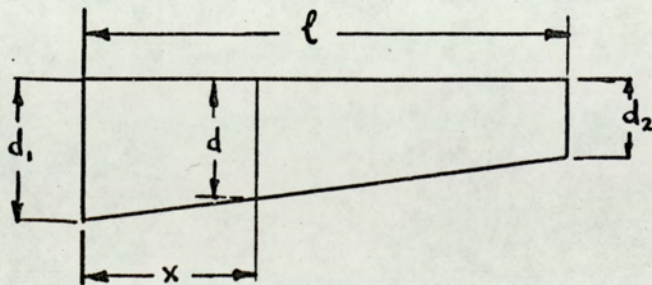


Fig. 6E.



Hence in 6.4.2 the limits for  $y$  are  $\pm(d_1 - mx)/2$  and for  $x$ , 0 and  $l$

$$\text{Then } U = \frac{Eb}{24} \int_0^l (d_1 - mx)^3 [G(x,u)]^2 dx \quad (6.4.3)$$

$$\text{or } U = \mathcal{F}(u_i)$$

Also the potential energy of the nodal forces and couples

$$\Omega = -F_1 w_1 - M_1 \theta_1 - F_2 w_2 - M_2 \theta_2 \quad (6.4.4)$$

and the total potential energy of the element  $V = U + \Omega$  or

$$V = -F_i u_i + \mathcal{F}(u_i) \quad i = 1, 2, 3, 4 \quad (6.4.5)$$

Then using the principle of stationary total potential energy

$$\delta V = 0$$

$$\text{and hence } F_i = \frac{\partial}{\partial u_i} \{ \mathcal{F}(u_i) \} \quad (6.4.6)$$

Initially, because of the complicated expressions obtained when the two terms in 6.4.3 are multiplied together, it was thought that, for small tapers, the  $m^2$  and  $m^3$  terms could be neglected. After multiplying other terms (i.e. terms containing  $d_1$  and  $m$ ) together and integrating 6.4.3 gives an expression in terms of  $u_i u_j$  ( $i, j = 1, 2, 3, 4$ ). The partial differentiation of 6.4.6. then results in an expression for each nodal force (or moment) in turn, each being a function of the  $u_i$ 's. The 4 coefficients so obtained are the elements of one row of the stiffness matrix. Since there are 4 partial differentiations, all 4 rows of the stiffness matrix are obtained.

In matrix form this stiffness matrix is:-



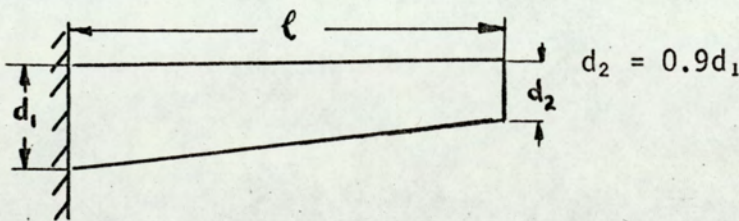
$$[K] = \frac{Eb}{12} \begin{bmatrix} \frac{d_1^2}{\ell^3}(18d_2-6d_1) & \frac{6d_1^2d_2}{\ell^2} & -\frac{d_1^2}{\ell^3}(18d_2-6d_1) & \frac{d_1^2}{\ell^2}(12d_2-6d_1) \\ & \frac{d_1^2}{\ell}(d_1+3d_2) & -\frac{6d_1^2d_2}{\ell^2} & \frac{d_1^2}{\ell}(3d_2-d_1) \\ & & \frac{d_1^2}{\ell^3}(18d_2-6d_1) & -\frac{d_1^2}{\ell^2}(12d_2-6d_1) \\ \text{Symmetric} & & & \frac{d_1^2}{\ell}(9d_2-5d_1) \end{bmatrix}$$

(6.4.7)

As far as the author is aware, such a stiffness matrix has not previously been presented.

Example 1

As an initial check on the stiffness matrix of 6.4.7 a tapered cantilever with an end load was considered



Since  $w_1 = \theta_1 = 0$

$$F_2 = k_{33}w_2 + k_{34}\theta_2 \quad \text{where } k_{33} = \frac{Eb}{12} \cdot 10.2 \frac{d_1^3}{\ell^3}$$

$$k_{34} = \frac{Eb}{12} \cdot (-4.8 \frac{d_1^3}{\ell^2})$$

$$M_2 = k_{43}w_2 + k_{44}\theta_2 \quad \text{where } k_{43} = k_{34}$$

$$k_{44} = \frac{Eb}{12} \cdot 3.1 \frac{d_1^3}{\ell}$$



Since in this case  $M_2 = 0$ ,  $\theta_2 = -\frac{k_{43}}{k_{44}} w_2$

and hence  $w_2 = \frac{0.360F_2 \ell^3}{EI_1}$  where  $I_1 = \frac{1}{12} b d_1^3$

In this case, conventional beam theory gives the solution

$$w_2 = \frac{12F_2 \ell^3}{Eb d_1^3} \left[ \left( \frac{d_1}{d_1-d_2} \right)^3 \ln \frac{d_1}{d_2} - \left( \frac{d_1}{d_1-d_2} \right)^2 - \frac{1}{2} \frac{d_1}{d_1-d_2} \right]$$

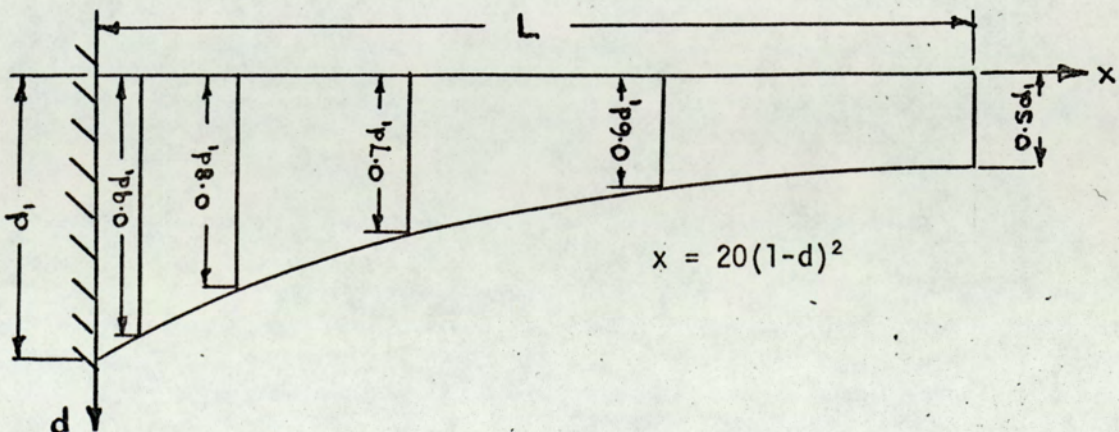
and when  $d_2 = 0.9d_1$

$$w_2 = \frac{0.3605F_2 \ell^3}{EI_1}$$

The finite element result is therefore about 0.1% low which seems very satisfactory.

### Example 2

As a further check it was decided to apply this method to a cantilever of parabolic profile so that by varying the lengths of the individual elements different values of the ratio  $d_1/d_2$  would be used.





The beam was divided into 5 elements as shown.

For convenience  $d_1$  was taken as 1 so that  $L = 5$ , but any other pair of values having the same ratio could be used as the deflection involves the non-dimensional factor  $(\frac{L}{d_1})^3$ . Similarly the end load  $F_9$  is also taken as unity.

A computer program (Prog.3) was written to evaluate the individual elements of the stiffness matrix, to assemble the stiffness matrix for the beam and to calculate the values of the displacements. After re-introduction of  $F$ ,  $E$  and  $b$  the end deflection obtained was

$$\underline{\underline{\frac{12}{Eb} \cdot 101.68F.}}$$

Beam theory now gives an end deflection

$$w = \frac{12}{Eb} F \int_0^5 \frac{(5-x)^2}{(1-\sqrt{\frac{x}{20}})^3} dx$$

This integral was evaluated numerically with the aid of a digital computer. To minimise errors, 50 divisions were used and the result obtained was

$$\underline{\underline{w = \frac{12}{Eb} 101.38F}}$$

The finite element solution is therefore about 0.3% high, which again seems quite satisfactory, especially as this error could almost certainly be reduced by dividing the beam into more elements.



The position is not however quite so satisfactory if it is observed that due to neglecting the  $m^2$  and  $m^3$  terms in 6.4.3, the stiffness matrix 6.4.7 contains terms which are unbalanced between  $d_1$  and  $d_2$ .

For example consider the following

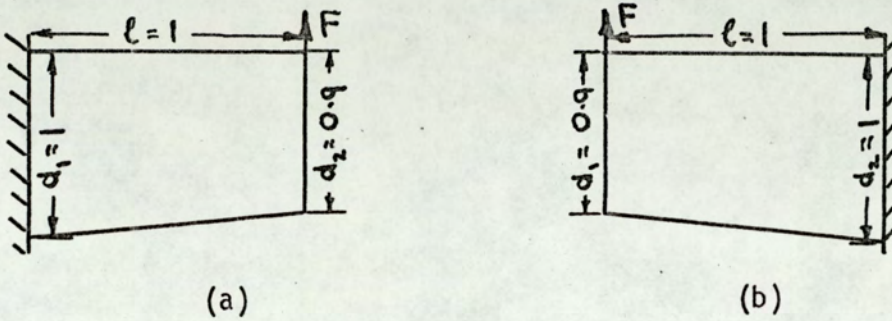


Fig. 6F.

(a) has already been dealt with and gives an end deflection of

$$0.360 \frac{F\ell^3}{EI_1} \text{ (about 0.1\% error).}$$

But (b) is the same beam reversed and should give the same deflection.

The equations are now

$$F = k_{11}w_1 + k_{12}\theta_1$$

$$0 = k_{12}w_1 + k_{22}\theta_1$$

Substituting for  $k_{11}$ ,  $k_{12}$  and  $k_{22}$  gives

$$w_1 = 0.367 \frac{F\ell^3}{EI_1} \quad \text{i.e. about 2\% error.}$$

The error in the end deflection therefore depends on the direction of the taper, the greatest error occurring when  $d_1 < d_2$ .

This is obviously unsatisfactory as actual beams may taper in either



direction. So long as there is a lack of balance between  $d_1$  and  $d_2$  terms in the stiffness matrix of 6.4.7 this difference must, however, appear, and the basic cause of this unbalance was thought to be the omission of  $m^2$  and  $m^3$  terms in the expansion of 6.4.3. The full expansion of  $(d_1 - mx)^3$  was accordingly used in deriving a more accurate stiffness matrix below.

### 6.5 Improved stiffness matrix for a tapered element

When the complete expansion of  $(d_1 - mx)^3$  is given in 6.4.3

$$U = \frac{Eb}{24} \int_0^{\ell} (d_1^3 - 3d_1^2mx + 3d_1m^2x^2 - m^3x^3)[G(x,u)]^2 dx$$

$$\text{where } G(x,u) = \left(-\frac{6}{\ell^2} + \frac{12x}{\ell^3}\right)w_1 + \left(-\frac{4}{\ell} + \frac{6x}{\ell^2}\right)\theta_1 + \left(\frac{6}{\ell^2} - \frac{12x}{\ell^3}\right)w_2 + \left(-\frac{2}{\ell} + \frac{6x}{\ell^2}\right)\theta_2$$

If partial differentiation with respect to  $u_i$  is carried out before integration then

$$F_i = \frac{\partial U}{\partial u_i} = \frac{Eb}{12} \int_0^{\ell} (d_1 - mx)^3 G(x,u)g_i dx$$

where  $g_i$  is the coefficient of  $u_i$  in  $G(x,u)$

Since  $G(x,u)$  contains terms in  $w_1 \theta_1 w_2 \theta_2$  the expression for  $F_i$  will be of the form  $k_{i1} w_1 + k_{i2} \theta_1 + k_{i3} w_2 + k_{i4} \theta_2$  and each of the  $k_{ij}$  ( $i = 1,2,3,4$ ;  $j = 1,2,3,4$ ) must be found separately.

For example consider the coefficient of  $\theta_1$  in the expression for  $F_1$  i.e.  $k_{12}$ .



For convenience  $\ell$  is taken as unity. Since the dimensions of each  $k_{ij}$  are known  $\ell$ ,  $\ell^2$  or  $\ell^3$  is easily inserted as appropriate at a later stage.

$$k_{12} = \frac{Eb}{12} \int_0^1 (d_1^3 - 3d_1^2mx + 3d_1m^2x^2 - m^3x^3) (-4 + 6x)(-6 + 12x)dx$$

After multiplication and integration the substitution  $m = (d_1 - d_2)/\ell$  is made ( $m = d_1 - d_2$  in this case where  $\ell$  is taken as unity) and re-introducing the  $\ell$

$$k_{12} = \frac{Eb}{12} \cdot \frac{1}{\ell^2} (3d_1^3 + 1.2d_1^2d_2 + 0.6d_1d_2^2 + 1.2d_2^3).$$

The other 15 elements of the stiffness matrix are found in the same way. The complete matrix is

$$\frac{Eb}{12} \begin{bmatrix} \frac{1}{\ell^3} \left[ \begin{matrix} 4.2d_1^3 + 1.8d_1^2d_2 \\ + 1.8d_1d_2^2 + 4.2d_2^3 \end{matrix} \right] & \frac{1}{\ell^2} \left[ \begin{matrix} 3d_1^3 + 1.2d_1^2d_2 \\ + 0.6d_1d_2^2 + 1.2d_2^3 \end{matrix} \right] & -k_{11} & \frac{1}{\ell^2} \left[ \begin{matrix} 1.2d_1^3 + 0.6d_1^2d_2 \\ + 1.2d_1d_2^2 + 3d_2^3 \end{matrix} \right] \\ & \frac{1}{\ell} \left[ \begin{matrix} 2.2d_1^3 + d_1^2d_2 \\ + 0.4d_1d_2^2 + 0.4d_2^3 \end{matrix} \right] & -k_{12} & \frac{1}{\ell} \left[ \begin{matrix} 0.8d_1^3 + 0.2d_1^2d_2 \\ + 0.2d_1d_2^2 + 0.8d_2^3 \end{matrix} \right] \\ \text{Symmetric} & & -k_{11} & -k_{14} \\ & & & \frac{1}{\ell} \left[ \begin{matrix} 0.4d_1^3 + 0.4d_1^2d_2 \\ + d_1d_2^2 + 2.2d_2^3 \end{matrix} \right] \end{bmatrix} \quad (6.5.1)$$

While these expressions are more complicated than those obtained using only a partial expansion of  $(d_1 - mx)^3$ , the discrepancy between right- and left-hand versions of the same beam now disappears and it is found that bigger differences between  $d_1$  and  $d_2$  compared with the



values used in 6.4 can be used without increasing the errors in the displacements.

It will also be seen in 6.5.1 above, that when the taper is zero  $d_1 = d_2$  and the stiffness matrix here and the less accurate version of 6.4.7 reduce to exactly the same form as the stiffness matrix derived for a uniform beam in 6.1.1 since  $\frac{bd_1^3}{12} = I$ .

As a check of this improved stiffness matrix, a cantilever was considered as a single element acted on by an end force and an end couple separately.

An expression for the end deflection of a cantilever subjected to an end force has already been found

$$w = \frac{12F}{Eb} \frac{l^3}{d_1^3} \left[ \frac{d_1^3}{(d_1-d_2)^3} \ln \left( \frac{d_1}{d_2} \right) - \frac{d_1^2}{(d_1-d_2)^2} - \frac{d_1}{2(d_1-d_2)} \right]$$

Similarly if an end couple  $M$  is applied, the end deflection may be shown to be

$$w = \frac{6Ml^2}{Ebd_1^2d_2} \quad \text{where } d_2 \text{ is the depth of the beam at its free end.}$$

For various values of  $d_2/d_1$  the end deflections were calculated for an end force and an end couple acting separately using these expressions. Values of end deflections were also found for a single finite element using the stiffness matrix of 6.5.1 and the



error in the value obtained by the finite element method was found in each case. The results are shown in Table 6.1.

Ratio of depths $d_2/d_1$	Percentage error in end deflection	
	End force	End couple
0.1	-9.5	-30.2
0.2	-1.4	- 2.4
0.5	-1.9	+ 3.4
0.8	-0.5	+ 0.2
1.0	0	0
1.25	-1.0	- 0.2
1.5	-3.6	- 1.5
2.0	-12.3	- 7.3
5.0	-61.3	-54.1

TABLE 6.1

While these results will not necessarily apply to beams with other types of loading, the similarity between the errors for a force and a couple suggest that they may at least be used as a guide. It will be seen that within the range  $0.8 < d_2/d_1 < 1.25$  errors do not exceed 1% and it is suggested that values within this range should be used.

It is interesting to note that errors for both forces and couples increase rapidly at values of  $d_2/d_1$  of about 0.2 and 1.5. It will be noted that 1.5 is not the reciprocal of 0.2 and the errors at



$d_2/d_1 = \frac{1}{0.2} = 5$  are very different from the errors at  $d_2/d_1 = 0.2$ .

This lack of symmetry between the two ends of the beam was thought worthy of further investigation.

6.6 Further investigation of the errors in the end deflection of a finite element of varying taper

As shown in Table 6.1 above, for values of  $d_2/d_1$  outside the range 0.8 to 1.25, the stiffness matrix of 6.5.1 gives increasingly inaccurate results for the end deflection of a cantilever using only one element. To investigate this effect, the cantilever of Fig. 6G. with an end couple was considered.

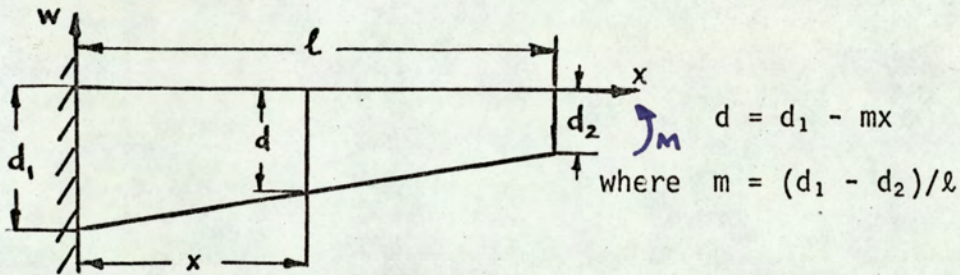


Fig. 6G

$d = d_1 - mx$   
 where  $m = (d_1 - d_2)/l$

From the usual expression for the curvature of a beam

$EI \frac{d^2w}{dx^2} = M$ , and noting that  $I = \frac{b}{12} (d_1 - mx)^3$  it may be shown

that the deflection  $w$  is given by

$$w \cdot \frac{Eb}{12M} = \frac{1}{2m^2(d_1-mx)} - \frac{x}{2md_1^2} - \frac{1}{2m^2d_1} \tag{6.6.1}$$

If  $-1 < (1 - \frac{d_2}{d_1}) \frac{x}{l} < 1$ , the first term may be expanded as a series giving

$$w \cdot \frac{Eb}{12M} = \frac{1}{2d_1^3}x^2 + \frac{1-r}{2d_1^3l}x^3 + \frac{(1-r)^2}{2d_1^3l^2}x^4 + \dots + \frac{1}{2d_1^3}(\frac{1-r}{l})^{p-2}x^p + \dots \tag{6.6.2}$$

where  $r = d_2/d_1$ .



It may be noted that if  $r = 1$  (i.e. a uniform beam) all terms except the first are zero, so that an exact value of  $w$  is obtained with a single term.

Now for a single finite element, the assumed shape is given by

$$w = a_1 + a_2 x + a_3 x^2 + a_4 x^3 \quad (6.6.3)$$

From the known end conditions  $w_1 = \theta_1 = 0$  and the known nodal forces  $F_2 = 0$ ,  $M_2 = M$  the end deflection  $w_2$  and the end slope  $\theta_2$  may be found by using the stiffness matrix 6.5.1. Then since  $w_1 = \theta_1 = 0$ , obviously in 6.6.3 above  $a_1 = a_2 = 0$  and from the values of  $w_2$  and  $\theta_2$ ,  $a_3$  and  $a_4$  may be found.

These are

$$a_3 = \frac{12M}{Eb} \frac{2.5(8r^2+3r-1)}{d_1^3(r^6+4r^5+10r^4+20r^3+10r^2+4r+1)}$$

$$a_4 = \frac{12M}{Eb} \frac{2.5(-3r^3-r^2+r+3)}{d_1^3(r^6+4r^5+10r^4+20r^3+10r^2+4r+1)}$$

By comparing the coefficients of 6.6.2 and 6.6.3 it will be seen that although the two expansions agree in that the constant and the coefficient of  $x$  are both zero, the coefficients of  $x^2$  and  $x^3$  are different. The assumed series 6.6.3 does not merely truncate 6.6.2 but modifies the first two coefficients.

It is therefore not possible to find the error in the finite element solution by summing terms containing  $x^4$  and higher powers in 6.6.2 but since 6.6.1 is exact, the difference between 6.6.3 and 6.6.1



will give the error. Hence by substituting  $x = l$  in these two equations the error in the end deflection is found.

$$\text{This is } \left[ \frac{5r(5r^3+2r^2+r+2)}{r^6+4r^5+10r^4+20r^3+10r^2+4r+1} - 1 \right] \times 100\% \quad (6.6.4)$$

Substitution of a particular value of  $r$  in 6.6.4 is found to give the same value as that obtained by direct comparison and previously recorded in Table 6.1.

Since with this particular type of loading  $a_1 = a_2 = 0$   
6.6.3 reduces to  $w = a_3x^2 + a_4x^3$   
and  $\frac{d^2w}{dx^2} = 2a_3 + 6a_4x$

There will therefore be a point of contraflexure when  
 $2a_3 - 6a_4x = 0$  i.e. when  $x = -a_3/3a_4$ .

Now if  $a_3$  and  $a_4$  have opposite signs this will give a positive value of  $x$ .

$r < 1$   $a_4$  is positive for all values of  $r$   
 $a_3$  is negative if  $8r^2 + 3r - 1 < 0$   
i.e. when  $r < 0.21$  (the only positive value of  $r$ )

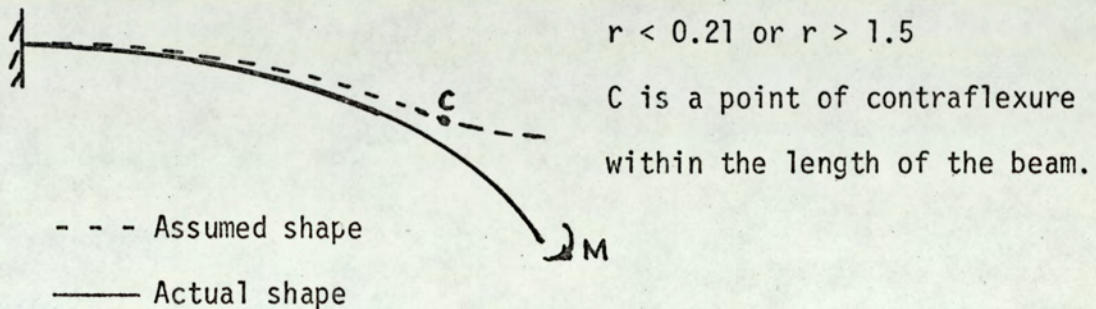
$r > 1$   $a_3$  is positive for all values of  $r$   
 $a_4$  is negative for all values of  $r$

Hence  $-a_3/3a_4$  is always positive but if  $\frac{-(8r^2+3r-1)l}{3(-3r^3-r^2+r+3)} < l$

the point of contraflexure will lie within the length of the beam. This occurs if  $r > 1.5$  approx.



If therefore  $r < 0.21$  or  $r > 1.5$  the point of contraflexure will lie within the length of the beam and will move towards the fixed end as  $r$  becomes smaller or greater respectively. The difference between the actual and assumed shapes of the beam will then increase rapidly



It is gratifying to observe that these two values of  $r$  are in complete agreement with values of 0.2 and 1.5 already noted from Table 6.1 at which errors begin to increase rapidly.

It should perhaps be repeated that while these exact results will not necessarily apply to other types of loading there is evidence to suggest that similar values of  $r$  will be obtained, so on no account should  $r$  be less than 0.2 or greater than 1.5

It is probably safer to use a more restricted range  $0.8 < r < 1.25$  to obtain a higher degree of accuracy, while if the stiffness matrix of 6.5.1 is applied to a uniform beam the error in the end deflection is zero.



In view of the results obtained here, the stiffness matrix of 6.5.1 was used in subsequent work, the above limits on the ratio of depths being observed.

### 6.7 End deflection of a uniform wedge

In 6.6 the behaviour of a single tapered element of a beam was investigated. In cases where a distributed load is applied, the beam must be divided into a number of elements so that equivalent "lumped" loads may be applied at the nodes. It was thought that the wedge shown in Fig.6.H, a problem for which an exact solution has been obtained in 3.3 would be a suitable test for the finite element method using the improved stiffness matrix of 6.5.1. For comparison the end deflection given by elementary beam theory was also calculated.

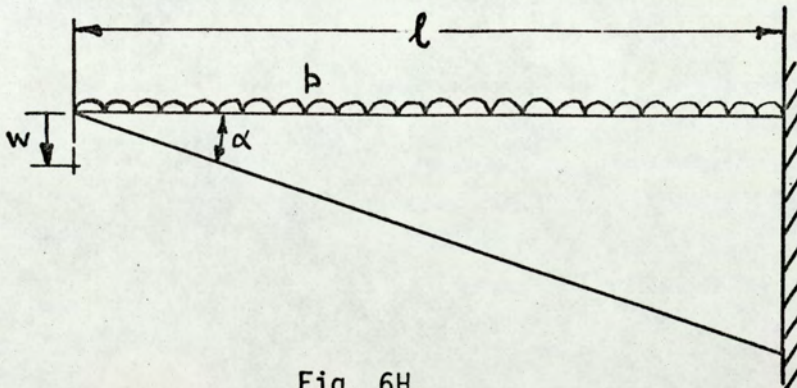


Fig. 6H.

The three methods used to find the end deflection were:-

- (a) Exact solution using the methods of the theory of elasticity.

The result found in 3.3.6 above is repeated here

$$w = \frac{pl}{E(\tan\alpha - \alpha)} \left[ (1+\nu) + (1-\nu) \frac{\alpha}{\tan\alpha} + 2\ln(\sec\alpha) \right]$$



(b) Elementary beam theory

$$\text{This gave } w = \frac{6p\ell}{E\alpha^3} \quad (6.7.1)$$

(c) Finite element solution using the improved stiffness matrix for a tapered beam-type element of 6.5.1. In this case 20 elements were used, for the first 19 of which a ratio  $d_2/d_1 = 0.8$  was used. The lengths of the elements will therefore decrease as the free end of the beam is approached, but these 19 elements will account for 98.6% of the length of the beam.

The length of the twentieth element will then be the remaining 1.4% of the length of the beam and  $d_2$  will be zero. This value of  $d_2$  may give rise to considerable error for this particular element, but since it represents such a small part of the whole the effect on the beam as a whole should be negligible. The stiffness matrix for the beam was assembled and the displacements calculated by means of a computer program (Prog.4.).

The results obtained for the end deflection using the three methods are shown in Table 6.2.



Angle $\alpha$ degrees	End deflection $\div p\ell/Eb$		
	(a)Exact solution	(b)Beam theory	(c)Finite element (20 elements)
5	9027.2	8959.8	8954.3
10	1127.9	1094.5	1093.8
15	333.9	311.9	311.7
20	140.6	124.4	124.4
25	71.8	59.2	59.1
30	41.3	31.2	31.2

TABLE 6.2

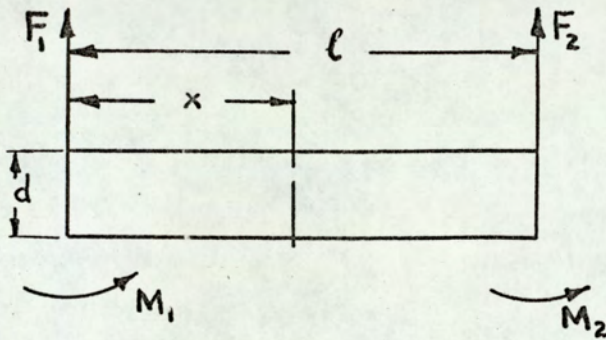
It will be seen that (b) and (c) give almost identical results for all values of  $\alpha$ , thus providing another check on the use of the finite element method. It is interesting to note that both these methods will give inaccurate results since they both neglect all stresses except the longitudinal stress, while method (a) allows for all three coplanar stresses. The resulting error is however only about 0.5% when  $\alpha = 5^\circ$ , but this increases to about 25% when  $\alpha = 30^\circ$ . This confirms that the simple beam theory will give satisfactory results providing the depth of a beam is small in comparison with its length, but as these two dimensions become similar the beam theory will give increasingly inaccurate results.

6.8 Effect of shear stress on the stiffness matrix of an element of a beam

Table 6.2 shows that the finite element method gives rather



poor results for the end deflection of a wedge as the angle of taper increases. This is almost completely due to the neglect of shear stresses which will affect the beam deflection appreciably for large tapers. Severn shows [11] how the effect of shear stress may be allowed for in the stiffness matrix of a parallel beam. This method assumes that stresses vary in a particular way, and to obtain experience in the use of this method the stiffness matrix for a uniform beam was first derived, and the same method was then applied to a tapered element.



The assumed stresses for the element shown in Fig. 6J were:-  
 Bending stress  $\sigma = y(A_1 + A_2)x$   
 Shear stress  $\tau = (1 - 4y^2/d^2)A_3$  (6.8.1)

Fig. 6J.

Also from Fig. 6J  $\sigma = M_1y/I - F_1xy/I$  (6.8.2)

Comparison of the coefficients of 6.8.1 and 6.8.2 gives  $A_1$  and  $A_2$ .

Equilibrium of stresses requires that  $\frac{\partial \sigma}{\partial x} + \frac{\partial \tau}{\partial y} = 0$  and hence  $A_3$  may be found.

Assume initially that the right hand end of the element is fixed

$$\text{Then } \begin{Bmatrix} \sigma \\ \tau \end{Bmatrix} = \begin{bmatrix} (-12/bd^3)xy & (12/bd^3)y \\ f & 0 \end{bmatrix} \begin{Bmatrix} F_1 \\ M_1 \end{Bmatrix}$$

where  $f = (-3/2bd)(1 - 4y^2/d^2)$



and hence

$$\begin{Bmatrix} \epsilon \\ \gamma \end{Bmatrix} = \frac{1}{E} \begin{bmatrix} (-12/bd^3)xy & (12/bd^3)y \\ 2(1+\nu)f & 0 \end{bmatrix} \begin{Bmatrix} F_1 \\ M_1 \end{Bmatrix}$$

For a linear elastic material the complementary strain energy is equal to the strain energy

$$\begin{aligned} \text{Hence } U^* &= b \int_0^{\ell} dx \int_0^d \{\sigma\}^t \{\epsilon\} dy \\ &= \frac{1}{EB} \int_0^{\ell} \left( \frac{6}{d^3} x^2 F_1^2 + \frac{6}{5} \frac{(1+\nu)}{d} F_1^2 - \frac{12}{d^3} x F_1 M_1 + \frac{6}{d^3} M_1^2 \right) dx \end{aligned} \quad (6.8.3)$$

(a) Uniform element

Since  $d$  is constant 6.8.3 is easily integrated giving

$$U^* = \frac{1}{EB} \left[ \frac{2}{d^3} \ell^3 F_1^2 + \frac{6}{5} (1+\nu) \frac{\ell}{d} F_1^2 - \frac{6}{d^3} \ell^2 F_1 M_1 + \frac{6}{d^3} \ell M_1^2 \right] \quad (6.8.4)$$

Also the complementary energy of the nodal forces is

$$\Omega^* = -F_1 w_1 - M_1 \theta_1$$

and the total complementary energy

$$V^* = U^* + \Omega^*$$

Using the principle of stationary total complementary energy

$$\delta V^* = 0 \quad \therefore w_1 = \frac{\partial U^*}{\partial F_1} \quad \text{and} \quad \theta_1 = \frac{\partial U^*}{\partial M_1}$$

Hence from 6.8.4

$$\begin{Bmatrix} w_1 \\ \theta_1 \end{Bmatrix} = \frac{1}{E} \begin{bmatrix} r_1 & r_2 \\ r_2 & r_3 \end{bmatrix} \begin{Bmatrix} F_1 \\ M_1 \end{Bmatrix}$$

$$\text{where } r_1 = \frac{4\ell^3}{bd^3} + \frac{12}{5}(1+\nu) \frac{\ell}{bd}$$

$$r_2 = -\frac{6\ell^2}{bd^3}$$

$$r_3 = \frac{12\ell}{bd^3}$$



The flexibility matrix may be inverted, and substituting for  $r_1, r_2$  and  $r_3$

$$\begin{Bmatrix} F_1 \\ M_1 \end{Bmatrix} = \frac{12}{\ell^2 + 12g} \frac{EI}{\ell} \begin{bmatrix} 1 & \frac{\ell}{2} \\ \frac{\ell}{2} & \frac{\ell^2}{3} + g \end{bmatrix} \begin{Bmatrix} w_1 \\ \theta_1 \end{Bmatrix} \quad \text{where } g = (1+\nu)d^2/5$$

This gives only one quarter of the stiffness matrix for the element, but using its symmetry  $k_{ij} = k_{ji}$ .

Also equilibrium conditions required that  $F_2 = -F_1$  so that  $k_{3j} = -k_{1j}$ , and  $M_2 = F_1\ell - M_1$  giving  $k_{4j} = \ell k_{1j} - k_{2j}$ .

The complete stiffness matrix is then found to be

$$\frac{12}{\ell^2 + 12g} \frac{EI}{\ell} \begin{bmatrix} 1 & \frac{\ell}{2} & -1 & \frac{\ell}{2} \\ & \frac{\ell^2}{3} + g & -\frac{\ell}{2} & \frac{\ell^2}{6} - g \\ & & 1 & -\frac{\ell}{2} \\ \text{Symmetric} & & & \frac{\ell^2}{3} + g \end{bmatrix} \quad (6.8.5)$$

which agrees with the result obtained by Severn.

(b) Tapered element

If  $d_1$  and  $d_2$  are the depths at the ends of the beam (see Fig.6E of 6.4), then, assuming uniform taper  $d = d_1 - mx$  where  $m = (d_1 - d_2)/\ell$ .



Hence from 6.8.3

$$U^* = \frac{1}{Eb} \left[ \left\{ \frac{3}{m} \frac{\ell^2}{d_2^2} - \frac{6}{m^2} \frac{\ell}{d_2} + \frac{6}{m^3} \ln \left( \frac{d_1}{d_2} \right) + \frac{6}{5} (1+\nu) \frac{1}{m} \ln \left( \frac{d_1}{d_2} \right) \right\} F_1^2 \right. \\ \left. - \left\{ \frac{6}{m} \frac{\ell}{d_2^2} - \frac{6}{m^2} \left( \frac{1}{d_2} - \frac{1}{d_1} \right) \right\} F_1 M_1 + \frac{3}{m} \left\{ \frac{1}{d_2^2} - \frac{1}{d_1^2} \right\} M_1^2 \right]$$

Again  $w_1 = \frac{\partial U^*}{\partial F_1}$  and  $\theta_1 = \frac{\partial U^*}{\partial M_1}$

Hence 
$$\begin{Bmatrix} w_1 \\ \theta_1 \end{Bmatrix} = \frac{1}{E} \begin{bmatrix} r_1 & r_2 \\ r_2 & r_3 \end{bmatrix} \begin{Bmatrix} F_1 \\ M_1 \end{Bmatrix}$$

where  $r_1 = \frac{6}{m} \frac{\ell^2}{d_2^2} - \frac{12}{m^2} \frac{\ell}{d_2} + \left\{ \frac{12}{m^3} + \frac{12}{5} \frac{(1+\nu)}{m} \right\} \ln \left( \frac{d_1}{d_2} \right)$

$$r_2 = - \left\{ \frac{6}{m} \frac{\ell}{d_2^2} - \frac{6}{m^2} \left( \frac{1}{d_2} - \frac{1}{d_1} \right) \right\} \tag{6.8.6}$$

$$r_3 = \frac{6}{m} \left( \frac{1}{d_2^2} - \frac{1}{d_1^2} \right)$$

As in (a), the flexibility matrix may be inverted to give one quarter of the stiffness matrix for the element and the same methods as in (a) may be used to find the other elements of the matrix.

Hence 
$$[K] = \frac{Eb}{r_1 - r_4} \begin{bmatrix} 1 & \frac{\ell d_1}{d_1 + d_2} & -1 & \frac{\ell d_2}{d_1 + d_2} \\ \frac{r_1}{r_3} & -\frac{\ell d_1}{d_1 + d_2} & \frac{\ell^2 d_1}{d_1 + d_2} - \frac{r_1}{r_3} & \\ & 1 & -\frac{\ell d_2}{d_1 + d_2} & \\ \text{Symmetric} & & \frac{r_1}{r_3} - \frac{\ell^2 (d_1 - d_2)}{d_1 + d_2} & \end{bmatrix} \tag{6.8.7}$$



where  $r_1, r_2, r_3$  are as given in 6.8.6

and  $r_4 = r_2^2/r_3$

It may be shown that when  $d_1 = d_2$  the stiffness matrix of 6.8.7 reduces to exactly the same form as the matrix of 6.8.5 derived for a uniform element.

It was initially found that the stiffness matrix of 6.8.7 was giving very inaccurate values for the end deflection of a tapered cantilever. Further investigations showed that the error appeared to be in the calculated value of  $r_1$ . It was further found that the first two terms in the expression for  $r_1$  in 6.8.6 almost exactly cancelled  $\frac{12}{m^3} \ln\left(\frac{d_1}{d_2}\right)$  in the last term, so that a small error in any one of these terms could result in a very large error in the value of  $r_1$ .

This difficulty was avoided by writing  $\frac{d_1}{d_2}$  as  $1 - \left(\frac{d_1}{d_2} - 1\right)$  and so expanding  $\ln\left(\frac{d_1}{d_2}\right)$  as a series. This is only possible if

$-1 < \frac{d_1}{d_2} - 1 < 1$  or  $0 < \frac{d_1}{d_2} < 2$ . It is then found that the first two

terms of  $r_1$  cancel with the first two terms of the expansion after multiplication by  $-\frac{12}{m^2}$  so that

$$r_1 = \frac{12\ell^3}{d_2^3} \left\{ \frac{1}{3} - \frac{1}{4} \left( \frac{d_1}{d_2} - 1 \right) + \frac{1}{5} \left( \frac{d_1}{d_2} - 1 \right)^2 - \frac{1}{6} \left( \frac{d_1}{d_2} - 1 \right)^3 + \dots \right\} + \frac{12}{5} (1+\nu) \frac{\ell}{d_1 - d_2} \ln\left(\frac{d_1}{d_2}\right) \quad (6.8.8)$$



A computer will easily sum this series to any required degree of accuracy. It was found that inclusion of terms greater than  $10^{-4}$  gave satisfactory results and this required the evaluation of 8 terms when  $d_1/d_2 = 1.25$ , but note that the series will converge increasingly slowly as  $d_1/d_2$  approaches 2 or 0. In the case of the upper limit this difficulty can be avoided by increasing the number of elements, but there appears to be no way of overcoming the difficulty as  $d_1/d_2$  approaches 0.

Reference to 6.8.6 shows that when  $d_1$  (or  $d_2$ ) = 0 then  $r_1$ ,  $r_2$  and  $r_3$  all become infinite and it is therefore impossible to evaluate the elements of the stiffness matrix of 6.8.7. This difficulty appears to arise from the physical nature of the problem of a beam of zero depth carrying a shear force and therefore subjected to an infinite shear stress. In the case of the uniform wedge tapering to a point discussed later in this section, a satisfactory result was obtained by using a small but finite depth at the pointed end. This may introduce a small error, but does enable a solution to be obtained.

The uniform wedge previously considered in 3.3 and 6.7 gave solutions which were in good agreement for small values of  $\alpha$ , but the finite element method of 6.7 gave increasingly poor results as  $\alpha$  increased, due to the total neglect of the effects of shear stress. This problem was re-examined using the stiffness matrix of 6.8.7. Unfortunately, as noted above,  $r_1$ ,  $r_2$  and  $r_3$  all became infinite for the last element where  $d_2 = 0$ . To avoid this difficulty a common ratio  $d_2/d_1 = 0.9$  was used for 85 elements which accounted for



99.99% of the beam. The remaining 0.01% was neglected. It was also thought possible that replacing a distributed load by a number of point loads might affect the shear deflection as a constant shear force is assumed in each element whereas it actually varies. (The same problem is not encountered with moments as the finite element method allows for variation of bending moment within the element). A second solution was therefore obtained for 100 elements of equal length and assuming an arbitrary ratio  $d_2/d_1 = 0.5$  for the last element. The results obtained by these two methods were almost identical, thus confirming that the neglect of the last element and the arbitrary ratio chosen for  $d_2/d_1$  have negligible effect on the end deflection.

Taking the solution from the stress function of 3.3 as exact and taking  $\nu = 0.3$ , Fig.6.8.1 shows how the errors for the two finite element solutions, i.e. (a) neglecting and (b) allowing for shear stress, vary with the angle of taper. It will be seen that both methods give reasonable results up to about  $10^\circ$ , and the solution using shear stress gives acceptable results up to perhaps  $20^\circ$ . For larger angles the errors increase rapidly, and the allowance for shear stress appears almost exactly to halve the error obtained when shear stress is neglected. Unfortunately the assumed stress pattern of 6.8.1 differs increasingly from the actual stress distribution, so that even 6.8.7 gives poor results for large angles.

The assumed stresses are easily calculated from 6.8.1 and the exact expressions for the stresses  $\sigma_r$  etc. in a uniform wedge have already been derived in 3.3.5. By the usual method of transformation



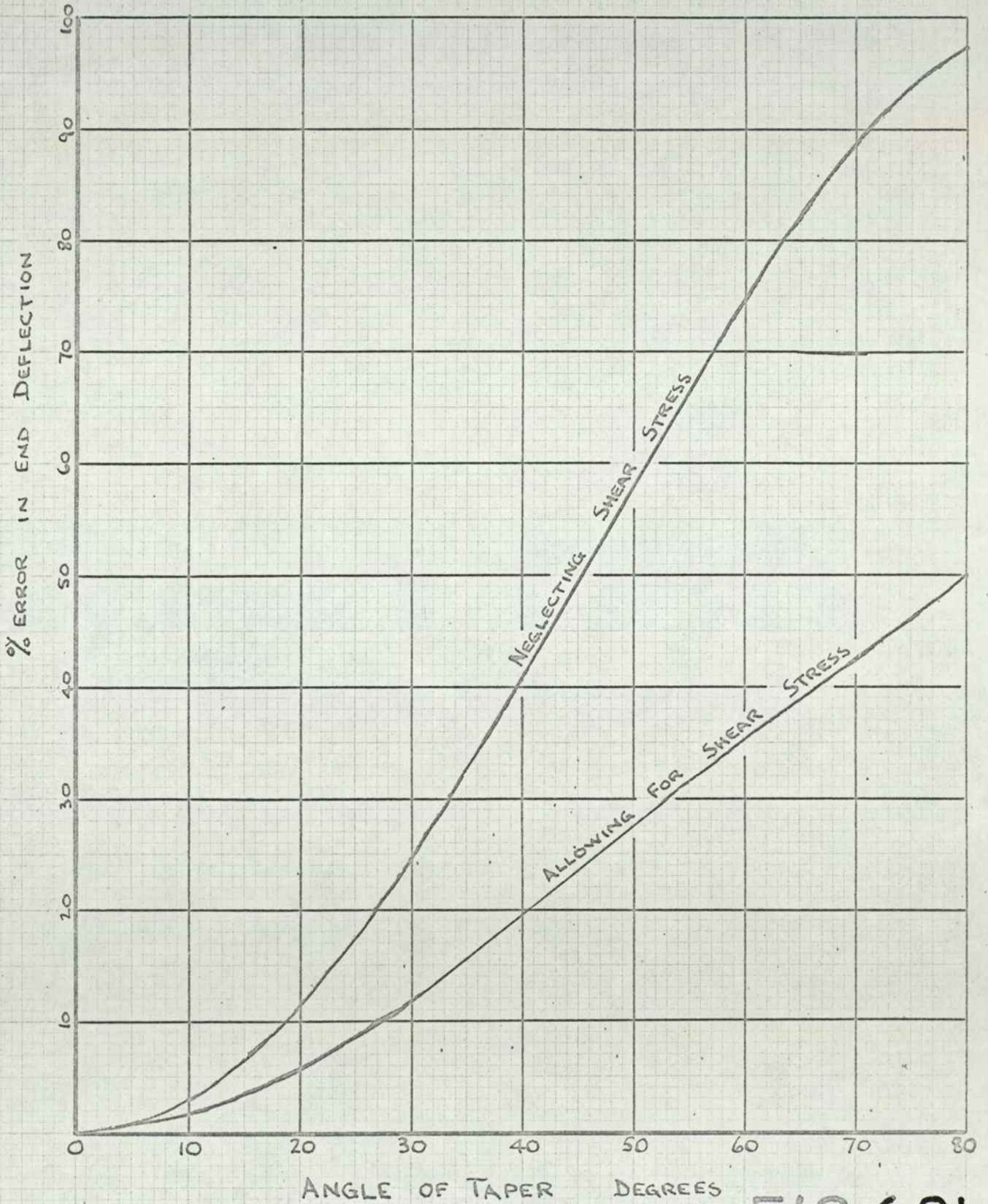
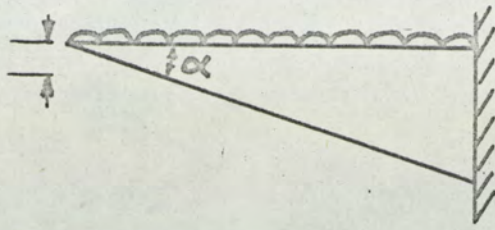


FIG. 6.8.1



of coordinates it is then possible to find the stresses  $\sigma_x$  and  $\tau_{xy}$  corresponding to the assumed bending and shear stresses.

Fig. 6.8.2 shows that for an angle of taper of  $10^\circ$  it is not possible to show any difference between the exact and assumed values of  $\sigma_x$ , and while the exact and assumed shear stresses differ considerably their values are small in comparison with  $\sigma_x$ . At  $50^\circ$  exact and assumed values of  $\sigma_x$  are still in reasonable agreement, but because of the much larger relative values of  $\tau_{xy}$  compared with the  $10^\circ$  taper the great differences between exact and assumed values are now of considerable importance. As Fig. 6.8.2 shows, at  $50^\circ$  the error in the end deflection is about 27% and becomes even greater at larger angles.

### 6.9 General solution for a tapered beam

So far, only cantilevers had been considered, and because the same two displacements were always zero, a particular type of stiffness matrix was obtained. In this section a solution was obtained for a beam with any number of supports (rigid or elastic) which could be at any point on the beam. A computer program (Prog.5) was written to compile the stiffness matrix and to determine the displacements in the usual way. The improved stiffness matrix of 6.5.1 was used, so that the effect of shear stress was neglected, but this will have negligible effect in most beam problems. If, however, it is desired to include shear effects, the stiffness matrix 6.8.7 could be used instead of 6.5.1 giving increased accuracy (slight in most cases) at the expense of increased computation time.



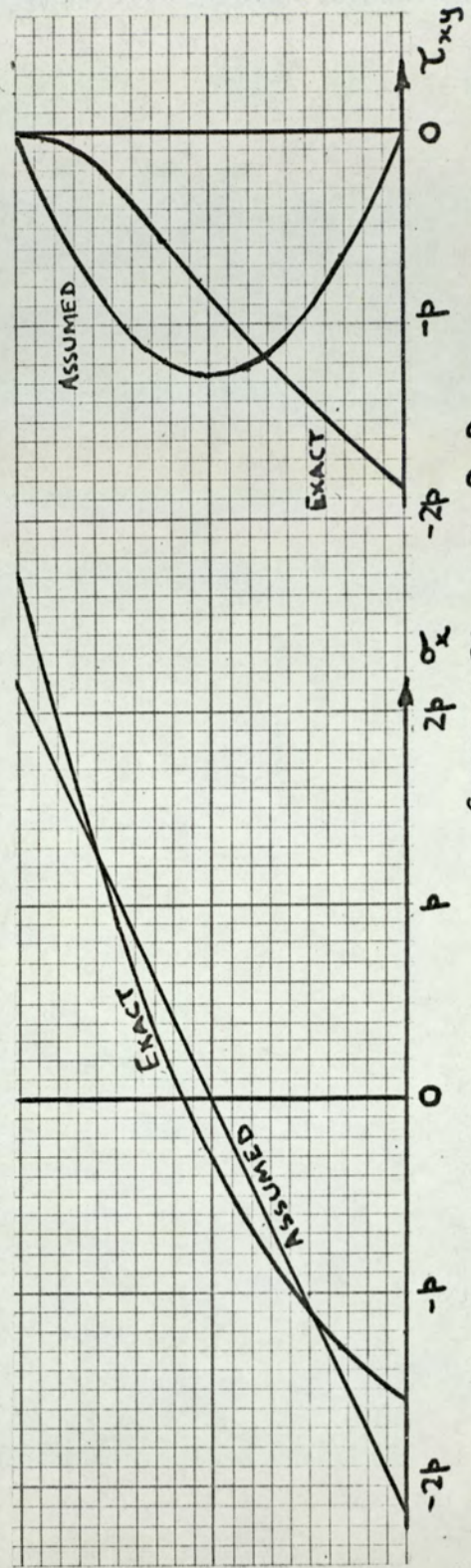
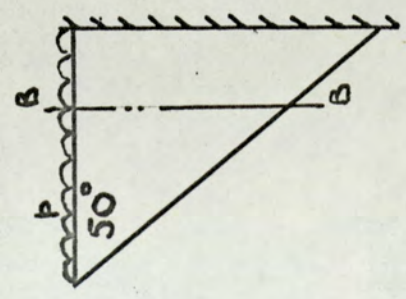
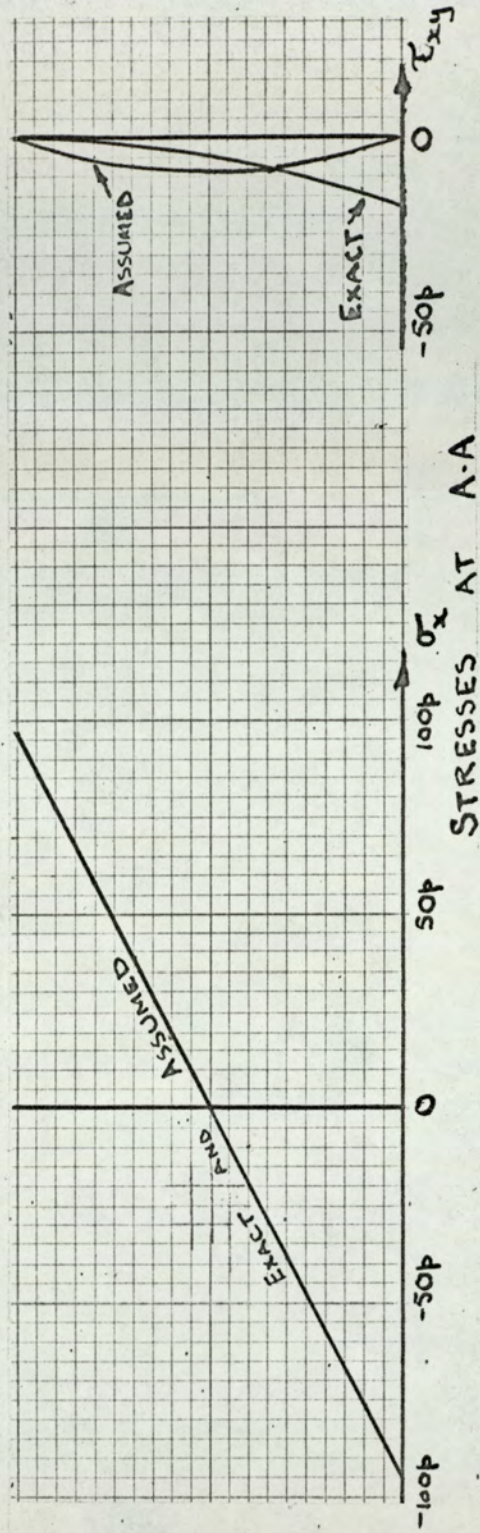
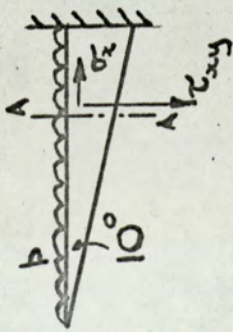


FIG. 68.2.

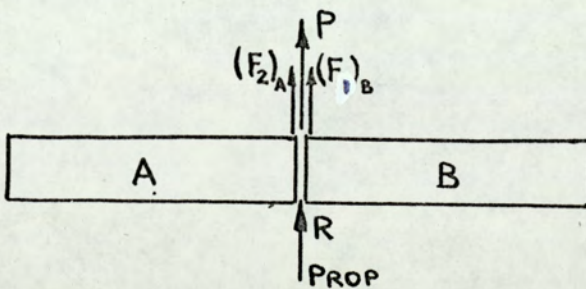


In order to allow a support at any node, if the beam is divided into  $N$  elements, the stiffness matrix must contain  $2N + 2$  rows. The appropriate row and column are then deleted for each rigid support since the displacement is then zero. This procedure is described in more detail in the Appendix.

Once the displacements have been calculated it is then a simple matter to substitute back to find the nodal forces and couples, and so to calculate the maximum bending stress at each node. Prog 5 was written so that all these values could be determined.

The values of the forces at all supports were also required, and care was necessary in allowing for any force applied at a node.

For example consider two adjacent elements with a prop and an applied force  $P$  at their common node as shown in Fig. 6K.



It is required to find the prop reaction force  $R$ .

Fig. 6K.

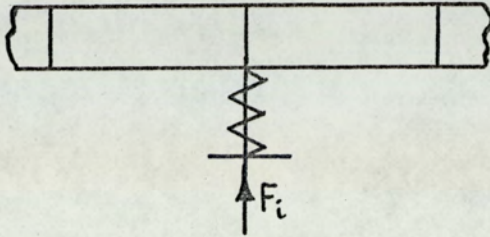
When the displacements at the 3 nodes shown have been calculated, multiplication by the appropriate element of the stiffness matrix will give  $(F_2)_A + (F_1)_B$ . Since the node is in equilibrium

$$R + (F_2)_A + (F_1)_B + P = 0$$

and since  $P$  is known  $R$  is easily calculated.



In the case of an elastic support of known stiffness the method described below was used.



Consider an elastic support at a node where the deflection is  $u_i$ . Then the nodal force  $F_i = -k_s u_i$  where  $k_s$  is the stiffness of the support.

Fig. 6L.

Also  $F_i = k_{ij} u_j \quad j = i-2, i-1, \dots, i+3$

Equating these two expressions for  $F_i$  gives

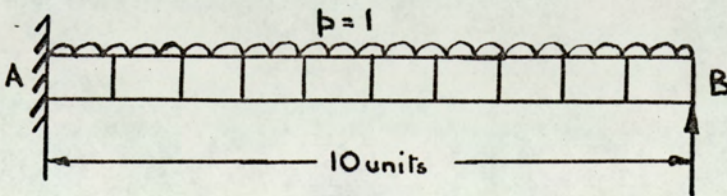
$$-k_s u_i = k_{i,i-2} u_{i-2} + \dots + k_{i,i} u_i + \dots + k_{i,i+3} u_{i+3}$$

or  $0 = k_{i,i-2} u_{i-2} + \dots + (k_{i,i} + k_s)u_i + \dots$

i.e. an elastic support is treated by adding its stiffness to the element on the leading diagonal of the stiffness matrix at that node and taking the nodal force as zero.

The program was checked in the following examples.

Example 1



$b = 12$   
 $d = 1$   
 $E = 3000$



This was a cantilever with a rigid prop carrying a uniformly distributed load. This load was replaced by nodal forces using the static lumping method and 10 elements were used. The results obtained from Prog. 5 were:-

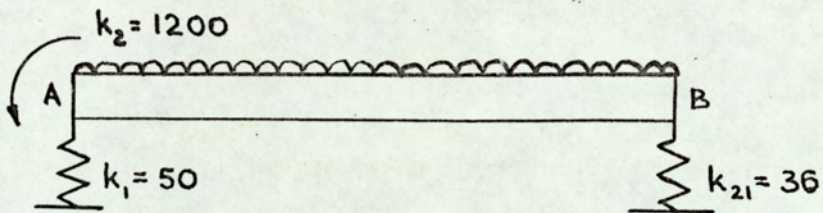
Prop load 3.76 units (3.75 exact value)

Maximum bending moment -7.05 (-7.03)

Maximum deflection - 0.0179 at 6 units from A (-0.0180 at 5.7)

It will be seen that there is very good agreement between the two sets of results

Example 2



Example 1 was modified by introducing the three flexibilities shown in the supports.

The finite element method using Prog.5 gave results:-

Prop load at B 4.27 units (4.266 exact value)

Deflection at B 0.1187 units (0.1185 exact value)

Prog. 5 therefore has been shown to give satisfactory values for prop forces, maximum deflections etc. for beams with either rigid or flexible supports



Further checks were made with several rigid supports, and with a mixture of rigid and flexible supports. These results are not given here, but in all cases it was found that errors in the finite element results were very small, and these could be reduced to negligible proportions by increasing the number of elements.

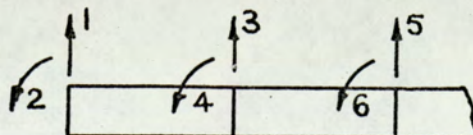
6.10 Use of the general program for a tapered beam (Prog.5)

This program may be used for any linear elastic beam of rectangular section of constant width with any number of supports, either rigid or elastic, and with any type of loading. The solution gives the deflection, bending moment and maximum bending stress at each node, and the force and/or moment at each support.

The following information is presented on data cards:-

1. The value of  $E$  in  $\text{MN/m}^2$ .
2. The width of the beam in mm.
3. The number of elements into which the beam is to be divided.
4. Corresponding values of distance from the left hand end of the beam and its depth at that point starting at the end of the beam. All dimensions to be in mm.

For the remaining sections the following notation is used. Each node is associated with two coordinates, the first (odd) of which denotes a vertical displacement or force (upwards positive) and the second (even) applies to the slope or moment (anticlockwise positive)

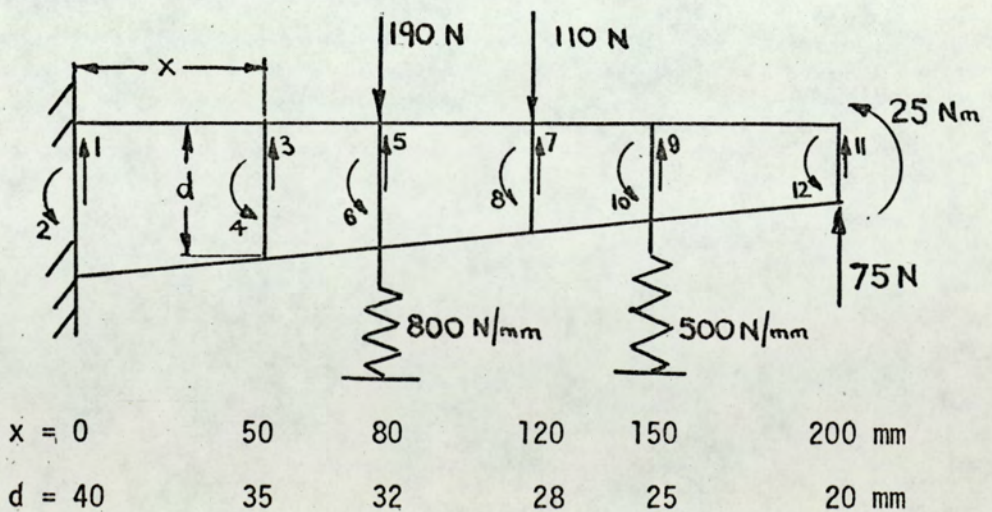




5. Number of rigid supports. (0 if no rigid supports and omit card 6).
6. Position of rigid supports (i.e. give the numbers of the coordinates for which the displacements are zero).
7. Number of elastic supports (0 if no elastic supports and omit card 8).
8. Corresponding values of position (see 6) and stiffness in N/mm (= kN/m) of the elastic supports.
9. Number of applied forces and couples taken together.
10. Corresponding values of position (see 6) and magnitude of any applied force or couple. Values to be in N(forces) Nm x 10<sup>3</sup> (couples).

Values will then be printed for the distance from the left-hand end of the beam in mm, the deflection in mm, the bending moment in Nm, the stress in MN/m<sup>2</sup>, each reaction in N, and each fixing moment in Nm.

Example





The beam shown has a constant width of 18 mm, is rigidly clamped at its left-hand end and there are two elastic supports. Three forces and a couple are applied.  $E = 5000 \text{ MN/m}^2$ . The following data cards are required:-

1. 5000
2. 18
3. 5
4. 0 40 50 35 80 32 120 28 150 25 200 20
5. 2
6. 1 2
7. 2
8. 5 800 9 500
9. 4
10. 5 -190 7 -110 11 75 12 25000

The results of this program are printed in Fig. 6.10.1.

### 6.11 Finite element method applied to a plane stress problem

In the case of a beam-type finite element, there are only four degrees of freedom per element, and since these elements are joined end to end the assembly of the stiffness matrix is relatively simple. It was thought that more would be learned about the complexities of the finite element method by considering a plane stress problem, using triangular elements, for each of which there are six degrees of freedom. In addition, since the assemblage of elements may be arranged in a variety of ways, the assembly of the stiffness matrix will now be considerably more complicated.



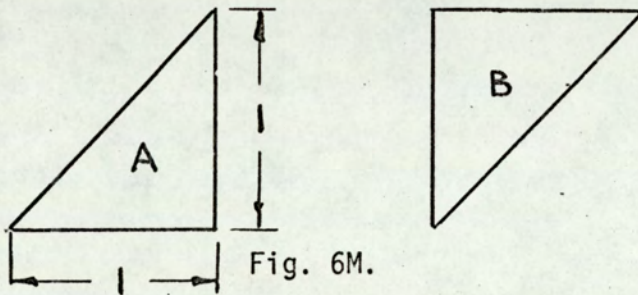
X	DEFLN	B M	STRESS	REACTION	FIXING MT
0,00	0,00	13,123	2,73	384,56	13,123
50,00	-0,02	-6,105	-1,66		
80,00	-0,01	-17,642	-5,74	11,26	
120,00	0,10	-25,875	-11,00		
150,00	0,34	-28,750	-15,33	-170,83	
200,00	1,27	-25,000	-20,83		

FIG. 6.10.1



Since beam-type elements have been shown to give very satisfactory results for bending problems, it was thought that it would be interesting to see how triangular elements could be used in beams [12].

The first requirement was an arrangement of elements which will exactly fit the shape of the beam, and the simplest possible arrangement is a pair of right- and left-hand right-angled  $45^\circ$  triangles, called for convenience A and B triangles, as shown in Fig. 6M.



These may be fitted together to extend either horizontally or vertically. The stiffness matrix for each of these triangles is then required, and since it was envisaged that the global nodes would be numbered as shown in Fig. 6N, the element nodes were numbered in a similar order, i.e. nodal numbers increase upwards and to the left.

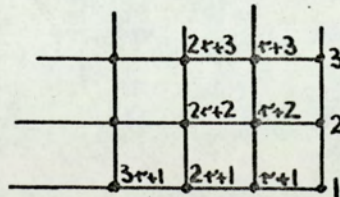


Fig. 6N.



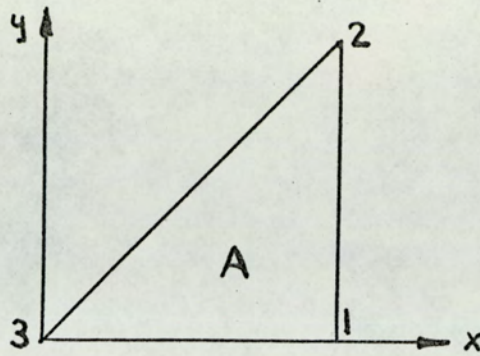


Fig. 6P

Now for triangle A assume that the horizontal and vertical components of the displacement of any point within the element are:-

$$u = \alpha_1 + \alpha_2 x + \alpha_3 y$$

$$v = \alpha_4 + \alpha_5 x + \alpha_6 y$$

where the values of the parameters  $\alpha$  are adjustable.

This displacement pattern is the simplest possible for a plane triangle and implies that each of the three stresses  $\sigma_x$ ,  $\sigma_y$ ,  $\tau_{xy}$  is uniform within any one element.

Now the displacement components  $u$  and  $v$  anywhere within the element may be expressed in terms of the nodal displacements  $u_1, v_1, \dots, v_3$  (or more conveniently as  $u_i$ ,  $i = 1, 2, \dots, 6$ ). The strains can then be found in terms of the  $u_i$ 's, and from the usual linear stress-strain relationships the stresses may be similarly found. Then the strain energy of the element

$$U = \frac{b}{2} \iint \{\sigma\}^t \{\epsilon\} dx dy \quad \text{where } b \text{ is the thickness of the element.}$$

The potential energy of the nodal forces is

$$\Omega = -F_i u_i \quad i = 1, 2, \dots, 6$$



Hence, by using the principle of stationary total potential energy it may be shown that the stiffness matrix for the element is given by:-

$$[K] = b \iint [B]^t [D] [B] dx dy$$

$$\text{where } [B] = \frac{1}{2\Delta} \begin{bmatrix} b_1 & 0 & b_2 & 0 & b_3 & 0 \\ 0 & c_1 & 0 & c_2 & 0 & c_3 \\ c_1 & b_1 & c_2 & b_2 & c_3 & b_3 \end{bmatrix}$$

$$\text{and } [D] = \frac{E}{1-\nu^2} \begin{bmatrix} 1 & \nu & 0 \\ \nu & 1 & 0 \\ 0 & 0 & (1-\nu)/2 \end{bmatrix}$$

$$\begin{aligned} \text{in } [B] \quad b_1 &= y_2 - y_3 \\ c_1 &= x_3 - x_2 \quad \text{etc.} \end{aligned}$$

It may also be shown that the stresses in an element are given by

$$\{\sigma\} = [D] [B] \{u_i\}$$

so that once the nodal displacements have been determined the calculation of stresses is fairly straightforward.

In the case of the present "A" triangle  $b_1 = 1$ ,  $c_1 = -1$ ,  $b_2 = 0$ ,  $c_2 = 1$ ,  $b_3 = -1$ ,  $c_3 = 0$ .

It is then found that:



$$[K]_A = \frac{Eb}{2(1-\nu^2)} \begin{bmatrix} \frac{3-\nu}{2} & -\frac{(1+\nu)}{2} & -\frac{(1-\nu)}{2} & \nu & -1 & \frac{(1-\nu)}{2} \\ & \frac{3-\nu}{2} & \frac{1-\nu}{2} & -1 & \nu & -\frac{(1-\nu)}{2} \\ & & \frac{1-\nu}{2} & 0 & 0 & -\frac{(1-\nu)}{2} \\ & & & 1 & -\nu & 0 \\ & \text{Symmetric} & & & 1 & 0 \\ & & & & & \frac{1-\nu}{2} \end{bmatrix}$$

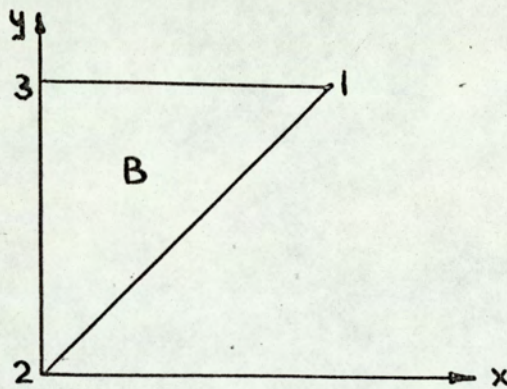


Fig. 6Q.

Similarly for triangle B.

This is numbered in accordance with the chosen scheme. Again let the perpendicular sides be of unit length.

$$\begin{aligned} \text{Then } b_1 &= -1, & b_2 &= 0, & b_3 &= 1 \\ c_1 &= 0, & c_2 &= 1, & c_3 &= -1 \end{aligned}$$



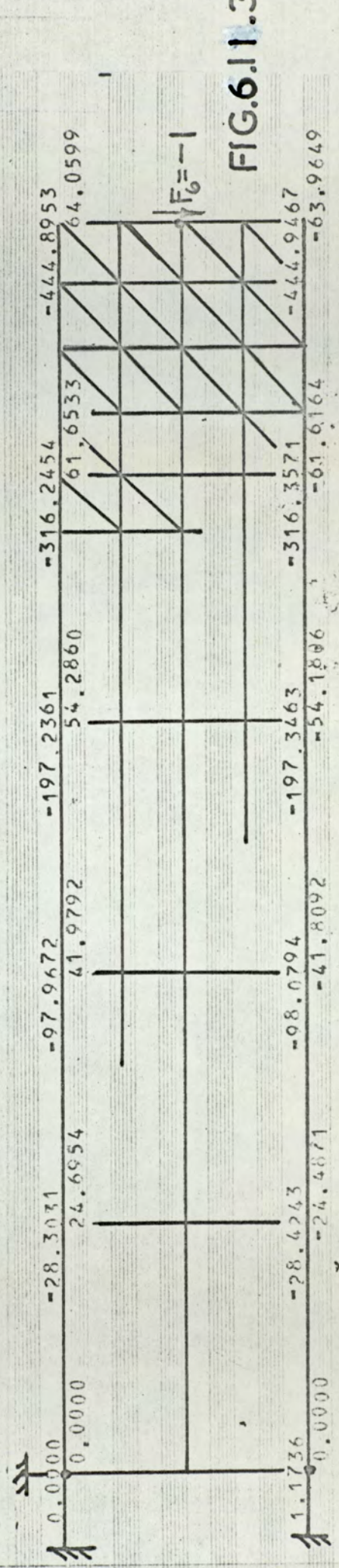
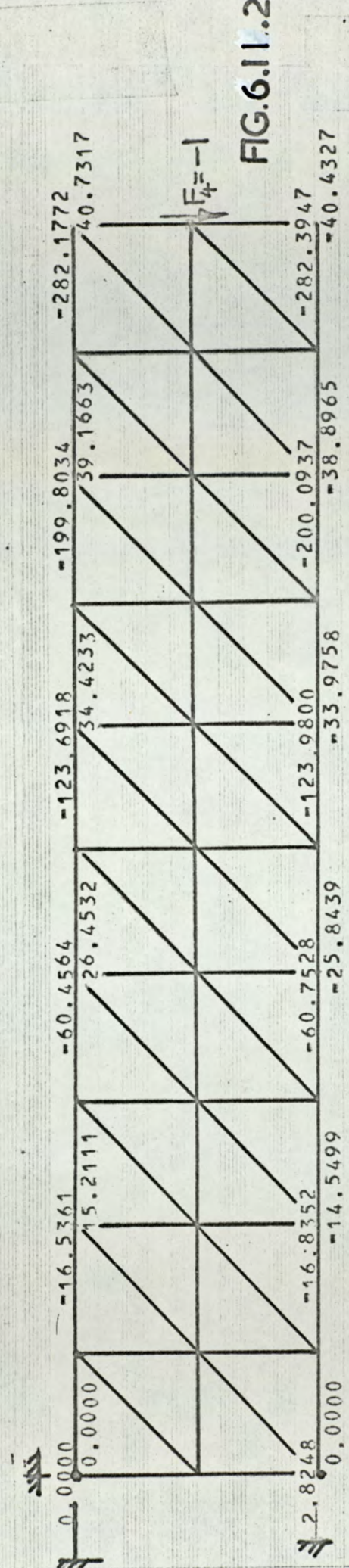
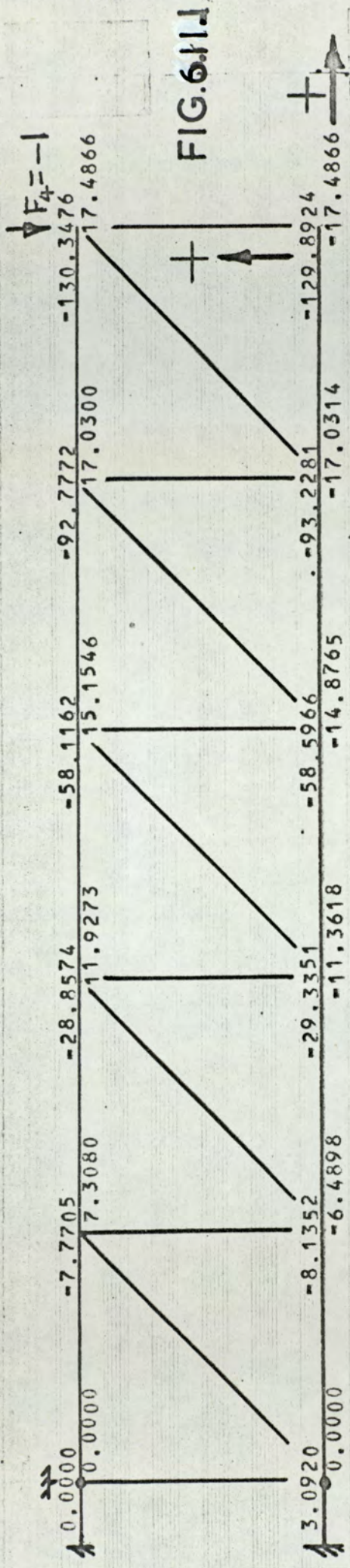
$$[K]_B = \frac{Eb}{2(1-\nu^2)} \begin{bmatrix} 1 & 0 & 0 & -\nu & -1 & \nu \\ \frac{1-\nu}{2} & -\frac{(1-\nu)}{2} & 0 & \frac{1-\nu}{2} & -\frac{(1-\nu)}{2} & \\ & \frac{1-\nu}{2} & 0 & -\frac{(1-\nu)}{2} & \frac{1-\nu}{2} & \\ \text{Symmetric} & & 1 & \nu & -1 & \\ & & & \frac{3-\nu}{2} & -\frac{(1-\nu)}{2} & \\ & & & & \frac{3-\nu}{2} & \end{bmatrix}$$

The procedure for assembling the stiffness matrix for an assemblage of A and B elements, according to the rules previously established based on compatibility and equilibrium, is explained in the Appendix.

Examples on beams treated as plane stress problems

A simple arrangement of 10 triangular elements was first used to form a beam 1 unit deep and 5 units long. This is shown in Fig. 6.11.1. Constraints are applied so that the top left-hand corner of the beam is not allowed to move in any direction, and the bottom left hand corner is not allowed to move horizontally. A vertically downward unit force is then applied at the top right-hand corner ( $F_4 = -1$ ). The stiffness matrix is then assembled and the nodal displacements are found as for a beam type element. Fig. 6.11.1 shows the nodal displacements (factor  $F/Eb$  omitted), the upper line giving the vertical displacements (positive upwards) and the second line the horizontal displacements (positive to the







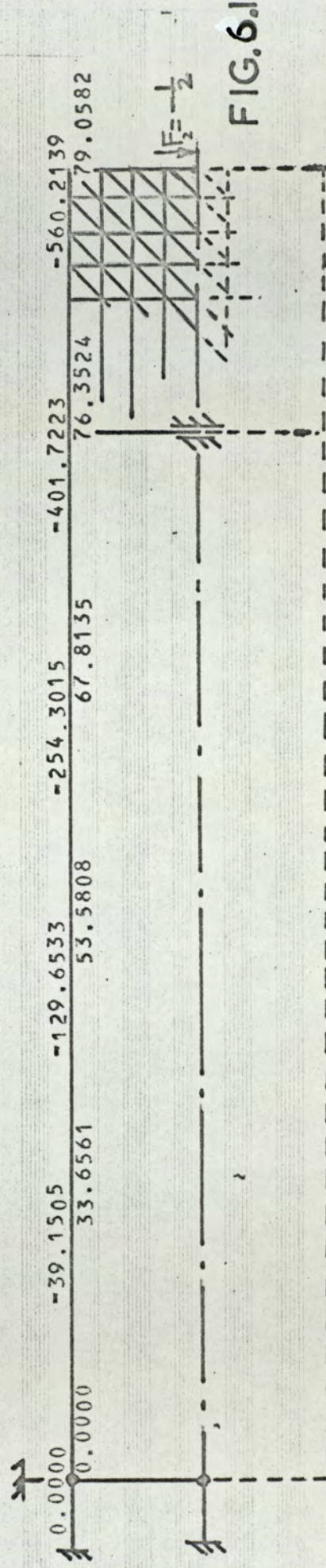
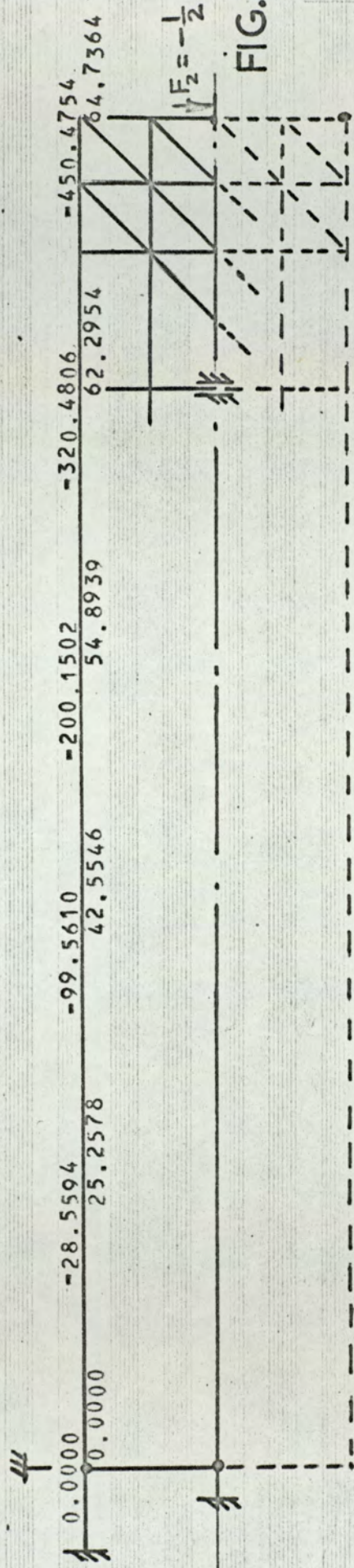
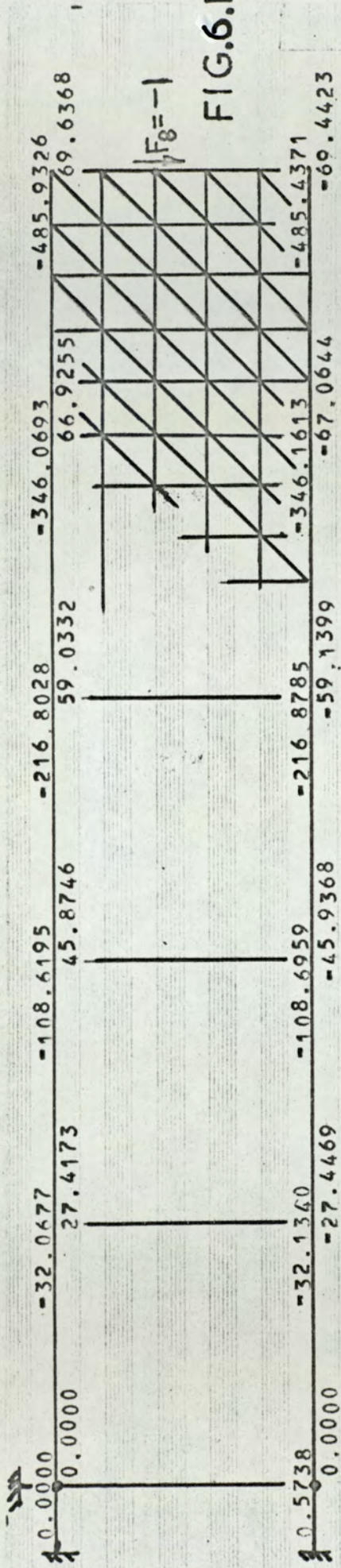
right). It will be seen that horizontal displacements at the top and bottom of the beam are nearly equal and opposite at the same distance from the end of the beam, and that vertical displacements at the top and bottom are nearly equal, both useful checks on the results. When one considers numerical results, however, a very different picture emerges. Treating the beam as a cantilever and neglecting the effect of shear stress, the vertical end deflection should be  $-\frac{F\ell^3}{3EI}$  and since  $\ell = 5d$ , and  $I = \frac{1}{12}bd^3$  this reduces to  $-600\frac{F}{Eb}$ .

The finite element method gives an end deflection of approximately  $-130\frac{F}{Eb}$ , i.e. less than a quarter of the correct answer. This poor result is due to the fact that stresses vary rapidly and change sign between the top and bottom of a beam, while this finite element method assumes a constant stress within each element. The chosen model is thus a poor one.

To achieve greater accuracy more elements were added, keeping the proportions of the beam unchanged (i.e.  $\ell = 5d$ ). The computer program was modified to allow for these additions and the results are shown in Figs. 6.11.2 to 6.11.4. In each case horizontal and vertical displacements are shown at intervals of  $\ell/5$  at the top and bottom surfaces of the beam, the factor  $F/Eb$  being omitted.

It will be seen that although with increasing numbers of elements the end deflection increases, even using 250 elements (Fig. 6.11.4) there is still more than a 20% error. Attempts to







increase the number of elements further were unsuccessful as the storage capacity of the computer was exceeded.

By using the symmetry of the beam and assuming that horizontal displacements on the neutral axis were zero the results of Fig. 6.11.5 were obtained using the top half of the beam only carrying half the total load. Results should be the same as those of Fig. 6.11.3 and there is in fact only about 1% difference. The same method was then applied to give the results of Fig. 6.11.6 using 320 elements (i.e. equivalent to 640 elements for the whole beam), and even this gave an end deflection which was about 7% low. The graph of Fig. 6.11.7 shows how the accuracy varies with the number of elements, and although a very dramatic increase in accuracy is shown, it appears that several thousand elements will be necessary to give any further significant improvement. This will probably be beyond the scope of any existing computer, as increasing the number of elements also increases the band-width of the stiffness matrix so that the number of elements of the stiffness matrix to be stored is approximately proportional to (Number of elements)<sup>1.5</sup>

It will be noted that if only two types of element (i.e. A and B triangles) are used, an arrangement which is unsymmetrical about the centre line of the beam must be obtained. To achieve symmetry another pair of triangles must be introduced, and these are as follows:-



CORRECT  
VALUE

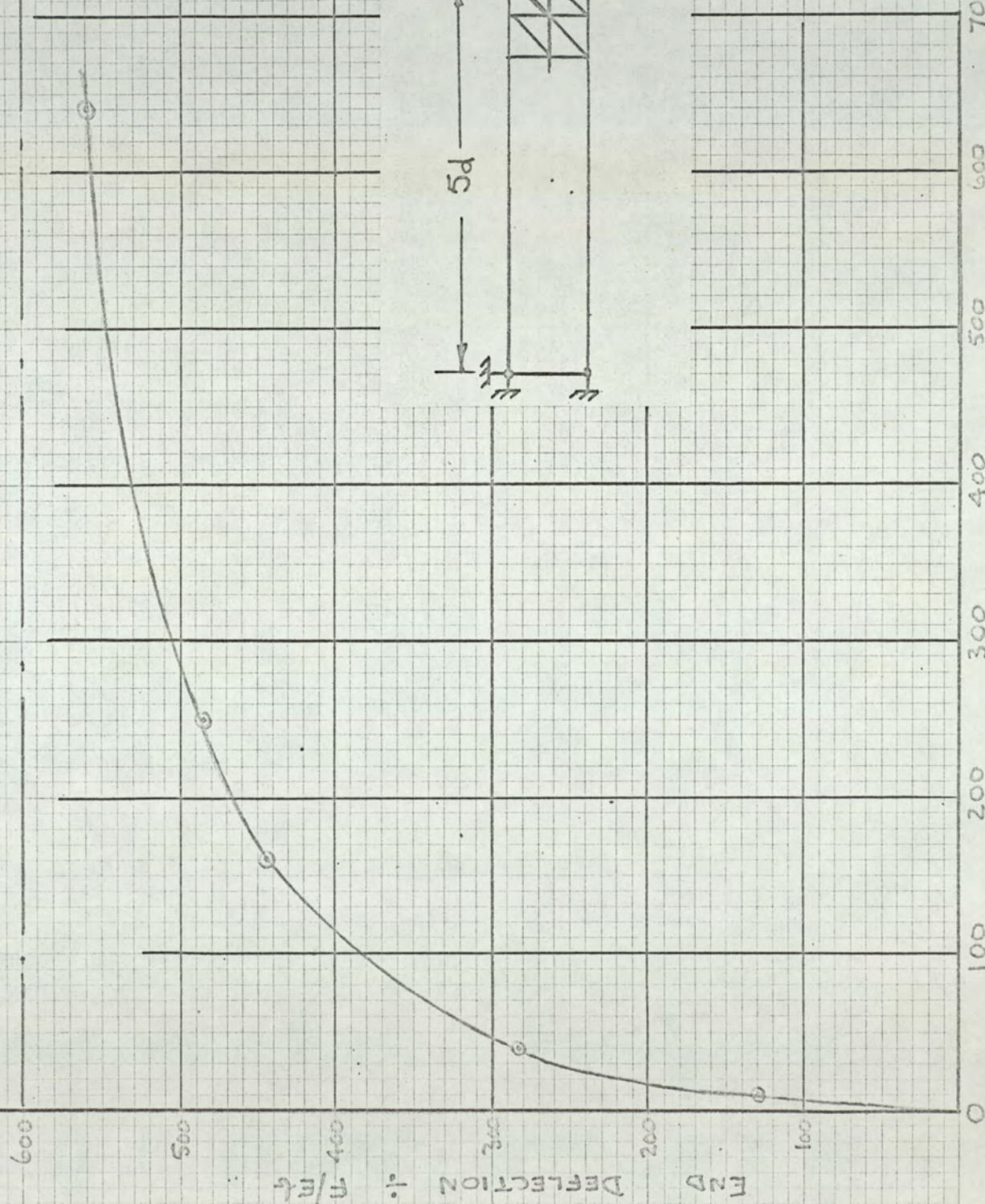
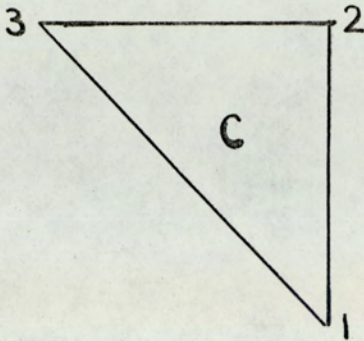


FIG. 6.11.7





Again, taking unit perpendicular sides

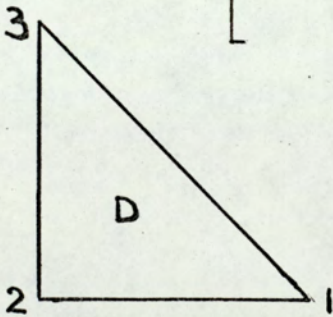
$$b_1 = 0, \quad b_2 = 1, \quad b_3 = -1$$

$$c_1 = -1, \quad c_2 = 1, \quad c_3 = 0$$

Fig. 6R.

$$[K]_C = \frac{Eb}{2(1-\nu^2)} \begin{bmatrix} \frac{1-\nu}{2} & 0 & -(\frac{1-\nu}{2}) & -(\frac{1-\nu}{2}) & 0 & \frac{1-\nu}{2} \\ & 1 & -\nu & -1 & \nu & 0 \\ & & \frac{3-\nu}{2} & \frac{1+\nu}{2} & -1 & -(\frac{1-\nu}{2}) \\ & & & \frac{3-\nu}{2} & -\nu & -(\frac{1-\nu}{2}) \\ & & & & 1 & 0 \\ & & & & & \frac{1-\nu}{2} \end{bmatrix}$$

Symmetric



$$b_1 = -1, \quad b_2 = 1, \quad b_3 = 0,$$

$$c_1 = 0, \quad c_2 = 1, \quad c_3 = -1.$$

Fig. 6S.

$$[K]_D = \frac{Eb}{2(1-\nu^2)} \begin{bmatrix} 1 & 0 & -1 & -\nu & 0 & \nu \\ & \frac{1-\nu}{2} & -(\frac{1-\nu}{2}) & -(\frac{1-\nu}{2}) & \frac{1-\nu}{2} & 0 \\ & & \frac{3-\nu}{2} & \frac{1+\nu}{2} & -(\frac{1-\nu}{2}) & -\nu \\ & & & \frac{3-\nu}{2} & -(\frac{1-\nu}{2}) & -1 \\ & & & & \frac{1-\nu}{2} & 0 \\ & & & & & 1 \end{bmatrix}$$

Symmetric



Using the four different triangles, the stiffness matrix was compiled for two different symmetrical arrangements of the same beam. Displacements for these two cases are shown in Figs. 6.11.8 and 6.11.9.

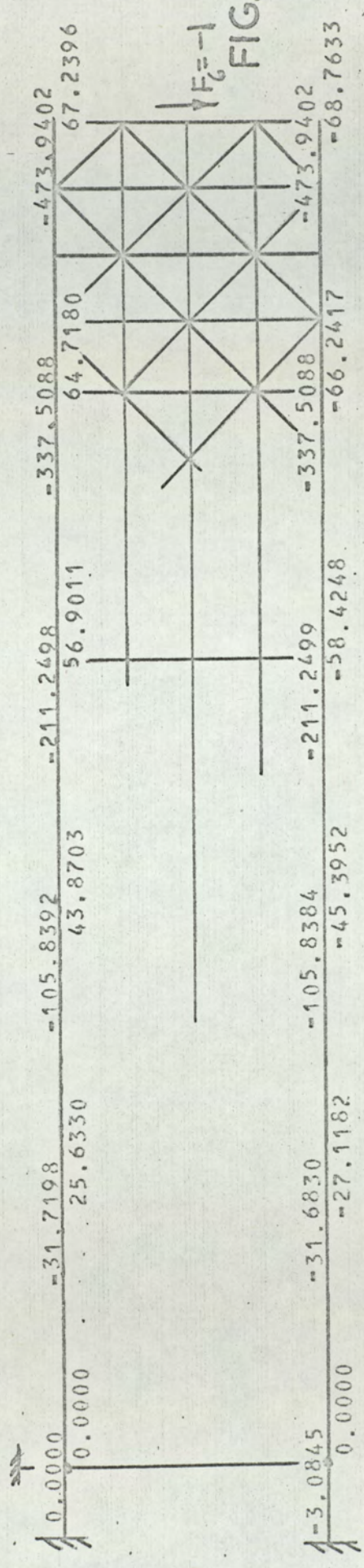
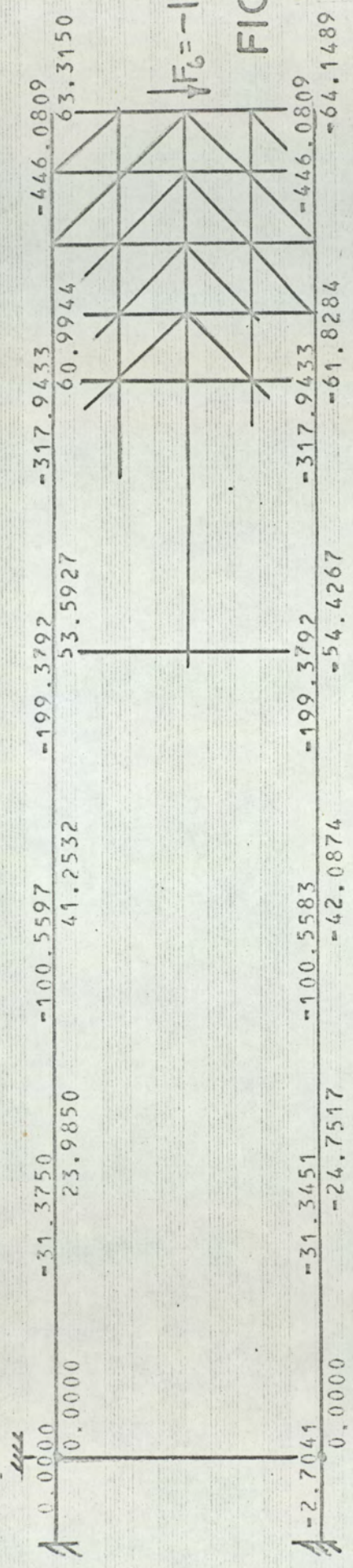
If these results are compared with those of Fig. 6.11.3, which is an unsymmetrical arrangement of the same number of elements, it will be seen that the improvement for the symmetrical arrangement is small.

Once the displacements have been found, the stresses are fairly easily found and Prog.6 calculates values of stresses for the beam arrangement of Fig. 6.11.9. Since there is no variation of stress within an element, stresses at the nodes are found by taking an average of the stresses in the surrounding elements. It is found that transverse and shear stresses are small in comparison with longitudinal stresses and Fig. 6.11.10 compares the nodal stresses at a distance of  $\lambda/5$  from the fixed end of the beam with the "exact" values as calculated from  $\sigma = \frac{My}{I}$ .

It will be seen that, as for displacements, the finite element method results for stresses are too low. In the case considered the end deflection is about 21% low and the stresses 14% low.

It is therefore concluded that because of the high stress gradients in a beam, treatment as a plane-stress problem by the finite element method will give serious errors in both displacements and stresses, even when using a large number of elements. Much more accurate results will be obtained more easily by using beam-type







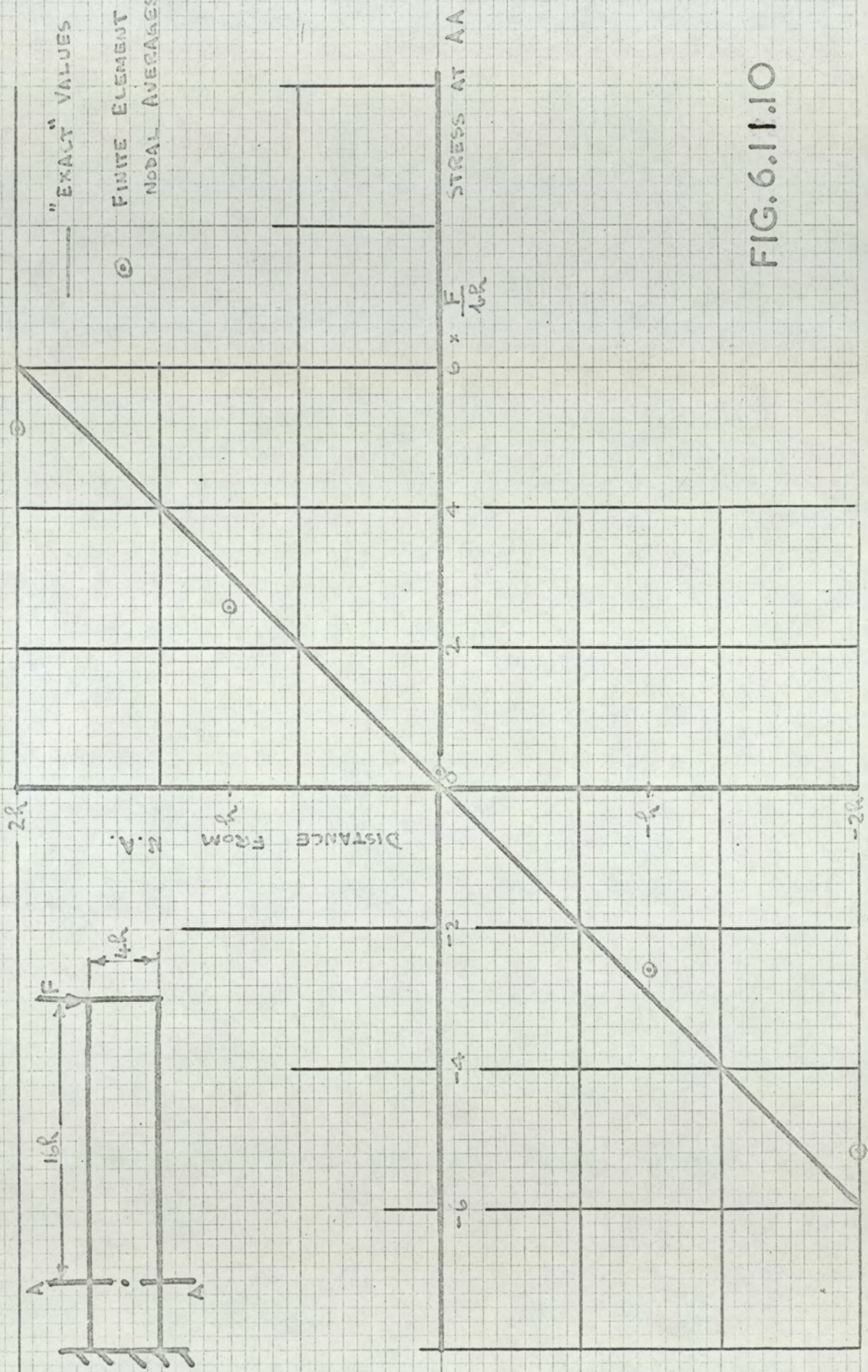


FIG. 6.11.10



elements, especially if allowance is made for the shear stress as shown in 6.8.

Alternatively a more elaborate plane stress program could have been developed using more than three nodes for each triangular element and so allowing for stress variation within the element, [22] [23]. In view of the excellent results obtained using beam-type elements this was not however thought to be necessary.



CHAPTER 7

SOLUTION OF LINEAR VISCOELASTIC PROBLEMS  
USING FINITE ELEMENT METHODS

In the previous chapter, finite element methods were applied to linear elastic materials. Also in 3.4 it was shown that if the solution of an elastic problem is known then the use of the correspondence rule should enable the corresponding viscoelastic problem to be solved. In particular it was seen that if stresses remain constant, or nearly so, a solution may be obtained by using time-dependent values of Young's modulus and Poisson's ratio  $E(t)$  and  $\nu(t)$  respectively. It is then only necessary to use the values of  $E(t)$  and  $\nu(t)$  for a particular value of  $t$  to solve a particular problem for a viscoelastic material instead of using the constant values  $E$  and  $\nu$  for an elastic material.

In this chapter, three viscoelastic problems were considered. In each case any variation of stress was small so that the use of time-dependent "constants" could be justified. Theoretical solutions of these three problems were obtained by using finite element methods, and the results obtained were compared with experimental results. Since each of the problems was self-contained theoretical and experimental results are given consecutively for each case so that comparison of the results is easily made.



In each case it is assumed that the viscoelastic behaviour of the material is described by elastic dilatation and 3-parameter distortion models as this fits the experimental creep test results of 4.1 for Perspex very well. This means that  $E(t)$  and  $\nu(t)$  will vary according to equations 3.4.11 and 3.4.12.

### 7.1 Perspex frame

The Portal frame shown in Fig. 7.1.1 was the subject of this investigation. An elastic structure of this type has already been investigated in 6.2, and an expression for the deflection in the direction of the load is given in 6.2.1.

Now for an elastic structure, the relation between the nodal forces  $\{F\}^e$  and the nodal displacements  $\{u\}^e$  is  $\{F\}^e = [K] \{u\}^e$ , where  $[K]$  is the stiffness matrix. Since each element in the stiffness matrix has a common factor  $E$ , which is constant for an elastic material, this relation may be written as  $\{F\}^e = E[K_1]\{u\}^e$  where the elements of  $[K_1]$  are functions of  $I$  and  $l$  only and are therefore constants.

The Laplace transform with respect to time is

$$\{\bar{F}\}^e = E [K_1] \{\bar{u}\}^e$$

and using the correspondence rule to obtain the result for a viscoelastic material,  $E$  is replaced by

$$\frac{9KG(\zeta + s)}{(3K+G)s + 3K\gamma + G\zeta} \quad (\text{see 3.4.6})$$



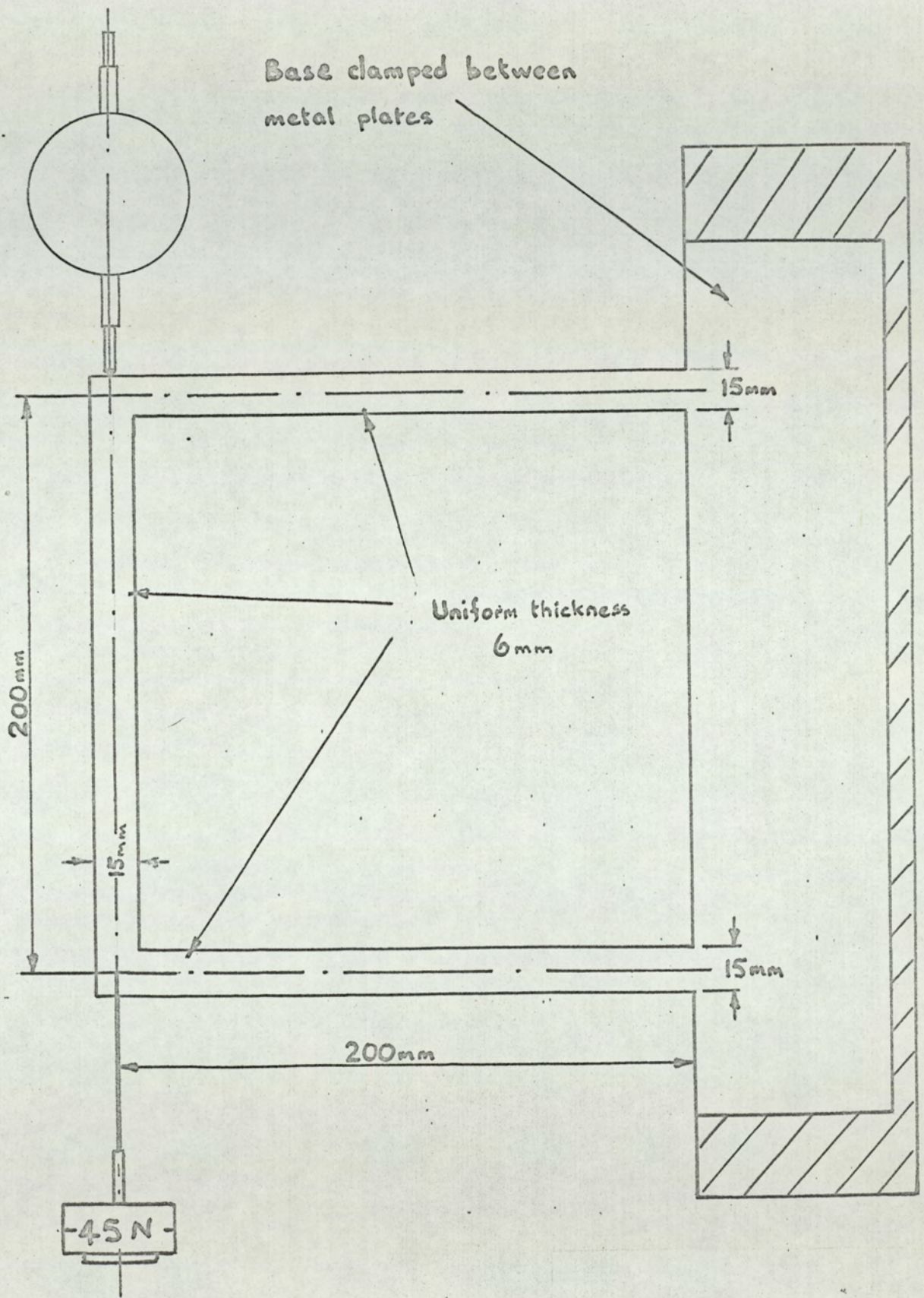


FIG. 7.1.1



Now to find displacements

$$\{\bar{u}\} = \frac{(3K+G)s + 3K\gamma + G\zeta}{9KG(\zeta + s)} [K]^{-1} \{F\}^e$$

and for a system of constant forces, this reduces to

$$\{u\} = [1 + EC(1 - e^{-\zeta t})] \{u\}^e \quad (7.1.1)$$

since  $\{u\}^e = \frac{\{F\}}{E [K]^{-1}}$

Using the values of E, C and  $\zeta$  from 4.1.1 for Perspex the values of the nodal displacements  $\{u\}$  could then be calculated from the elastic displacements  $\{u\}^e$ . In this case only the deflection in the direction of the force was calculated. Using the dimensions of the frame in Fig. 7.1.1 together with the initial value of E of 3000 MN/m<sup>2</sup> from 4.1.1., it was calculated that a load of 45N would give a maximum stress of approximately 20 MN/m<sup>2</sup> which was about the limiting stress beyond which non-linear effects became significant previously found for Perspex in 4.1. Equation 6.2.1 then gave an elastic deflection of 4.24 mm, and the viscoelastic deflection found from 7.1.1 was then given by

$$u = 4.24 [1 + 0.18(1 - e^{-0.58t})] \text{ mm} \quad (7.1.2)$$

where t is the time in hours.

These results are shown in Fig. 7.1.2



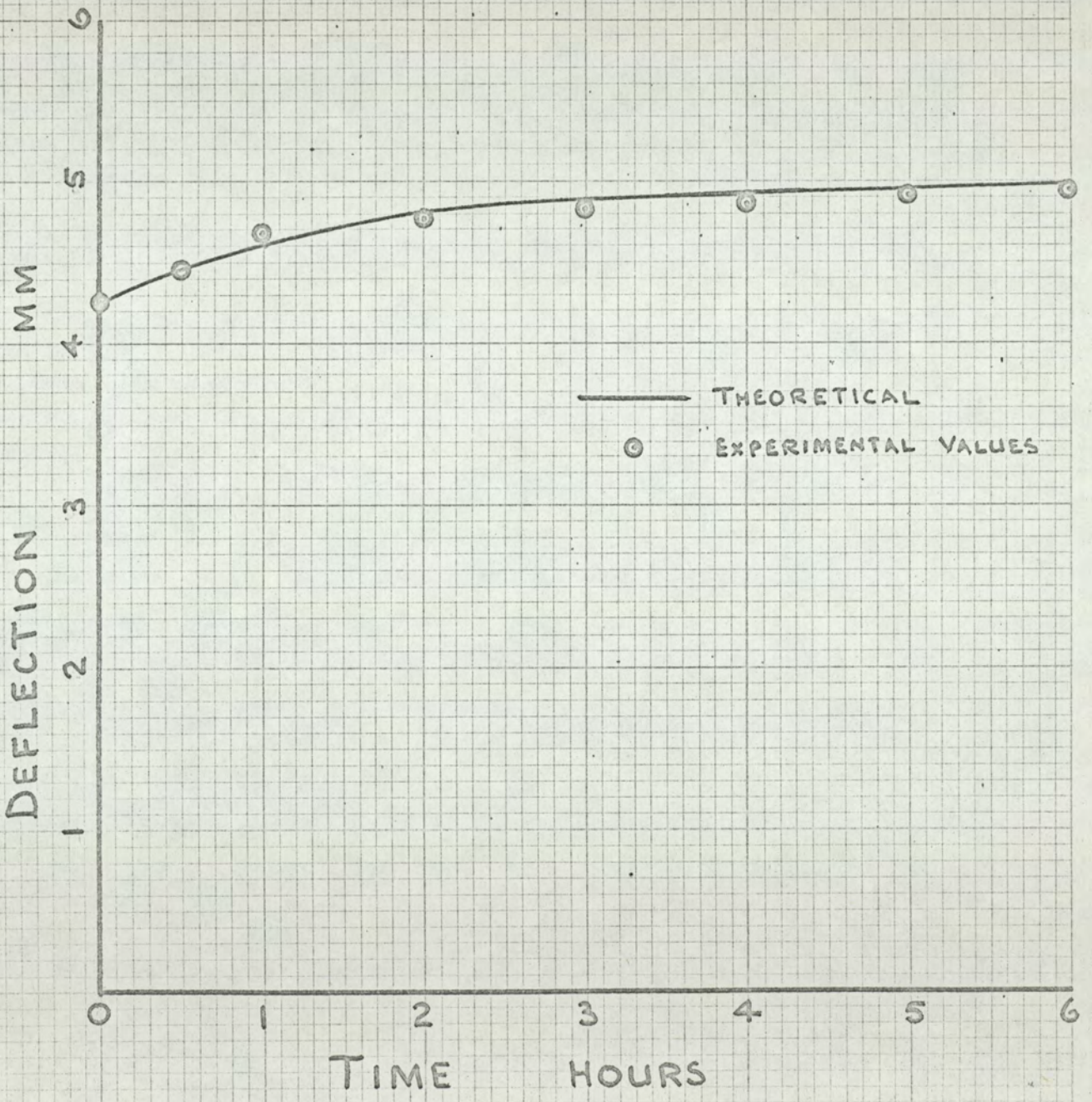
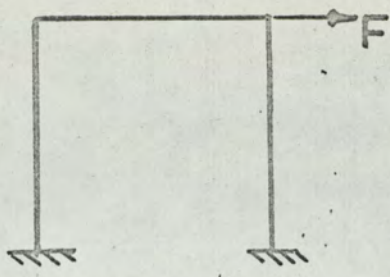


FIG.7.1.2



To confirm these results a Perspex frame was made to the dimensions of Fig. 7.1.1, a load of 45N was applied and the deflection was measured with a dial gauge for 0 to 6 hours. These experimental results are also shown in Fig. 7.1.2.

It is seen that the theoretical and experimental results are in very close agreement, thus justifying the use of (a) the finite element method of 6.2 as applied to elastic frames, and (b) the time-dependent value of  $E(t)$  which gave equation 7.1.1

## 7.2 Cylinder of varying wall thickness subjected to an internal pressure

A solution for a uniform cylinder has been obtained without the use of numerical methods in 4.4. It may be recalled that an "exact" solution for the change of radius of a cylinder of uniform thickness subjected to an internal pressure was obtained by assuming that the parameter  $\beta$  remained constant, and that this assumption was justified. An "exact" solution for a cylinder of varying wall thickness presents much more difficulty, although Hetenyi [13] obtains a solution for an elastic cylinder in terms of Bessel functions, the result being expressed as an infinite series.

By using the stiffness matrix for a tapered element the finite element method is used now to obtain a solution for a viscoelastic cylinder of varying thickness.



It will again be shown that variations of stress are small and accordingly the use of time-dependent values of  $E(t)$  and  $\nu(t)$  may be justified.

As previously noted in 4.4 any local bending of a longitudinal slice of the cylinder wall will be opposed by adjacent parts of the cylinder, and the problem is therefore analogous to that of a beam on a flexible base. It was first necessary therefore to see how this base would modify the stiffness matrix for a longitudinal beam type element. Again in 4.4, it was seen that the radial stiffness per unit length  $k = Eh/r^2$ , and if this stiffness is multiplied by the length of the element and then "lumped" at the nodes, the resulting stiffness at each end of the element  $k' = k\ell/2$  where  $\ell$  is the length of the element.

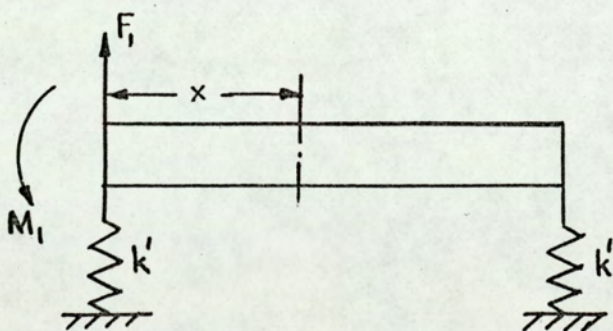


Fig. 7A

Consider first, a uniform elastic element as shown in Fig. 7A, and for convenience let the right-hand end be fixed.

Then  $M = M_1 - F_1x + k'w_1x$  since the stiffness  $k'$  will introduce a downward force of  $k'w_1$ .



The total complementary energy

$$\begin{aligned} V^* &= U^* + \Omega^* \\ &= \int_0^l \frac{M^2}{2EI} dx - F_1 w_1 - M_1 \theta_1 \end{aligned}$$

For stationary total complementary energy  $\frac{\partial V^*}{\partial F_1} = 0$  and  $\frac{\partial V^*}{\partial M_1} = 0$

Two equations are thus obtained which may be arranged to give one quarter of the stiffness matrix for the element

$$\begin{Bmatrix} F_1 \\ M_1 \end{Bmatrix} = \begin{bmatrix} \frac{12EI}{l^3} + k' & \frac{6EI}{l^2} \\ \frac{6EI}{l^2} & \frac{4EI}{l} \end{bmatrix} \begin{Bmatrix} w_1 \\ \theta_1 \end{Bmatrix}$$

By comparison with the stiffness matrix of 6.1.1 it will be seen that  $k'$  has been added to  $k_{11}$ . Similarly if the left-hand end of the element is fixed the last quarter of the stiffness matrix may be obtained, and it is found that  $k'$  is added to  $k_{33}$ . Since the original parts of the stiffness matrix of 6.1.1 are in no way altered by the stiffness of the base, this same method may be applied to a tapered element, i.e. the stiffness matrix of 6.5.1 was modified by adding  $k'$  to  $k_{11}$  and to  $k_{33}$ .

In addition, due to the effect of adjacent parts of the cylinder, the simple modulus  $E$  must be replaced by the modified form  $E/(1-\nu^2)$  in the stiffness matrix.

Finally, to obtain a solution for a viscoelastic cylinder, the constants  $E$  and  $\nu$  must be replaced by their time-dependent forms so



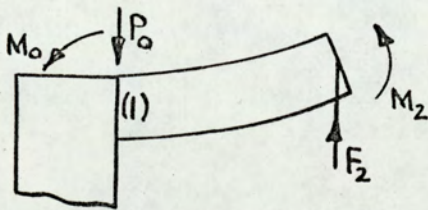
that in the stiffness matrix of 6.5.1 E is replaced by  $E(t)/\{1-[v(t)]^2\}$  where values of E(t) and v(t) are found from 3.4.11 and 3.4.12.

Also, since k' is a function of E the time-dependent value k'(t) must be found by replacing E by E(t). i.e.  $k'(t) = E(t)h/r^2$ .

It was shown in 4.4 that the deflected shape of the cylinder could be regarded as being the deflection due to a ring load and couple superimposed on the "free" expansion of the cylinder. In calculating this "free" expansion time-dependent values of E(t) and v(t) must be used and this value is now given by:-

$$\Delta r = \frac{pr^2}{E(t)h} \left(1 - \frac{v(t)}{2}\right)$$

If the first element of the slice of the cylinder as shown in Fig. 7B is now considered, displacements are prescribed at end (1)



i.e.  $w_1 = -\Delta r$  and  $\theta_1 = 0$

The equations for the right-hand end of the element then become:-

Fig. 7B

$$F_2 = k_{31}(-\Delta r) + k_{32}(0) + k_{33}w_2 + k_{34}\theta_2$$

$$M_2 = k_{41}(-\Delta r) + k_{42}(0) + k_{43}w_2 + k_{44}\theta_2$$

where  $k_{ij}$  is one of the elements of the stiffness matrix of 6.1.1 modified as noted above. These equations are most easily fitted to the remainder if they are rewritten as:-



$$F_2 + k_{31}\Delta r = k_{33}w_2 + k_{34}\theta_2$$

$$M_2 + k_{41}\Delta r = k_{43}w_2 + k_{44}\theta_2$$

That is  $k_{31}\Delta r$  and  $k_{41}\Delta r$  are added to  $F_2$  and  $M_2$  (the applied nodal force and moment) for the first element only, and the first two elements are omitted from the corresponding rows of the stiffness matrix.

The force and stiffness matrices are then assembled in the usual way and the deflections  $\{w\}$  are found with the aid of a digital computer. Finally the net increase of radius at any node  $j$  is  $w_j - \Delta r$ .

Since a solution for a uniform cylinder was obtained in 4.4, this result was checked by the present finite element method. 20 elements were used, each 10 mm long.

The results are shown in Fig. 7.2.1. and to check for possible errors due to the use of too few elements the calculations were repeated using 80 elements of 2.5 mm length. Differences were less than 0.1% so this source of error is not important.

It is interesting to compare the results of Fig. 7.2.1 with those previously obtained by the "exact" method shown in Fig. 4.4.1. It will be seen that the results are identical for  $t = 0$ , a further check on the accuracy of the finite element method. In the region where local effects are important (0 - 40 mm) there is a small but increasing difference between the two sets of results. For example







at  $x = 20$  mm, the finite element method gives a value about 1/4% less than the "exact" value at  $t = 1$  hour, and this difference increases to about 1/2% at 6 hours. This difference is probably due to the assumed constant value of  $\beta$  in the "exact" method, an assumption which is not necessary in the finite element solution. It would therefore seem that the finite element solution may be more accurate here.

The results predicted by this finite element method were also checked experimentally. The dimensions taken from the Perspex cylinder used in the test which were required for the theoretical solution were:- Radius  $r = 74.6$  mm, wall thickness  $h = 3.18$  mm, Pressure  $p = 0.1$  MN/m<sup>2</sup>. As noted below in the description of the experimental procedure the values of the viscoelastic parameters previously found for a stress of 5 MN/m<sup>2</sup> were used in equation 3.4.11 i.e.  $E = 3100$  MN/m<sup>2</sup>,  $C = 0.06 \times 10^{-3}$  m<sup>2</sup>/MN and  $\zeta = 0.58h^{-1}$ . Also an initial value was taken for Poisson's ratio  $\nu = 0.35$  [14].

Details of the computer calculations are shown in Prog.7, which may be used for either a constant or varying wall thickness. Theoretical values of deflection, bending moment and longitudinal and hoop stresses were calculated, some of the results being shown in Fig. 7.2.2 for various distances from the fixed end of the cylinder at different times. It should be noted that the value of stress given is for either the inside or the outside of the shell, the greater value being given. In Fig. 7.2.3 the variation of stress with distance at both surfaces is plotted for  $t = 0$ .



	T= 0	1	2	3	4	5	6
X= 0.0	0.0000	0.0000	0.0000	0.0000	0.0000	0.0000	0.0000
DEFLN	-5.9881	-5.9747	-5.9683	-5.9651	-5.9634	-5.9624	-5.9619
B M	4.7259	4.7179	4.7141	4.7122	4.7112	4.7106	4.7103
LONG STRESS	1.6541	1.7048	1.7300	1.7433	1.7504	1.7544	1.7565
HOOP STRESS							
X= 2.5	0.0017	0.0019	0.0019	0.0020	0.0020	0.0020	0.0020
DEFLN	-3.7520	-3.7482	-3.7466	-3.7458	-3.7454	-3.7452	-3.7451
B M	3.3991	3.3969	3.3959	3.3954	3.3952	3.3951	3.3950
LONG STRESS	1.2616	1.2986	1.3170	1.3266	1.3319	1.3347	1.3363
HOOP STRESS							
X= 5.0	0.0060	0.0064	0.0066	0.0068	0.0069	0.0069	0.0069
DEFLN	-2.0123	-2.0148	-2.0163	-2.0171	-2.0175	-2.0178	-2.0179
B M	2.3669	2.3684	2.3693	2.3698	2.3700	2.3702	2.3703
LONG STRESS	1.0774	1.1022	1.1145	1.1210	1.1245	1.1264	1.1275
HOOP STRESS							
X= 7.5	0.0116	0.0125	0.0129	0.0132	0.0133	0.0134	0.0134
DEFLN	-0.7219	-0.7279	-0.7310	-0.7327	-0.7336	-0.7341	-0.7344
B M	1.6013	1.6048	1.6067	1.6077	1.6082	1.6085	1.6087
LONG STRESS	1.0438	1.0583	1.0655	1.0693	1.0713	1.0725	1.0731
HOOP STRESS							
X= 10.0	0.0178	0.0191	0.0198	0.0202	0.0204	0.0205	0.0206
DEFLN	0.1817	0.1744	0.1707	0.1687	0.1677	0.1671	0.1667
B M	1.2808	1.2764	1.2742	1.2731	1.2724	1.2721	1.2719
LONG STRESS	1.1876	1.1931	1.1958	1.1972	1.1979	1.1983	1.1986
HOOP STRESS							
X= 12.5	0.0239	0.0256	0.0265	0.0271	0.0274	0.0275	0.0276
DEFLN	0.7666	0.7596	0.7561	0.7542	0.7532	0.7527	0.7524
B M	1.6278	1.6237	1.6216	1.6205	1.6199	1.6195	1.6194
LONG STRESS	1.5615	1.5689	1.5724	1.5743	1.5753	1.5758	1.5761
HOOP STRESS							

FIG. 7.2.2



X= 15.0	DEFLN	0.0316	0.0328	0.0334	0.0338	0.0340	0.0341
	B M	1.0944	1.0916	1.0901	1.0892	1.0888	1.0886
	LONG STRESS	1.8223	1.8206	1.8197	1.8192	1.8190	1.8188
	HOOB STRESS	1.8714	1.8753	1.8773	1.8785	1.8791	1.8794
X= 16.5	DEFLN	0.0368	0.0382	0.0390	0.0394	0.0397	0.0398
	B M	1.2403	1.2383	1.2373	1.2367	1.2364	1.2363
	LONG STRESS	1.9088	1.9077	1.9071	1.9068	1.9066	1.9065
	HOOB STRESS	2.1045	2.1084	2.1105	2.1116	2.1122	2.1125
X= 20.0	DEFLN	0.0412	0.0428	0.0437	0.0441	0.0444	0.0446
	B M	1.2509	1.2499	1.2494	1.2492	1.2490	1.2490
	LONG STRESS	1.9152	1.9146	1.9143	1.9141	1.9140	1.9140
	HOOB STRESS	2.2755	2.2792	2.2811	2.2822	2.2827	2.2831
X= 22.5	DEFLN	0.0447	0.0464	0.0474	0.0479	0.0482	0.0484
	B M	1.1714	1.1713	1.1713	1.1713	1.1713	1.1713
	LONG STRESS	1.8680	1.8679	1.8679	1.8679	1.8679	1.8679
	HOOB STRESS	2.3936	2.3969	2.3987	2.3996	2.4001	2.4004
X= 25.0	DEFLN	0.0474	0.0492	0.0503	0.0508	0.0511	0.0513
	B M	1.0376	1.0383	1.0386	1.0389	1.0390	1.0390
	LONG STRESS	1.7886	1.7890	1.7892	1.7893	1.7894	1.7894
	HOOB STRESS	2.4684	2.4713	2.4729	2.4737	2.4742	2.4744
X= 27.5	DEFLN	0.0494	0.0513	0.0524	0.0529	0.0533	0.0535
	B M	0.8772	0.8784	0.8791	0.8795	0.8797	0.8798
	LONG STRESS	1.6934	1.6942	1.6946	1.6948	1.6949	1.6950
	HOOB STRESS	2.5095	2.5120	2.5133	2.5140	2.5144	2.5146



X= 30.0      DEFLN      0.0507      0.0527      0.0544      0.0547      0.0549  
                   B M      0.7105      0.7119      0.7132      0.7135      0.7136  
                   LONG STRESS      1.5944      1.5954      1.5961      1.5963      1.5964  
                   HOOP STRESS      2.5254      2.5274      2.5285      2.5294      2.5296

X= 32.5      DEFLN      0.0516      0.0536      0.0553      0.0557      0.0559  
                   B M      0.5507      0.5524      0.5539      0.5542      0.5543  
                   LONG STRESS      1.4997      1.5007      1.5016      1.5018      1.5019  
                   HOOP STRESS      2.5202      2.5251      2.5265      2.5267      2.5269

X= 35.0      DEFLN      0.0520      0.0541      0.0558      0.0562      0.0564  
                   B M      0.4068      0.4086      0.4101      0.4104      0.4106  
                   LONG STRESS      1.4143      1.4154      1.4163      1.4165      1.4166  
                   HOOP STRESS      2.5099      2.5112      2.5123      2.5125      2.5126

X= 37.5      DEFLN      0.0522      0.0542      0.0560      0.0563      0.0565  
                   B M      0.2835      0.2852      0.2866      0.2869      0.2870  
                   LONG STRESS      1.3411      1.3422      1.3430      1.3432      1.3432  
                   HOOP STRESS      2.4896      2.4906      2.4914      2.4915      2.4916

X= 40.0      DEFLN      0.0522      0.0542      0.0559      0.0563      0.0565  
                   B M      0.1822      0.1837      0.1845      0.1852      0.1853  
                   LONG STRESS      1.2810      1.2819      1.2824      1.2828      1.2829  
                   HOOP STRESS      2.4661      2.4669      2.4673      2.4676      2.4677

X= 42.5      DEFLN      0.0520      0.0540      0.0558      0.0561      0.0563  
                   B M      0.1025      0.1038      0.1049      0.1051      0.1052  
                   LONG STRESS      1.2338      1.2345      1.2350      1.2353      1.2354  
                   HOOP STRESS      2.4423      2.4429      2.4432      2.4434      2.4435



X= 40.0    DEF LN    0.0481    0.0517    0.0537    0.0555    0.0549    0.0559    0.0560  
           B M        0.0407    0.0427    0.0437    0.0446    0.0443    0.0447    0.0448  
           LONG STRESS    1.1971    1.1983    1.1989    1.1994    1.1992    1.1995    1.1996  
           HOOP STRESS    2.4192    2.4199    2.4203    2.4206    2.4205    2.4206    2.4207

X= 47.5    DEF LN    0.0479    0.0514    0.0534    0.0552    0.0546    0.0555    0.0557  
           B M        -0.0014    0.0001    0.0009    0.0016    0.0013    0.0017    0.0018  
           LONG STRESS    1.1738    1.1730    1.1735    1.1739    1.1737    1.1740    1.1740  
           HOOP STRESS    2.4001    2.3999    2.4001    2.4003    2.4003    2.4004    2.4004

X= 50.0    DEF LN    0.0476    0.0512    0.0532    0.0549    0.0543    0.0552    0.0554  
           B M        -0.0291    -0.0281    -0.0275    -0.0271    -0.0272    -0.0270    -0.0269  
           LONG STRESS    1.1902    1.1896    1.1893    1.1890    1.1891    1.1890    1.1889  
           HOOP STRESS    2.3948    2.3950    2.3951    2.3951    2.3951    2.3951    2.3951

X= 52.5    DEF LN    0.0474    0.0509    0.0529    0.0546    0.0540    0.0550    0.0551  
           B M        -0.0455    -0.0448    -0.0444    -0.0441    -0.0442    -0.0441    -0.0441  
           LONG STRESS    1.1999    1.1995    1.1993    1.1991    1.1992    1.1991    1.1991  
           HOOP STRESS    2.3879    2.3884    2.3886    2.3887    2.3887    2.3887    2.3888

X= 55.0    DEF LN    0.0471    0.0507    0.0526    0.0544    0.0537    0.0547    0.0549  
           B M        -0.0531    -0.0527    -0.0526    -0.0524    -0.0525    -0.0524    -0.0524  
           LONG STRESS    1.2045    1.2043    1.2041    1.2041    1.2041    1.2040    1.2040  
           HOOP STRESS    2.3805    2.3810    2.3813    2.3815    2.3814    2.3816    2.3816

X= 57.5    DEF LN    0.0470    0.0505    0.0524    0.0541    0.0535    0.0545    0.0547  
           B M        -0.0544    -0.0544    -0.0543    -0.0543    -0.0543    -0.0543    -0.0543  
           LONG STRESS    1.2053    1.2052    1.2052    1.2052    1.2052    1.2052    1.2052  
           HOOP STRESS    2.3731    2.3737    2.3741    2.3743    2.3742    2.3744    2.3744



X= 60.0	DEFLN	0.0503	0.0523	0.0533	0.0540	0.0543
	B M	-0.0517	-0.0517	-0.0518	-0.0518	-0.0518
	LONG STRESS	1.2036	1.2037	1.2037	1.2037	1.2037
	HOOP STRESS	2.3670	2.3673	2.3675	2.3676	2.3676
X= 62.5	DEFLN	0.0502	0.0521	0.0532	0.0538	0.0544
	B M	-0.0463	-0.0464	-0.0465	-0.0466	-0.0466
	LONG STRESS	1.2004	1.2005	1.2006	1.2006	1.2006
	HOOP STRESS	2.3611	2.3614	2.3615	2.3616	2.3617
X= 65.0	DEFLN	0.0501	0.0520	0.0531	0.0537	0.0543
	B M	-0.0396	-0.0397	-0.0398	-0.0399	-0.0399
	LONG STRESS	1.1964	1.1965	1.1966	1.1966	1.1966
	HOOP STRESS	2.3561	2.3564	2.3565	2.3566	2.3566
X= 67.5	DEFLN	0.0500	0.0520	0.0530	0.0537	0.0542
	B M	-0.0323	-0.0325	-0.0326	-0.0327	-0.0328
	LONG STRESS	1.1921	1.1923	1.1923	1.1924	1.1924
	HOOP STRESS	2.3521	2.3523	2.3524	2.3525	2.3526
X= 70.0	DEFLN	0.0465	0.0519	0.0530	0.0536	0.0541
	B M	-0.0250	-0.0255	-0.0256	-0.0257	-0.0257
	LONG STRESS	1.1878	1.1881	1.1882	1.1882	1.1882
	HOOP STRESS	2.3487	2.3492	2.3493	2.3494	2.3494
X= 72.5	DEFLN	0.0465	0.0519	0.0530	0.0536	0.0541
	B M	-0.0186	-0.0191	-0.0192	-0.0193	-0.0193
	LONG STRESS	1.1840	1.1843	1.1844	1.1844	1.1844
	HOOP STRESS	2.3465	2.3469	2.3470	2.3471	2.3471



It will be seen that the maximum stress is the longitudinal stress at the inside surface at the fixed end. This stress decreases rapidly as the distance from the fixed end increases, and at about 9 mm from the end the greatest stress becomes the longitudinal stress at the outside surface. At about 14 mm from the end the hoop stress at the outside surface becomes the largest stress, and from about 50 mm the two hoop stresses are almost equal and are twice as large as the longitudinal stresses which are also almost equal. These latter are of course the membrane stresses.

Although stresses for times other than  $t = 0$  are not plotted it is shown in Fig. 7.2.2 that the stress which changes most rapidly with time is the hoop stress at the fixed end of the cylinder. This is entirely due to the increase of Poisson's ratio with time. This local effect dies out very rapidly at increasing distance from the fixed end; in 6 hours the hoop stress at the fixed end increases by about 6%, while at 10 mm from the end the increase is only about 1% in the same time.

Theoretical values of the variation of radius with distance are plotted in Fig. 7.2.4 for three values of time. This figure shows that theoretically there is a rapid increase of radius to a maximum value at about 40 mm from the fixed end. There is then a gradual decrease for about another 40 mm after which the radius remains almost constant for any distance from the end. The surface of the cylinder therefore takes the form of a damped cosine wave which is almost completely damped out after one cycle. This pattern is the



THEORETICAL VALUES

AT  $t=0$

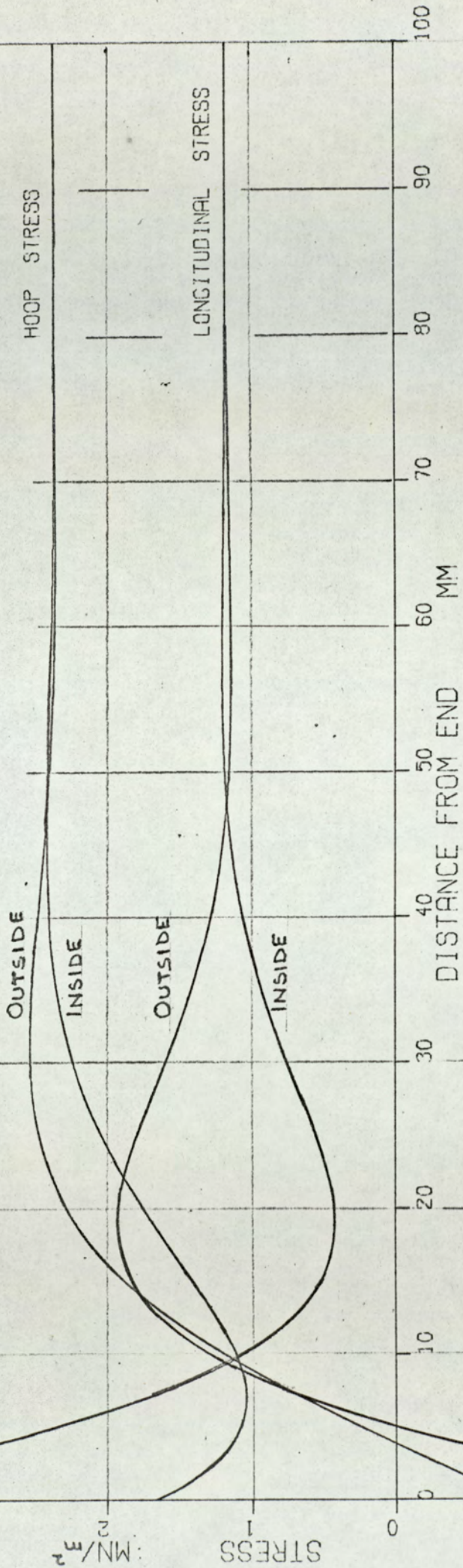
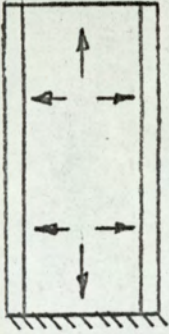


FIG. 7.2.3



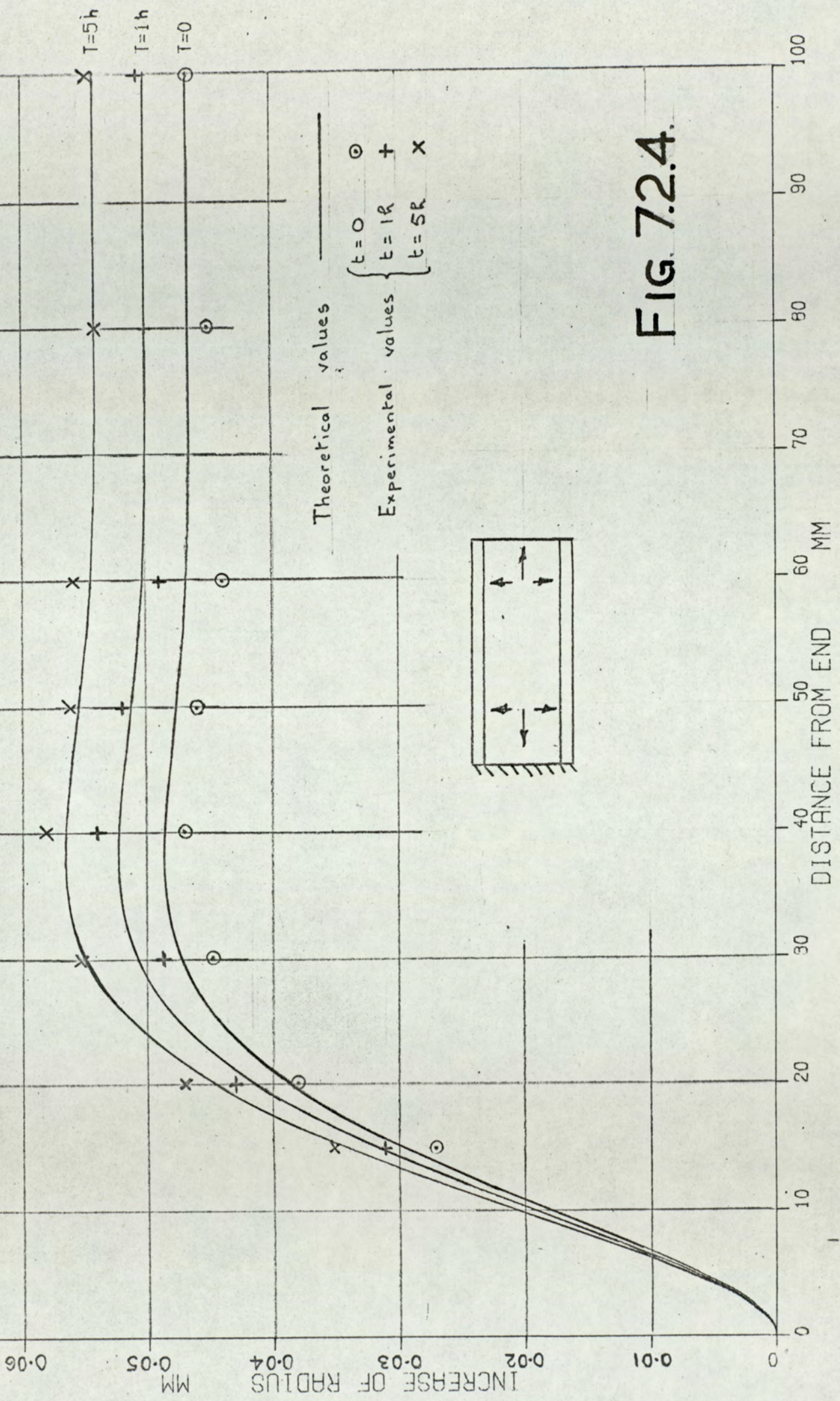


FIG 7.2.4.

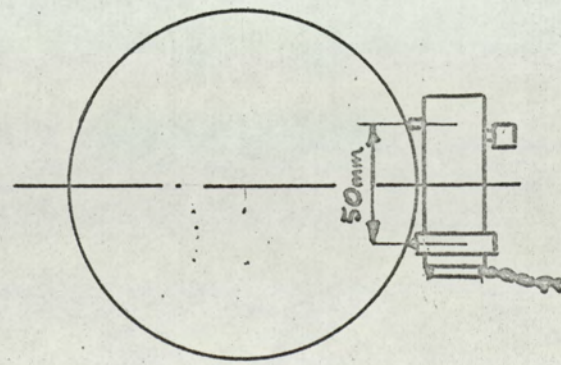
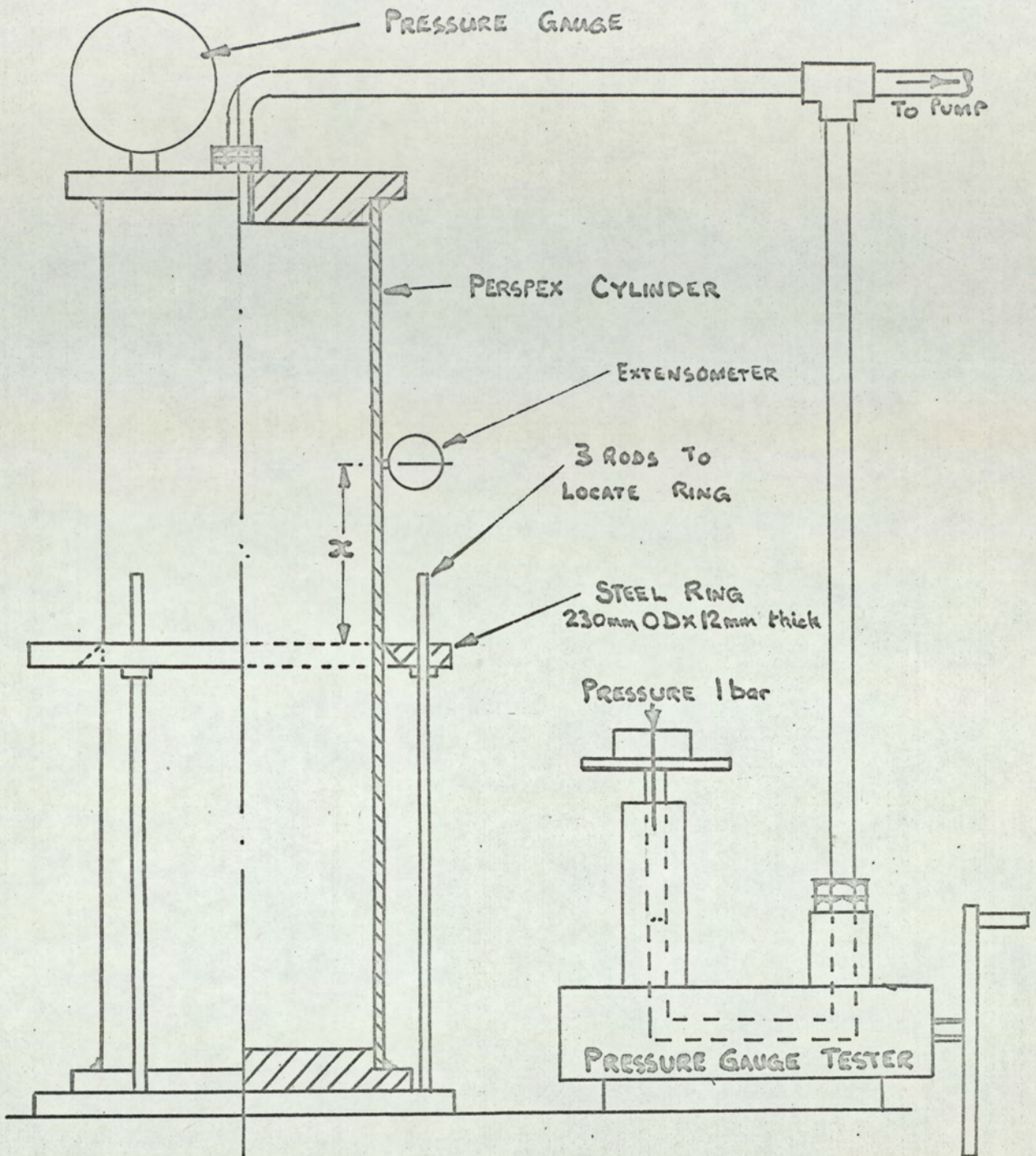


same for all times, but the radius increases with time at all distances. No change in the position of the point of maximum displacement is apparent, although there may be some movement which is too small to be shown. Reference to 4.4 above shows that the point of maximum deflection should move slightly away from the fixed end with increasing time, but that the distance changes by only about 1/2% in 6 hours. A change of this order would not be seen on the graph.

To verify these theoretical results it was decided to measure the change of radius of a Perspex cylinder subjected to an internal pressure. The nominal dimensions of the cylinder were 6 in external diameter and 1/8 in wall thickness. The cylinder was accurately measured and the values obtained and used in the finite element program above were :- Mean radius 74.6 mm, wall thickness 3.18 mm.

The cylinder was 18 in long and was fitted with 1 in thick Perspex and plugs which were cemented in position as shown in Fig. 7.2.5. Calculations showed that the local effects of these ends would decay in a distance of about 50 mm, so that there would be a central portion of the cylinder over 300 mm in length over which conditions would be almost exactly uniform. In the centre of this portion a rigidly held end was simulated by a well-fitting sharp-edged steel ring which could be considered rigid in comparison with the cylinder. The change of radius was therefore negligible at this position, and due to symmetry, the slope would also be zero.





PLAN SHOWING POSITION OF EXTENSOMETER

FIG.7.2.5



The cylinder was filled with oil, and an internal pressure applied by means of a hand-operated pump. To ensure that the pressure remained constant, a dead-weight pressure gauge tester was connected in the oil-line. As the cylinder expanded the piston in the gauge tester slowly fell and an occasional stroke of the pump was required to raise the piston clear off its seat to ensure constant pressure in the cylinder.

The Philips extensometer previously used for creep tests was fitted to the cylinder in such a way that it measured the change in length of a chord of 50 mm original length. Simple proportion would then give the change of radius.

A series of readings were taken with the extensometer attached at various distances from the simulated end and while a constant pressure of 1 bar ( $=0.1 \text{ MN/m}^2$ ) was maintained, extensometer readings were taken for a period of 6 hours. Pressures higher than 1 bar were initially attempted, but caused fracture of the cylinder at stresses much lower than those previously applied in the creep tests of 4.1. With the pressure actually used, stresses did not exceed about  $5 \text{ MN/m}^2$ , so that in obtaining theoretical values for the change of radius, values of  $E$ ,  $C$  and  $\zeta$  previously found for  $5 \text{ MN/m}^2$  were used rather than the average values for stresses up to  $20 \text{ MN/m}^2$  as used for the frame of 7.1.

These experimental values of increase of radius are shown in Fig. 7.2.4 so that a direct comparison may be made with the theoretical



results previously obtained by the finite element method. There is, in general, quite good agreement between the two sets of results, the maximum difference being about 6% which may be regarded as satisfactory for most engineering purposes.

Possible sources of error are:-

1. Difficulties in obtaining accurate creep test results at low stresses which require small loads so that friction effects may become important.
2. Two sets of extensometer readings were involved (creep tests and cylinder test), and it is estimated that there are errors of up to 2% in each case.
3. There is some doubt about the value for Poisson's ratio. A figure of 0.35 seems to be generally accepted for Perspex [14], but the value was not measured for the material used.
4. Possible variations in the thickness of the cylinder, but these are likely to be small.
5. Difficulties in maintaining a constant temperature.

Although the maximum variation during any one test was  $1.5^{\circ}\text{C}$ , the variation between sets of results was up to  $3^{\circ}\text{C}$ .

Temperature changes of this order should however produce little change in the properties of Perspex [6] and this was verified by repeating some of the creep tests at different temperatures within the range  $\pm 2^{\circ}\text{C}$  of the average temperature.

It was not found possible to compare the theoretical results for a tapered cylinder with experimental values, but it has been



shown that the finite element method used gives satisfactory results for a uniform cylinder. Since the method employed is basically the finite element method applied to tapered beams which has been checked by other theoretical methods (6.4 and 6.7 above) and experimentally (9.3 below), it seems reasonable to believe that equally satisfactory results will be obtained for a tapered cylinder.

This investigation was therefore concluded by considering theoretically the effect of a small taper near the end of the cylinder.

Since the maximum (longitudinal) stress exceeds the membrane hoop stress for only about 5 mm from the fixed end it is obviously wasteful of material to use a uniform wall thickness and design the cylinder to withstand this purely local stress. By using a 5% taper for 45 mm from the end, stresses at and near the end are reduced and Fig. 7.2.6 shows that the effect of this taper is to reduce the longitudinal stress at the fixed end to almost exactly the same value as the hoop stress at 45 mm from the end, thus making more efficient use of the quantity of material used. This could be of interest where weight and cost are important considerations.

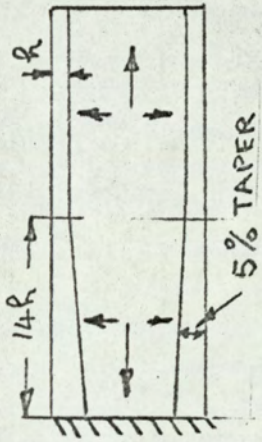
### 7.3 Application of the finite element method to a plane stress viscoelastic problem

Although bending problems are not handled particularly well as plane stress problems because of the number of elements needed,



THEORETICAL VALUES

AT  $t = 0$



HOOP STRESS

LONGITUDINAL STRESS

OUTSIDE

INSIDE

OUTSIDE

INSIDE

100

90

80

70

60

50

40

30

20

10

0

DISTANCE FROM END  
MM

$MN/m^2$

STRESS

-2

-1

0

1

2

3

4

FIG. 7.2.6.



the finite element method gives much better results when stress gradients are smaller. An application to this type of problem is reported by Webber [14] using a 9 in x 9 in x 1/4 in\* sheet of Perspex which was stressed by compressive forces applied to two opposite edges while the other edges and the two faces were left free as shown in Fig. 7C. Buckling was prevented so that there were stresses only in the plane of the sheet, and these stresses were assumed uniform throughout its thickness.

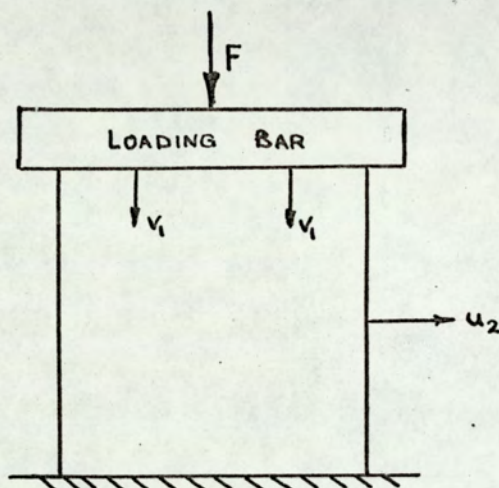


Fig. 7C.

The force  $F$  was such that there was nominally a uniform stress of 4000 lbf/in<sup>2</sup> applied to a horizontal cross-section, and displacements were measured at several points. but the only ones of interest here are the downward displacement of the loading bar  $v_1$  (average of 2 readings) and the horizontal displacement at the centre of a vertical face  $u_2$ . Because of friction at the top and bottom edges transverse movements were almost absent here, and the horizontal

---

\* Imperial units are used throughout in this section so that direct comparisons may be made with Webber's results.



friction forces involved converted what would otherwise have been a uniform stress system into one in which stresses varied in both directions.

Experimental values of  $v_1$  and  $u_2$  were obtained by Webber and also his finite element solution gave theoretical values. In order to obtain the latter, creep tests were carried out and parameters evaluated assuming Maxwell distortion and elastic dilatation.

A comparison of Webber's experimental and theoretical results shows that although good agreement is obtained for times of 2 to 5h approximately, differences are greater for earlier and later times. The present author thought that by assuming 3-parameter distortion and elastic dilatation better agreement might be obtained over the whole period.

Using the results of Webber's creep tests the three parameters were first evaluated and the values giving the best average fit with experimental results in the range 0 - 4000 lbf/in<sup>2</sup> were:-

$$E = 420 \times 10^3 \text{ lbf/in}^2, \quad C = 0.5 \times 10^{-6} \text{ in}^2/\text{lbf}, \quad \zeta = 0.3h^{-1}$$

$$\text{i.e. } \epsilon = \left\{ \frac{1}{420 \times 10^3} + 0.5 \times 10^{-6} (1 - e^{-0.3t}) \right\} \sigma \quad (7.3.1)$$

---

Due to the symmetry of the system only one-quarter of the Perspex sheet need be considered, so the stiffness matrix assembly of Prog.6 was modified to give the square assemblage of Fig. 7D.



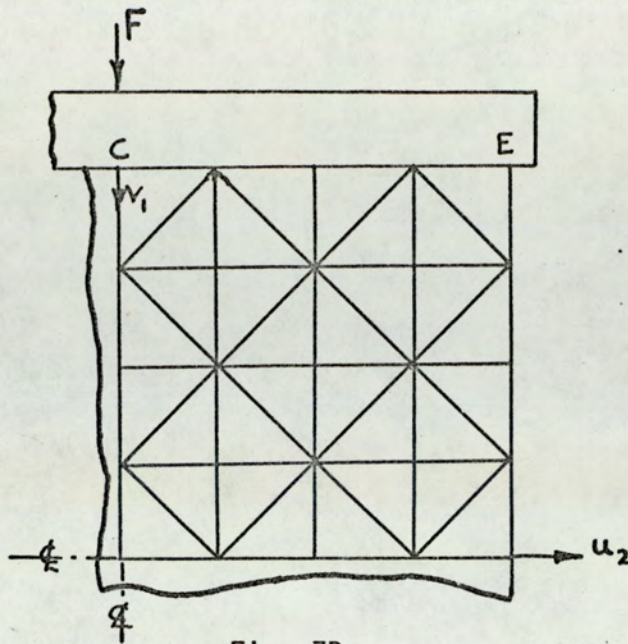


Fig. 7D

Horizontal and vertical displacements were set to zero on the vertical and horizontal centre lines respectively and also no horizontal movement was allowed at the top edge.

An axial force  $F$  was applied so as to give a nominal uniform compressive stress of  $4000 \text{ lbf/in}^2$  - the value used by Webber.

This force was first shared between the nodes to give a uniform pressure on the top edge of the plate, and initial (elastic) values of  $E(420 \times 10^3 \text{ lbf/in}^2)$  and  $\nu(0.35)$  were then used to evaluate the elements of the stiffness matrix.

The initial elastic displacements were then obtained from the computer program, and the stresses calculated in the usual way from these displacements. It was immediately clear that the vertical displacements at the upper nodes were not equal. In other words Webber's assumption that a rigid loading bar (which must give equal displacements) applies a uniform pressure is incorrect due to



the effect of the horizontal friction force. A uniform pressure does in fact give maximum deflection near the centre line i.e. at C of Fig. 7D with (in this case) about a 20% smaller value at the edge at E.

The computer program was then further modified to equate the vertical displacements at these upper nodes. This was achieved by adding first the rows and then the columns of the stiffness matrix which apply to these vertical displacements. Similarly the sum of the forces is taken and for convenience was assumed to act on the vertical centre line so that all vertical displacements were also referred to this point. This method gave a vertical displacement which was the average of the values obtained by assuming uniform pressure. Rather surprisingly the value of the horizontal displacement  $u_2$  was reduced by about 10% compared with the value obtained with uniform pressure. This appears to result from the tendency of the edges of the plate to be deflected less than the centre when a uniform pressure is applied as noted above. To achieve equal deflections the pressure must therefore be increased near the edges of the plate. This will cause increased horizontal friction forces to act inwards on the top and bottom edges of the plate, and the resulting horizontal compressive stress will tend to reduce the horizontal displacement  $u_2$ .

Having obtained the elastic solution, the viscoelastic problem was solved by using a time-dependent value of E as given in 3.4.11. Since the initial value of E is known, and taking an initial value of



$\nu$  as 0.35, the value of  $K$ , which is constant, is then found.

Finally using this value of  $K$  together with  $E(t)$  the value of  $\nu(t)$  the time-dependent value of  $\nu$  is found. For a given value of  $t$  the elements of the stiffness matrix are then evaluated from calculated values of  $E(t)$  and  $\nu(t)$  and the displacements and stresses are then found in the usual way.

The results of these calculations are shown in Fig. 7.3.1 which compares the experimental and theoretical (Maxwell) results of Webber and the theoretical values for 3-parameter distortion of the present author. It will be seen that this latter gives improved results for  $v_1$  over most of the period, but that agreement is not so good for  $u_2$ . Since the theoretical (Maxwell) results here were obtained from the incorrect assumption of uniform pressure, Webber's values for  $u_2$  should probably be reduced by about 10% so that there is then little difference between the Maxwell (Webber's) and the 3-parameter (present author's) theoretical values for  $u_2$ .

It should be noted that the values of  $E(t)$  used here strictly apply only if the stresses are constant. Since the value of  $E(t)$  depends on the stress history only, when non-linear effects are neglected, each stress will be associated with its own value of  $E(t)$ . It would appear that for the 3 values of stress there will be 3 values of  $E(t)$ , and therefore of  $\nu(t)$  for each element, and calculations would then become extremely complicated.



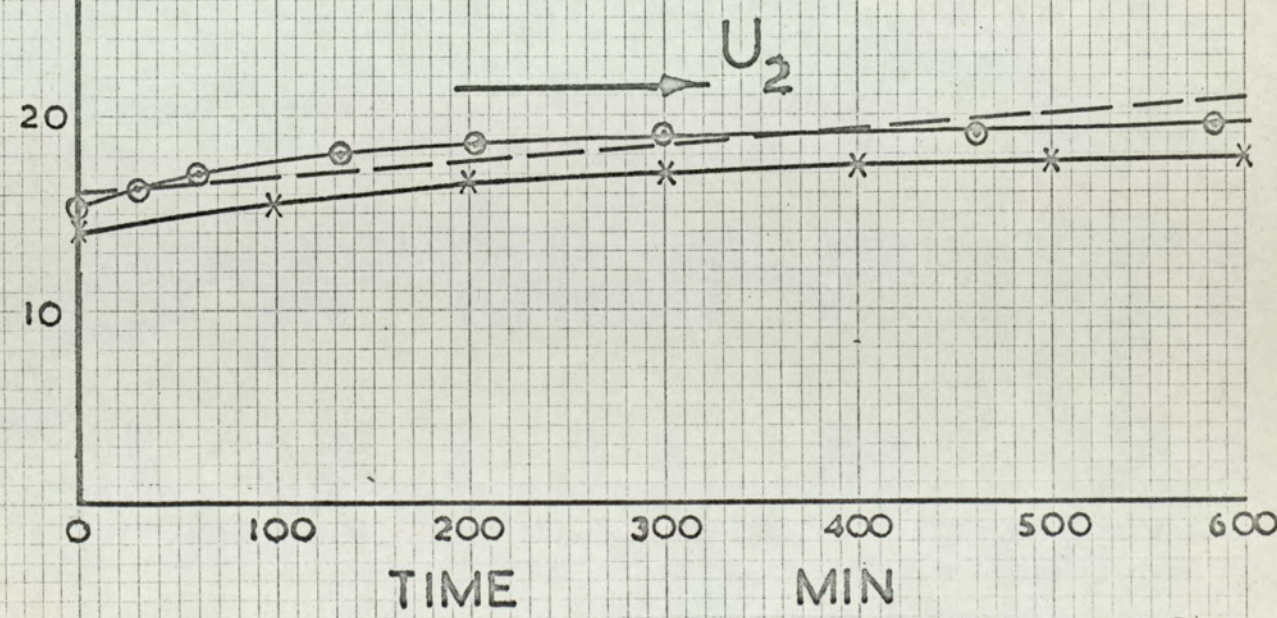
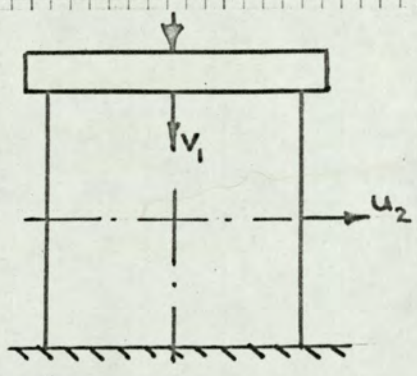
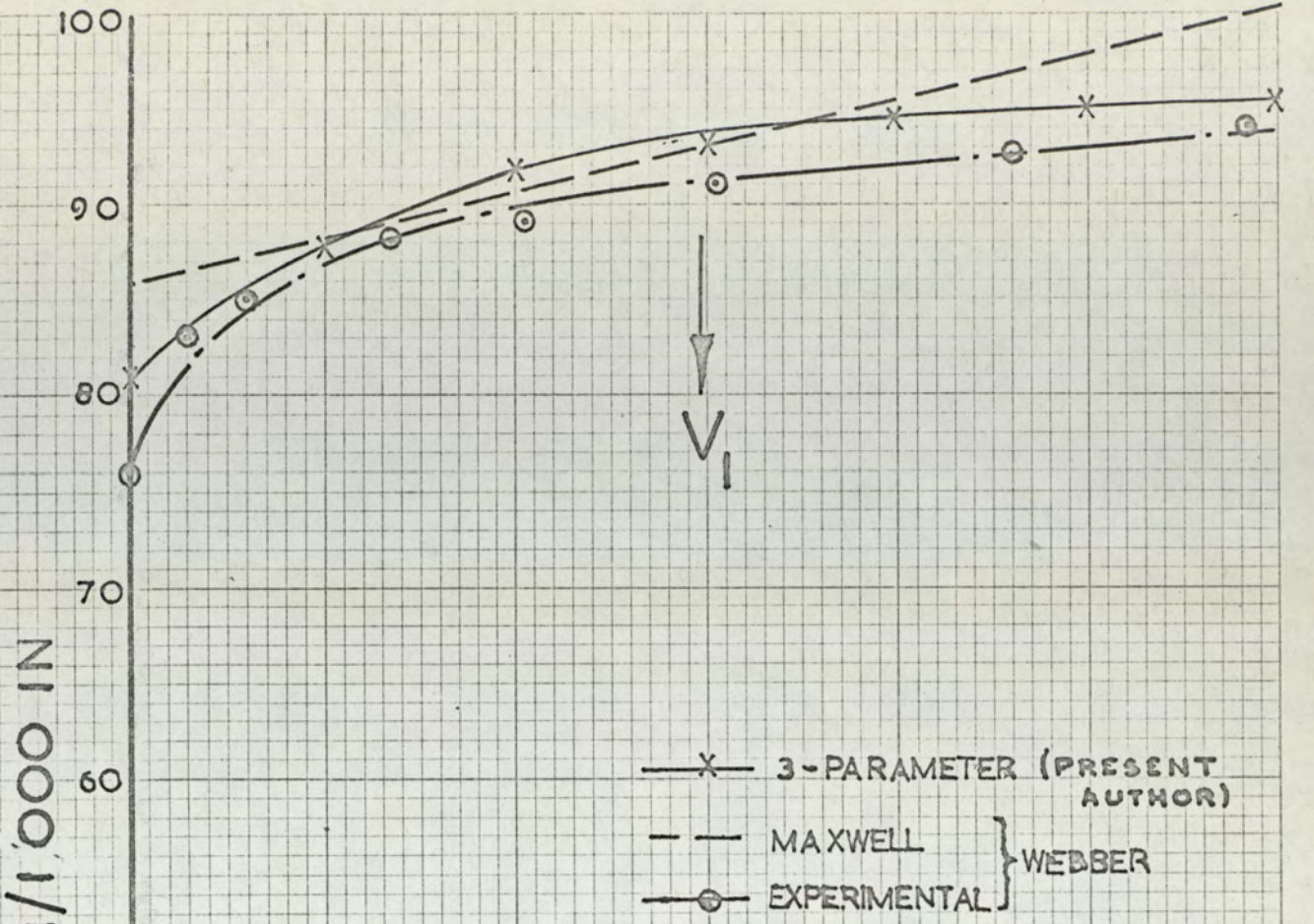


FIG.7.3.1



To attempt to find the errors due to the use of only one value of  $E(t)$  {for a given value of  $t$ } for the whole solid, the maximum variation of stress was first found from the previous results, and this was found to be about 10% in 10 h. It was then assumed that the stress varied linearly with time, and by combining the strains due to constant and ramp stresses as given in 3.4.8 and 4.2.1, a modified expression for  $E(t)$  was obtained

$$E(t) = \frac{E}{1 + EC\{1 - [(\sigma_0 - \frac{r}{\zeta})e^{-\zeta t} - \frac{r}{\zeta}]/[\sigma_0 + rt]\}} \quad (7.3.2)$$

where  $r = \frac{d\sigma}{dt}$  and  $\sigma_0$  is the initial stress

Using the observed rate of change of stress with respect to time the approximate value of  $r$  is  $0.01\sigma_0$  (Stress units)/h, and using 7.3.2 it is found that  $E(t)$  differs very slightly from the value obtained when the stress is constant. Even using a value of  $r = 0.1\sigma_0$  i.e. 10 times the observed rate of change, the maximum change in the value of  $E(t)$  is only about  $1\frac{1}{2}\%$ . (An increase in the stress slightly raises the value of  $E(t)$ .) Since this is such a small difference, it seems that a value of  $E(t)$  found when the stress is constant should introduce only small errors. Since also the use of one value of  $E(t)$  for all stresses and all elements drastically simplifies the calculations, it is considered that this approximation is well justified.

Further consideration of the method used to calculate displacements in this problem suggested that the re-calculation of the value



of each element in the stiffness matrix for each value of  $t$ , due to the variation of  $\nu(t)$  is very wasteful of computer time.

Using the method of Zienkiewicz et al [15] the strain in a two-dimensional constant stress system is given in 3.4.10

$$\begin{aligned}\epsilon_x &= \left\{ \frac{1}{E} + C(1-e^{-\zeta t}) \right\} \sigma_x - \left\{ \left( \frac{1}{2G} - \frac{1}{E} \right) + \frac{C}{2}(1-e^{-\zeta t}) \right\} \sigma_y \\ &= \frac{1}{E}(\sigma_x - \nu\sigma_y) + C(1-e^{-\zeta t})(\sigma_x - 0.5\sigma_y)\end{aligned}$$

$$\text{or } \epsilon_x = \frac{1}{E}(\sigma_x - \nu\sigma_y) + \frac{1}{\mathcal{E}}(\sigma_x - N\sigma_y) \quad (7.3.3)$$

$$\mathcal{E} = \frac{1}{C(1-e^{-\zeta t})} \quad \text{and } N = 0.5$$

If the stresses vary, only the value of  $\mathcal{E}$  will be affected, but its value is likely to be little different from that obtained when the stress is constant since  $\mathcal{E}$  is the time-dependent part of  $E(t)$ , which has been shown to vary little with variation of stress.

Consideration of equation 7.3.3 shows that the strains and therefore the displacements in a viscoelastic solid acted on by constant forces will have two components, (a) elastic displacements  $\{u_e\}$  found by using the initial (elastic) values of  $E$  and  $\nu$  and (b) viscous displacements  $\{u_v\}$  found by using  $\mathcal{E}$  which is time-dependent and  $N$  which has a constant value of 0.5.



The relative values of the displacements in each case will depend on the values of Young's modulus and Poisson's ratio, while their absolute magnitudes depend on the value of Young's modulus. The net displacements may therefore be regarded as the sum of two different displacement patterns, one of which  $\{u_e\}$  is of constant magnitude while the magnitude of the other  $\{u_v\}$  varies with time. The proportions of the net displacements  $\{u\} = \{u_e\} + \{u_v\}$  will therefore vary with time due to the change in  $\{u_v\}$ .

As only two displacement patterns are required, the stiffness matrix need be evaluated twice only, once using  $E$  and  $\nu$  to find  $u_c$  and again using  $\underline{E}(t_1)$  and  $N = 0.5$  to find  $\{u_{v1}\}$  at time  $t_1$ . The values of  $\{u_e\}$  are stored and the values of  $\{u_{v2}\}$  at time  $t_2$  are found by proportion i.e.  $\{u_{v2}\} = \frac{\underline{E}(t_1)}{\underline{E}(t_2)} \{u_{v1}\}$

Having found the net displacements the stresses are calculated using  $1/E(t) = 1/E + 1/\underline{E}(t)$ .

This method was applied to the problem under consideration, and it was found that displacements and stresses were almost identical to those previously found by using  $E(t)$  and  $\nu(t)$  to evaluate the stiffness matrix. Using the present method it was found that for seven values of  $t$ , the computer time was almost halved, and the saving would be even greater with more values of  $t$ , since further values of  $\{u_v\}$  are very quickly obtained by proportion. The method used is shown in Prog.8.



The same method could also be applied if the forces vary. In this case a step-by-step approach would be used, calculating the values of  $\{u_e\}$  and  $\{u_v\}$  for each increment of load, and finally obtaining the sums of all the separate displacements. Even here only two evaluations of the stiffness matrix would be required, since each displacement would now be proportional to the force.

In this chapter, finite element solutions have been obtained for three different types of linear viscoelastic problem, the first two using beam-type elements and the third using constant strain triangles. In all three cases good agreement was obtained between theoretical and experimental results.

However, to be able to use linear viscoelastic theory for the test material, Perspex, all stresses had to be kept fairly small (say less than  $20 \text{ MN/m}^2$ ). If higher stresses are to be used some form of non-linear theory is required, and this is investigated in the next two chapters, first using a non-linear elastic material and then a non-linear viscoelastic material.



## CHAPTER 8

### BENDING OF NON-LINEAR ELASTIC BEAMS

The finite element method using beam-type elements has been applied successfully to a variety of elastic and viscoelastic problems. In all cases previously considered, however, a linear relation between stress and strain has been assumed. While this condition may be satisfied almost exactly by metals stressed up to the elastic limit, the behaviour of most plastics is markedly non-linear.

In this section the easier case of a non-linear elastic material is considered before applying a similar method to the more difficult case of a viscoelastic material in 9.3. below.

#### 8.1 Strains in a non-linear beam

If the effect of shear stress is neglected, plane transverse sections of a beam will remain plane during bending for any type of stress strain relation. The strain will therefore always be proportional to the distance from the neutral axis, but the stress will vary in a manner which depends on its relation to strain, i.e. the constitutive relation for the material.

If the maximum strain is  $\hat{\epsilon}$  at a distance  $\frac{d}{2}$  from the neutral axis, then the radius of curvature is



$$R = - \frac{d}{2\hat{\epsilon}}$$

and hence 
$$\frac{d^2w}{dx^2} = - \frac{2\hat{\epsilon}}{d} \tag{8.1.1}$$

If then, for a particular beam, the relation between  $\hat{\epsilon}$  and  $x$  is known, the usual double integration will give the deflection at any point. Since the curvature of a beam will depend, in some way, on the bending moment, it is first necessary to be able to determine the maximum strain for a given moment.

Also, to use a finite element solution, since  $E$  appears in the stiffness matrix for a linear material, an equivalent quantity will be required for a non-linear material.

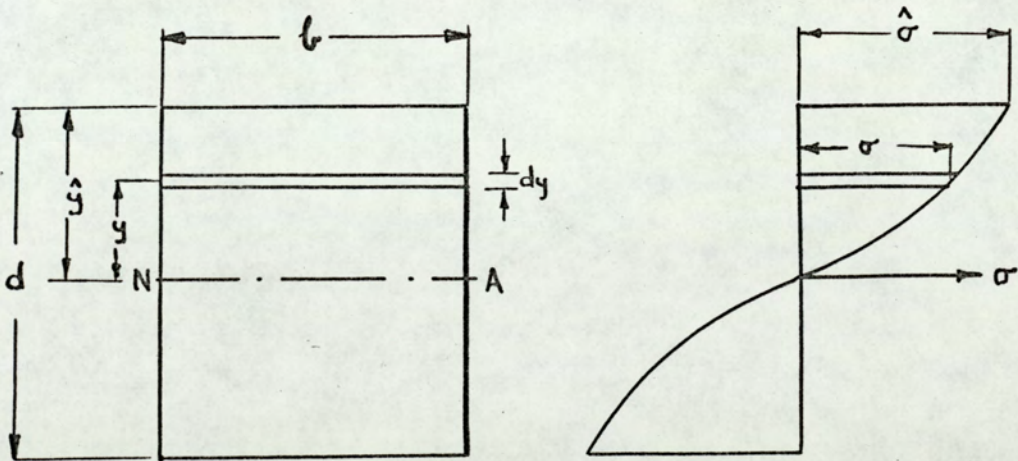


Fig. 8A.

Consider the cross-section of a beam with the stress variation shown, and assume that the same stress-strain relation applies in both tension and compression.



At a distance  $y$  from the neutral axis the stress is  $\sigma$ , and the longitudinal force on an element of thickness  $dy$  is  $\sigma b dy$ . This force has a moment about NA of  $\sigma bdy \cdot y$ . Hence for the whole cross-section the bending moment

$$M = 2 \int_0^{\hat{y}} \sigma b y dy$$

But since plane transverse sections still remain plane

$$y = \frac{\epsilon}{\hat{\epsilon}} \hat{y} \quad \text{and} \quad dy = \frac{\hat{y}}{\hat{\epsilon}} d\epsilon$$

where  $\epsilon$  is the strain at a distance  $y$  from NA  
and  $\hat{\epsilon}$  is the maximum strain at  $y = \hat{y}$

Then 
$$M = 2 \int_0^{\hat{\epsilon}} \sigma b \frac{\epsilon}{\hat{\epsilon}} \hat{y} \cdot \frac{\hat{y}}{\hat{\epsilon}} d\epsilon$$

and since 
$$\hat{y} = \frac{d}{2}$$

$$M = \frac{bd^2}{2} \frac{1}{\hat{\epsilon}^2} \int_0^{\hat{\epsilon}} \sigma \epsilon d\epsilon \tag{8.1.2}$$

---

---

Hence if the bending moment at a particular section is known and values of  $\frac{1}{\hat{\epsilon}^2} \int_0^{\hat{\epsilon}} \sigma \epsilon d\epsilon$  have been calculated for different values of  $\hat{\epsilon}$  it is then possible (by interpolation if necessary) to find the value of  $\hat{\epsilon}$  at that section.

Now for a linear elastic material



$$M = \frac{EI}{R} \quad \text{and} \quad R = \frac{\hat{y}}{\hat{\epsilon}} = \frac{d}{2\hat{\epsilon}} \quad \text{for any material}$$

Hence 
$$E = \frac{6M}{bd^2\hat{\epsilon}}$$

If the expression found for M is now substituted, the equivalent value of E for a non-linear material will be found to be

$$E_e = \frac{3}{\hat{\epsilon}^3} \int_0^{\hat{\epsilon}} \sigma \epsilon \, d\epsilon \quad (8.1.3)$$

---

---

This expression also applies to a linear material, as if the substitution  $\sigma = E\epsilon$  is made it reduces to E.

Having found the value of  $\hat{\epsilon}$  from the known value of M, the corresponding value of  $E_e$  may then be calculated and this will then be used in the finite element program instead of the value of E used previously. Note that  $E_e$  is not a constant but will vary with the value of M.

## 8.2 Finite element solution using a non-linear stress-strain law

It should be noted that if there is a non-linear relation between stress and strain, beam deflections will not be directly proportional to forces or couples.

This may be shown by reference to a single uniform finite element of a beam as shown in Fig. 8B.



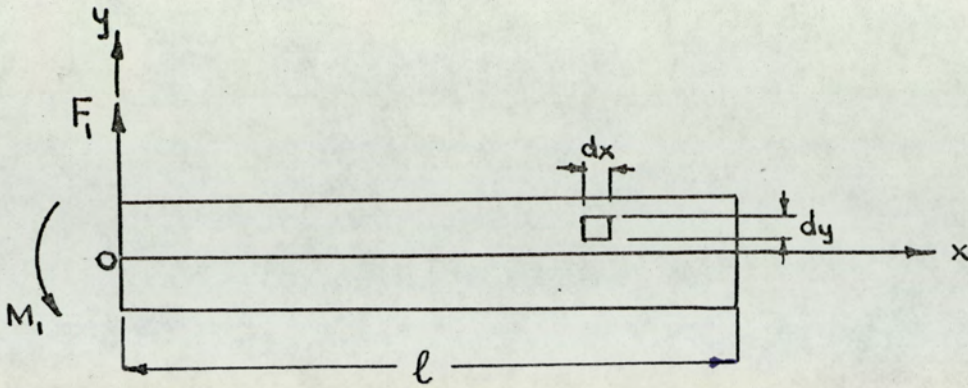


Fig. 8B.

Since the strain energy per unit volume is  $\int_0^\epsilon \sigma d\epsilon$  the strain energy of an element of beam  $dx \times dy$  is given by

$$dU = b dx dy \int_0^\epsilon \sigma d\epsilon$$

Also  $\epsilon = -y/R$

and using the same method as that applied to a tapered element in 6.4 it may be shown that

$\epsilon = -y[G(x,u)]$  where  $G(x,u)$  is a function of  $x$  and the nodal displacements as given in 6.4.2.

If now a non-linear stress-strain relationship  $\sigma = a\epsilon^n$  is assumed, the total strain energy of the element is given by

$$U = \frac{-2ba}{(n+1)(n+2)} \left(-\frac{d}{2}\right)^{n+2} \int_0^l [G(x,u)]^{n+1} dx$$

Again, using the methods of 6.4 any nodal force  $F_i$  may be found

from  $F_i = \frac{\partial U}{\partial u_i}$



so that  $F_1 = \frac{\partial U}{\partial w_1}$  which gives

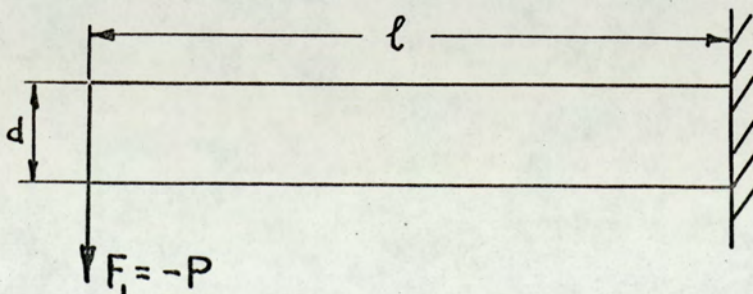
$$F_1 = \frac{-2ba}{n+2} \left(-\frac{d}{2}\right)^{n+2} \int_0^{\ell} [G(x,u)]^n \left(-\frac{6}{\ell^2} + \frac{12x}{\ell^3}\right) dx \quad (8.2.1)$$

Now if  $n = 1$  (i.e. a linear elastic material) this expression is easily integrated, but for a non-linear material  $n$  will not have the value 1 and even if integration is possible, because of the presence of the  $[G(x,u)]^n$  term there will be a non-linear relation between the nodal forces and nodal displacements.

In a similar way  $M_1 = \frac{\partial U}{\partial \theta_1}$  will give a non-linear relation between the end moment and the displacements.

Now if the usual finite element method of the form  $\{F\} = [K]\{u\}$  is used, a linear relationship between forces and displacements is assumed within any one element. The only way in which the non-linearity can be allowed for is by using a different value of  $E_e$  for each element. Although the relation between forces and displacements is then only approximate for a single element, it was thought that if enough elements were used a reasonably accurate result would be obtained for the whole beam. To check if this was so the following example was examined.

Example 1





Consider the cantilever of rectangular section  $b \times d$  carrying an end load  $-P$ . A non-linear stress-strain relation  $\sigma = \pm a\epsilon^2$  was assumed. [To allow for + and - stresses the + sign is used for a + strain and the - sign for a - strain].

For convenience, in the finite element method,  $a, b, d, P$  and  $l$  were all taken as unity.

The number of elements was first decided, and then, to find the bending moments at the nodes, a value of  $E$  was assumed. This value was arbitrary and was taken as unity. The nodal displacements were then calculated by using the computer program previously developed for linear beams (Prog. 5). The bending moment  $M$  at each node was then easily calculated. Then substituting  $\sigma = + a\epsilon^2$  (the + sign is used here since all values of  $M$  are positive, and  $\epsilon$  is positive for positive values of  $y$ ) in equation 8.1.2 it may be shown that

$$\hat{\epsilon} = \sqrt{\frac{8M}{bd^2a}} \quad \text{so that the value of } \hat{\epsilon} \text{ may be calculated at each node.}$$

Again using  $\sigma = + a\epsilon^2$  in 8.1.3 it is found that  $E_e = 3/4a\hat{\epsilon}$  so that from the known values of  $\hat{\epsilon}$ , values of  $E_e$  were calculated at each node. Average values of  $E_e$  were then calculated for each element by taking the arithmetic mean of the values at the ends of the element. These values of  $E_e$  were then used for each element in compiling the stiffness matrix for Prog.5 instead of the constant value of  $E$  used for elastic materials.

Finally, using this modified stiffness matrix and the known nodal forces, the nodal displacements were calculated. The precise



form of the relationship between the end deflection and the other parameters is found below, so  $a$ ,  $b$ ,  $d$ ,  $P$  and  $l$  are now re-introduced.

Using various numbers of elements the finite element method described above gave the results shown in Table 8.1.

Cantilever with an end force

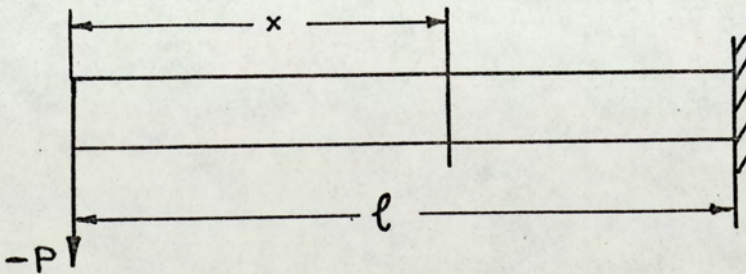
$$\sigma = a\epsilon^2$$

$$\text{Factor } f = \sqrt{\frac{P l^5}{bd^4a}}$$

Number of elements	1	2	5	10	20
End deflection/f	-3.771	-2.600	-2.311	-2.274	-2.265

TABLE 8.1

It appears that as the number of elements increases the values obtained for the end deflection are converging on the exact value. It is possible to verify that this is so in this case.



$$\sigma = a\epsilon^2$$

$$\int_0^{\hat{\epsilon}} \sigma \epsilon d\epsilon = \frac{a\hat{\epsilon}^4}{4}$$

so that from 8.1.2.

$$\hat{\epsilon} = \pm \sqrt{\frac{8M}{bd^2a}}$$



$$\text{Also } M = Px \text{ and } \frac{d^2w}{dx^2} = -\frac{2\epsilon}{d}$$

$$\text{Hence } \frac{d^2w}{dx^2} = -\frac{2}{d} \sqrt{\frac{8Px}{bd^2a}}$$

Integrating twice and inserting the end conditions gives

$$w = \sqrt{\frac{32P}{bd^4a}} \left( -\frac{4}{15}x^{5/2} + \frac{2}{3}l^{3/2}x - \frac{2}{5}l^{5/2} \right)$$

so that when  $x = 0$

$$w = -2.263 \sqrt{\frac{Pl^5}{bd^4a}}$$

---

If this result is compared with the previous values obtained by the finite element method it will be seen that the finite element values converge on this exact result as the number of elements is increased. and that when 20 elements are used the finite element result is only 0.1% higher than the correct value.

It does therefore appear that this modified finite element method will give satisfactory results for non-linear materials.

In the previous example the stress-strain relation chosen  $\sigma = a \epsilon^2$  was such that if it is written  $\sigma = E\epsilon$ , the value of  $E$  increases with increasing stress. It is much more likely with engineering materials that the value of  $E$  will fall as the stress increases. A further example using this type of relationship was investigated.



Example 2

The cantilever of Example 1 was again used, but a stress-strain relationship  $\sigma = a \epsilon - c \epsilon^2$  was assumed. This is the type of result obtained from many plastics. To simplify the working, values  $a = 1$  and  $c = 0.04$  were used. Accordingly  $\sigma = \epsilon - 0.04\epsilon^2$ .

The finite element method described in Example 1 was again used, the only difference being in the expressions for  $\hat{\epsilon}$  and  $E_e$ . In this case equation 8.1.2 gives

$$M = \frac{bd^2}{2} (\hat{\epsilon}/3 - 0.01\hat{\epsilon}^2)$$

A quadratic equation must now be solved for  $\hat{\epsilon}$  giving

$$\hat{\epsilon} = \frac{50}{3} - \sqrt{\frac{2500}{9} - \frac{200M}{bd^2}}$$

[There is a second root, but this gives a strain which is increasing as the stress falls and is not likely to apply to a real material].

This value of strain is now used in 8.1.3 giving

$$E_e = 1 - 0.03\hat{\epsilon}$$

For convenience,  $b$ ,  $d$ ,  $P$  and  $l$  were again taken as unity.

Values of  $E_e$  were found at each node and average values were calculated for each element as above. The displacements were then found using various numbers of elements. The values obtained for the end deflection are shown in Table 8.2.



Number of elements	1	2	5	10	20
End deflection	-4.534	-4.732	-4.793	-4.801	-4.803

TABLE 8.2

By considering the curvature of the beam an exact solution is again possible

$$\frac{d^2w}{dx^2} = -\frac{2\hat{\epsilon}}{d} = -\frac{2}{d} \left( \frac{50}{3} - \sqrt{\frac{2500}{9} - 200 \frac{Px}{bd^2}} \right)$$

Integrating twice, inserting the end conditions and taking b, d, P and  $\ell$  as unity as above gives an end deflection of -4.804. Comparison with the finite element results given in Table 8.2 shows that the finite element solution converges very rapidly on the correct solution, and even using only 2 elements the error is only 1.5%.

Using 2 elements, the relative values of  $E_e$  at the nodes are:- at the free end 1.0, at the centre of the beam 0.90 and at the fixed end 0.77. There is thus a variation in  $E_e$  of the order of 10% in each element. As a guide to the use of this finite element method for non-linear materials it is suggested that sufficient elements should be used to limit changes of  $E_e$  to about 10% in any one element. The figures above then suggest that errors are not likely to exceed about 1%.



### 8.3 Finite element solution using numerical values of stress and strain

In 8.2 non-linear bending problems were solved by using a stress-strain law of the type  $\sigma = a \epsilon^n$ . Here, instead of trying to find a mathematical relationship of this type between stress and strain, only corresponding values of stress and strain (which would normally be obtained direct from a tensile test) were used.

It was first necessary to find the maximum strain at a given section of the beam for a known bending moment. This corresponds to equation 8.1.2 in the previous section.

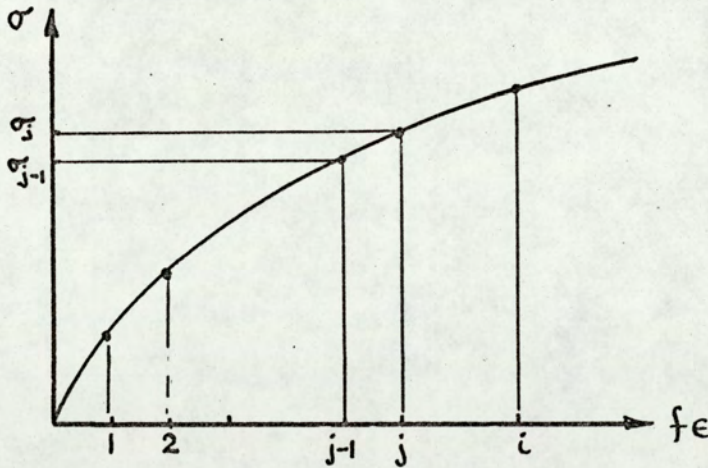


Fig. 8C.

Consider the case where  $N$  values of stress and corresponding equally-spaced values of strain are known. For convenience the values of  $\epsilon$  are multiplied by a factor  $f$  so that values of  $f\epsilon$  are 1,2,3 ...  $N$ . Assume that the stress-strain graph is a straight line between each pair of points. (Enough points must be used to justify this assumption.)



Then between  $f_{\epsilon} = j - 1$  and  $f_{\epsilon} = j$

$$\sigma = \sigma_{j-1} + (\sigma_j - \sigma_{j-1})(f_{\epsilon} - [j-1])$$

$$\int_{j-1}^j \sigma f_{\epsilon} d(f_{\epsilon}) = \int_{j-1}^j \{ \sigma_{j-1}(f_{\epsilon}) + (\sigma_j - \sigma_{j-1})[(f_{\epsilon})^2 - (j-1)(f_{\epsilon})] \} d(f_{\epsilon})$$

Hence

$$\int_0^i \sigma f_{\epsilon} d(f_{\epsilon}) = \sum_{j=1}^i \left[ \frac{1}{2} \sigma_{j-1} \{ j^2 - (j-1)^2 \} + (\sigma_j - \sigma_{j-1}) \left\{ \frac{1}{3} j^3 - \frac{1}{2} (j-1)j^2 + \frac{1}{6} (j-1)^3 \right\} \right] \quad (8.3.1)$$

$$\text{Now } \frac{1}{\epsilon_i^2} \int \sigma \epsilon d\epsilon = \left( \frac{f}{i} \right)^2 \int \frac{\sigma f_{\epsilon} d(f_{\epsilon})}{f^2} = \frac{1}{i^2} \int \sigma f_{\epsilon} d(f_{\epsilon})$$

$$\text{Now let } m_i = \frac{1}{\epsilon_i^2} \int_0^i \sigma \epsilon d\epsilon \quad (8.3.2)$$

Values of  $m_i$  may then be found for  $i = 1, 2, \dots, N$  by dividing the right hand side of equation 8.3.1 by  $i^2$ .

Since the bending moment  $M = \frac{bd^2}{2} \frac{1}{\hat{\epsilon}^2} \int_0^{\hat{\epsilon}} \sigma \epsilon d\epsilon$  (equation 8.1.2) by comparing values of  $\frac{2M}{bd^2}$  with  $m_i$  two adjacent values of  $i$  will be found such that one value of  $m_i$  is lower and the other higher than  $2M/bd^2$ . A good approximation for the value of  $\hat{\epsilon}$  is then found by linear interpolation between these two values of  $m_i$ .



Also from 8.1.3 the equivalent value of E is  $\frac{3}{\hat{\epsilon}^3} \int_0^{\hat{\epsilon}} \sigma \epsilon \, d\epsilon$

so that  $E_i = 3\left(\frac{f}{i}\right)^3 \int_0^i \frac{\sigma f \epsilon \, d(f\epsilon)}{f^2}$

or  $E_i = 3 \frac{m_i}{ig}$  (8.3.3)

where  $g = \frac{1}{f}$  = Increment of strain for unit increase of  $i$ .

Values of  $E_i$  may thus be calculated for each value of  $i$ , and the value of  $E_e$  may be found by linear interpolation between adjacent values of  $E_i$  for a known value of  $\hat{\epsilon}$ .

This numerical method was checked by assuming a relation  $\sigma = a_1\epsilon + a_2\epsilon^2 + a_3\epsilon^3$  so that exact values of  $m_i$  and  $E_i$  could be obtained by integration. Curves of the type shown below in Fig. 8D were obtained.

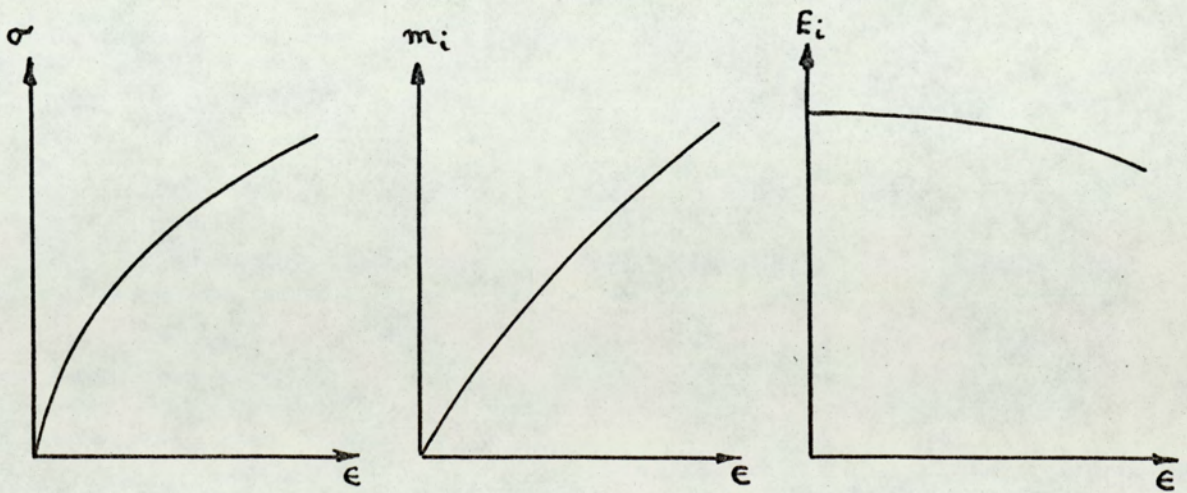


Fig. 8D



The numerical method gave values of  $m_i$  and  $E_i$  which in all cases differed by considerably less than 1% from the exact values obtained by integration, and almost any degree of accuracy could be obtained by increasing the number of points used from the stress-strain graph, although this would increase computation time. In the case considered a total of 12 points was found to be satisfactory.

The program for a tapered beam (Prog.5) was then modified to apply to non-linear beams (Prog.9). After calculating the  $N$  values of  $m_i$  and  $E_i$  from given values of stress and strain, as detailed above, a value of  $E$  was assumed to determine the displacements. If there are no redundant supports the bending moments will be independent of the elastic properties of the material and so any assumed value of  $E$  may be used to find displacements which are then used to calculate the exact values of the bending moments. For a beam with redundant supports, however, the reactions at the supports, and therefore the bending moments, do depend on the properties of the material, and the bending moments found from the assumed value of  $E$  will be approximate. In this case an iterative process as described below is required to give satisfactory values of bending moments and displacements.

From the bending moments found above, values of  $E_e$  may be found at the nodes. Consideration was given to the possibility of forming a new stiffness matrix by assuming a linear variation of  $E_e$  along the beam element, but although this is not difficult in the case of a parallel beam (e.g.  $k_{12} = (4E_1 + 2E_2)I/l^2$ ) individual elements become



much more complicated with a tapered beam. Since the variation of  $E_e$  within each beam element is likely to be small it was decided that the extra complexity would have little effect on the accuracy of the calculations and accordingly a mean value  $(E_1 + E_2)/2$  was used for each element, and this appears to be satisfactory, from calculated results.

Having found these values of  $E_e$  the elements of the stiffness matrix are then re-computed and new values of the displacements are determined. If there are no redundant supports these are the required values, otherwise iteration must continue until a satisfactory degree of convergence is obtained. The criterion for this was taken as a change of less than 0.2% of  $\sum \text{abs}(u_j)$ . Other criteria could be applied, but this was found to be satisfactory giving convergence in about 4 iterations in the cases considered.

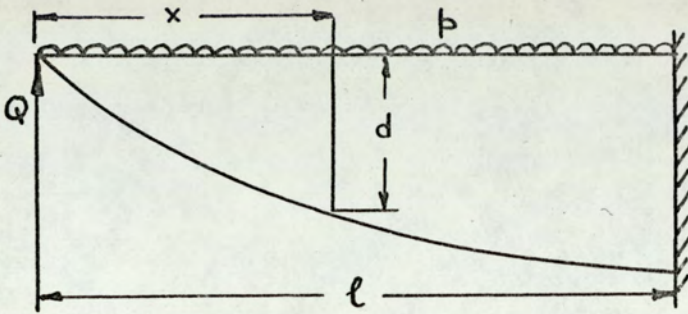
The finite element method has so far been checked and found to give satisfactory results in the following cases (i) Linear-elastic tapered beam with no redundant supports (ii) Linear-elastic parallel beam with both rigid and elastic redundant supports (iii) Non-linear elastic parallel beam with no redundant supports, for various stress-strain laws.

It was finally decided to combine these variations and to check the method for a non-linear elastic tapered beam with a redundant support, using only numerical values of stress and strain.



Considerable difficulty was found in formulating a problem which could be readily checked, but results were calculated for the following propped tapered cantilever.

Example



For checking only it was

assumed that:

$$\left. \begin{aligned} \sigma &= a \epsilon^{\frac{1}{3}} \\ d &= c x^{\frac{3}{7}} \end{aligned} \right\} \quad (8.3.4)$$

Note that these relationships are not used in the finite element method; instead numerical values of  $\sigma$  and  $d$  are calculated for chosen values of  $\epsilon$  and  $x$ , and only these numerical values are used.

It is perhaps unfortunate that in choosing a simple stress strain relationship which would allow the necessary double integration, the form chosen results in a value  $E = \infty$  at  $\epsilon = 0$ . This is of course an impossibility with any practical material as it would require that there should be no initial rate of strain with a gradually applied stress. Since however this peculiarity is unfavourable to obtaining a good finite element result owing to the large variation of  $E$ , it was decided to proceed and to see if a satisfactory result was still possible.

A finite element solution was obtained using 20 elements in Prog. 9 and reading in the required values of the beam width ( $l_m$ ) the



rate of loading  $p(1 \text{ MN/m})$  the length of beam  $\ell(10 \text{ m})$  and values of  $\sigma$ ,  $\epsilon$  and  $d$  calculated from 8.3.4 and using  $a = 300$  and  $c = 0.5$ . Results are given in Table 8.3 below.

Because of the form of the relationships chosen in 8.3.4 an exact solution is possible here.

Let  $\sigma = a \epsilon^n$  where  $n = 1/3$

Then from 8.1.2  $M = \frac{bd^2}{2} \frac{a}{n+2} \hat{\epsilon}^n$

giving  $\hat{\epsilon} = \left[ \frac{2(n+2)}{bd^2a} M \right]^{\frac{1}{n}}$

Also  $M = \frac{1}{2} px^2 - Qx$  where  $Q$  is the prop reaction

and  $\frac{d^2w}{dx^2} = - \frac{2\hat{\epsilon}}{d}$

where  $d = cx^m$   $m = 3/7$ .

Hence by integrating twice, inserting the end conditions and substituting the known values of  $n$ ,  $m$ ,  $b$ ,  $p$ ,  $\ell$ ,  $a$  and  $c$  from above, the following equation results:-

$$Q^3 - 10Q^2 + 37.5Q - 50 = 0$$

from which  $Q = 3.11 \text{ MN}$ .

It is then found that at the point of maximum deflection

$$\frac{1}{32} x^4 - 0.778x^3 + 7.26x^2 - 30.1x + 40 = 0$$



giving a value of  $x = 2.40$  m.

The maximum deflection is then found to be  $-0.0354$  m .

These results are compared with those from the finite element solution in Table 8.3.

	Exact solution	Finite element
Prop load	3.11 MN	2.97 MN
Maximum deflection	$-0.0354$ m at $x = 2.4$ m.	$-0.0362$ m at $x = 2.5$ m

TABLE 8.3

Remembering that the chosen stress-strain relation must cause difficulties in the finite element solution where stresses are small the agreement between the two sets of results is reasonably satisfactory. This example does at least show that it is not necessary to assume a stress-strain law to use the non-linear finite element program, but by using Prog.9 only corresponding values of stress and strain are required. In this present example 24 pairs of values were used, but in many cases a smaller number will be sufficient since the value of  $E$  will change less rapidly than in this case.

The information required to use this non-linear finite element program is detailed below.



It may be noted here that this program was successfully used for a non-linear viscoelastic material in 9.3.

#### 8.4 General computer solution for non-linear materials (Prog.9)

Much of this program is the same as Prog.5, but the first 6 cards 1b to 6b as detailed below are to be used in place of cards 1, 2 and 3 of Prog.5 .

- 1b Number of elements
- 2b Number of points from the stress-strain graph excluding the origin
- 3b Assumed value of E to determine moments
- 4b Scale of strain axis i.e. strain represented by  $i = 1$ .
- 5b Values of stress in order for equal strain increments
- 6b Width of beam

Followed by cards 4 to 10 of Prog.5.

#### Example

The following values of stress ( $\text{MN/m}^2$ ) and strain are known

Point number i	1	2	3	4	5	6
Strain $\epsilon$	0.01	0.02	0.03	0.04	0.05	0.06
Stress $\sigma$	10	19	27	33	38	42



The following data cards would be used:

1b N

2b 6

3b 800 (An approximate average value of E from above data)

4b 0.01

5b 10 19 27 33 38 42

6b B

+ cards 4 to 10 of Prog.5.



CHAPTER 9

NON-LINEAR VISCOELASTICITY

9.1 Non-linear behaviour of plastics

The behaviour of any plastic may be considered linear only within a limited stress range. Even Perspex, which probably behaves more linearly than most other plastics, shows considerable non-linear effects at stresses greater than about 20 MN/m<sup>2</sup> as shown in 4.1.

In the absence of any easily used non-linear viscoelastic theory, various suggestions have been made for a stress-strain-time relationship, but none has proved completely satisfactory. For example, one possible relation suggested by Marin & Pao [16] is

$$\epsilon = \sigma/E + D\sigma^m(1 - Pe^{-pt}) \quad (9.1.1)$$

where E, D, m, P and p are constants.

In this form the behaviour of Perspex in a creep test is described quite well by:-

$$\epsilon = \sigma/3500 + 35 \times 10^{-6} \sigma^{1.5} (1 - 0.997e^{-0.58t})$$

There is of course no particular virtue in an equation of the type of 9.1.1 per se, since it can only represent the results of experiments in a convenient form, and the problems of non-linear viscoelasticity go much deeper than finding a suitable form of equation to describe material behaviour.



For example consider the application of a tensile stress  $\sigma_1$  which is then removed at time T as shown in Fig. 9A.

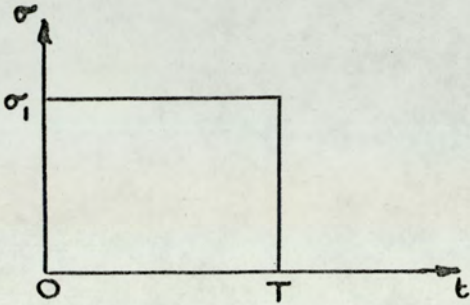


Fig. 9A

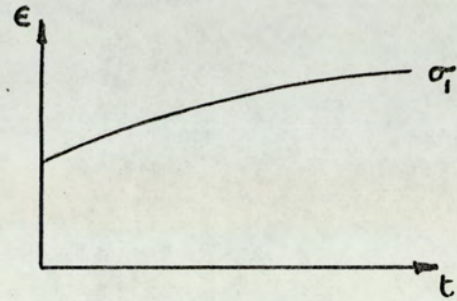


Fig. 9B

The results of a creep test for a constant stress  $\sigma_1$  may be found from a curve of the type shown in Fig. 9B, or alternatively these results could be embodied in an equation as in 9.1.1. For times  $t > T$  the stress history of the material may be regarded as a stress  $\sigma_1$  applied at  $t = 0$  with an additional stress  $-\sigma_1$  applied at  $t = T$ . According to the principle of linear superposition the recovery strain at time  $t$  ( $t > T$ ) should then be given by

$$\epsilon_r(t) = \epsilon_1(t) - \epsilon_1(t-T) \quad (9.1.2)$$

where  $\epsilon_1(t)$  is the strain due to a stress  $\sigma_1$  acting for time  $t$ .

Turner shows [17] however that for propylene homopolymer there are considerable differences between the predictions of 9.1.2 and experimental results, due apparently to the breakdown of the superposition principle for non-linear behaviour. In view of the more linear behaviour of Perspex, the present author thought that equation 9.1.2 might give better results for this material, but preliminary tests gave unsatisfactory results due mainly to the difficulty of repeating



results either with the same specimen or with other specimens cut from the same sheet of material. Investigations by Lockett & Turner [21] show that the behaviour of propylene homopolymer is affected by previous stressing even when it shows no residual strain. Although this effect may not be large, it may considerably influence the small strains to be measured during recovery. While the recovery strain due to a single application and removal of stress may be difficult to predict, it is shown [21] that a much more orderly state of affairs is found when the stress is repeatedly applied and removed. As this is much more likely in practice than the single application and removal of a stress the present author decided that the strains due to intermittent loading should be investigated rather than the predictions of 9.1.2.

### 9.2 Intermittent loading of a tensile test piece

In spite of the failure of the method of superposition of strains shown in [17], Turner shows [18] that although the results of a single stress application and removal may be unpredictable, if several stress cycles are considered linear superposition of strains may be used. The residual strain at the end of N cycles  $(\epsilon_r)_N$  is shown to be

$$(\epsilon_r)_N = \epsilon_c(T) \sum_{x=1}^N \left[ \left( \frac{t'_x}{T} \right)^n - \left( \frac{t'_x}{T} - 1 \right)^n \right] \quad (9.2.1)$$

where T is the duration of the creep period in each cycle

t' is the total duration of each cycle

$\epsilon_c(T)$  is the creep strain at the end of the first creep period

n is the slope of the log(strain)-log(time) graph for a constant stress i.e. creep test.



Also the creep strain after N creep periods is given by

$$(\epsilon_c)_N = (\epsilon_r)_{N-1} + \epsilon_c(T) \quad (9.2.2.)$$

Turner also shows that if  $(\epsilon_r)_N$  and  $(\epsilon_c)_N$  are plotted against  $\log(\text{time})$ , the results are almost two straight lines.

(i) It seems unlikely that this method may be used only for the material tested by Turner (polypropylene), so using the results for Perspex from the creep tests of 4.1 the results for a constant stress of  $15 \text{ MN/m}^2$  were found to be  $\epsilon_c(T) = 5.3 \times 10^{-3}$  after 6 min and the slope of the  $\log(\text{strain})$ - $\log(\text{time})$  graph  $n = 0.015$ . Taking  $T = 6 \text{ min}$  and  $t' = 12 \text{ min}$  (i.e. equal loading and recovery periods) the series of 9.2.1 and 9.2.2. were easily evaluated for various values of  $x$  by using a digital computer. The results are shown in Fig. 9.2.1.

(ii) Since linear viscoelastic theory is much more convenient to use, it is reasonable to enquire how well the predictions of linear viscoelastic theory agree with those of 9.2.1 and 9.2.2.

Hence, by assuming 3-parameter linear viscoelasticity

i.e.  $\epsilon(t) = \sigma \left[ \frac{1}{E} + C(1 - e^{-\zeta t}) \right]$  and so calculating  $\epsilon(t)$  for any value of  $t$ , the following series were obtained by superposition of strains:-

$$(\epsilon_r)_N = \sum_{x=1}^N \epsilon_c(xt') - \sum_{x=1}^N \epsilon_c(xt' - T) \quad (9.2.3)$$

$$(\epsilon_c)_N = \sum_{x=0}^{N-1} \epsilon_c(xt' + T) - \sum_{x=0}^{N-1} \epsilon_c(xt') \quad (9.2.4)$$







These series were again evaluated by means of a computer, using the parameters of 4.1 to calculate  $\epsilon_c(t)$ .

(iii) Finally using a Denison creep testing machine and Philips extensometer experimental values for  $(\epsilon_r)_N$  and  $(\epsilon_c)_N$  were obtained for the same cycle i.e. a stress of  $15 \text{ MN/m}^2$  applied for 6 min and then removed for 6 min.

The results of (i), (ii) and (iii) are shown in Fig. 9.2.1 and it will be seen that while there is very good agreement between the predictions of equations 9.2.1 and 9.2.2 and experimental results, linear viscoelasticity gives rather poorer results, even though the parameters used fit the experimental creep results for  $15 \text{ MN/m}^2$  very well. It would seem that even at this comparatively low stress the basic non-linear behaviour of the material is more apparent when the stress varies than when it remains constant. It is possible, of course, that a more complicated viscoelastic model, while still fitting the creep test results, would give better results in the intermittent loading test, but in view of the accuracy of equations 9.2.1 and 9.2.2 this was not investigated at this stage, but it might be worth further investigation.

It should be noted that in Figs. 9.2.1, 9.2.2 and 9.2.3 the time scale shows the time for which the stress is applied and not the total elapsed time. i.e.  $t = xT$ , where  $x$  is the cycle number and  $T$  is the time for which the stress is applied in each cycle.



Using the same values of  $T$  and  $t'$  (6 and 12 mins respectively) (i) and (iii) were repeated using a stress of  $30 \text{ MN/m}^2$  which is well beyond the linear range of Perspex, and so the results of (ii) were not evaluated. In this case  $\epsilon_c(T) = 11.4 \times 10^{-3}$  and  $n = 0.035$ .

Fig. 9.2.2 shows theoretical and experimental results, and also compares the strain due to a constant stress with that due to the same stress applied intermittently. It is obvious that an intermittent stress results in a smaller strain than a constant stress. The numbers 1, 2, 4 etc. on the graph are the cycle numbers, i.e. values of  $x$ .

It will again be seen that the results of equations 9.2.1 and 9.2.2 agree extremely well with experimental results.

Turner does state that this behaviour pattern has been established for several different polymers, and here it has also been shown to apply to Perspex.

It was finally decided to apply the same method to a stress cycle which varies between two stresses, neither of which is zero. The resultant strains are now predicted from equations 9.2.1 and 9.2.2 for a stress  $\sigma_1$  and adding a second series for a stress  $\sigma_2$  which is first applied at  $t = T$  for a period  $t' - T$ , where  $t'$  is the cycle time for both stresses giving:-



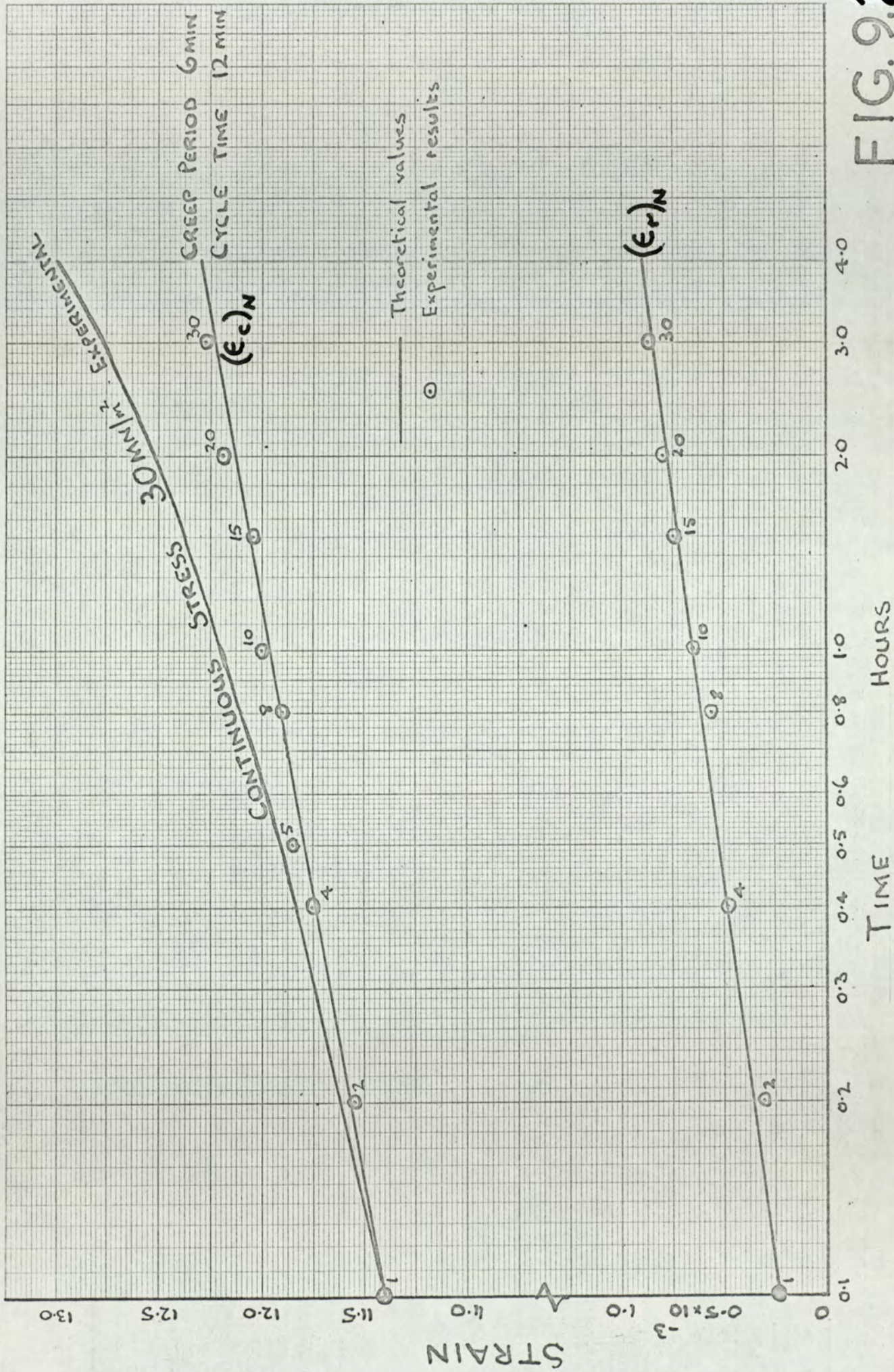


FIG. 9.2.2.2



$$\begin{aligned}
 (\epsilon_r)_N &= \epsilon_{c_1}(T) \sum_{x=1}^N \left[ \left( \frac{t'x}{T} \right)^{n_1} - \left( \frac{t'x}{T} - 1 \right)^{n_1} \right] \\
 &+ \epsilon_{c_2}(t'-T) \sum_{x=1}^{N-1} \left[ \left( \frac{t'x}{t'-T} \right)^{n_2} - \left( \frac{t'x}{t'-T} - 1 \right)^{n_2} \right] + \epsilon_{c_2}(T - t') \quad (9.2.5)
 \end{aligned}$$

$$\begin{aligned}
 (\epsilon_c)_N &= \epsilon_{c_1}(T) \sum_{x=1}^{N-1} \left[ \left( \frac{t'x}{T} \right)^{n_1} - \left( \frac{t'x}{T} - 1 \right)^{n_1} \right] + \epsilon_{c_1}(T) \\
 &+ \epsilon_{c_2}(t'-T) \sum_{x=1}^{N-1} \left[ \left( \frac{t'x}{t'-T} \right)^{n_2} - \left( \frac{t'x}{t'-T} - 1 \right)^{n_2} \right] \quad (9.2.6)
 \end{aligned}$$

where  $\epsilon_{c_1}(T)$  and  $\epsilon_{c_2}(t'-T)$  are the creep strains due to constant stresses of  $\sigma_1$  and  $\sigma_2$  at times  $T$  and  $t'-T$  respectively.

A comparison of theoretical and experimental results was obtained for Perspex stressed for periods of 6 min each at 30 MN/m<sup>2</sup> and 15 MN/m<sup>2</sup>. The values used in equations 9.2.5 and 9.2.6 were as before i.e.  $\epsilon_{c_1}(T) = 11.4 \times 10^{-3}$ ,  $n_1 = 0.035$  and  $\epsilon_{c_2}(t'-T) = 5.3 \times 10^{-3}$ ,  $n_2 = 0.015$ .

The results are shown in Fig. 9.2.3 and it will be seen that agreement between the two sets of values is not as good as was the case with a single stress. Since, however, the maximum difference is about 2% the theoretical results obtained by using this method should be accurate enough for most engineering purposes.



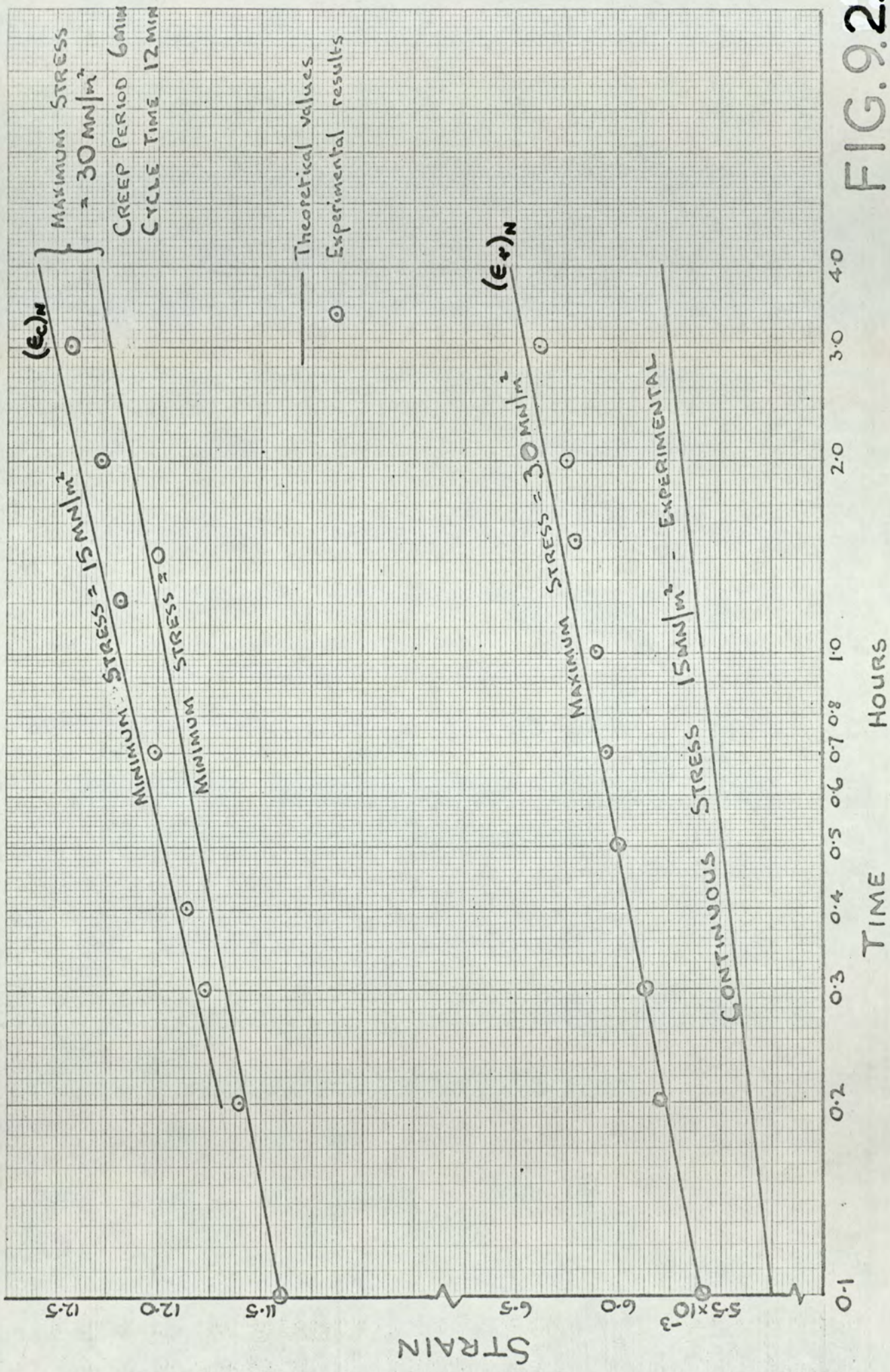


FIG. 9.2.3



Turner argues [18] that when  $\sigma_2 = 0$  linear superposition may be used because the residual strains are small. In the case just considered where  $\sigma_2 \neq 0$  residual strains are not small and linear superposition no longer gives accurate results as also noted by Turner [17].

Fig. 9.2.3 also shows that the maximum strain  $(\epsilon_c)_N$  is not greatly affected by the value of the lower stress. In this case  $(\epsilon_c)_N$  is only about 5% greater when the stress is reduced to  $15 \text{ MN/m}^2$  than when it is removed completely. On the other hand the minimum strain  $(\epsilon_r)_N$  is considerably increased by the higher stress, and here it is about 15% greater than the strain due to a constant stress of  $15 \text{ MN/m}^2$ . This pattern of behaviour is to be expected as the greater residual strains due to the higher stress will affect the lower strains much more than the strains caused by the lower stress will affect the maximum strain.

It would therefore seem that equations 9.2.1 and 9.2.2 will predict extremely accurately the strains due to the intermittent application of a single stress in a cycle which is repeated at regular intervals. Linear viscoelastic theory is, on the other hand, likely to give fairly poor results for this type of loading. In the case of Perspex the results of the test shown in Fig.9.2.1 show that while the strains predicted by linear viscoelastic theory may be up to 5% low at the end of a creep period, the strain at the end of a recovery period may be overestimated by as much as 50%. Since this latter strain is, however, very small the absolute error



in the strain is not large, and these linear viscoelastic calculations would probably be accurate enough for most design purposes.

It also appears that equations 9.2.5 and 9.2.6 may be used to extend this method to apply to a stress variation between two constant stress levels. The results here are not quite as good as those for a single stress, but are still quite adequate for design calculations.

Since all the experimental data required for this method is obtained from a simple creep test, and the series are easily summed by a computer, very little extra work will give a great deal of useful information in cases where the stress varies in a known manner.

### 9.3 The deflection of a tapered non-linear viscoelastic beam

Beam deflections obtained using the finite element method have been found to agree well, in those cases where they could be checked, with results of other theoretical methods. While this is encouraging it was thought that experimental verification was required.

A symmetrical tapered Perspex beam having the dimensions shown in Fig. 9.3.1 was simply supported at its ends and loaded at mid-span. Although the extension of the bottom face of the beam will tend to be partly taken up by the required increase in length of the beam due to its curvature, calculations suggested that the span might increase by up to about 0.5 mm. To allow the span to change by this amount, one end of the beam was supported on a roller, while the other rested



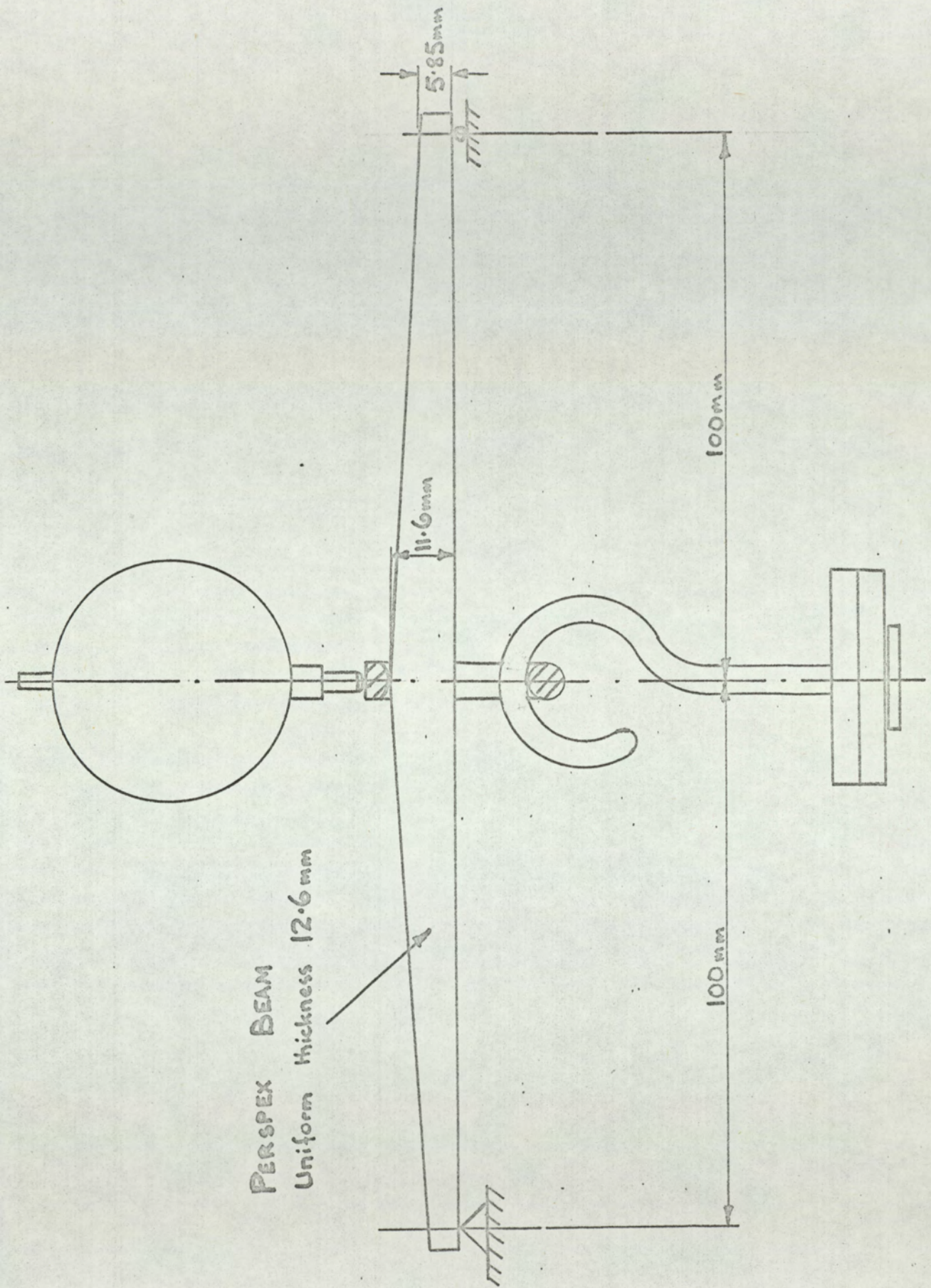


FIG. 9.3.1



on a knife-edge, and some slight increase in span was indeed noticed when the largest forces were applied. A change of span of this order would increase the deflection by less than 1% and this effect was accordingly neglected.

Central loads of up to 180N (giving a maximum stress of about  $30 \text{ MN/m}^2$ ) were applied, and for each load the central deflection was measured over a period of 6 hours. With the shape of beam used, maximum stress occurs at mid span, but was only about 10% less than the maximum at a quarter span (the exact figure varying with the load on the beam). The non-linearity shown at the higher stresses will therefore affect about half the length of the beam, and should show clearly in the central deflection.

To obtain a finite element solution Prog. 9 was used. It was assumed that the stress did not vary with time at a given point, and accordingly that the behaviour of a small element of beam would be exactly the same as for the creep tests of 4.1. This assumption was found to be reasonable, as the finite element solution showed a maximum change of stress at the outer layers of the beam of about 2%. The stress at the outside of the beam does in fact decrease slightly with increasing time, while the stress increases nearer the neutral axis.

Using values of stress and strain from 4.1, values of  $m_i$  and  $E_i$  were calculated from 8.3.2 and 8.3.3. A strain increment  $g$  (8.3.3) of 0.002 was used, and values of  $m_i$  and  $E_i$  were calculated for 0.1,



0.5, 2, 4 and 6 hours. Using 20 elements each 10 mm long and supplying beam dimensions, positions of constraints and details of loading (one central force), Prog.9 was used and the deflections and stresses found for several different loads. The variation of central deflection with time for various loads is shown in Fig. 9.3.2, both experimental and finite element results being given. It will be seen that there is very good agreement between the two sets of results for all loads and times, the maximum difference being about 2%, and an error of this magnitude could well be accounted for by errors in measuring strains in the creep tests. Calculations showed that if the initial (elastic) value of  $E$  had been used throughout errors of over 10% would have appeared, so the non-linear method used gives a considerable improvement in accuracy.

It may therefore be concluded that the finite element method developed for non-linear elastic materials will also give good results for non-linear viscoelastic materials, providing that the stress at a particular point in the beam remains almost constant. In cases where the stress does vary appreciably with time (e.g. if there is a redundant support), the strain at any point will depend on the previous stress history. It is however shown in 7.3 that, for a linear viscoelastic material, considerable variations of stress have little effect on the value of  $E(t)$ . With a non-linear viscoelastic material the ratio stress/strain is now a function of stress as well as of time, but even so it seems likely that the values of  $E_i$  will be fairly insensitive to variations in stresses.



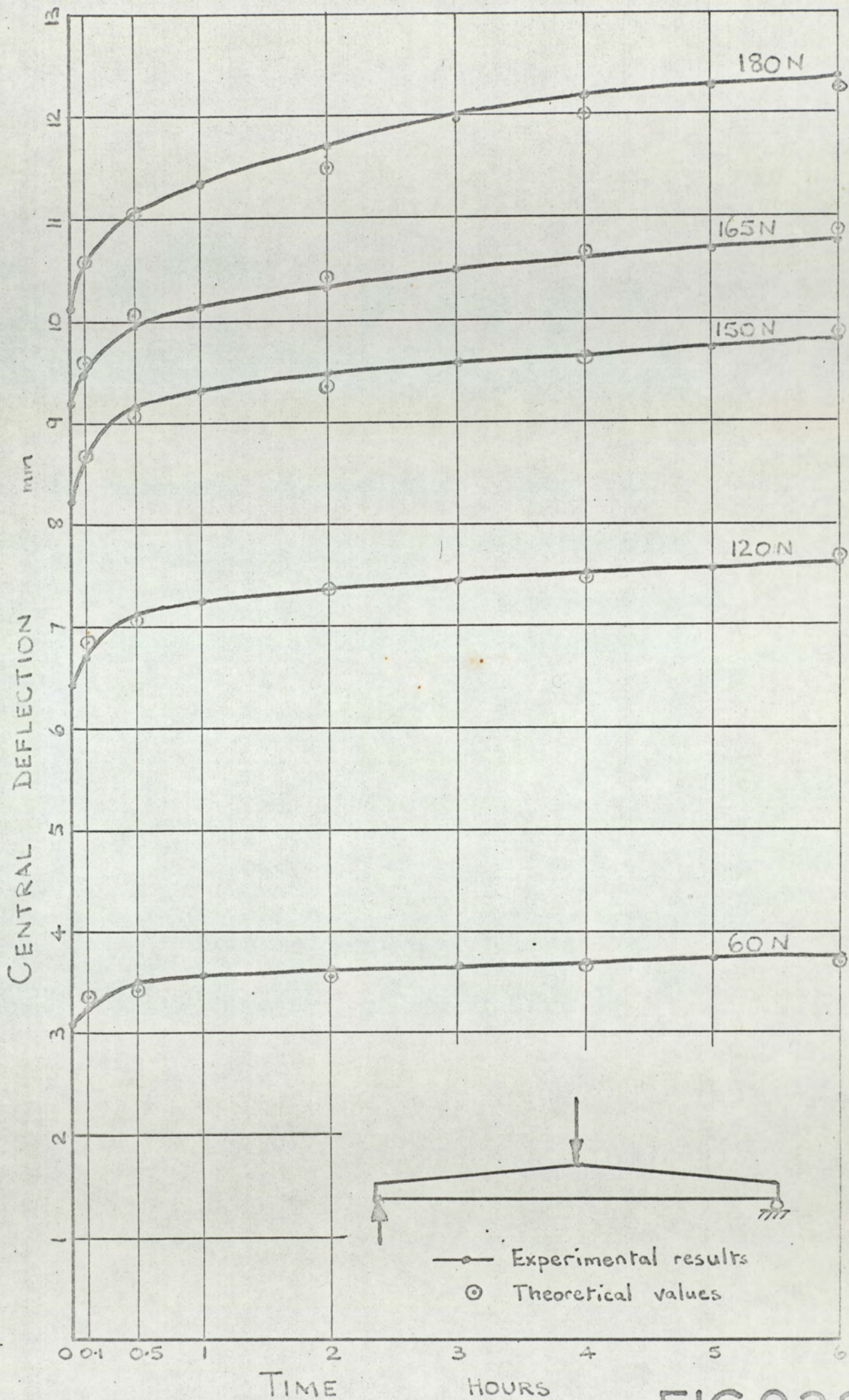


FIG.9.3.2



Providing then that the final stresses are used to determine the values of  $E_i$  (and this is done automatically by using the iterative method of 8.3 which is incorporated in Prog.9) errors due to stress variation are likely to be fairly small.

#### 9.4 Design in plastics

Design problems for plastics are much more complicated than for metals. These complications are due to (a) the time-dependence of the mechanical properties of plastics and (b) the non-linear relation between stress and strain for most plastics, except for very moderate stresses.

##### Linear viscoelasticity

If linear viscoelasticity is assumed, the initial problem is to obtain a relationship between stress, strain and time which will fit the observed behaviour of the material used. The mathematics of this approach has been well developed, and a combination of Maxwell and/or Kelvin elements will usually be found to agree with experimental results for certain materials [2] [19].

The assumption of linearity implies that if the behaviour of the material in one type of test is known, then its behaviour in any other type of test may be predicted. Since the tensile creep test is probably the simplest type of test, this is normally used to obtain the parameters for the viscoelastic model. It is then necessary to make one further assumption concerning the dilatation of the material and then the results of torsion and other tests may be predicted.



The further assumption mentioned above concerns the elastic bulk modulus  $K$ . The possible assumptions are:-

- (i)  $K$  is infinite and hence  $\nu$  has a constant value of 0.5
- (ii)  $\nu$  is constant and  $K$  will then vary in some unprescribed manner.
- (iii)  $K$  is constant but finite and  $\nu$  will vary
- (iv)  $K$  varies in a way which can be described by Maxwell and Kelvin elements, and again  $\nu$  will vary.

Of these assumptions (i) and (ii) do not appear to agree with observations [17], while (iii) seems to agree approximately with experimental results [19]. A more accurate expression would probably be given by (iv), but in view of the doubtful nature of the assumed linearity the extra complication seems to be unjustified. Assumption (iii) therefore seems to be a good compromise between accuracy and simplicity.

The results of the creep tests on Perspex in 4.1 were adequately represented for stresses up to about  $20 \text{ MN/m}^2$  by linear viscoelastic theory based on a 3-parameter distortion model and assumption (iii) above for dilatation. The mathematics of this linear theory then shows that calculations for a viscoelastic material are similar to those for an elastic material except that the elastic constants of the elastic theory are replaced by time-dependent variables. As calculations for an elastic material are usually based on the constants  $E$  and  $\nu$ , a similar approach is convenient for viscoelastic materials.

The use of a time-dependent modulus  $E(t)$  is demonstrated in calculating the deflection of the Perspex frame in 7.1. This is a



uni-axial stress problem, for any one member, in which the bending stress varies with position but not with time. The use of a time-dependent  $E(t)$ , the value of which could be found from the earlier creep tests could then be expected to predict the deflection of the frame extremely accurately, and this was found to be the case. Also, as both tensile and compression bending stresses occur, the results of 7.1 demonstrate that there cannot be much difference between the behaviour of Perspex in tension and compression, at least up to a stress of  $20 \text{ MN/m}^2$ .

By using linear viscoelastic theory, the strains in a particular direction due to several stresses may be superimposed, and 3.4 shows how this linear theory may be applied to a two-dimensional stress system. It is also demonstrated that the constants  $E$  and  $\nu$  of an elastic material are replaced by variables  $E(t)$  and  $\nu(t)$  for a viscoelastic material.

Hence, having obtained a stress-strain-time relationship, the designer is then confronted with a time-dependent modulus  $E(t)$  and a time-dependent Poisson's ratio  $\nu(t)$ , the appropriate values of which must be used at a particular time. This may not present any particular problems in some cases; for example, in a long internally-pressurized cylinder, the longitudinal and hoop stresses are not time-dependent being statically determinate, and the increase of diameter is easily obtained in the usual way using the appropriate values of  $E(t)$  and  $\nu(t)$ .



While the assumption of constant stresses is exactly true for the membrane stresses in a cylinder (providing the pressure remains constant), any local bending stresses may vary slightly with time. This is so in the case of the Perspex cylinder investigated in 7.2, but the variation of the net longitudinal and hoop stresses is small and it is shown theoretically that, at least for Perspex, the actual variation of stresses with time has little effect on the value of  $E(t)$ . It also follows that the value of  $v(t)$  will be little different to the value obtained when the stresses remain constant. In 7.2 therefore values of  $E(t)$  and  $v(t)$  are calculated for constant stresses and it is shown that the measured increase of radius of the cylinder agrees quite well with the calculated values.

Similarly, good agreement is obtained between theoretical and calculated values of the deflections of a square of Perspex subjected to a compressive stress described in 7.3. Here also stresses vary somewhat with time but it is found that the values of  $E(t)$  and  $v(t)$  calculated for constant stresses give satisfactory results.

Even when a solution is obtained for a particular problem, the designer's work is not finished as he must then decide what criteria to use to determine maximum permissible loads etc. Turner suggests [19] that for plastics, strain is probably a more suitable limit than stress, and that accordingly the strain should not exceed some prescribed limit during the life of the part.



This criterion does, however, cast considerable doubt on this linear design approach, as with most plastics at strains well below a suitable upper limit, the behaviour of the material will be very markedly non-linear.

#### Non-linear viscoelasticity

If linear viscoelasticity is not to be assumed, the stress-strain-time equation may be replaced by sets of curves plotted from experimental results. These are perhaps best visualised as sections through a 3-dimensional surface in which the 3 perpendicular axes are stress, strain and time (usually on a logarithmic scale). Sections perpendicular to any axis give the usual creep (constant stress), isometric (constant strain), and isochronous (constant time) curves.[17]. Curves for many common plastics have been published [6].

The limiting strain criterion is now easily applied, resulting in either a maximum stress or a limit on the life of the part, but this approach is only reliable if all stresses remain constant, and since the way in which Poisson's ratio varies is extremely uncertain, two- and three-dimensional problems now present great difficulties.

Even uniaxial stress problems now become very complicated unless the stress remains constant. The basic difficulty in non-linear viscoelasticity is that strains cannot be obtained by simple superposition and while methods have been suggested for predicting the results of stress variations [20] the amount of experimental work necessary to obtain the required functions appears to be impracticable. [21].



Lockett and Turner [21] also show that when a uniaxial stress is removed, although no residual strain may be shown after a certain time, the response to a further stress application will be affected. A much simplified strain-time relation is also obtained for several creep-recovery cycles, the stress being constant for each creep period, and it is then removed completely during recovery.

Turner [18] shows how the strain during creep-recovery cycles may be predicted from creep tests only. As expected the strains due to an intermittently applied stress are less than those due to the same stress applied continuously, so that if the maximum strain criterion is applied here, a higher stress may be used when the loading is intermittent, than when the load is continuous.

One set of results for a square wave stress is given in 9.2 and it also seems that the same method may be applied to this type of variation between two stresses, neither of which is zero.

A second type of non-linear viscoelastic problem is discussed in 9.3. This is the problem of the loading of a non-linear tapered Perspex beam. It is shown that, since this is a uniaxial stress system and the stresses vary only slightly with time, the deflection may be calculated extremely accurately by using only the results of the earlier creep tests in conjunction with the non-linear elastic bending theory described in 8.3.



While the methods indicated extend the scope of non-linear viscoelastic design for a uniaxial system, further progress appears uncertain until

- (i) the response to a single arbitrary stress input can be predicted from the previous stress history, and the theory then extended to 2 and 3-dimensional systems.
- (ii) a satisfactory criterion corresponding to the von Mises yield criterion is available for a viscoelastic material.

At the moment, neither of these objectives seems to be in sight, so some sort of approximation to (i) above is necessary. One possibility with small stress variations is to neglect the change, and 9.3 shows how this gives good results with a beam. A second line of approach might be to superimpose strains when the variations of stress are small, but remembering that this may cause some inaccuracy.



## CHAPTER 10

### GENERAL DISCUSSION

Quite simple theoretical solutions are possible for some engineering problems in which it is possible to make certain simplifying assumptions. A good example of this approach is the use of simple bending theory for elastic materials in which all stresses except those acting along the length of the beam are ignored. This method gives extremely good results providing its limitations are known and it is not used for cases in which the simplifying assumptions cannot be justified, for example in the case of a short deep beam where shear stresses are important.

In cases where a simplified solution gives poor results, the theory of linear elasticity may be used to obtain an exact result, but this usually involves a great deal of algebraic manipulation, and the solution may become so complex that this method of approach may not be practicable for everyday design work. One case in which this method does work is given in 3.3 where elasticity theory gives an exact value for the end deflection of a loaded wedge. It is also shown that for small angles of taper the simple beam theory gives quite good results (6.7).

The viscoelastic behaviour of plastics differs from that of



elastic materials in being time dependent but it was seen that the actual behaviour of Perspex could be adequately represented by suitable mathematical models which assumed a linear relationship between stress and strain for stresses not exceeding about 20 MN/m<sup>2</sup>. It was further seen that if the solution of a linear problem is known, by using a correspondence rule the solution of the viscoelastic problem is (at least in theory) possible. In all except the simplest cases, however, the inversion of the Laplace transform, which is a necessary part of the solution, may present considerable difficulties. For simple one- and two-dimensional constant stress systems solutions are possible and it was demonstrated that the form of the viscoelastic solution is similar to the elastic solution with the elastic constants replaced by corresponding time-dependent variables. These variables are readily calculated from the known parameters evaluated from (say) a set of creep tests. It was also shown, that small variations of stress have little effect on the values of these time-dependent variables for Perspex.

If, then, the solution is known for an elastic problem in which the stresses remain constant or nearly so, the solution of the corresponding viscoelastic problem may be obtained without difficulty.

As was noted above, however, exact solutions for elastic materials may be very complex, so various numerical methods were investigated and it was decided that the most promising of these, for the types of problems to be solved, was the finite element method, using beam type elements. It was seen that the bending of uniform beams could



be treated in this way and that frame deflection problems could be similarly solved.

The stiffness matrix was then derived for a tapered element and the accuracy of this finite element method was then further improved by modifying the stiffness matrix to allow for the effect of shear stresses in both uniform and tapered elements. The accuracy of the finite element method was considerably improved by this allowance for shear effects in the case of the loaded wedge for which an exact solution had been previously obtained.

To complete this part of the work, a computer program was written to solve, using this finite element method, beam problems for uniform or tapered beams for any type of loading and with any number of either rigid or elastic supports.

An alternative finite element method using constant strain triangles was applied to beams which were treated as plane-stress problems. This was found to give very inaccurate values for both deflections and stresses due to the large variations of stress across the depth of the beam. The accuracy was improved by increasing the number of elements, but even with a large number of elements the results were much inferior to those obtained by using beam-type elements.

Finite element methods were then applied to three linear visco-elastic problems. These were (i) a frame (ii) a pressurized cylinder



and (iii) a square plate subjected to compressive stresses. In the first of these, stresses were independent of time and nearly so in (ii) and (iii). In all three cases the finite element solution obtained by using the time-dependent variables  $E(t)$  and  $\nu(t)$  calculated from expressions which are strictly true only for constant stresses was found to agree well with experimental results.

Finally, the problems of non-linear viscoelasticity were considered. A method of predicting strains due to the alternation of two stresses was shown to agree fairly well with measured values. A theoretical solution was also obtained for the deflection of a non-linear tapered Perspex beam. The theoretical values of deflection agreed extremely well with experimental results even when stresses considerably exceeded the linear range of the material. The method used here could in fact be applied to any non-linear bending problem and requires only corresponding values of stress and strain such as could be easily obtained from creep tests.



CHAPTER 11

CONCLUSIONS

The following conclusions may be deduced from the work recorded here.

1. A finite element method using beam type elements will satisfactorily solve bending problems for linear elastic, linear viscoelastic and non-linear viscoelastic uniform and tapered beams.
2. Bending problems are not well suited to solution as plane-stress problems using constant strain triangles due to the variation in stress across the beam, but this approach is satisfactory in cases where stress gradients are smaller than in beams.
3. The linear viscoelastic behaviour of plastics may be described in terms of mathematical models which may then be used to predict the behaviour of the material under a variety of conditions.
4. If the solution of a particular problem for an elastic material is known the use of the correspondence rule will give the solution for a linear viscoelastic material. The solution may, however, be complex and the use of a numerical method may be preferable.



5. Linear viscoelastic problems are readily solved by a finite element method using time-dependent values of  $E(t)$  and  $\nu(t)$ . These results are not strictly accurate in cases where the stresses vary with time, but errors will be small if the variations of stress are not large.
  
6. Non-linear viscoelastic problems are much more difficult to solve than linear ones. Relatively simple solutions are possible for some problems (e.g. the strains due to alternating stresses).

The non-linear bending problem of Chapter 8 was solved so readily by the numerical method of 8.3 that it might be rewarding to see if the same method can be used for beams of other than rectangular cross-section.

Regarding the behaviour of plastics, it would be interesting to investigate the effect of using more complicated mathematical models of material behaviour than the three-parameter model mainly used by the present author. It would also be of interest to investigate theoretically and experimentally how the value of  $E(t)$  is affected for different types of stress variation, possibly using several different materials.

Since the behaviour of all plastics is to some extent non-linear it would be extremely useful if the method of 8.3 for a uniaxial



stress system could be extended to two- and three-dimensional systems. This would, however, need much more information about how the value of Poisson's ratio varies with stress and time than appears to be available at present.

A satisfactory criterion for the failure of plastics is still awaited, but in view of the number of parameters involved a very great deal of experimental work will probably be necessary to obtain any useful results.

The intermittent loading tests of 9.2 show that the strain continues to increase with time. A vibratory force producing alternate tensile and compressive stresses in the material may produce the same type of result. Further investigation of this possibility may be worth while.



## ACKNOWLEDGEMENTS

The author wishes to thank:-

Mr. T. H. Richards who, as supervisor, gave generously of his time to provide assistance and guidance throughout.

Members of the technical staff who gladly gave assistance in the workshops and laboratories.

The Governors and Principal of Dudley Technical College who made it possible for the author to undertake this work.



APPENDIX

COMPUTER PROGRAMS

The programs detailed below were written for an I.C.L. 1905 computer, and the language used was ALGOL. Initially, to gain experience in writing computer programs, problems such as the plate bending problem of 5.1(c) were solved by using the computer for the evaluation of a number of terms and the summation of the resulting series. Since there are no particular points of interest in this or similar programs they are not shown here.

The first program involving any real difficulty was Prog.1 required to calculate the change of radius of a viscoelastic cylinder. The expression of 4.4.4

$$\frac{pr^2}{h} \left\{ \frac{1}{E} \left( 1 - \frac{\nu}{2} \right) - \frac{3}{4} C (1 - e^{-\zeta t}) \right\} \{ 1 - e^{-\beta x} (\cos \beta x + \sin \beta x) \}$$

was to be evaluated for various values of  $x$  and  $t$ . This was achieved by using a double loop, first keeping the value of  $t$  constant in the outer loop and then using all the different values of  $x$  in the inner loop. To save computer time the value of  $e^{-\zeta}$  was initially computed and then values of  $e^{-\zeta t}$  ( $t = 2, 3, \dots$ ) were readily found by multiplications such as  $e^{-2\zeta} = e^{-\zeta} \cdot e^{-\zeta}$  at the end of the  $t$  loop. Values of  $e^{-\beta x}$  were found in the same way. For convenience in printing out the results the required deflections were all calculated and stored in a two-dimensional array  $W[I, T]$  before being printed.



Prog.2 was used to solve the 10 simultaneous equations obtained by using a finite element method to solve a beam problem. In this case the values of the elements of the stiffness matrix were read in from cards and the equations then solved by Gaussian elimination (It is perhaps worth recording that the Gauss-Seidel iterative method was first tried, but gave very inaccurate results and used a great deal of computer time. The failure of this method here is probably due to the very small value of F compared with those of the other terms in each equation [8].

Gaussian elimination, on the other hand worked extremely well. This method requires that starting with the first row some multiple of each pivot row ( $P = 1, 2 \dots N-1$ ) is subtracted from each row below ( $I = P+1, \dots N$ ) so that the elements to the left of the leading diagonal are made equal to zero. Prog.2 does in fact save unnecessary calculations by omitting this subtraction when an element is already zero. The form of the modified equations is then as shown below.

$$\begin{Bmatrix} H_1 \\ \vdots \\ H_{10} \end{Bmatrix} = \begin{bmatrix} x & x & & & x \\ & & & & \\ & & \text{Etc} & & \\ & & & & \\ & & & & x \end{bmatrix} \begin{Bmatrix} u_1 \\ \vdots \\ u_{10} \end{Bmatrix}$$

where x denotes a non-zero element.

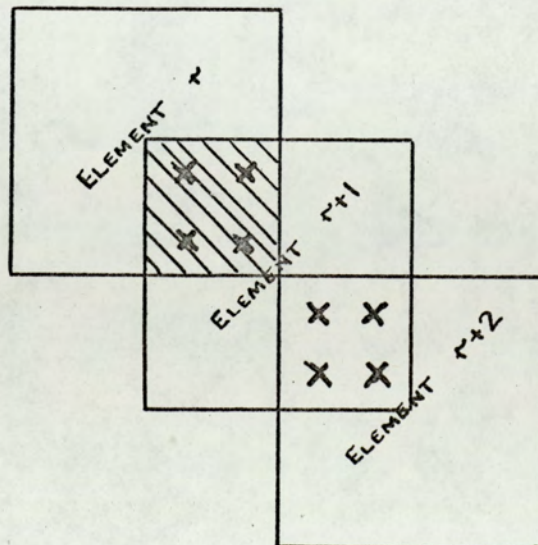
$u_{10}$  can then be found immediately, and by substitution of this value in the row above  $u_9$  is calculated and so on until  $u_1$  is found.



With only a few elements, the method of reading in values used above is satisfactory, but with many elements it is almost essential to use the computer to evaluate individual elements of the stiffness matrix. This is easily achieved by supplying the values of  $E$ ,  $I$  and  $\ell$  for a uniform beam, or of  $E$ ,  $b$ ,  $d_1$ ,  $d_2$  and  $\ell$  for the tapered beam element of 6.5. If the elements of the stiffness matrix of this one element are represented by  $c_{ij}$  ( $i, j = 1, 2, 3, 4$ ), the last 4 of these values  $c_{ij}$  ( $i, j = 3, 4$ ) must be temporarily stored for addition to the first 4 values of  $c_{ij}$  ( $i, j = 1, 2$ ) of the next element since two elements are joined at the common node. The required additions for adjacent elements  $r, r + 1$ , are:-

$$\begin{aligned} (c_{33})_r + (c_{11})_{r+1}, & \quad (c_{34})_r + (c_{12})_{r+1} \\ (c_{43})_r + (c_{21})_{r+1}, & \quad (c_{44})_r + (c_{22})_{r+1} \end{aligned}$$

This is perhaps more obvious in the diagram below where the additions above occupy the shaded area common to elements  $r$  and  $r + 1$ . Similar additions will be required for elements  $r + 1$  and  $r + 2$  etc. until the last element is reached.









By moving every element of the  $i^{\text{th}}$  row  $i - 1$  spaces to the left all the non-zero elements may be stored in the form:-

$$\begin{bmatrix} 0 & 0 & 0 & k_{11} & k_{12} & k_{13} & k_{14} \\ 0 & 0 & k_{21} & k_{22} & k_{23} & k_{24} & 0 \\ 0 & k_{31} & x & k_{33} & x & x & k_{36} \\ k_{41} & x & x & k_{44} & x & k_{46} & 0 \\ 0 & k_{53} & x & k_{55} & x & x & k_{58} \\ k_{63} & x & x & k_{66} & x & k_{68} & 0 \\ 0 & k_{75} & x & k_{77} & x & x & x \\ k_{85} & x & x & x & x & x & 0 \\ & & & \text{etc.} & & & \end{bmatrix}$$

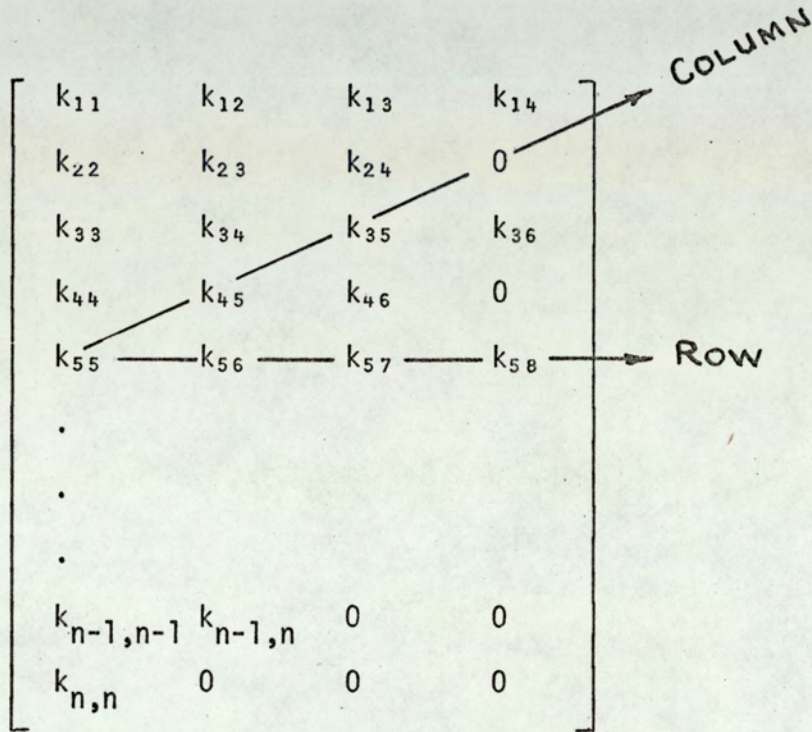
The Gaussian elimination method is again used to find the displacements, with due account being taken of the distorted form of the storage arrangement.

Prog.4 is a program written to find the deflection at the end of the wedge of 6.8. In addition to the finite element solution obtained in the same way as in Prog.3, values are also obtained using simple beam theory and using the methods of the theory of elasticity.

Prog.5 is a more general program which may be used for a tapered beam with any number of rigid or elastic supports. Prog.4 makes use of the banded nature of the stiffness matrix, but as it is also symmetrical about the leading diagonal only this diagonal and the elements on one side of it need be stored. This method of storage



is used in Prog.5 as shown below and because of the distorted form of the matrix care is again necessary in using the Gaussian elimination method to find the displacements.

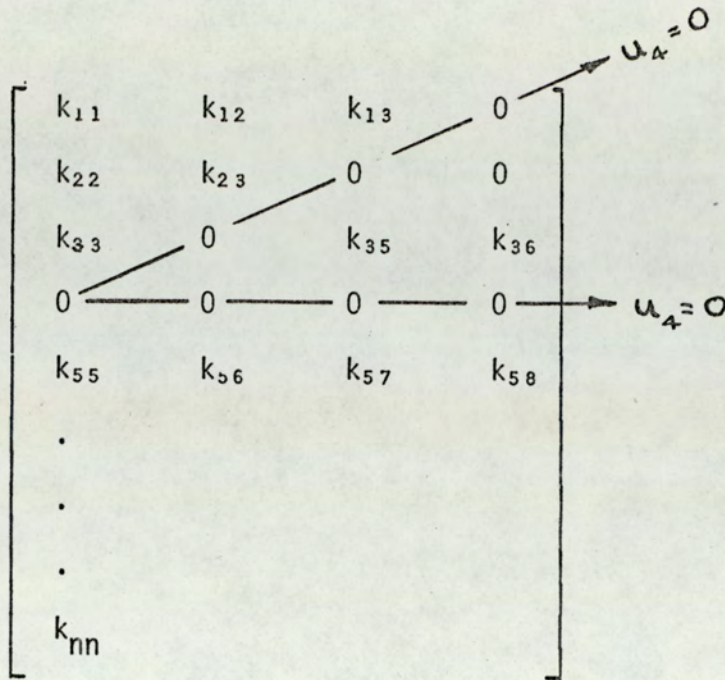


Note that rows are still horizontal, but columns of the true stiffness matrix are now stored on diagonal lines. The first element of each row stored is the leading diagonal element of the true matrix, and the band width is now reduced to only 4 elements.

If a constraint is applied so that a particular displacement is zero, the elements of the appropriate rows and columns of the stiffness matrix are now all zero.

e.g. if  $u_4 = 0$ , the stiffness matrix becomes:-





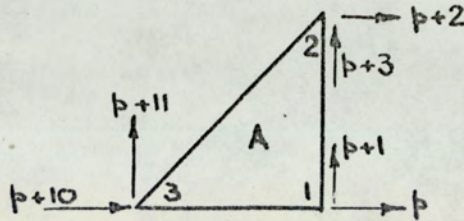
During the elimination process all such rows and columns are missed since all the elements are already zero and therefore no further action is needed.

The plane stress problem of 6.11 was solved by using Prog.6. The assembly of the stiffness matrix is now more complicated because not only does each shape of triangle have a different stiffness matrix but since the triangles may be fitted together in a variety of ways (unlike beam elements which can only fit end to end) the summation of stiffnesses must take account of the relative position of the triangles.

In Prog.6, four different triangles are used, and the elements of their different stiffness matrices are first evaluated from the expressions of 6.11. Using the symmetry of the matrices, only the elements of the upper half of each matrix are in fact used. The nodes of each triangular element must then be related to the global nodes, and since there is a regular pattern in the arrangement of



elements, this is not difficult. For example, consider an "A" triangle in the arrangement of Fig. 6.11.9.



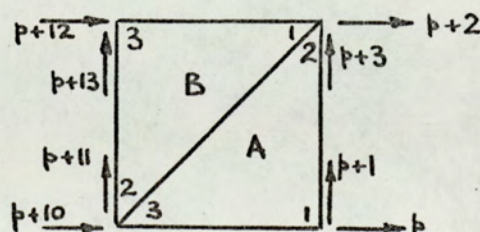
The element nodes 1,2,3 correspond to global nodes  $m, m+1, m+5$  where  $m = 1, 2, 3$  etc. depending on the position of the element. The generalized coordinate numbers at these global nodes are  $p, p+1, p+2, p+3, p+10$  and  $p+11$ .

The contribution of an A triangle to the  $p^{\text{th}}$  row of the combined stiffness matrix will therefore be of the form:-

$$\begin{array}{c}
 p^{\text{th}} \text{ column} \\
 \downarrow \\
 \begin{array}{cccccccccccc}
 a_{11} & a_{12} & a_{13} & a_{14} & 0 & 0 & 0 & 0 & 0 & 0 & a_{15} & a_{16}
 \end{array} \\
 \downarrow
 \end{array}$$

Other rows are obtained in the same way and Prog.6 first takes the contribution of all the A triangles making  $k_{p1} = a_{11}$  etc.

B triangles are treated in the same way adding stiffnesses where necessary. For example the upper right-hand corner (element node 2) of an A triangle is always joined to node 1 of a B triangle.



The  $p+2^{\text{th}}$  row of the stiffness matrix for combined A and B triangles is therefore:-







Once the combined stiffness matrix has been assembled, displacements are found using the same method as in Prog.5.

Stresses may then be calculated from the nodal displacements  $\{u_i\}$  using

$$\{\sigma\} = [D] [B] \{u_i\} \quad [24]$$

where  $[D]$  and  $[B]$  are as given in 6.11.

$[D]$  will be the same for all elements since it is a function of  $E$  and  $\nu$  only, and  $[B]$  will be the same for each triangle of a particular shape. It was therefore convenient to evaluate the  $[B]$  matrix for an "A" triangle, to pre-multiply this by  $[D]$  and so obtain

$$\{\sigma\} = [M] \{u_i\}$$

where  $[M]$  is a function of  $E$ ,  $\nu$  and the lengths of the perpendicular sides of an A triangle. Stresses in each A triangle were then determined from the values of  $u_i$  for a particular triangle.

In the same way stresses in the B, C and D triangles were calculated.

The change of radius of a cylinder of varying wall thickness may be found by using Prog.7. This is similar in many ways to Prog.5 as far as the assembly and storage of the stiffness matrix is concerned. As explained in 7.1 any longitudinal slice of the cylinder will behave as a beam on a flexible base, and the same section also shows how the stiffness and force matrices are modified by this "flexible base".



The stiffness elements for a tapered beam are used, and since the "free" change of radius and the stiffnesses depend on time-dependent values of  $E$  and  $\nu$  a time loop is added to calculate these values from equations 3.4.11 and 3.4.12 for each time value. Each element of the stiffness matrix is then evaluated in the usual way.

When the deflections due to the local end effects have been found by the same methods as in previous programs, the addition of the "free" expansion will give the net change of radius. Bending moments may be found by using the usual relation between nodal moments and displacements, and local bending stresses at the inside and outside surfaces of the cylinder are then easily determined by the usual bending equation. The net longitudinal stress is the sum of this bending stress and the usual membrane stress  $\frac{pr}{2h}$ .

The hoop stresses at the two surfaces are then found from

$$\sigma_h = E \frac{w}{r} + \nu \sigma_\ell$$

where  $w$  is the change of radius and  $\sigma_\ell$  is the longitudinal stress [5].

In addition to the printed values of change of radius, bending moment and stress, graphs of change of radius and stresses at the inner and outer surfaces were drawn by the graph plotter using the cubic curve-fitting sub-routine HGPSCURVE. For each graph, the coordinates of all points were stored, and after drawing each curve the pen was raised and moved to the starting coordinates of the next curve.



Since theoretical values were used there were no discontinuities in any of the curves for the uniform cylinder, and smooth curves were obtained (see Figs. 7.2.3 and 7.2.4). Fig. 7.2.6 however shows the variation of stress in a cylinder which is tapered near its end. While there is no discontinuity of stress at the end of the tapered portion ( $x = 45$  mm) there is a discontinuity in the rate of change of stress and HGPSCURVE tries to smooth out this sudden change of slope. To avoid this, each curve is drawn in two separate parts, i.e. from 0 to 45 mm and from 45 mm to 100 mm.

The plane stress viscoelastic problem of 7.3 was solved by using a finite element method. The stiffness matrix is assembled by modifying Prog.6 so that the assembled triangular elements now form a square, which is a simple matter of shortening the list at the start of each 'DO' loop during compilation. Since only a quarter of the Perspex square was considered due to its double symmetry, vertical constraints were applied to all nodes on the horizontal centre line, and horizontal constraints on the vertical centre line.

Using these modifications Prog.8 was written. A further difference from Prog.6 is that in Prog.8 allowance is made for the fact that vertical displacements at all nodes on the top edge of the square are to be equal. Since the columns in the stiffness matrix corresponding to the generalized coordinates of these nodes will now correspond to equal displacements they may be added, and to satisfy equilibrium the corresponding rows must also be added, and so must the appropriate nodal forces. This may be shown by a



simple example.

$$\begin{Bmatrix} F_1 \\ F_2 \\ F_3 \end{Bmatrix} = \begin{bmatrix} a & b & c \\ b & d & e \\ c & e & f \end{bmatrix} \begin{Bmatrix} u_1 \\ u_2 \\ u_3 \end{Bmatrix}$$

If  $u_1 = u_2$  this may be rewritten as

$$\begin{Bmatrix} F_1 + F_2 \\ 0 \\ F_3 \end{Bmatrix} = \begin{bmatrix} a+2b+d & 0 & c+e \\ 0 & 0 & 0 \\ c+e & 0 & f \end{bmatrix} \begin{Bmatrix} u_1 \\ 0 \\ u_3 \end{Bmatrix}$$

Values of  $u_1$  and  $u_2$  may then be found by inverting the stiffness matrix and are automatically equal.

This summation of stiffness elements is used in Prog.8. As described in 7.3, the variation of displacements with time is allowed for by calculating two sets of displacements from two stiffness matrices, the first evaluated from initial values of  $E$  and  $\nu$ , and the second using  $\bar{E}$  and  $N$  as given in equation 7.3.3. The net displacements are then the sums of these two sets of values, and the stresses are then found from the displacements by using the time-dependent values of  $E$  and  $\nu$ ,  $E(t)$  and  $\nu(t)$  as given in 3.4.11 and 3.4.12.

Prog.9 used for non-linear bending problems does not differ greatly from Prog.5, the main difference being that instead of a known value of  $E$  an equivalent quantity which depends on the maximum



stress must now be used. This requires that values of  $m_i$  and  $E_i$  as given in 8.3.2 and 8.3.3 shall be evaluated for all values of  $i$ . An iterative method of solution is used, and an additional loop is therefore included in Prog.9, at the end of which the sum of all the displacements is compared with the previous sum. Calculations are concluded when the difference between successive values is less than 0.2%.



# PROG. I

21/01/71

COMPILED BY XALE MK. 4B

```
'SENDTO'(ED,ICLA-DEFAULT(0),.PROGRAM)
'BEGIN' 'REAL' P,R,H,E,NU,B,C,D,BX,VC,Z,CT,DT,RE,NF,VT,A;
'INTEGER' I,X,T;
'REAL' 'ARRAY' W(0:20,0:6);
P:=1.5;
R:=75; H:=6.25;
E:=3000; NU:=0.35; VC:=0.068 -3; Z:=0.47;
A:=P*R*R/H; CT:=1/EXP(Z); DT:=1; RE:=1/E; NF:=1-0.5*NU;
B:=(3*(1-NU*NU)/(R*R*H*H))↑0.25; C:=EXP(10*B);
'FOR' T:=0 'STEP' 1 'UNTIL' 6 'DO'
'BEGIN' D:=1; VT:=VC*(1-DT);
'FOR' I:=0 'STEP' 1 'UNTIL' 20 'DO'
'BEGIN' X:=10*I; BX:=B*X;
W[I,T]:=A*(NF*RE+0.75*VT)*(1-(COS(BX)+SIN(BX))/D);
D:=D*C;
'END';
DT:=DT*CT;
'END';
SPACE(12); WRITETEXT('('T=%0%'')');
'FOR' T:=1,2,3,4,5,6 'DO'
PRINT(T,9,0); NEWLINE(2);
'FOR' I:=0 'STEP' 1 'UNTIL' 20 'DO'
'BEGIN' X:=10*I; WRITETEXT('('X=')');
PRINT(X,3,0);
'FOR' T:=0 'STEP' 1 'UNTIL' 6 'DO'
PRINT(W[I,T],4,4);
NEWLINE(2);
'END';
'END';
```







# PROG. 3

27/07/70

COMPILED BY XALE MK. 4B

```

'BEGIN' 'REAL' D1,D2,X1,X2,FAC,SUM,L;
'INTEGER' N,K,Q,T,AL,AC,P,I,J, LAST,FIN;
N:=READ;
'BEGIN' 'REAL' 'ARRAY' C[1:4,1:4],CP[3:4,1:4],U,F[1:N],A[1:N,1:7];
'FOR' I:=1 'STEP' 1 'UNTIL' N 'DO' F[I]:=READ;
'FOR' I:=1 'STEP' 1 'UNTIL' N 'DO'
'FOR' J:=1 'STEP' 1 'UNTIL' 7 'DO'
A[I,J]:=0; D1:=1; X1:=0;
'FOR' K:=2 'STEP' 2 'UNTIL' N+2 'DO'
'BEGIN' D2:=D1-0.1; X2:=20*(1-D2)*(1-D2);
L:=X2-X1;
'COMMENT' *EB/12; C[1,1]:=D1*D1*(18*D2-6*D1)/(L*L*L);
C[1,2]:=6*D1*D1*D2/(L*L);
C[1,3]:=-C[1,1];
C[1,4]:=D1*D1*(12*D2-6*D1)/(L*L);
C[2,1]:=C[1,2];
C[2,2]:=D1*D1*(D1+3*D2)/L;
C[2,3]:=-C[1,2];
C[2,4]:=D1*D1*(3*D2-D1)/L;
'FOR' J:=1 'STEP' 1 'UNTIL' 4 'DO'
C[3,J]:=-C[1,J];
C[4,1]:=C[1,4];
C[4,2]:=C[2,4];
C[4,3]:=C[3,4];
C[4,4]:=D1*D1*(9*D2-5*D1)/L;
D1:=D2; X1:=X2;
'IF' K=2 'THEN' 'GOTO' SKIP;
I:=K-3;
'IF' I=1 'THEN' 'GOTO' JUMP;
'IF' K=N+2 'THEN'
'BEGIN' C[1,1]:=0; C[1,2]:=0; C[2,1]:=0; C[2,2]:=0;
'END';
A[I,2]:=CP[3,1]; A[I,3]:=CP[3,2];
A[I+1,1]:=CP[4,1]; A[I+1,2]:=CP[4,2];
JUMP: A[I,4]:=CP[3,3]+C[1,1]; A[I,5]:=CP[3,4]+C[1,2];
A[I+1,3]:=CP[4,3]+C[2,1]; A[I+1,4]:=CP[4,4]+C[2,2];
'IF' K=N+2 'THEN' 'GOTO' COMP;
A[I,6]:=C[1,3]; A[I,7]:=C[1,4];
A[I+1,5]:=C[2,3]; A[I+1,6]:=C[2,4];
SKIP: 'FOR' Q:=3,4 'DO'
'FOR' T:=1 'STEP' 1 'UNTIL' 4 'DO'
CP[Q,T]:=C[Q,T];
COMP: 'END';
'FOR' I:=1 'STEP' 1 'UNTIL' N 'DO'
'BEGIN' 'FOR' J:=1 'STEP' 1 'UNTIL' 7 'DO'
PRINT(A[I,J],6,4); NEWLINE(2);
'END';
PAPERTHROW;
'FOR' P:=1 'STEP' 1 'UNTIL' N-1 'DO'
'BEGIN' LAST:='IF' P+3 'LE' N 'THEN' P+3 'ELSE' N;
'FOR' I:=P+1 'STEP' 1 'UNTIL' LAST 'DO'
'BEGIN' 'IF' A[I,P+4-I]=0 'THEN' 'GOTO' ELIM
'ELSE' FAC:=A[I,P+4-I]/A[P,4];
F[I]:=F[I]-F[P]*FAC;

```



```

'FOR'J:=P+4-I'STEP'1'UNTIL'P+7-I'DO'
A[I,J]:=A[I,J]-A[P,I-P+J]*FAC;
ELIM: 'END';
'END';
U[N]:=F[N]/A[N,4];
'FOR'I:=N-1'STEP'-1'UNTIL'1'DO'
'BEGIN'SUM:=F[I];
FIN:='IF'I'LE'N-3'THEN'7'ELSE'N-I+4;
'FOR'J:=5'STEP'1'UNTIL'FIN'DO'
SUM:=SUM-A[I,J]*U[I+J-4];
U[I]:=SUM/A[I,4];
'END;
NEWLINE(4);
'FOR'I:=1'STEP'1'UNTIL'N'DO'
'BEGIN'WRITETEXT('(U)');PRINT(I,2,0);
WRITETEXT('(I=)');PRINT(U[I],4,4);
NEWLINE(2);
'END';
'END';
'END';

```

0.0000	0.0000	0.0000	1308.7500	-109.2000	-33.7500	9.4500
0.0000	0.0000	-109.2000	19.9550	-10.8000	2.0250	0.0000
0.0000	-33.7500	-10.8000	38.7420	-6.7620	-4.9920	2.3040
9.4500	2.0250	-6.7620	5.5010	-2.6880	0.8320	0.0000
0.0000	-4.9920	-2.6880	6.1706	-1.4040	-1.1786	0.7500
2.3040	0.8320	-1.4040	2.3470	-0.9000	0.3850	0.0000
0.0000	-1.1786	-0.9000	1.5119	-0.4167	-0.3333	0.2667
0.7500	0.3850	-0.4167	1.0850	-0.3333	0.1800	0.0000
0.0000	-0.3333	-0.3333	0.3333	-0.2667	0.0000	0.0000
0.2667	0.1800	-0.2667	0.3000	0.0000	0.0000	0.0000

Storage arrangement for the stiffness matrix of PROG. 3  
(Eb/12 omitted).



# PROG. 4

10/02/72

COMPILED BY XALE MK. 5C

```
'SEND TO' ( ED,ASTD-DEFAULT(0),.PROGRAM)
'WORK' (ED,WORK FILE (0))
'BEGIN' 'REAL' D1,D2,FAC,SUM,L,LP,AR,TANA,V1,V2,V3:
        'INTEGER' N,K,Q,T,P,I,J,LAST,FIN,AN,M:
        N:=READ; M:=READ:
        'BEGIN' 'REAL' 'ARRAY' C[1:4,1:4],CP[3:4,1:4],U,F[1:N],
                A[1:N,1:7], FD[1:4]:
                WRITETEXT('('FINITEXELEMENT'('30S')'POLARXCOORDS
                        '('30S')'BEAMXTHEORY')');
                NEWLINE(2);
        'FOR' AN:=5 'STEP' 5 'UNTIL' M 'DO'
        'BEGIN' PRINT(AN,2,0); WRITETEXT('('DEGREES')');
                NEWLINE(2);
                AR:=AN*3.14159/180; TANA:=SIN(AR)/COS(AR);
                'FOR' I:=1 'STEP' 1 'UNTIL' N 'DO'
                'FOR' J:=1 'STEP' 1 'UNTIL' 7 'DO'
                A[I,J]:=0; D1:=TANA;
                'FOR' K:=2 'STEP' 2 'UNTIL' N+2 'DO'
                'BEGIN' 'IF' K=N+2 'THEN'
                        'BEGIN' C[1,1]:=0;C[1,2]:=0;C[2,1]:=0;
                                C[2,2]:=0;L:=0; 'GOTO' TIP;
                        'END';
                        D2:=0.8*D1; L:=(D1-D2)/TANA;
                        FD[1]:=D1*D1*D1; FD[2]:=D1*D1*D2;
                        FD[3]:=D1*D2*D2; FD[4]:=D2*D2*D2;
                        'IF' K=N 'THEN' 'BEGIN'
                                D2:=0; L:=D1/TANA; 'END';
                                C[1,1]:=(4.2*FD[1]+1.8*FD[2]+1.8*FD[3]
                                        +4.2*FD[4])/(L*L*L);
                                C[1,2]:=(3*FD[1]+1.2*FD[2]+0.6*FD[3]
                                        +1.2*FD[4])/(L*L);
                                C[1,3]:=-C[1,1];
                                C[1,4]:=(1.2*FD[1]+0.6*FD[2]+1.2*FD[3]
                                        +3*FD[4])/(L*L);
                                C[2,1]:=C[1,2];
                                C[2,2]:=(2.2*FD[1]+FD[2]+0.4*FD[3]
                                        +0.4*FD[4])/L;
                                C[2,3]:=-C[1,2];
                                C[2,4]:=(0.8*FD[1]+0.2*FD[2]+0.2*FD[3]
                                        +0.8*FD[4])/L;
                                'FOR' J:=1 'STEP' 1 'UNTIL' 4 'DO'
                                C[3,J]:=-C[1,J];
                                C[4,1]:=C[1,4];
                                C[4,2]:=C[2,4];
                                C[4,3]:=C[3,4];
                                C[4,4]:=(0.4*FD[1]+0.4*FD[2]+FD[3]
                                        +2.2*FD[4])/L;
                                'IF' K=2 'THEN' 'GOTO' SKIP;
                                I:=K-3; F[I]:=0.5*(LP+L); F[I+1]:=0;
                                'IF' I=1 'THEN' 'GOTO' JUMP;
                                A[I,2]:=CP[3,1]; A[I,3]:=CP[3,2];
                                A[I+1,1]:=CP[4,1]; A[I+1,2]:=CP[4,2];
                                A[I,4]:=CP[3,3]+C[1,1];
                                A[I,5]:=CP[3,4]+C[1,2];
                                A[I+1,3]:=CP[4,3]+C[2,1];
                                A[I+1,4]:=CP[4,4]+C[2,2];
                                'IF' K=N+2 'THEN' 'GOTO' COMP;
```

TIP:

JUMP:



```

A[I,6]:=C[1,3]; A[I,7]:=C[1,4];
A[I+1,5]:=C[2,3]; A[I+1,6]:=C[2,4];
SKIP: 'FOR' Q:=3,4 'DO'
      'FOR' T:=1,2,3,4 'DO'
      CP[Q,T]:=C[Q,T]; D1:=D2; LP:=L;
COMP: 'END';
      'FOR' P:=1 'STEP' 1 'UNTIL' N-1 'DO'
      'BEGIN' LAST:='IF' P+3 'LE' N 'THEN' P+3 'ELSE' N;
      'FOR' I:=P+1 'STEP' 1 'UNTIL' LAST 'DO'
      'BEGIN' 'IF' A[I,P+4-I]=0 'THEN' 'GOTO' ELIM
      'ELSE' FAC:=A[I,P+4-I]/A[P,4];
      F[I]:=F[I]-F[P]*FAC;
      'FOR' J:=P+5-I,P+6-I,P+7-I 'DO'
      A[I,J]:=A[I,J]-A[P,I-P+J]*FAC;
ELIM: 'END';
      'END';
      U[N]:=F[N]/A[N,4];
      'FOR' I:=N-1 'STEP' -1 'UNTIL' 1 'DO'
      'BEGIN' SUM:=F[I];
      FIN:='IF' I 'LE' N-3 'THEN' 7 'ELSE' N-I+4;
      'FOR' J:=5 'STEP' 1 'UNTIL' FIN 'DO'
      SUM:=SUM-A[I,J]*U[I+J-4];
      U[I]:=SUM/A[I,4];
      'END';
      V1:=12*U[N-1];
      V2:=(1+NU+(1-NU)*AR/TANA+2*LN(1/COS(AR)))
      /(TANA-AR);
      V3:=6/(TANA*TANA*TANA);
      PRINT(V1,6,1); PRINT(V2,36,1); PRINT(V3,36,1);
      NEWLINE(4);
      'END';
      'END';
      'END';

```



# PROG. 5

13/04/72

COMPILED BY XALE MK. 5C

```
'SEND TO' ( ED,ASTD=DEFAULT(0),.PROGRAM)
'WORK' (ED,WORK FILE (0))
'BEGIN' 'REAL' X1,X2,D1, D2,E,B,FAC,SUM,L,MT,AA;
'INTEGER' EN,N,BW,EL,I,J,I1,JJ,FIRST, LAST,SA,Z,P,M,NC,NL,R,S;
E:=READ; B:=READ;
EN:=READ; N:=2*EN+2; BW:=4;
'BEGIN' 'REAL' 'ARRAY' C[1:4,1:4],CP[3:4,3:4],U,F,KS[1:N],
K,KM,Q[1:N,1:4],G,X,D,V[1:N],FD[1:4];
X2:=READ; D2:=READ;
CP[3,3]:=CP[3,4]:=CP[4,4]:=0;
'FOR' I:=1 'STEP' 1 'UNTIL' N 'DO'
'BEGIN' F[I]:=G[I]:=0; V[I]:=1;
'FOR' J:=1 'STEP' 1 'UNTIL' BW 'DO'
K[I,J]:=0;
'END';
'FOR' EL:=1 'STEP' 1 'UNTIL' EN 'DO'
'BEGIN' X1:=X2; D1:=D2;
I:=2*EL-1;
X[I]:=X1; D[I]:=D1;
X2:=READ; D2:=READ; L:=X2-X1;
FD[1]:=D1*D1*D1; FD[2]:=D1*D1*D2; FD[3]:=D1*D2*D2;
FD[4]:=D2*D2*D2;
C[1,1]:=(4.2*FD[1]+1.8*FD[2]+1.8*FD[3]+4.2*FD[4])/(L*L*L);
C[1,2]:=(3*FD[1]+1.2*FD[2]+0.6*FD[3]+1.2*FD[4])/(L*L);
C[1,3]:=-C[1,1];
C[1,4]:=(1.2*FD[1]+0.6*FD[2]+1.2*FD[3]+3*FD[4])/(L*L);
C[2,2]:=(2.2*FD[1]+FD[2]+0.4*FD[3]+0.4*FD[4])/L;
C[2,3]:=-C[1,2];
C[2,4]:=(0.8*FD[1]+0.2*FD[2]+0.2*FD[3]+0.8*FD[4])/L;
C[3,3]:=-C[1,3]; C[3,4]:=-C[1,4];
C[4,4]:=(0.4*FD[1]+0.4*FD[2]+FD[3]+2.2*FD[4])/L;
KM[I,1]:=C[1,2]; KM[I,2]:=C[2,2];
KM[I,3]:=C[2,3]; KM[I,4]:=C[2,4];
K[I,1]:=C[1,1]+CP[3,3]; K[I,2]:=C[1,2]+CP[3,4];
K[I,3]:=C[1,3]; K[I,4]:=C[1,4];
K[I+1,1]:=C[2,2]+CP[4,4]; K[I+1,2]:=C[2,3];
K[I+1,3]:=C[2,4];
CP[3,3]:=C[3,3]; CP[3,4]:=C[3,4]; CP[4,4]:=C[4,4];
'END';
X[N-1]:=X2; D[N-1]:=D2;
K[N-1,1]:=CP[3,3]; K[N-1,2]:=CP[3,4]; K[N,1]:=CP[4,4];
'FOR' I:=1 'STEP' 1 'UNTIL' N 'DO'
'FOR' J:=1 'STEP' 1 'UNTIL' BW 'DO'
Q[I,J]:=K[I,J];
NC:=READ;
'IF' NC=0 'THEN' 'GOTO' NOCO;
'FOR' R:=1 'STEP' 1 'UNTIL' NC 'DO'
'BEGIN' Z:=READ; U[Z]:=0; V[Z]:=0;
'FOR' J:=1 'STEP' 1 'UNTIL' BW 'DO'
K[Z,J]:=0;
FIRST:= 'IF' Z>BW 'THEN' Z-BW+1 'ELSE' 1;
'FOR' I:=Z-1 'STEP'-1 'UNTIL' FIRST 'DO'
K[I,Z-I+1]:=0;
'END';
NOCO:
EL:=READ;
'IF' EL=0 'THEN' 'GOTO' ZEK;
'FOR' P:=1 'STEP' 1 'UNTIL' EL 'DO'
```



```

'BEGIN' I:=READ; KS[I]:=READ;
          K[I,1]:=K[I,1]+KS[I]*12/(E*B); V[I]:=2;
'END';
ZEK: NL:=READ;
'FOR' S:=1 'STEP' 1 'UNTIL' NL 'DO'
'BEGIN' Z:=READ; G[Z]:=READ; F[Z]:=G[Z]*12/(E*B);
'END';
'FOR' P:=1 'STEP' 1 'UNTIL' N-1 'DO'
'BEGIN' 'IF' K[P,1]=0 'THEN' 'GOTO' FINP;
        LAST:= 'IF' P 'LE' N-BW+1 'THEN' P+BW-1 'ELSE' N;
'FOR' I:=P+1 'STEP' 1 'UNTIL' LAST 'DO'
'BEGIN' 'IF' K[P,I-P+1]=0 'THEN' 'GOTO' FINI;
        FAC:=K[P,I-P+1]/K[P,1];
        F[I]:=F[I]-F[P]*FAC;
        'FOR' J:=1 'STEP' 1 'UNTIL' P-I+BW 'DO'
          K[I,J]:=K[I,J]-K[P,I-P+J]*FAC;
FINI: 'END';
FINP: 'END';
SUBS: 'FOR' I:=N 'STEP' -1 'UNTIL' 1 'DO'
'BEGIN' 'IF' K[I,1]=0 'THEN' 'GOTO' ZU;
        SUM:=F[I];
        'IF' I=N 'THEN' 'GOTO' VAL;
        SA:= 'IF' I>N-BW+1 'THEN' N-I+1 'ELSE' BW;
'FOR' J:=2 'STEP' 1 'UNTIL' SA 'DO'
        SUM:=SUM-K[I,J]*U[I+J-1];
        U[I]:=SUM/K[I,1];
VAL: 'END';
ZU: 'FOR' I:=1 'STEP' 1 'UNTIL' N 'DO'
'BEGIN' F[I]:=0;
        FIRST:= 'IF' I>BW 'THEN' I-BW+1 'ELSE' 1;
        LAST:= 'IF' I<N-BW+1 'THEN' I+BW-1 'ELSE' N;
'FOR' J:=FIRST 'STEP' 1 'UNTIL' LAST 'DO'
'BEGIN' P:= 'IF' J<I 'THEN' J 'ELSE' I;
        Z:= 'IF' J<I 'THEN' I-J+1 'ELSE' J-I+1;
        F[I]:=F[I]+Q[P,Z]*U[J];
'END';
        F[I]:=F[I]*E*B/12;
        'IF' V[I]=0 'THEN' F[I]:=F[I]-G[I];
        'IF' V[I]=2 'THEN' F[I]:=-KS[I]*U[I];
'END';
        NEWLINE(2);
        WRITETEXT('('('4S')'X('14S')'DEFLN('14S')'B%M('16S')'
        STRESS('14S')'REACTION('11S')'FIXING%MT')'); NEWLINE(4);
'FOR' I:=1 'STEP' 2 'UNTIL' N-1 'DO'
'BEGIN' 'IF' I=N-1 'THEN'
        'BEGIN' KM[I,1]:=C[1,4]; KM[I,2]:=C[2,4];
          KM[I,3]:=C[3,4]; KM[I,4]:=C[4,4];
          MT:=- (KM[I,1]*U[I-2]+KM[I,2]*U[I-1]+KM[I,3]*U[I]
          +KM[I,4]*U[I+1])*E*B/12;
          'GOTO' STRE;
        'END';
        MT:=(KM[I,1]*U[I]+KM[I,2]*U[I+1]+KM[I,3]*U[I+2]
        +KM[I,4]*U[I+3])*E*B/12;
        AA:=6*MT/(B*D[I]*D[I]);
        PRINT(X[I],3,2); PRINT(U[I],10,2); PRINT(MT/1000,13,3);
        PRINT(AA,15,2);
        'IF' V[I]=2 'THEN' 'BEGIN' PRINT(F[I],13,2);
          'GOTO' FLE;
        'END';
        'IF' V[I]=0 'THEN' PRINT(F[I],14,2) 'ELSE' SPACE(20);
FLE: 'IF' V[I+1]=0 'THEN' PRINT(F[I+1]/1000,12,3);
'IF' V[I+1]=2 'THEN' PRINT(F[I+1]/1000,12,3);
        NEWLINE(2);
'END';
'END';

```



# PROG. 6

```

'SEND TO' ( ED,ASTD-DEFAULT(U),.PROGRAM)
'WORK' (ED,WORK FILE (0))
  'BEGIN'
  'REAL' NU,FAC,SUM,AB,B1,B2,B3,C1,C2,C3,NF;
  'INTEGER' I,J,N,I1,JJ,R,Z,FIRST,LAST,P,SA,BW,NB;
  R:=4;
  BW:=2*R+4; N:=10*R*(R+1)+BW-2;
  NB:=BW*2;
  'BEGIN'
  'REAL' 'ARRAY' A,B,C,D[1:6,1:6],U,F[1:N],K[1:N,1:NB],
  M[1:3,1:6],SIG[1:N,1:3], X[1:6];
  NU:=0.3;
  NF:=(1-NU)/2;
  A[1,1]:=(3-NU)/2; A[1,2]:=-(1+NU)/2; A[1,3]:=-(1-NU)/2;
  A[1,4]:=NU; A[1,5]:=-1; A[1,6]:=(1-NU)/2;
  A[2,2]:=A[1,1]; A[2,3]:=A[1,6]; A[2,4]:=-1; A[2,5]:=NU;
  A[2,6]:=A[1,3]; A[3,3]:=A[2,3]; A[3,4]:=A[3,5]:=0;
  A[3,6]:=A[1,3]; A[4,4]:=1; A[4,5]:=-NU; A[4,6]:=A[5,6]:=0;
  A[5,5]:=1; A[6,6]:=A[1,6];
  B[1,1]:=1; B[1,2]:=B[1,3]:=0; B[1,4]:=-NU; B[1,5]:=-1;
  B[1,6]:=NU; B[2,2]:=A[1,6]; B[2,3]:=A[1,3];
  B[2,4]:=B[3,4]:=0; B[2,5]:=B[2,2]; B[2,6]:=A[1,3];
  B[3,3]:=B[2,2]; B[3,5]:=A[1,3]; B[3,6]:=B[2,2];
  B[4,4]:=1; B[4,5]:=NU; B[4,6]:=-1;
  B[5,5]:=A[1,1]; B[5,6]:=A[1,2]; B[6,6]:=A[1,1];
  C[1,1]:=C[1,6]:=C[6,6]:=A[1,6];
  C[1,2]:=C[1,5]:=C[2,6]:=C[5,6]:=0;
  C[1,3]:=C[1,4]:=C[3,6]:=C[4,6]:=A[1,3];
  C[2,2]:=C[5,5]:=1; C[2,4]:=C[3,5]:=-1;
  C[2,3]:=C[4,5]:=-NU; C[2,5]:=NU;
  C[3,3]:=C[4,4]:=A[1,1]; C[3,4]:=-A[1,2];
  D[1,1]:=D[6,6]:=1; D[1,2]:=D[1,5]:=D[2,6]:=D[5,6]:=0;
  D[1,3]:=D[4,6]:=-1; D[1,4]:=D[3,6]:=-NU; D[1,6]:=NU;
  D[2,2]:=D[2,5]:=D[5,5]:=A[1,6];
  D[2,3]:=D[2,4]:=D[3,5]:=D[4,5]:=A[1,3];
  D[3,3]:=D[4,4]:=A[1,1]; D[3,4]:=-A[1,2];
  'FOR' I:=1 'STEP' 1 'UNTIL' N 'DO'
  'BEGIN' F[I]:=0; U[I]:=0;
    'FOR' J:=1 'STEP' 1 'UNTIL' NB 'DO'
      K[I,J]:=0;
  'END';
  'FOR' Z:=1,15,21,33,41,53,61,73,81,93,101,113,121,133,141,153,
  161,173,181,193 'DO'
  'BEGIN' 'FOR' I1:=Z,Z+4 'DO'
    'BEGIN' 'FOR' I:=I1,I1+1,I1+2,I1+3,I1+BW-2,
    I1+BW-1 'DO'
      'BEGIN' P:= 'IF' I 'LE' I1+3 'THEN' I-I1+1
      'ELSE' I-I1-BW+7;
      'FOR' J:=2-P 'STEP' 1 'UNTIL' 5-P,
      I1-I+BW-1,I1-I+BW 'DO'
        'BEGIN' 'IF' J<1 'THEN' 'GOTO' FIR;
        JJ:='IF' J'LE' 5-P 'THEN' I-I1+J 'ELSE' I-I1+J-BW+6;
        K[I,J]:=K[I,J]+A[P,JJ];
      'END';
    'END';
  'END';
  'FOR' Z:=3,15,23,35,43,55,63,75,83,95,103,115,123,135,143,155,
  163,175,183,195 'DO'
  'BEGIN' 'FOR' I1:=Z,Z+4 'DO'

```



```

      'BEGIN' 'FOR' I:=I1,I1+1,I1+BW-4 'STEP' 1
      'UNTIL' I1+BW-1 'DO'
      'BEGIN' P:= 'IF' I 'LE' I1+1 'THEN' I-I1+1
      'ELSE' I-I1-BW+7;
      'FOR' J:=2-P,3-P, I1-I+BW-3 'STEP' 1
      'UNTIL' I1-I+BW 'DO'
      'BEGIN' 'IF' J<1 'THEN' 'GOTO' SEC;
JJ:= 'IF' J 'LE' 3-P 'THEN' I-I1+J 'ELSE' I-I1+J-BW+6;
      K[I,J]:=K[I,J]+B[P,JJ];
SEC: 'END'; 'END'; 'END'; 'END';
      'FOR' Z:=3,11,23,31,43,51,63,71,83,91,103,111,123,131,143,
      151,163,171,183,191 'DO'
      'BEGIN' 'FOR' I1:=Z,Z+4 'DO'
      'BEGIN' 'FOR' I:=I1,I1+1,I1+2,I1+3,I1+NB-2,I1+NB-1 'DO'
      'BEGIN' P:= 'IF' I 'LE' I1+3 'THEN' I-I1+1
      'ELSE' I-I1-NB+7;
      'FOR' J:=2-P 'STEP' 1 'UNTIL' 5-P,
      I1-I+NB-1, I1-I+NB 'DO'
      'BEGIN' 'IF' J<1 'THEN' 'GOTO' THR;
      JJ:= 'IF' J 'LE' 5-P 'THEN' I-I1+J
      'ELSE' I-I1+J-NB+6;
      K[I,J]:=K[I,J]+C[P,JJ];
THR: 'END';
      'END';
      'FOR' I:=I1,I1+1,I1+NB-4 'STEP' 1 'UNTIL' I1+NB-1
      'DO' 'BEGIN' P:= 'IF' I 'LE' I1+1 'THEN' I-I1+1
      'ELSE' I-I1-NB+7;
      'FOR' J:=2-P,3-P,I1-I+NB-3 'STEP' 1
      'UNTIL' I1-I+NB 'DO'
      'BEGIN' 'IF' J<1 'THEN' 'GOTO' FUR;
      JJ:= 'IF' J 'LE' 3-P 'THEN' I-I1+J
      'ELSE' I-I1+J-NB+6;
      K[I,J]:=K[I,J]+D[P,JJ];
FUR: 'END';
      'END';
      'END';
INV: 'END';
      P:=0.5*BW; F[P]:=-1; BW:=BW+2;
      'FOR' Z:=N-BW+5,N-1,N 'DO'
      'BEGIN' U[Z]:=0;
      'FOR' J:=1 'STEP' 1 'UNTIL' BW 'DO'
      K[Z,J]:=0;
      FIRST:= 'IF' Z>BW 'THEN' Z-BW+1 'ELSE' 1;
      'FOR' I:=Z-1 'STEP' -1 'UNTIL' FIRST 'DO'
      K[I,Z-I+1]:=0;
      'END';
      'FOR' P:=1 'STEP' 1 'UNTIL' N-1 'DO'
      'BEGIN' 'IF' K[P,1]=0 'THEN' 'GOTO' FINP;
      LAST:= 'IF' P 'LE' N-BW+1 'THEN' P+BW-1 'ELSE' N;
      'FOR' I:=P+1 'STEP' 1 'UNTIL' LAST 'DO'
      'BEGIN' 'IF' K[P,I-P+1]=0 'THEN' 'GOTO' FINI;
      FAC:=K[P,I-P+1]/K[P,1];
      F[I]:=F[I]-F[P]*FAC;
      'FOR' J:=1 'STEP' 1 'UNTIL' P-I+BW 'DO'
      K[I,J]:=K[I,J]-K[P,I-P+J]*FAC;
FINI: 'END';
FINP: 'END';
SUBS: 'FOR' I:=N 'STEP' -1 'UNTIL' 1 'DO'
      'BEGIN' 'IF' K[I,1]=0 'THEN' 'GOTO' ZU;
      SUM:=F[I]*2*(1-NU*NU);

```



```

'IF' I=N 'THEN' 'GOTO' VAL;
SA:= 'IF' I>N-BW+1 'THEN' N-I+1 'ELSE' BW;
'FOR' J:=2 'STEP' 1 'UNTIL' SA 'DO'
    SUM:=SUM-K[I,J]*U[I+J-1];
    U[I]:=SUM/K[I,1];
VAL:
ZU:
'END';
SPACE(56); WRITETEXT('('DISPLACEMENTS')'); NEWLINE(4);
'FOR' I1:=1 'STEP' 10 'UNTIL' 201 'DO'
'BEGIN' 'FOR' J:=I1 'STEP' 2 'UNTIL' I1+8 'DO'
    PRINT(ULI,16,4);
    'FOR' I:=I1+1 'STEP' 2 'UNTIL' I1+9 'DO'
        PRINT(ULI,16,4);
    NEWLINE(3);
'END';
PAPERTHROW;
B1:=C2:=1; B2:=C3:=0; B3:=C1:=-1;
M[1,1]:=B1; M[1,2]:=NU*C1; M[1,3]:=B2; M[1,4]:=NU*C2;
M[1,5]:=B3; M[1,6]:=NU*C3; M[2,1]:=NU*B1; M[2,2]:=C1;
M[2,3]:=NU*B2; M[2,4]:=C2; M[2,5]:=NU*B3; M[2,6]:=C3;
M[3,1]:=NF*C1; M[3,2]:=NF*B1; M[3,3]:=NF*C2;
M[3,4]:=NF*B2; M[3,5]:=NF*C3; M[3,6]:=NF*B3;
'FOR' I1:=1 'STEP' 20 'UNTIL' 191 'DO'
'BEGIN' 'FOR' I:=I1,I1+4,I1+12,I1+16 'DO'
'BEGIN' X[1]:=ULI; X[2]:=U[I+1]; X[3]:=U[I+2]; X[4]:=U[I+3];
    X[5]:=ULI+10; X[6]:=U[I+11];
    'FOR' J:=1,2,3 'DO'
        'BEGIN' SUM:=0;
        'FOR' P:=1,2,3,4,5,6 'DO'
            SUM:=SUM+M[J,P]*X[P];
            SIG[I,J]:=SUM/(1-NU*NU);
        'END'; 'END'; 'END';
B1:=C3:=-1; B2:=C1:=0; B3:=C2:=1;
M[1,1]:=B1; M[1,2]:=NU*C1; M[1,3]:=B2; M[1,4]:=NU*C2;
M[1,5]:=B3; M[1,6]:=NU*C3; M[2,1]:=NU*B1; M[2,2]:=C1;
M[2,3]:=NU*B2; M[2,4]:=C2; M[2,5]:=NU*B3; M[2,6]:=C3;
M[3,1]:=NF*C1; M[3,2]:=NF*B1; M[3,3]:=NF*C2;
M[3,4]:=NF*B2; M[3,5]:=NF*C3; M[3,6]:=NF*B3;
'FOR' I1:=1 'STEP' 20 'UNTIL' 191 'DO'
'BEGIN' 'FOR' I:=I1+1,I1+5,I1+13,I1+17 'DO'
'BEGIN' X[1]:=U[I+1]; X[2]:=U[I+2]; X[3]:=U[I+9];
    X[4]:=U[I+10]; X[5]:=U[I+11]; X[6]:=U[I+12];
    'FOR' J:=1,2,3 'DO'
        'BEGIN' SUM:=0;
        'FOR' P:=1,2,3,4,5,6 'DO'
            SUM:=SUM-M[J,P]*X[P];
            SIG[I,J]:=SUM/(1-NU*NU);
        'END'; 'END'; 'END';
B1:=C3:=-1; B2:=C2:=1; B3:=C1:=0;
M[1,1]:=B1; M[1,2]:=NU*C1; M[1,3]:=B2; M[1,4]:=NU*C2;
M[1,5]:=B3; M[1,6]:=NU*C3; M[2,1]:=NU*B1; M[2,2]:=C1;
M[2,3]:=NU*B2; M[2,4]:=C2; M[2,5]:=NU*B3; M[2,6]:=C3;
M[3,1]:=NF*C1; M[3,2]:=NF*B1; M[3,3]:=NF*C2;
M[3,4]:=NF*B2; M[3,5]:=NF*C3; M[3,6]:=NF*B3;
'FOR' I1:=1 'STEP' 20 'UNTIL' 191 'DO'
'BEGIN' 'FOR' I:=I1+2,I1+6,I1+10,I1+14 'DO'
'BEGIN' X[1]:=U[I]; X[2]:=U[I+1]; X[3]:=U[I+10]; X[4]:=U[I+11];
    X[5]:=U[I+12]; X[6]:=U[I+13];
    'FOR' J:=1,2,3 'DO'
        'BEGIN' SUM:=0;
        'FOR' P:=1,2,3,4,5,6 'DO'

```



```

        SUM:=SUM-M[J,P]*X[P];
        SIG[I,J]:=SUM/(1-NU*NU);
'END'; 'END'; 'END';
B1:=C3:=0; B2:=C2:=1; B3:=C1:=-1;
M[1,1]:=B1; M[1,2]:=NU*C1; M[1,3]:=B2; M[1,4]:=NU*C2;
M[1,5]:=B3; M[1,6]:=NU*C3; M[2,1]:=NU*B1; M[2,2]:=C1;
M[2,3]:=NU*B2; M[2,4]:=C2; M[2,5]:=NU*B3; M[2,6]:=C3;
M[3,1]:=NF*C1; M[3,2]:=NF*B1; M[3,3]:=NF*C2;
M[3,4]:=NF*B2; M[3,5]:=NF*C3; M[3,6]:=NF*B3;
'FOR' I1:=1 'STEP' 20 'UNTIL' 191 'DO'
'REGIN' 'FOR' I:=I1+3,I1+7,I1+11,I1+15 'DO'
'BEGIN' X[1]:=U[I-1]; X[2]:=U[I]; X[3]:=U[I+1]; X[4]:=U[I+2];
        X[5]:=U[I+11];X[6]:=U[I+12];
        'FOR' J:=1,2,3 'DO'
        'BEGIN' SUM:=0;
        'FOR' P:=1,2,3,4,5,6 'DO'
            SUM:=SUM+M[J,P]*X[P];
            SIG[I,J]:=SUM/(1-NU*NU);
        'END'; 'END'; 'END';
SPACE(56); WRITETEXT('('STRESSES')'); NEWLINE(4);
'FOR' I1:=1 'STEP' 10 'UNTIL' 191 'DO'
'BEGIN' 'FOR' P:=1,2,3 'DO'
        'FOR' I:=I1 'STEP' 1 'UNTIL' I1+7 'DO'
            PRINT(SIG[I,P],7,4);
        NEWLINE(3);
'END';
'END';
'END';

```



# PROG.7

```

'BEGIN' 'REAL' L,R,PR,E,RE,NU,KB,VC,Z,DE,KS,CT,DT,D1,D2,
        FAC,SUM,X,TAP;
'INTEGER' N,T,I,J,LAST,FIN,P;
N:=98; L:=2.5;
'BEGIN' 'REAL' 'ARRAY' C[1:4,1:4],CP[3:4,3:4],DR[-1:N-1],F[1:N],
        U[-1:N],K[1:N,1:4],FD[1:4],W,M,S,HS[-1:N,0:6],A,B[-1:N];
R:=74.6; D1:=3.18; TAP:=0;
PR:=0.1;
E:=3100; NU:=0.35; VC:=0.068 -3; Z:=0.58; RE:=1/E;
CT:=1/EXP(Z); DT:=1; KB:=E/(3*(1-2*NU));
'FOR' T:=0 'STEP' 1 'UNTIL' 6 'DO'
'BEGIN' E:=1/(RE+VC*(1-DT));
        NU:=0.5-E/(6*KB);
        DE:=E/(12*(1-NU*NU));
'FOR' I:=1 'STEP' 1 'UNTIL' N 'DO'
'FOR' J:=1 'STEP' 1 'UNTIL' 4 'DO'
        K[I,J]:=0;
'FOR' I:=-1 'STEP' 2 'UNTIL' N-1 'DO'
'BEGIN' D2:=D1-TAP*L;
        KS:=E*D1/(R*R); DR[I]:=PR*R*R*(1-NU/2)/(E*D1);
        FD[1]:=D1*D1*D1; FD[2]:=D1*D1*D2;
        FD[3]:=D1*D2*D2; FD[4]:=D2*D2*D2;
        C[1,1]:=DE*(4.2*FD[1]+1.8*FD[2]+1.8*FD[3]+4.2*FD[4])
            /(L*L*L);
        C[1,2]:=DE*(3*FD[1]+1.2*FD[2]+0.6*FD[3]+1.2*FD[4])
            /(L*L);
        C[1,3]:=-C[1,1];
        C[1,4]:=DE*(1.2*FD[1]+0.6*FD[2]+1.2*FD[3]+3*FD[4])
            /(L*L);
        C[2,2]:=DE*(2.2*FD[1]+FD[2]+0.4*FD[3]+0.4*FD[4])/L;
        C[2,3]:=-C[1,2];
        C[2,4]:=DE*(0.8*FD[1]+0.2*FD[2]+0.2*FD[3]+0.8*FD[4])/L;
        C[3,3]:=C[1,1];
        C[3,4]:=-C[1,4];
        C[4,4]:=DE*(0.4*FD[1]+0.4*FD[2]+FD[3]+2.2*FD[4])/L;
        A[I]:=C[1,2]; A[I+1]:=C[2,2]; B[I]:=C[2,4];
'IF' I=-1 'THEN'
'BEGIN' F[1]:=C[1,3]*DR[I];
        F[2]:=C[1,4]*DR[I];
'GOTO' ENDEL;
'END';
        K[I,1]:=C[1,1]+CP[3,3]+KS*L;
        K[I,2]:=C[1,2]+CP[3,4];
        K[I,3]:=C[1,3];
        K[I,4]:=C[1,4];
        K[I+1,1]:=C[2,2]+CP[4,4];
        K[I+1,2]:=C[2,3];
        K[I+1,3]:=C[2,4];
'IF' I=1 'THEN' 'GOTO' ENDEL;
        F[I]:=F[I+1]:=0;
        CP[3,3]:=C[3,3];
        CP[3,4]:=C[3,4];
        CP[4,4]:=C[4,4];
        D1:=D2;
'END';
ENDEL;
'END';

```



```

'FOR' P:=1 'STEP' 1 'UNTIL' N-1 'DO'
'BEGIN' LAST:= 'IF' P 'LE' N-3 'THEN' P+3 'ELSE' N;
      'FOR' I:=P+1 'STEP' 1 'UNTIL' LAST 'DO'
      'BEGIN' 'IF' K[P,I-P+1]=0 'THEN' 'GOTO' FINI
      'ELSE' FAC:=K[P,I-P+1]/K[P,1];
      F[I]:=F[I]-F[P]*FAC;
      'FOR' J:=1 'STEP' 1 'UNTIL' P-I+4 'DO'
      K[I,J]:=K[I,J]-K[P,I-P+J]*FAC;
FINI:      'END';
'END';
U[N]:=F[N]/K[N,1];
'FOR' I:=N-1 'STEP' -1 'UNTIL' 1 'DO'
'BEGIN' SUM:=F[I];
      FIN:= 'IF' I 'LE' N-3 'THEN' 4 'ELSE' N-I+1;
      'FOR' J:=2 'STEP' 1 'UNTIL' FIN 'DO'
      SUM:=SUM-K[I,J]*U[I+J-1];
      U[I]:=SUM/K[I,1];
'END';
D1:=3.18; U[-1]:=-DR[-1]; U[0]:=0;
'FOR' I:=-1 'STEP' 2 'UNTIL' N-3 'DO'
'BEGIN' M[I,T]:=A[I]*(U[I]-U[I+2])+A[I+1]*U[I+1]+B[I]*U[I+3];
      S[I,T]:=6*(ABS(M[I,T]))/(D1*D1)+PR*R/(2*D1);
      D1:=D1-TAP*L;
'END';
'FOR' I:=-1 'STEP' 2 'UNTIL' N-3 'DO'
'BEGIN'
W[I,T]:=U[I]+DR[I];
HS[I,T]:=E*W[I,T]/R+NU*S[I,T];
'END';
DT:=DT*CT;
'END' OF T LOOP;
SPACE(26); WRITETEXT('('T=%0%%')');
'FOR' T:=1,2,3,4,5,6 'DO'
PRINT(T,9,0); NEWLINE(2);
'FOR' I:=-1 'STEP' 2 'UNTIL' N-3 'DO'
'BEGIN' X:=0.5*L*(I+1); WRITETEXT('('X=')');
PRINT(X,3,1); WRITETEXT('('%DEFLN%')'); SPACE(5);
'FOR' T:=0 'STEP' 1 'UNTIL' 6 'DO'
PRINT(W[I,T],4,4);
NEWLINE(1); SPACE(11); WRITETEXT('('%B%M%%')');
'FOR' T:=0 'STEP' 1 'UNTIL' 6 'DO'
PRINT(M[I,T],4,4);
NEWLINE(1); SPACE(11); WRITETEXT('('LONG%STRESS')');
'FOR' T:=0 'STEP' 1 'UNTIL' 6 'DO'
PRINT(S[I,T],4,4);
NEWLINE(1); SPACE(11); WRITETEXT('('HOOP%STRESS')');
'FOR' T:=0 'STEP' 1 'UNTIL' 6 'DO'
PRINT(HS[I,T],4,4); NEWLINE(3);
'END';
'END';
'END';

```



# PROG.8

12/06/72

COMPILED BY XALE MK. 5C

```
'SEND TO' ( ED,ASTD-DEFAULT(0),.PROGRAM)
'WORK' (ED,WORK FILE      )
  'BEGIN'
  'REAL' NU,FAC,SUM,AB,B1,B2,B3,C1,C2,C3,NF,KB,VC,ZE,T,VF,E,
    T1,T2,EP;
  'INTEGER' I,J,N,I1,JJ,R,Z,FIRST,LAST,P,SA,BW,NB;
  R:=4;
  BW:=2*R+4;  N:=50;
  NB:=BW+2;
  'BEGIN'
  'REAL' 'ARRAY' A,B,C,D[1:6,1:6],U,F[1:N],K[1:N,1:22],V[1:N],
    M[1:3,1:6],SIG[1:N,1:3], X[1:6];
  NU:=0.35; E:=4.2*100000; KB:=E/(3*(1-2*NU));
  VC:=0.5/1000000; ZE:=0.3;
  'FOR' I:=1 'STEP' 1 'UNTIL' N 'DO' U[I]:=0;
  'FOR' T:=0 'STEP' 5/3 'UNTIL' 10 'DO'
  'BEGIN' 'IF' T 'NE' 0 'THEN'
    'BEGIN' T1:=T-5/3; T2:=T;
      E:=1/(VC*(1/EXP(ZE*T1)-1/EXP(ZE*T2))); NU:=0.5;
    'END';
    'IF' T>2 'THEN'
    'BEGIN' 'FOR' I:=1 'STEP' 1 'UNTIL' N 'DO'
      V[I]:=V[I]*EP/E; 'GOTO' XXX; 'END';
  NF:=(1-NU)/2;
  BW:=12;
  A[1,1]:=(3-NU)/2; A[1,2]:=-1; A[1,3]:=-1; A[1,4]:=NU; A[1,5]:=-1; A[1,6]:=(1-NU)/2;
  A[2,2]:=A[1,1]; A[2,3]:=A[1,6]; A[2,4]:=-1; A[2,5]:=NU;
  A[2,6]:=A[1,3]; A[3,3]:=A[2,3]; A[3,4]:=A[3,5]; A[3,6]:=0;
  A[4,4]:=1; A[4,5]:=-NU; A[4,6]:=A[5,6]; A[5,5]:=1; A[6,6]:=A[1,6];
  B[1,1]:=1; B[1,2]:=B[1,3]; B[1,4]:=-NU; B[1,5]:=-1;
  B[1,6]:=NU; B[2,2]:=A[1,6]; B[2,3]:=A[1,3];
  B[2,4]:=B[3,4]; B[2,5]:=B[2,2]; B[2,6]:=A[1,3];
  B[3,3]:=B[2,2]; B[3,5]:=A[1,3]; B[3,6]:=B[2,2];
  B[4,4]:=1; B[4,5]:=NU; B[4,6]:=-1;
  B[5,5]:=A[1,1]; B[5,6]:=A[1,2]; B[6,6]:=A[1,1];
  C[1,1]:=C[1,6]; C[1,5]:=C[2,6]; C[1,4]:=C[3,6]; C[1,3]:=C[4,6]; C[1,2]:=C[5,6]; C[1,1]:=C[6,6]; C[1,6]:=A[1,6];
  C[2,2]:=C[5,5]; C[2,4]:=C[3,5]; C[2,3]:=C[4,5]; C[2,5]:=NU;
  C[3,3]:=C[4,4]; C[3,4]:=-A[1,2];
  D[1,1]:=D[6,6]; D[1,2]:=D[1,5]; D[1,3]:=D[2,6]; D[1,4]:=D[3,6]; D[1,5]:=D[4,6]; D[1,6]:=NU;
  D[2,2]:=D[2,5]; D[2,3]:=D[3,5]; D[2,4]:=D[4,5]; D[2,5]:=A[1,6];
  D[3,3]:=D[4,4]; D[3,4]:=-A[1,2];
  'FOR' I:=1 'STEP' 1 'UNTIL' N 'DO'
  'BEGIN' F[I]:=0; V[I]:=0;
    'FOR' J:=1 'STEP' 1 'UNTIL' 22 'DO'
      K[I,J]:=0;
  'END';
  'FOR' Z:=1,13,21,33 'DO'
  'BEGIN' 'FOR' I1:=Z,Z+4 'DO'
    'BEGIN' 'FOR' I:=I1,I1+1,I1+2,I1+3,I1+BW-2,
      I1+BW-1 'DO'
```



```

        'BEGIN' P:= 'IF' I 'LE' I1+3 'THEN' I-I1+1
                                'ELSE' I-I1-BW+7;
        'FOR' J:=2-P 'STEP' 1 'UNTIL' 5-P,
                I1-I+BW-1, I1-I+BW 'DO'
                'BEGIN' 'IF' J<1 'THEN' 'GOTO' FIR;
JJ:='IF' J'LE' 5-P 'THEN' I-I1+J 'ELSE' I-I1+J-BW+6;
                K[I,J]:=K[I,J]+A[P,JJ];
FIR:  'END'; 'END'; 'END'; 'END';
        'FOR' Z:=3,15,23,35 'DO'
        'BEGIN' 'FOR' I1:=Z,Z+4 'DO'
                'BEGIN' 'FOR' I:=I1,I1+1,I1+BW-4 'STEP' 1
                        'UNTIL' I1+BW-1 'DO'
                'BEGIN' P:= 'IF' I 'LE' I1+1 'THEN' I-I1+1
                                'ELSE' I-I1-BW+7;
                'FOR' J:=2-P,3-P, I1-I+BW-3 'STEP' 1
                        'UNTIL' I1-I+BW 'DO'
                'BEGIN' 'IF' J<1 'THEN' 'GOTO' SEC;
JJ:='IF' J'LE' 3-P 'THEN' I-I1+J 'ELSE' I-I1+J-BW+6;
                K[I,J]:=K[I,J]+B[P,JJ];
SEC:  'END'; 'END'; 'END'; 'END';
        'FOR' Z:=3,11,23,31 'DO'
        'BEGIN' 'FOR' I1:=Z,Z+4 'DO'
                'BEGIN' 'FOR' I:=I1,I1+1,I1+2,I1+3,I1+NB-2,I1+NB-1 'DO'
                        'BEGIN' P:= 'IF' I 'LE' I1+3 'THEN' I-I1+1
                                'ELSE' I-I1-NB+7;
                'FOR' J:=2-P 'STEP' 1 'UNTIL' 5-P,
                        I1-I+NB-1, I1-I+NB 'DO'
                'BEGIN' 'IF' J<1 'THEN' 'GOTO' THR;
                JJ:= 'IF' J 'LE' 5-P 'THEN' I-I1+J
                        'ELSE' I-I1+J-NB+6;
                K[I,J]:=K[I,J]+C[P,JJ];
THR:  'END';
        'END';
        'FOR' I:=I1,I1+1,I1+NB-4 'STEP' 1 'UNTIL' I1+NB-1
        'DO' 'BEGIN' P:= 'IF' I 'LE' I1+1 'THEN' I-I1+1
                                'ELSE' I-I1-NB+7;
        'FOR' J:=2-P,3-P, I1-I+NB-3 'STEP' 1
                'UNTIL' I1-I+NB 'DO'
        'BEGIN' 'IF' J<1 'THEN' 'GOTO' FUR;
                JJ:= 'IF' J 'LE' 3-P 'THEN' I-I1+J
                        'ELSE' I-I1+J-NB+6;
                K[I,J]:=K[I,J]+D[P,JJ];
FUR:  'END';
        'END';
        'END';
INV:  'END';
        BW:=22;
        'FOR' Z:=2,12,22,32,41,42,43,45,47,49,4,6,8,10 'DO'
        'BEGIN' V[Z]:=0;
                'FOR' J:=1 'STEP' 1 'UNTIL' BW 'DO'
                        K[Z,J]:=0;
                FIRST:= 'IF' Z>BW 'THEN' Z-BW+1 'ELSE' 1;
                'FOR' I:=Z-1 'STEP'-1 'UNTIL' FIRST 'DO'
                        K[I,Z-I+1]:=0;
        'END';
K[1,1]:=K[1,1]+K[3,1]+K[5,1]+K[7,1]+K[9,1]+2*(K[1,3]+K[1,5]+K[1,7]
+K[1,9]+K[3,3]+K[3,5]+K[3,7]+K[5,3]+K[5,5]+K[7,3]);
K[1,2]:=K[1,2]+K[2,2]+K[2,4]+K[2,6]+K[2,8];
K[1,4]:=K[1,4]+K[3,2]+K[4,2]+K[4,4]+K[4,6];
K[1,6]:=K[1,6]+K[3,4]+K[5,2]+K[6,2]+K[6,4];

```



```

K[1,8]:=K[1,8]+K[3,6]+K[5,4]+K[7,2]+K[8,2];
'FOR' J:=10 'STEP' 1 'UNTIL' 22 'DO'
K[1,J]:=K[1,J]+K[3,J-2]+K[5,J-4]+K[7,J-6]+K[9,J-8];
'FOR' Z:=3,5,7,9 'DO' 'BEGIN'
  'FOR' J:=1 'STEP' 1 'UNTIL' BW 'DO'
    KLZ,JJ:=0;
    FIRST:= 'IF' Z>BW 'THEN' Z-BW+1 'ELSE' 1;
    'FOR' I:=Z-1 'STEP' -1 'UNTIL' FIRST 'DO'
      KLI,Z-I+1:=0;
'END';
F[1]:=-10000;
'FOR' P:=1 'STEP' 1 'UNTIL' N-1 'DO'
'BEGIN' 'IF' K[P,1]=0 'THEN' 'GOTO' FINP;
  LAST:= 'IF' P 'LE' 29 'THEN' P+21 'ELSE' 50;
  'FOR' I:=P+1 'STEP' 1 'UNTIL' LAST 'DO'
  'BEGIN' 'IF' K[P,I-P+1]=0 'THEN' 'GOTO' FINI;
    FAC:=K[P,I-P+1]/K[P,1];
    F[I]:=F[I]-F[P]*FAC;
    'FOR' J:=1 'STEP' 1 'UNTIL' P-I+22 'DO'
      K[I,J]:=K[I,J]-K[P,I-P+J]*FAC;
  'END';
FINI:
FINP:
SUBS: 'FOR' I:=N 'STEP' -1 'UNTIL' 1 'DO'
'BEGIN' 'IF' K[I,1]=0 'THEN' 'GOTO' ZU;
  SUM:=F[I]*2*(1-NU*NU)/E;
  'IF' I=N 'THEN' 'GOTO' VAL;
  SA:= 'IF' I>29 'THEN' 51-I 'ELSE' 22;
  'FOR' J:=2 'STEP' 1 'UNTIL' SA 'DO'
    SUM:=SUM-K[I,J]*V[I+J-1];
    V[I]:=SUM/K[I,1];
VAL:
ZU:
XXX: 'FOR' Z:=3,5,7,9 'DO' V[Z]:=V[1];
'FOR' I:=1 'STEP' 1 'UNTIL' N 'DO' U[I]:=U[I]+V[I]; EP:=E;
WRITETEXT('('T=)'); PRINT(T,2,2);
SPACE(44); WRITETEXT('('DISPLACEMENTS)'); NEWLINE(4);
'FOR' I1:=1 'STEP' 10 'UNTIL' 41 'DO'
'BEGIN' 'FOR' I:=I1 'STEP' 2 'UNTIL' I1+8 'DO'
  PRINT(U[I],16,4);
  'FOR' I:=I1+1 'STEP' 2 'UNTIL' I1+9 'DO'
    PRINT(U[I],16,4);
  NEWLINE(3);
'END';
NEWLINE(10);
VF:=VC*(1-1/EXP(ZE*T));
E:=1/(1/420000+VF); NU:=0.5-E/(6*KB);
B1:=C2:=1; B2:=C3:=0; B3:=C1:=-1;
M[1,1]:=B1; M[1,2]:=NU*C1; M[1,3]:=B2; M[1,4]:=NU*C2;
M[1,5]:=B3; M[1,6]:=NU*C3; M[2,1]:=NU*B1; M[2,2]:=C1;
M[2,3]:=NU*B2; M[2,4]:=C2; M[2,5]:=NU*B3; M[2,6]:=C3;
M[3,1]:=NF*C1; M[3,2]:=NF*B1; M[3,3]:=NF*C2;
M[3,4]:=NF*B2; M[3,5]:=NF*C3; M[3,6]:=NF*B3;
'FOR' I1:=1 'STEP' 10 'UNTIL' 21 'DO'
'BEGIN' 'FOR' I:=I1,I1+4,I1+12,I1+16 'DO'
'BEGIN' X[1]:=U[I]; X[2]:=U[I+1]; X[3]:=U[I+2]; X[4]:=U[I+3];
  X[5]:=U[I+10]; X[6]:=U[I+11];
  'FOR' J:=1,2,3 'DO'
  'BEGIN' SUM:=0;
  'FOR' P:=1,2,3,4,5,6 'DO'
    SUM:=SUM+M[J,P]*X[P];
  SIG[I,J]:=SUM*E/(1-NU*NU);

```



```

'END'; 'END'; 'END';
B1:=C3:=-1; B2:=C1:=0; B3:=C2:=1;
M[1,1]:=B1; M[1,2]:=NU*C1; M[1,3]:=B2; M[1,4]:=NU*C2;
M[1,5]:=B3; M[1,6]:=NU*C3; M[2,1]:=NU*B1; M[2,2]:=C1;
M[2,3]:=NU*B2; M[2,4]:=C2; M[2,5]:=NU*B3; M[2,6]:=C3;
M[3,1]:=NF*C1; M[3,2]:=NF*B1; M[3,3]:=NF*C2;
M[3,4]:=NF*B2; M[3,5]:=NF*C3; M[3,6]:=NF*B3;
'FOR' I1:=1 'STEP' 10 'UNTIL' 21 'DO'
'BEGIN' 'FOR' I:=I1+1,I1+5,I1+13,I1+17 'DO'
'BEGIN' X[1]:=U[I+1]; X[2]:=U[I+2]; X[3]:=U[I+9];
X[4]:=U[I+10]; X[5]:=U[I+11]; X[6]:=U[I+12];
'FOR' J:=1,2,3 'DO'
'BEGIN' SUM:=0;
'FOR' P:=1,2,3,4,5,6 'DO'
SUM:=SUM-M[J,P]*X[P];
SIG[I,J]:=SUM*E/(1-NU*NU);
'END'; 'END'; 'END';
B1:=C3:=-1; B2:=C2:=1; B3:=C1:=0;
M[1,1]:=B1; M[1,2]:=NU*C1; M[1,3]:=B2; M[1,4]:=NU*C2;
M[1,5]:=B3; M[1,6]:=NU*C3; M[2,1]:=NU*B1; M[2,2]:=C1;
M[2,3]:=NU*B2; M[2,4]:=C2; M[2,5]:=NU*B3; M[2,6]:=C3;
M[3,1]:=NF*C1; M[3,2]:=NF*B1; M[3,3]:=NF*C2;
M[3,4]:=NF*B2; M[3,5]:=NF*C3; M[3,6]:=NF*B3;
'FOR' I1:=1 'STEP' 10 'UNTIL' 21 'DO'
'BEGIN' 'FOR' I:=I1+2,I1+6,I1+10,I1+14 'DO'
'BEGIN' X[1]:=U[I]; X[2]:=U[I+1]; X[3]:=U[I+10]; X[4]:=U[I+11];
X[5]:=U[I+12]; X[6]:=U[I+13];
'FOR' J:=1,2,3 'DO'
'BEGIN' SUM:=0;
'FOR' P:=1,2,3,4,5,6 'DO'
SUM:=SUM-M[J,P]*X[P];
SIG[I,J]:=SUM*E/(1-NU*NU);
'END'; 'END'; 'END';
B1:=C3:=0; B2:=C2:=1; B3:=C1:=-1;
M[1,1]:=B1; M[1,2]:=NU*C1; M[1,3]:=B2; M[1,4]:=NU*C2;
M[1,5]:=B3; M[1,6]:=NU*C3; M[2,1]:=NU*B1; M[2,2]:=C1;
M[2,3]:=NU*B2; M[2,4]:=C2; M[2,5]:=NU*B3; M[2,6]:=C3;
M[3,1]:=NF*C1; M[3,2]:=NF*B1; M[3,3]:=NF*C2;
M[3,4]:=NF*B2; M[3,5]:=NF*C3; M[3,6]:=NF*B3;
'FOR' I1:=1 'STEP' 10 'UNTIL' 21 'DO'
'BEGIN' 'FOR' I:=I1+3,I1+7,I1+11,I1+15 'DO'
'BEGIN' X[1]:=U[I-1]; X[2]:=U[I]; X[3]:=U[I+1]; X[4]:=U[I+2];
X[5]:=U[I+11]; X[6]:=U[I+12];
'FOR' J:=1,2,3 'DO'
'BEGIN' SUM:=0;
'FOR' P:=1,2,3,4,5,6 'DO'
SUM:=SUM+M[J,P]*X[P];
SIG[I,J]:=SUM*E/(1-NU*NU);
'END'; 'END'; 'END';
SPACE(56); WRITETEXT('('STRESSES)'); NEWLINE(4);
'FOR' I1:=1 'STEP' 10 'UNTIL' 31 'DO'
'BEGIN' 'FOR' P:=1,2,3 'DO'
'FOR' I:=I1 'STEP' 1 'UNTIL' I1+7 'DO'
PRINT(SIG[I,P],10,1);
NEWLINE(3);
'END';
PAPERTHROW;
'END';
'END';
'END';

```



# PROG. 9

10/02/72

COMPILED BY XALE MK. 5C

```

'SEND TO' ( ED,ASTD-DEFAULT(0),.PROGRAM)
'WORK' (ED,WORK FILE (0))
'BEGIN' 'REAL' X1,X2,D1,D2,B,FAC,SUM,L,SUMSIG,INT,AM,MT,SC,PSUM,NSUM;
'INTEGER' EN,N,BW,EL,I,J,FIRST,LAST,SA,Z,P,NC,NL,R,S,NS,NI;
EN:=READ; NS:=READ; N:=2*EN+2; BW:=4;
'BEGIN' 'REAL' 'ARRAY' C[1:4,1:4],CP[3:4,3:4],K,KM,Q[1:N,1:4],
U,F,KS,A,M,E,G,X,D[1:N],FD[1:4],SIG,MM,EE[0:NS];
'INTEGER' 'ARRAY' V[1:N];
E[2]:=READ; SC:=READ; SIG[0]:=SUM:=INT:=SUMSIG:=0;
'FOR' I:=1 'STEP' 1 'UNTIL' NS 'DO'
'BEGIN' SIG[I]:=READ;
SUM:=SUM+0.5*SIG[I-1]*(I*I-(I-1)*(I-1))+(SIG[I]-SIG[I-1])
*(I*I*I/3-(I-1)*I*I/2+(I-1)*(I-1)*(I-1)/6);
MM[I]:=SUM/(I*I);
EE[I]:=MM[I]*3/(SC*I);
'END';
B:=READ;
'FOR' I:=1 'STEP' 2 'UNTIL' N-1 'DO'
'BEGIN' X[I]:=READ; D[I]:=READ; E[I]:=E[2];
'END';
'FOR' I:=1 'STEP' 1 'UNTIL' N 'DO'
'BEGIN' G[I]:=0; V[I]:=1;
'END';
NC:=READ;
'IF' NC=0 'THEN' 'GOTO' NOCO;
'FOR' R:=1 'STEP' 1 'UNTIL' NC 'DO'
'BEGIN' Z:=READ; V[Z]:=0;
'END';
NOCO:
EL:=READ;
'IF' EL=0 'THEN' 'GOTO' ZEK;
'FOR' P:=1 'STEP' 1 'UNTIL' EL 'DO'
'BEGIN' I:=READ; KS[I]:=READ; V[I]:=2;
'END';
ZEK:
NL:=READ;
'FOR' S:=1 'STEP' 1 'UNTIL' NL 'DO'
'BEGIN' Z:=READ; G[Z]:=READ;
'END';
NI:=1;
PSUM:=NSUM:=0;
MAT:
CP[3,3]:=CP[3,4]:=CP[4,4]:=0;
'FOR' I:=1 'STEP' 1 'UNTIL' N 'DO'
'BEGIN' U[I]:=0;
'FOR' J:=1 'STEP' 1 'UNTIL' BW 'DO'
K[I,J]:=0;
'END';
'FOR' EL:=1 'STEP' 1 'UNTIL' EN 'DO'
'BEGIN' I:=2*EL-1; X1:=X[I]; X2:=X[I+2]; D1:=D[I]; D2:=D[I+2];
L:=X2-X1;
FD[1]:=D1*D1*D1; FD[2]:=D1*D1*D2; FD[3]:=D1*D2*D2;
FD[4]:=D2*D2*D2;
C[1,1]:=(4.2*FD[1]+1.8*FD[2]+1.8*FD[3]+4.2*FD[4])/(L*L*L);
C[1,2]:=(3*FD[1]+1.2*FD[2]+0.6*FD[3]+1.2*FD[4])/(L*L);
C[1,3]:=-C[1,1];
C[1,4]:=(1.2*FD[1]+0.6*FD[2]+1.2*FD[3]+3*FD[4])/(L*L);
C[2,2]:=(2.2*FD[1]+FD[2]+0.4*FD[3]+0.4*FD[4])/L;
C[2,3]:=-C[1,2];
C[2,4]:=(0.8*FD[1]+0.2*FD[2]+0.2*FD[3]+0.8*FD[4])/L;

```



```

C[3,3]:=-C[1,3]; C[3,4]:=-C[1,4];
C[4,4]:=(0.4*FD[1]+0.4*FD[2]+FD[3]+2.2*FD[4])/L;
'FOR' P:=1 'STEP' 1 'UNTIL' 4 'DO'
'FOR' J:=P 'STEP' 1 'UNTIL' 4 'DO'
C[P,J]:=C[P,J]*(E[I]+E[I+2])/2;
KM[I,1]:=C[1,2]; KM[I,2]:=C[2,2];
KM[I,3]:=C[2,3]; KM[I,4]:=C[2,4];
K[I,1]:=C[1,1]+CP[3,3]; K[I,2]:=C[1,2]+CP[3,4];
K[I,3]:=C[1,3]; K[I,4]:=C[1,4];
K[I+1,1]:=C[2,2]+CP[4,4]; K[I+1,2]:=C[2,3];
K[I+1,3]:=C[2,4];
CP[3,3]:=C[3,3]; CP[3,4]:=C[3,4]; CP[4,4]:=C[4,4];
'END';
K[N-1,1]:=CP[3,3]; K[N-1,2]:=CP[3,4]; K[N,1]:=CP[4,4];
'FOR' I:=1 'STEP' 1 'UNTIL' N 'DO'
'FOR' J:=1 'STEP' 1 'UNTIL' BW 'DO'
Q[I,J]:=K[I,J];
'FOR' Z:=1 'STEP' 1 'UNTIL' N 'DO'
'BEGIN' 'IF' V[Z]=0 'THEN'
'BEGIN'
'FOR' J:=1 'STEP' 1 'UNTIL' BW 'DO'
K[Z,J]:=0;
FIRST:='IF' Z>BW 'THEN' Z-BW+1 'ELSE' 1;
'FOR' I:=Z-1 'STEP'-1 'UNTIL' FIRST 'DO'
K[I,Z-I+1]:=0;
'END';
'IF' V[Z]=2 'THEN' K[Z,1]:=K[Z,1]+KS[Z]*12/B;
F[Z]:=G[Z]*12/B;
'END';
'FOR' P:=1 'STEP' 1 'UNTIL' N-1 'DO'
'BEGIN' 'IF' K[P,1]=0 'THEN' 'GOTO' FINP;
LAST:='IF' P 'LE' N-BW+1 'THEN' P+BW-1 'ELSE' N;
'FOR' I:=P+1 'STEP' 1 'UNTIL' LAST 'DO'
'BEGIN' 'IF' K[P,I-P+1]=0 'THEN' 'GOTO' FINI;
FAC:=K[P,I-P+1]/K[P,1];
F[I]:=F[I]-F[P]*FAC;
'FOR' J:=1 'STEP' 1 'UNTIL' P-I+BW 'DO'
K[I,J]:=K[I,J]-K[P,I-P+J]*FAC;
'END';
FINI: 'END';
FINP: 'END';
SUBS: 'FOR' I:=N 'STEP' -1 'UNTIL' 1 'DO'
'BEGIN' 'IF' K[I,1]=0 'THEN' 'GOTO' ZU;
SUM:=F[I];
'IF' I=N 'THEN' 'GOTO' VAL;
SA:='IF' I>N-BW+1 'THEN' N-I+1 'ELSE' BW;
'FOR' J:=2 'STEP' 1 'UNTIL' SA 'DO'
SUM:=SUM-K[I,J]*U[I+J-1];
VAL: U[I]:=SUM/K[I,1];
NSUM:=NSUM+ABS(U[I]);
ZU: 'END';
'IF' ABS(NSUM-PSUM)<0.002*NSUM
'THEN' 'GOTO' EXT;
PSUM:=NSUM; NSUM:=0;
'FOR' I:=1 'STEP' 2 'UNTIL' N-1 'DO'
'BEGIN' 'IF' I=N-1 'THEN'
'BEGIN' KM[I,1]:=C[1,4]; KM[I,2]:=C[2,4];
KM[I,3]:=C[3,4]; KM[I,4]:=C[4,4];
M[I]:=- (KM[I,1]*U[I-2]+KM[I,2]*U[I-1]+KM[I,3]*U[I]
+KM[I,4]*U[I+1])*B/12;
'GOTO' STRE;

```



```

      'END';
      M[I]:=(KM[I,1]*U[I]+KM[I,2]*U[I+1]+KM[I,3]*U[I+2]
+KM[I,4]*U[I+3])*B/12;
STRE:  MT:=2*M[I]/(B*D[I]*D[I]);      AM:=ABS(MT);
      M[I]:=M[I]/1000;
      'IF' AM>MM[NS] 'THEN'
      'BEGIN' WRITETEXT(('OVERSTRESSED%AT%I='));
           PRINT(I,2,0);
           'GOTO' ENU;
      'END';
      'IF' AM<MM[1] 'THEN'
      'BEGIN' E[I]:=EE[1];  A[I]:=SIG[1]*AM/MM[1];
      'GOTO' ABT;
      'END';
      'FOR' P:=2 'STEP' 1 'UNTIL' NS 'DO'
      'IF' AM<MM[P] 'THEN'
      'BEGIN' E[I]:=EE[P-1]+(EE[P]-EE[P-1])*(AM-MM[P-1])
           /(MM[P]-MM[P-1]);
           A[I]:=SIG[P-1]+(SIG[P]-SIG[P-1])*(AM-MM[P-1])
           /(MM[P]-MM[P-1]);
           'GOTO' ABT;
      'END';
ABT:  'END';
      NI:=NI+1;
      'GOTO' MAT;
EXT:  'FOR' I:=1 'STEP' 1 'UNTIL' N 'DO'
      'BEGIN' F[I]:=0;
           FIRST:= 'IF' I>BW 'THEN' I-BW+1 'ELSE' 1;
           LAST:= 'IF' I<N-BW+1 'THEN' I+BW-1 'ELSE' N;
           'FOR' J:=FIRST 'STEP' 1 'UNTIL' LAST 'DO'
           'BEGIN' P:= 'IF' J<I 'THEN' J 'ELSE' I;
                   Z:= 'IF' J<I 'THEN' I-J+1 'ELSE' J-I+1;
                   F[I]:=F[I]+Q[P,Z]*U[J];
           'END';
           F[I]:=F[I]*B/12;
      'END';
      NEWLINE(2);
      WRITETEXT(('('14S)'X('14S)'DEFLN('14S)'BXM('16S)'
STRESS('14S)'REACTION('11S)'FIXING%MT)');  NEWLINE(4);
      'FOR' I:=1 'STEP' 2 'UNTIL' N-1 'DO'
      'BEGIN'
           PRINT(X[I],3,2); PRINT(U[I],9,4); PRINT(M[I],12,4);
           PRINT(A[I],12,4);
           'IF' V[I]=2 'THEN' 'BEGIN' PRINT(F[I],12,4);
                   'GOTO' FLE;
                   'END';
           'IF' V[I]=0 'THEN' PRINT(F[I],12,4) 'ELSE' SPACE(20);
           'IF' V[I+1]=0 'THEN' PRINT(F[I+1]/1000,12,4);
           'IF' V[I+1]=2 'THEN' PRINT(F[I+1]/1000,12,4);
           'IF' V[I+1]=2 'THEN' PRINT(F[I+1],12,4);
           NEWLINE(2);
      'END';
      NEWLINE(6); PRINT(NI,30,0); WRITETEXT(('ITERATIONS'));
      'END';
ENU:  'END';

```



REFERENCES

1. TIMOSHENKO, S. and GOODIER, J.N. Theory of elasticity 1970 (McGraw-Hill).
2. WILLIAMS, M.L. Structural analysis of viscoelastic materials. AIAA Journal 1964, 2 (5), 785 - 808.
3. FLÜGGE, W. Viscoelasticity 1967 (Blaisdell Publishing Co.)
4. BOLEY, B.A. and WEINER, J.H. Theory of thermal stresses 1960 (John Wiley & Sons).
5. TIMOSHENKO, S. Strength of Materials Part II, 1956, (Van Nostrand Reinhold Co.).
6. OGORKIEWICZ, R.M. Engineering properties of thermoplastics, 1970 (Wiley Interscience).
7. BUTLER, R. and KERR, E. An introduction to numerical methods 1966 (Pitman).
8. McCracken, D.D. and DORN, W.S. Numerical methods and Fortran programming with applications to engineering and science. 1964 (Wiley).
9. LIVESLEY, R.K. Matrix methods of structural analysis 1964 (Pergamon).
10. McMINN, S.J. Matrices for structural analysis 1962 (E & F.N.Spon Ltd., London).
11. SEVERN, R.T. Inclusion of shear deflection in the stiffness matrix for a beam element. J.Strain Anal. 1970, 5 (4), 239 - 241.



12. ZIENKIEWICZ, O.C. The finite element method in engineering science. 1971 (McGraw-Hill).
13. HETENYI, M. Beams on elastic foundations 1946 (University of Michigan Press).
14. WEBBER, J.P.H. Stress analysis in viscoelastic bodies using finite elements and a correspondence rule with elasticity. J.Strain Anal. 1969, 4 (3), 236 - 243.
15. ZIENKIEWICZ, O.C., WATSON, M. and KING, I.P. A numerical method of viscoelastic stress analysis. Int.J.Mech.Sci. 1968 10, 807 - 827.
16. BAER, E. (Ed) Engineering Design for plastics 1964, (Chapman & Hall).
17. TURNER, S. The strain response of plastics to complex stress histories. Polymer Engineering & Science 1966, 6, 306 - 316.
18. TURNER, S. Mechanical Performance and design of polymers. Applied Polymer Symposia 1971, 17, 213 - 240.
19. TURNER, S. The foundations of possible engineering design methods for plastics. Trans.J.Plastics Inst 1966. 127 - 135.
20. GREEN, A.E. & RIVLIN, R.S. The mechanics of non-linear materials with a memory. Arch.Rational Mech.Anal. 1957, 1, 1 - 21.
21. LOCKETT, F.J. and TURNER, S. Non-linear creep plastics. J.Mech.Phys.Solids 1971, 19, 201 - 214.



22. PIAN, T.H.H. Derivation of element stiffness matrices by assumed stress distributions AIAA Journal 1964, 2 (7), 1333 - 1336.
23. McNIECE, G.M. and HUNNISETT, S.F. Mixed-displacement finite-element analysis with particular application using plane-stress triangles. J.Strain Anal. 1972, 7 (4), 243 - 252.
24. DUGDALE, D.S. and RUIZ, C. Elasticity for Engineers 1971, (McGraw-Hill).